



**International
Energy
Agency**

Condensation and Energy

Sourcebook

Report Annex XIV, Volume 1

**Energy Conservation in Buildings
and Community Systems Programme**

IEA — ANNEX XIV : CONDENSATION AND ENERGY

Volume 1

Sourcebook

INTERNATIONAL ENERGY AGENCY — ENERGY CONSERVATION IN
BUILDING AND COMMUNITY SYSTEMS

MARCH 1991

With many thanks to Beatrice Schotsmans, Arnold Janssens, Eric Senave and Pol Verbeek for reading, correcting and/or doing the layout of the final text-proposals for Annex 14. Owing to them, this Source Book is not only interesting to study but also pleasant to read.

PREFACE

THE INTERNATIONAL ENERGY AGENCY

The International Energy Agency (IEA) was established in 1975 within the framework of the Organisation for Economic Cooperation and Development (OECD) to implement an International Energy programme. A basic aim of the IEA is to foster cooperation among the 21 IEA Participating Countries to increase energy security through energy conservation, development of alternative energy sources and energy research, development and demonstration (RD&D). This is achieved in part through a programme of collaborative RD&D consisting of forty-two implementing Agreements, containing a total of over eighty separate energy RD&D projects.

ENERGY CONSERVATION IN BUILDING AND COMMUNITY SYSTEMS

As one element of the Energy Programme, the IEA sponsors research and development in a number of areas related to energy. In one of these areas, energy conservation in buildings, the IEA is backing various exercises to predict more accurately the energy use of buildings, including comparison of existing computer programmes, building monitoring, comparison of calculation methods, energy management systems, as well as air quality and inhabitants behaviour studies. Sixteen countries and the European Community, BELGIUM, CANADA, CEC, DENMARK, FEDERAL REPUBLIC OF GERMANY, FINLAND, GREECE, ITALY, JAPAN, NETHERLANDS, NEW ZEALAND, NORWAY, SWEDEN, SWITZERLAND, TURKEY, U.K., U.S.A., have elected to participate and have designed contracting parties to the Implementing Agreement, covering collaborative research in this area. This designation by the government of a number of private organisations as well as universities and government laboratories, as contracting parties, has provided a broader range of expertise to tackle the projects in the different technology areas than would have been the case if participation was restricted to governments alone. The importance of associating industry with government sponsored energy RD&D is recognised in the IEA, and every effort is made to encourage this trend.

THE EXECUTIVE COMMITTEE

Overall control of the programme is maintained by an Executive Committee, which not only monitors existing projects but also identifies new areas where collaborative effort may be beneficial. The Executive Committee ensures all projects to fit into a predetermined strategy without unnecessary overlap or duplication but with effective liaison and communication. Twenty-five projects have been initiated by the Executive Committee, more than half of which have been completed:

- ANNEX 1: Load energy determination of buildings (*)
- ANNEX 2: Ekistics & advanced community energy systems (*)
- ANNEX 3: Energy conservation in residential buildings (*)
- ANNEX 4: Glasgow commercial building monitoring (*)
- ANNEX 5: Air infiltration and ventilation centre (*)
- ANNEX 6: Energy systems and design of communities (*)
- ANNEX 7: Local government energy planning (*)

- ANNEX 8: Inhabitants behaviour with regard to ventilation (*)
- ANNEX 9: Minimum ventilation rates (*)
- ANNEX 10: Building HVAC system simulation (*)
- ANNEX 11: Energy auditing (*)
- ANNEX 12: Windows and fenestration (*)
- ANNEX 13: Energy management in hospitals (*)
- ANNEX 14: Condensation and energy (*)
- ANNEX 15: Energy efficiency of schools
- ANNEX 16: BEMS 1- User interfaces and system integration
- ANNEX 17: BEMS 2- Evaluation and emulation techniques
- ANNEX 18: Demand controlled ventilation systems
- ANNEX 19: Low slope roofs systems
- ANNEX 20: Air flow patterns
- ANNEX 21: Energy efficient communities
- ANNEX 22: Thermal modelling
- ANNEX 23: Air flow modelling
- ANNEX 24: Heat- air moisture transport in new and retrofitted insulated envelope parts
- ANNEX 25: Real time simulation and fault detection

ANNEX 14: CONDENSATION AND ENERGY

The idea to start an Annex on mould, surface condensation and energy grew in 1984-1985. In September 1985, a workshop was organised at the Leuven University, Belgium, focusing on the state of the art in different countries. This workshop revealed a real lack of overall knowledge and understanding, on the levels of data, modelling and measuring.

The Annex objectives were formulated as:

- providing architects, building owners and practitioners as well as researchers with a better knowledge and understanding of the physical backgrounds of mould and surface condensation, including the critical conditions for mould growth and the influencing material properties;
- to introduce better calculation models, taking into account air, heat and moisture transfer, in order to predict properly the phenomena of mould and surface condensation and to validate possible solutions;
- to develop energy conserving and cost effective strategies and complementary design methods, techniques and data for avoiding mould and surface condensation in new buildings or preventing further degradation in problem buildings.

At first 6, later 5 countries: BELGIUM, FEDERAL REPUBLIC OF GERMANY, ITALY, NETHERLANDS, U.K., joined together for 3 years of intensified research on mould and surface condensation. The shared work included case studies, common exercises and the draft of a source book, a catalogue of material properties and a guidelines booklet. Also the national research efforts were scheduled in accordance with the Annex 14 scheme and the results brought together and used as base for the Annex publications.

Seven working meetings of 3 days each were held, the first to build up a common knowledge, the last to discuss research and reports and to elaborate a common performance philosophy.

(*) completed

LIST OF EXPERTS CONTRIBUTING TO ANNEX 14

OPERATING AGENT

K.U.Leuven, Laboratory for Building Physics, represented by Prof. H. Hens, head of the lab.

NATIONAL EXPERTS

Belgium

ir. E. Senave, K.U.Leuven, Lab. for Building Physics, Leuven
 dr. ir. P. Standaert, Adviesbureau Physibel, Maldegem
 ir. B. Walley, NMH, National Housing Society, Brussels
 ir. P. Wouters, WTCB- CSTC, Belgian Building Research Institute, Brussels

Federal Republic of Germany

National coordinator: Dipl.-Ing. H. Erhorn,
 Fraunhofer institut für Bauphysik, Stuttgart
 Dipl.-Ing. W. Eisele, Fraunhofer Institut für Bauphysik, Stuttgart
 Dipl.-Ing. Z. Herbak, Fraunhofer Institut für Bauphysik, Stuttgart
 Dipl.-Ing. H. Künzel, Fraunhofer Institut für Bauphysik, Holzkirchen
 Dipl.-Ing. J. Reiß, Fraunhofer Institut für Bauphysik, Stuttgart
 Dr W. Raatschen, Dornier GmbH, Friedrichshafen
 Dipl.-Ing. R. Stricker, Fraunhofer Institut für Bauphysik, Stuttgart

Italy

National coordinator: Prof. C. Lombardi,
 Politecnico di Torino
 Ing. G. Casetta, Consulting engineer

Netherlands

National coordinator: ir. P.C.H. Vanderlaan,
 Rijksgebouwendienst, Den Haag
 ir. O. Adan, TNO-IBBC, Rijswijk
 ir. J.J.M. Cauberg, Cauberg-Huyghen Raadgevende Ingenieurs, Maastricht
 dr. ir. J. de Wit, T.U. Eindhoven, Fakulteit bouwkunde, Vakgroep Fago, Eindhoven
 ir. W. Lichtveld, Lichtveld, Buis en Partners, Utrecht
 ir. J. Oldengarm, TNO-IBBC, Rijswijk
 ir. A.C. Van der Linden, Rijksgebouwendienst, Den Haag
 ir. R.J.P. Van Hees, TNO-IBBC, Rijswijk

United Kingdom

National coordinator: Mr. C. Sanders,
 BRE, Scottish Laboratory, East Kilbride
 Prof. P. Burberry, UMIST, Department of Building Engineering, Manchester
 Dr. M. Denman, Sheffield City Polytechnic, Sheffield
 Dr. C. Hunter, BRE, Garston, Watford
 Dr. T. Orescyn, Bartlet School of Architecture and Planning,
 University College London

CONTENTS

PREFACE	i
CONTENTS	iv
SYMBOLS	ix
INTRODUCTION	xi
CHAPTER 1: MATERIAL PROPERTIES	
1.0 INTRODUCTION	1.1
1.1 HYGROTHERMAL PROPERTIES	1.3
1.1.1 Survey	1.3
1.1.2 Influencing parameters	1.3
1.1.3 Definitions	1.5
1.2 STANDARD LISTS	1.20
1.2.1 The concept "calculation value"	1.20
1.2.2 Examples of standard lists (see catalogue report)	1.21
1.2.3 Discussion	1.22
1.2.4 Conclusion	1.23
1.3 EXPERIMENTAL METHODS	1.23
1.3.1 Aim	1.23
1.3.2 Methods	1.23
1.3.3 Standards	1.27
1.4 EXPERIMENTAL RESULTS	1.28
1.4.1 Materials and components tested	1.28
1.4.2 Analysis of the data (see catalogue report)	1.29
1.4.3 Database	1.30
1.5 REFERENCES AND LITERATURE	1.30
CHAPTER 2: MOULD	
2.0 INTRODUCTION	2.1
2.1 MICROBIOLOGY OF MOULDS	2.3
2.2 SAMPLING TECHNIQUES	2.6
2.2.1 Air sampling	2.6
2.2.2 Surface sampling	2.8

2.2.3 Identification	2.8
2.3 IMPORTANT SPECIES IN HOUSING	2.8
2.3.1 Mould spore levels in dwellings	2.8
2.3.2 Prevalence of moulds on surfaces	2.13
2.4 LIMITING CONDITIONS FOR GROWTH	2.15
2.4.1 Temperature	2.15
2.4.2 Water activity on the surface	2.15
2.4.3 Air humidity	2.17
2.4.4 Nutrient availability and substrate	2.18
2.5 HEALTH HAZARDS	2.19
2.5.1 Mycotoxins and organic volatiles	2.19
2.5.2 Mould spores	2.20
2.5.3 Mites	2.21
2.6 SOME ELEMENTARY CONTROL STRATEGIES	2.21
2.6.1 Fungicidal strategy	2.22
2.7 REFERENCES	2.23
Appendix 2A: Identification of mould	2.32
CHAPTER 3: MODELLING: THERMAL ASPECTS	
3.0. INTRODUCTION	3.1
3.1 CONDUCTION	3.6
3.1.1 Theoretical background	3.6
3.1.2 Calculation methods	3.9
3.1.3 Experimental investigations	3.21
3.1.4 Applications	3.24
3.1.5 Conclusions	3.39
3.2 CONVECTION AND RADIATION	3.40
3.2.1 Introduction	3.40
3.2.2 Radiative heat transfer	3.40
3.2.3 Convective heat transfer	3.45
3.2.4 Total surface film coefficient	3.49
3.2.5 Influence of the reference temperature	3.49
3.2.6 Experimental investigations	3.50
3.2.7 Influence of furniture and the heating system	3.53
3.2.8 Practical method to define the surface film coefficient	3.59
3.3 REFERENCES	3.67

Appendix 3A - List of available PC Programs

CHAPTER 4: MODELLING: HYGRIC ASPECTS

4.1. INTRODUCTION,	4.1
4.2 VAPOUR IN THE AIR: A RECAPITULATION	4.1
4.3 MOISTURE IN MATERIALS	4.9
4.3.1 Hygroscopicity	4.9
4.3.2 Vapour transfer by diffusion	4.14
4.3.3 Capillary wetting and drying by diffusion	4.18
4.4 THE HYGRIC BALANCE OF AN ENCLOSURE: THE SINGLE-ZONE APPROXIMATION	4.20
4.4.1 No surface condensation, no hygroscopicity	4.20
4.4.2 Surface condensation, no hygroscopicity	4.33
4.4.3 Hygroscopic influences	4.46
4.4.4 Steady-state vapour diffusion through the envelope	4.74
4.4.5 Latent heat of evaporation	4.76
4.5 LITERATURE	4.77

CHAPTER 5: MODELLING: COMBINED HEAT, MOISTURE AND AIR TRANSPORT

5.1 INTRODUCTION	5.1
5.2 WHY COMBINED HAM MODELLING ?	5.2
5.2.1 Building physics and building models	5.2
5.2.2 HAM interactions	5.3
5.2.3 Combined HAM models and the Annex XIV task	5.3
5.2.4 A general HAM model classification	5.5
5.2.5 Potential users of HAM models	5.7
5.3 CLASSIFICATION OF HAM MODELS AND LEVELS OF COMPLEXITY	5.8
5.3.1 HAM model categories	5.8
5.3.2 Levels of detail	5.9
5.4 STATE-OF-ART OF COMBINED MODELLING	5.14
5.4.1 Examples of general purpose models	5.14
5.4.2 Building simulation models (category B)	5.16
5.4.3 Air infiltration models (category C)	5.17
5.4.4 Air flow simulation models (category D)	5.21
5.4.5 Special purpose and simplified modelling	5.24
5.5 CONCEPTS FOR MOISTURE STORAGE MODELLING	5.26

5.6	MODEL AND INPUT DATA REQUIREMENTS	5.27
5.6.1	Model documentation	5.27
5.6.2	Data requirements	5.27
5.6.3	Required level of detail	5.28
5.7	CASE STUDIES AND FIELD EXPERIMENTS	5.28
5.7.1	The model versus the real world	5.28
5.7.2	Feedback from practice to modelling	5.29
5.7.3	Case studies	5.29
5.7.4	Field experiments.	5.31
5.7.5	Discussions with respect to HAM modelling	5.34
5.7.6	Model validation.	5.35
5.8	PARAMETER STUDY	5.36
5.8.1	Introduction	5.36
5.8.2	Results	5.37
5.8.3	Remarks	5.45
5.10	REFERENCES	5.47
CHAPTER 6: BOUNDARY CONDITIONS		
6.0	INTRODUCTION	6.1
6.1	MOISTURE BALANCE OF A ROOM	6.1
6.2.1	Steady-state conditions	6.2
6.2.2	Non-steady-state effects	6.2
6.3.	INFLUENCE OF OCCUPANT BEHAVIOUR	6.2
6.3.1	Moisture production rates in rooms	6.3
6.3.2	Ventilation rates	6.8
6.3.3	Room temperature	6.10
6.3.4	Air and humidity distribution in buildings	6.10
6.4	INFLUENCE OF HEATING SYSTEM	6.11
6.4.1	Temperature stratification	6.11
6.4.2	Operating modes	6.11
6.5	INFLUENCE OF VENTILATION SYSTEM	6.14
6.5.1	Natural ventilation	6.14
6.5.2	Climatic influences	6.18
6.5.3	Moisture distribution within a zone	6.20
6.5.4	Interzonal moisture transfer	6.21

6.6	METEOROLOGICAL CONDITIONS	6.22
6.6.1	The local climate and the indoor air humidity	6.22
6.6.2	The local climate and the ventilation rate	6.25
6.6.3	Summary of findings	6.29
6.7	MEASURING TECHNIQUES	6.32
6.7.1	Room air temperature and surface temperatures	6.32
6.7.2	Humidity	6.36
6.7.3	Air exchange rates	6.38
6.8	REFERENCES	6.43

APPENDIX 6.A: Meteorological Data Base

APPENDIX 6.B: Calculation Procedure (to chapter 6.6)

SYMBOLS

symbol	unit	Physical quantities
a	-	absorbivity
a	m ² /s	thermal diffusivity
a _w	-	water activity
b	J/(m ² .K.s ²)	thermal effusivity
c	kg/m ³	water vapour concentration (humidity by volume)
c	J/(kg.K)	specific heat capacity
c'	J/(kg.K)	specific heat capacity of a wet material
d	m	thickness
e	-	emissivity
g _m	kg/(m ² .s)	density of moisture flow rate
k _a	s	air permeability
k _m	s	moisture conductivity
l	m	length
m	kg	mass
p	Pa	partial water vapour pressure
p'	Pa	partial water vapour saturation pressure
q	W/m ²	heat flow density
n	h ⁻¹ (s ⁻¹)	ventilation rate
r	-	reflectivity
t	s	time
u	%kg/kg	moisture content mass by mass
w	kg/m ³	moisture content mass by volume
x	g/kg	water vapour ratio (humidity by mass)

A	kg/(m ² s ²)	water sorption coefficient
D _w	m ² /s	moisture diffusivity
E _n		Energy consumption
G _m	kg/s	moisture flow rate , vapour production
K _a	s/m	air permeance
P	W/m ² .K	thermal permeance inside surface - outside
R	m ² .K/W	thermal resistance
S	-	degree of saturation
T	K	thermodynamic (absolute) temperature
U	W/m ² .K	thermal permeance

α	K ⁻¹	specific heat strain
δ _p	s	vapour permeability coupled to a vapour pressure gradient
δ _v	m ² /s	vapour permeability coupled to a vapour concentration gradient
ε	-	hygric strain
ρ	kg/m ³	volumic mass (density)
ρ _c	J/(m ³ .K)	volumic heat capacity
φ	-	relative humidity
μ	-	vapour resistance factor
μ _d	m	(equivalent) vapour diffusion thickness

ψ	$\%m^3/m^3$	moisture content volume by volume
ψ_a	$\%m^3/m^3$	air content
λ	$W/(mK)$	thermal conductivity
θ	$^{\circ}C$	temperature
θ_{rs}	$^{\circ}C$	dry resulting temperature
τ	-	transmissivity
	-	temperature ratio

SUBSCRIPTS

a	ambient
c	capillary
cv	convective
e	exterior
h	hygroscopic
i	interior
m	moisture
max	maximal
r	radiation
s	surface
sat	saturation
v	vapour
w	water, liquid

ABBREVIATIONS:

CFU	colony forming units
ERH	equilibrium relative humidity
IAQ	internal air quality
RUE	rational use of energy
MGF	mean growth factor
MW	mineral wool
MPS	extruded polystyrene
RH	relative humidity
TRY	test reference year

INTRODUCTION

Mould problems in dwellings are a rather widespread reality in the 5 countries, participating at Annex XIV, especially in the social housing sector. Statistical information, circulating during the working meetings, suggests some 20% of the social housing stock being affected in Belgium, some 15% in the Netherlands and some 25 to 30% of the low income housing in the U.K.

Mould germination on an inside surface becomes possible when the water activity on it stays higher, during a shorter or longer period, than a threshold-value ' a_w ', which is a function of different parameters.

Using the fact that, in steady-state or slowly changing conditions the water activity is nothing else but the relative humidity against the surface, the mould condition becomes:

$$p_{si} \geq a_w \cdot p'_{si}$$

p_{si} is the vapour pressure against the surface and p'_{si} the saturation pressure on the surface.

If $a_w = 1$, the mould condition turns to the surface condensation equation:

$$p_{si} \geq p'_{si}$$

This is equivalent to: "the dewpoint of the air against the surface is equal to or higher than the surface temperature".

THE SATURATION PRESSURE ON THE SURFACE (p'_{si})

is directly linked to the surface temperature θ_{si} :

$$\theta_{si} = \theta_0 + r \cdot (\theta_i - \theta_0)$$

with r the temperature ratio, which is a purely thermal property of each point on a wall, depending of the geometry (flat walls, 2- and 3- dimensional situations), the surface film coefficients and the dynamic reality.

THE VAPOUR PRESSURE AGAINST A SURFACE (p_{si})

follows directly from the air & vapour balance in and between rooms and between the building and the outside. Important elements in it are : the vapour production, the outside air ventilation, well or no surface condensation, hygroscopic inertia, intra and interroom moisture transport...

This short overview of theory learns that, to study the reality of mould and surface condensation, in relation with energy conservation and its emphasis

- on a better insulation quality, pronouncing the danger of real thermal bridges,
- on a minimisation of the heat losses by excess ventilation,
- on an economisation of heating system use,

one needs:

- a sound knowledge of material properties: chapter 1 of the source book. Otherwise, modelling the thermal and hygric response of the fabric remains theory;
- information on a 'a_w'-value: chapter 2 of the source book, studying 'moulds';
- an introduction in thermal modelling : chapter 3 of the source book, with as main point thermal bridging and surface film coefficients;
- some concepts of hygric modelling: chapter 4 of the source book, focussing on the hygroscopic inertia;
- an understanding of the heat-air-moisture combined transport: chapter 5 of the source book gives an overview of the actual knowledge, in relation with experimental results
- information on boundary conditions and building use data: chapter 6 of the source book

Chapter 1

MATERIAL PROPERTIES

Author:

H. Hens
LABORATORY FOR BUILDING PHYSICS
Celestijnenlaan 131, B-3001 Leuven (Heverlee)
Belgium

1.0 INTRODUCTION

In the understanding of mould problems and surface condensation, modelling plays an important role. The aim is to describe the heat, air, and moisture transfer in buildings, at surfaces and in and through the building envelope. To use the models properly, the knowledge of the material properties is of prime importance.

Chapter 1 introduces the "catalogue of building, insulating and finishing materials and their hygrothermal properties" (volume 3). This catalogue fills as much as possible the gaps, encountered in standard lists.

Information sources were:

- literature;
- the standard lists of Belgium, Germany, France, Italy, The Netherlands and the U.K.;
- all measurements, done at the "Laboratorium Bouwfysica" of the K.U.Leuven, reports of other labs.

As for the content of this chapter, one first has the array of hygrothermal properties, their exact definition, and their dependence on different parameters. Then follows a survey of standard lists, all collected in the volume 3, the catalogue report. One ends with an overview of measuring methods, results and the database, published in volume 3, the catalogue report.

Table 1.1: Array of hygrothermal properties

PROPERTY	SYMBOL	UNITS
<u>T: THERMAL</u>		
T.1 CAPACITIVE		
T.1.1 specific heat capacity	c	J/(kg.K)
T.1.2 volumetric heat capacity	ρc	J/(m ³ .K)
T.2 TRANSFER		
T.2.1 thermal conductivity	λ	W/(m.K)
T.2.2 (areal) thermal resistance	R	m ² .K/W
T.2.3 absorbtivity, emissivity, reflectivity, transmissivity	a, e, r, τ	-
T.3 COMBINED		
T.3.1 thermal diffusivity	a	m ² /s
T.3.2 thermal effusivity	b	J/(m ² .K.s ^{1/2})
T.4 CONSEQUENCE OF A CHANGE IN HEAT CONTENT		
T.4.1 specific thermal strain	α	K ⁻¹
<u>H: HYGRIC</u>		
H.1 CAPACITIVE		
H.1.1 moisture content	w	kg/m ³ ;
	u	%kg/kg;
	ψ	%m ³ /m ³
H.1.2 degree of saturation	S	%
H.1.3 specific moisture content	c_H	kg/m ³
H.2 TRANSFER		
H.2.1 vapour permeability, vapour resistance factor	δ_p, δ_v	s; m ² /s
	μ	-
H.2.2 diffusion thickness	μ_d	m
H.2.3 moisture conductivity	k_m	s
H.2.4 thermal diffusion coefficient	D_t	kg/(m ² .s.K)
H.3 COMBINED		
H.3.1 moisture diffusivity	D_w	m ² /s
H.3.2 water sorption coefficient	A	kg/(m ² .s ^{1/2})
H.4 CONSEQUENCE OF A CHANGE IN MOISTURE CONTENT		
H.4.1 hygric strain	ϵ	%
<u>A: AIR</u>		
A.1 CAPACITIVE		
A.1.1 air content	ψ_a	%m ³ /m ³
A.2 TRANSFER		
A.2.1 air permeability	k_a	s
A.2.2 air permeance	K_a	s/m

1.1 HYGROTHERMAL PROPERTIES

1.1.1 Array of hygrothermal properties (table 1.1)

For most building practitioners, hygrothermal properties reduce to "Thermal Conductivity". In reality, not only thermal, but also hygric and air properties are relevant. For each, a distinction has to be made between:

1. Capacitive properties: *"the possibility to store heat, moisture and air in a material"*
2. Transfer properties: *"the possibility of heat, air and moisture to flow in and through the material"*
3. Combined properties: *"a physically significant combination of capacitive and transfer properties"*
4. Properties, linked to changes in heat, moisture and air content. They are not discussed in this report.

1.1.2 Influencing parameters

For all materials, the hygrothermal properties are essentially theoretically defined quantities for use in calculations and are not absolute constants. Their value depends on parameters, the important ones being mentioned in tabel 1.2.

In principal, the relationship property = $f(\text{density, porous system, thickness, temperature, temperature difference, moisture content, time})$ has to be known. The functional dependence 'property- parameters' may follow from a physical understanding, the numerical relation has to be fitted by measurements. This demands such a tremendous amount of experimental work, that only partial results can be obtained.

Fortunately, within the interval of parameter values, encountered in buildings, the influence of parameters such as temperature difference remains rather unimportant, while the relationship with others can be linearised without major inaccuracy.

Table 1.2: Array hygrothermal properties - parameters

An important relationship is given a value 4, a less important relationship a value 2, limited relationship a value 1 and \pm no relationship a value 0.

PROPERTY	PARAMETER								
	M1	M2	M3	M4	AP1	AP2	AP3	T	Σ
T.1.1 c	2	0	0	0	1	0	4	0	7
T.1.2 ρc	2	4	0	0	1	0	4	0	11
T.2.1 λ	4	4	2	2	2	1	4	1	20
T.2.2 R	4	4	2	4	2	1	4	1	22
T.2.3 a, e, r, τ	4	0	0	0	2	0	1	1	8
T.3.1 a	2	1	1	0	1	0	1	0	6
T.3.2 b	4	4	2	0	2	0	4	1	17

H.1.1 w, u, ψ	1	4	4	0	0	0	0	1	10
H.2.1 μ	1	4	4	2	2	0	4	1	17
H.2.2 μd	1	4	4	4	2	0	4	1	19
H.2.3 k_m	1	4	4	0	2	0	4	1	16
H.2.4 D_t	1	4	4	0	2	0	4	1	16
H.3.1 D_w	1	4	4	0	2	0	4	1	16
H.3.2 A	1	4	4	0	1	0	4	1	15

A.1.1 w_a	0	4	4	0	0	0	4	1	13
A.2.1 k_a	1	4	4	0	1	0	4	1	15
A.2.2 K_a	0	4	4	4	1	0	2	1	16
Σ	30	57	47	15	24	2	56	14	244

PRODUCTION LINKED

M1: basic material

M2: density

M3: type, configuration, form, orientation of pores

M4: thickness

APPLICATION LINKED

AP1: temperature

AP2: temperature difference

AP3: moisture content, relative humidity

TIME

The array "Properties - parameters" (table 1.2) shows that the most important parameters are:

M1 : basic material

M2 : density

M3 : type, configuration, form, directivity of pores

AP3: moisture content, relative humidity

Of less importance are

AP1: temperature

M4 : thickness

T : time

The greatest parameter sensitivity is found for:

T.2.2 thermal conductivity

T.2.2 thermal resistance

H.2.2 diffusion thickness

In the catalogue, these facts are translated as follows:

M1, M3 The searching key: define the kind of material;

M2 Given for each material as a production linked parameter;

AP3 If known within the limits of temperatures, encountered in building constructions, the relation property - moisture content is given;

AP1,T,M4 If known and of practical use, relation given.

1.1.3 Definitions

DENSITY (symbol: ρ / units: kg/m^3)

We call density, the weight of 1 m^3 of dry material.

'Dry' is a standardised concept, rather than a physically exact notion: in fact, standards define as dry, stony or wooden materials dried at 105°C or plastics dried at a temperature, low enough not to enhance the material, until between two successive daily measurements, the weight decrease remains less than 1% of the starting weight.

In building applications, the density varies from $\approx 10 \text{ kg/m}^3$ for the lightest insulation until some 2500 à 3000 kg/m^3 for the heaviest stony, and 2700 à 11000 kg/m^3 for metallic materials, i.e. a difference in order of magnitude 3 (insulation versus stony) to 4 (insulation versus metallic).

THERMAL PROPERTIEST.1.1 SPECIFIC HEAT CAPACITY (symbol: c / units: J/(kg.K))

We call specific heat, the heat needed to change the temperature of a unit mass of material with 1 K. With the unit mass referring to the dry material, the specific heat capacity of a wet material c' becomes:

$$c' = c + 4187 \cdot \frac{w}{\rho} \quad (1.1)$$

with w the moisture content in the material in kg/m^3 .

Water has the highest specific heat capacity: $4187 \text{ J}/(\text{kg.K})$.

For building, insulating and finishing materials, c differs only slightly.

Generally speaking, we may distinguish between:

MATERIAL GROUP	c [J/(kg.K)]
Metallic	130 to 880
Stony	840
Polymeric	1470
Wood, wood based	1880

giving a difference in order of magnitude < 1 .

T.1.2 VOLUMETRIC HEAT CAPACITY (symbol: ρc / units: J/(m^3 .K))

The volumetric heat capacity is the heat, needed to change the temperature of a unit volume of dry material by 1 K. Referring to density and specific heat capacity, the volumic heat capacity of 1 m^3 of material is:

$$\begin{aligned} \text{DRY} &: \rho c \\ \text{WET} &: \rho c + 4187 \cdot w \end{aligned} \quad (1.2)$$

In all thermal phenomena, not c but ρc is the storage defining quantity. In it, the density causes clear differences in order of magnitude between insulating and stony materials:

$$\begin{aligned} \text{INSULATING} &: \rho c > 1.5 \cdot 10^4 \text{ J}/(\text{m}^3 \cdot \text{K}) \\ \text{STONY} &: \rho c > 2.5 \cdot 10^6 \text{ J}/(\text{m}^3 \cdot \text{K}) \end{aligned}$$

Owing to this, as a necessary condition to construct capacitive buildings, we have: use heavy materials!

T.2.1 THERMAL CONDUCTIVITY (symbol: λ / units:W/(m.K))

As exact definition of the thermal conductivity, we have:

"The thermal conductivity in a point of a material is the ratio between the 'density of heat flow'- vector and the 'temperature gradient'-vector in that point"

For isotropic materials, both vectors coincide and the thermal conductivity is a scalar. For anisotropic materials, they do not and the thermal conductivity becomes a tensor, represented by a (3x3)-matrix.

The technical definition of the thermal conductivity is coupled to the formula for the steady-state density of heat flow through a flat, infinitely extended single layer wall:

$$q = \frac{\lambda \cdot (\theta_1 - \theta_2)}{d} \quad \rightarrow \quad \lambda = \frac{q \cdot d}{\theta_1 - \theta_2} \quad (1.3)$$

or:

"The thermal conductivity of a material is the heat flowing in steady-state, during 1 s, from one side of a cube of 1 m³ of the material to the other, the temperature difference between both sides being 1 K, the other 4 sides being adiabatic"

Physically, the thermal conductivity is only a material property for non-porous materials.

In porous materials, heat not only flows through the material matrix by conduction, but also by:

DRY MATERIAL

- I - conduction through the pore filling gasses;
- II - radiation in the pores;
- III - convection in wide pores;

WET MATERIAL

I+II+III

- IV - conduction through the absorbed and capillary condensed water;
- V - water evaporation-> diffusion-> vapour condensation in the pores.

These six heat transfer modes are compressed in the quantity 'thermal conductivity', making it an 'equivalent' calculation value, which, because of the six modes, turns out to be extremely parameter dependent.

As range of calculating values, we have:

MATERIAL GROUP	λ [W/(m.K)]
Metallic	16 to 380
Stony	0.15 to 3.5
Polymeric, wood	0.10 to 0.25
Insulating	0.015 to 0.06

T.2.2 (AREAL) THERMAL RESISTANCE (symbol:R/ units:m².K/W)

The concept of an equivalent thermal conductivity does not work for cavities, gas filled spaces, heterogeneous layers, perforated blocks masonry work... For these, we have to turn to the thermal resistance.

The definition is based on, and the value calculated with the formula for the steady-state density of heat flow through a flat, infinitely extended single layer wall:

$$R = \frac{\theta_1 - \theta_2}{q} \quad (1.4)$$

R is a steady-state property, depending on the same heat transfer modes in an even more pronounced way as the thermal conductivity.

T.2.3 ABSORBTIVITY, EMISSIVITY, REFLECTIVITY, (TRANSMISSIVITY)

These surface properties are directly coupled to radiative heat transfer. As far as the 'grey surface'- concept holds, the 4 are defined as:

ABSORBTIVITY (a):

the ratio, for a given radiation temperature, between the absorbed density of radiative flow to the incident one;

EMISSIVITY (e): the ratio, for a given radiative temperature, between the emitted density of radiative flow and the 'black surface' emitted density;

REFLECTIVITY (r): the ratio, for a given radiation temperature, between the reflected density of radiative flow to the incident one;

TRANSMISSIVITY (τ): the ratio, for a given radiation temperature, between the transmitted density of radiative flow to the incident one;

For coloured surfaces, these definitions have to be narrowed to ratio's of spectral intensities instead of density.

In building physics, the grey body concept is used in a 'two temperatures interval' way:

- environmental I.R.-radiation ($T_r \approx 300K / a_L, e_L, r_L, \tau_L$)
- solar radiation ($T_r \approx 6000K / a_S, e_S, r_S, \tau_S$)

The following rules hold:

- environmental radiation: not depending on the colour; all materials and finishing layers, except the metallic ones, have an absorbtivity between 0.8 and 0.9.

$$a_L = e_L; a_L + r_L (+ \tau_L) = 1$$

- solar radiation: important influence of the colour of the surfaces
 $a_S(\text{white}) < a_S(\text{yellow}) < a_S(\text{red}) < a_S(\text{blue}) < a_S(\text{black})$

$$a_S + r_S (+ \tau_S) = 1$$

T.3.1 THERMAL DIFFUSIVITY (symbol: a / units: m^2/s)

We call thermal diffusivity, the ratio between thermal conductivity and volumic heat capacity:

$$a = \frac{\lambda}{\rho \cdot c} \quad (1.5)$$

For wet materials, the formula becomes:

$$a = \frac{\lambda(w)}{\rho \cdot c + 4187 \cdot w} \quad (1.6)$$

The diffusivity expresses the velocity of propagation, by conduction, of a local change of temperature in a material. Between materials, there is only a limited difference in a - value. Reason: thermal conductivity and density varying in the same way, both increasing or decreasing.

For all building materials, the thermal diffusivity has a low to very low value (... 10^{-6}), or, propagating a temperature change by conduction is a slow process.

T.3.2 THERMAL EFFUSIVITY (symbol:b/ units: $J/(m^2.K.s^{1/2})$)

We call thermal effusivity, the square root of the product of thermal conductivity and volumetric heat capacity:

$$b = \sqrt{\rho c \lambda} \quad (1.7)$$

For wet materials, the formula turns to:

$$b = \sqrt{(\rho c + 4187.w). \lambda(w)} \quad (1.8)$$

The effusivity expresses the ease, with which a material takes up and propagates heat by conduction. The property is closely linked to our physiological and psychological evaluation of materials: those with a high effusivity feel and are seen as cold, those with a low effusivity feel and are called warm.

Between materials, a significant difference in b-value exists, making the property a performance- criterion.

MATERIAL GROUP	b [$J/(m^2.K.s^{1/2})$]
Metallic	10000 to 36000
Stony	240 to 2900
Polymeric, wood	300 to 500
Insulating	16 to 70

HYGRIC PROPERTIESH.1.1 MOISTURE CONTENT (symbols: w, u, ψ /units: $\text{kg}/\text{m}^3, \text{kg}/\text{kg}, \text{m}^3/\text{m}^3$)

We call moisture content:

- MASS BY VOLUME,

the mass of moisture per unit volume of dry material:

$$w = \frac{m}{V} \quad (1.10)$$

- MASS BY MASS,

the mass of moisture per unit mass of dry material:

$$u = \frac{m}{M} \cdot 100 \quad (\%) \quad (1.11)$$

- VOLUME BY VOLUME,

the volume of moisture per unit volume of dry material:

$$\psi = \frac{V_m}{V} \cdot 100 \quad (\%) \quad (1.12)$$

Relations between these definitions:

$$u = 100 \cdot \frac{w}{\rho} \quad (\%); \quad \psi = w/10 \quad (\%) \quad (1.13)$$

The difference in numerical value between the three definitions, for the same moisture presence in the material, can be important and of direct psychological influence.

Example

Take 1 m^3 of concrete, density $2300 \text{ kg}/\text{m}^3$. For 100 kg moisture per unit volume, the three definitions give:

$$w = 100 \text{ kg}/\text{m}^3 ; \quad u = 4.35 \text{ kg}/\text{kg} ; \quad \psi = 10 \text{ m}^3/\text{m}^3$$

It's clear that the u -result seems the less severest.

With a very light mineral wool ($12 \text{ kg}/\text{m}^3$) the result becomes

$$w = 100 \text{ kg}/\text{m}^3 ; \quad u = 833 \text{ kg}/\text{kg} ; \quad \psi = 10 \text{ m}^3/\text{m}^3$$

Now the u -result seems disastrous, while the ψ -result looks rather reassuring

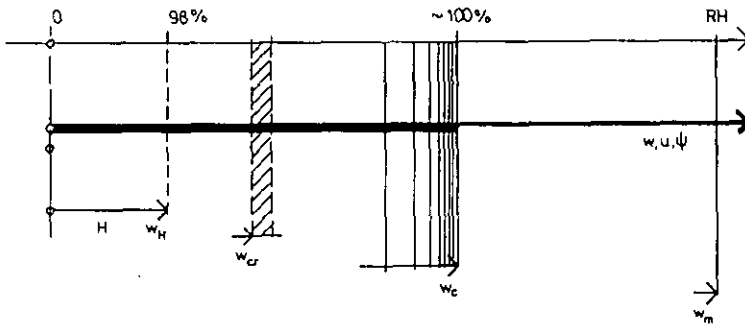


Figure 1.1: The moisture content scale

To avoid this psychological look to moisture content values, the following agreement is proposed:

- w is used for stony materials, i.e., materials with an unimportant hygric strain;
- u is used for wooden or wood based materials, i.e., materials with an important hygric strain;
- ψ is used for highly porous materials, such as insulating layers.

It is important to remember, that:

- a material can only become moist if it has a water or water vapour open porosity. Materials with zero porosity or closed pores, show a surface wetting, but no mass wetting;
- in all open porous materials, the moisture content can vary from zero (= dry) to saturation (= all water open pores filled). On this continuous scale, some important zones/ points exist (Figure 1.1).
- materials with only or predominantly macropores, undergo an important influence of gravity on the moisture content. Saturating them may become impossible.

From low to high moisture content, we have:

The ZERO POINT ($w = 0$).

For its definition: see 'Density'

The HYGROSCOPIC zone (w_R).

Most capillary- porous materials, show, depending on the pore system, a more or less pronounced hygroscopic behaviour, resulting in an equilibrium moisture content as function of the R.H.. On the moisture scale, this hygroscopic zone stretches from the zero point to a maximum hygroscopic moisture content, by definition the equilibrium value for a RH of 98%. In this hygroscopic zone, the materials show a moisture content hysteresis between wetting and drying (fig. 1.2). Hygroscopicity fixes the inside climate moisture content of a layer.

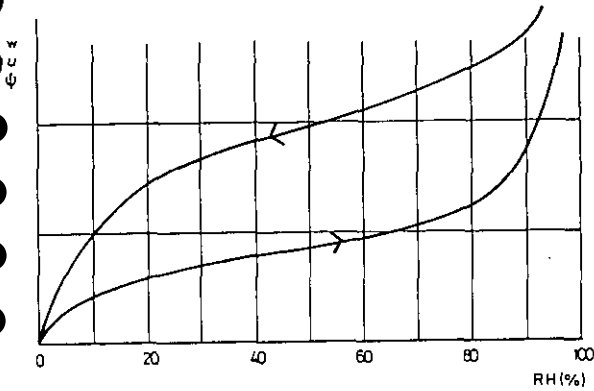


Figure 1.2: The hygroscopic hysteresis

The **CRITICAL** moisture zone (w_{cr}).

We call the critical moisture zone, that interval on the moisture scale, below which \pm only vapour transport occurs and above which vapour + water transport develops. On the microscale, the critical zone represents the lowest moisture content, showing continuous flow paths in the pore system. It plays an important role in drying phenomena and in interstitial condensation in or between capillary layers.

The **CAPILLARY** moisture content (w_c).

We call capillary moisture content, the value on the moisture scale, above which air-flow in and out the material becomes impossible. The capillary moisture content represents the highest value possible in capillary- porous materials, with no permanent water contact and the possibility of balanced wetting- drying. It is important in rain penetration, abundant surface condensation and interstitial condensation between a capillary and non-capillary layer.

The **SATURATION** or maximal moisture content (w_m).

All water open pores in the material are filled with water. Attaining saturation is only possible by vacuum- immersion. However, shifting on the moisture scale from capillary to maximal moisture content is inevitable, with capillary materials permanently in contact with water or having the possibility of unbalanced wetting- drying: wetting with little to no possibility of drying .

The interval between capillary and saturation moisture content also plays an important role in the frost resistance of the material: the smaller the interval, the greater the chance, in wet conditions, of frost damage.

H.1.2 DEGREE OF SATURATION (symbol: S/ unit:-)

We call degree of saturation, the ratio:

$$S = \frac{w}{w_m} \quad (1.14)$$

The degree of saturation uncouples to some extent the description of the moisture presence and the kind of material. It also facilitates the search for more general laws.

H.1.3 THE SPECIFIC MOISTURE CONTENT (symbol: c_w / unit:kg/m³)

We call specific moisture content the derivatives of the moisture content to the relative humidity or to the vapour pressure or to the suction potential.

H.2.1 VAPOUR PERMEABILITY, VAPOUR RESISTANCE FACTOR

(symbols: δ_p , δ_v , μ / units: s, m²/s, -)

As an exact definition of the vapour permeability, we have:

"The vapour permeability in a point of a material is the ratio between the 'density of vapour flow'- vector and the 'vapour pressure / vapour concentration gradient'-vector in that point"

For isotropic materials, both vectors coincide and the vapour permeability is a scalar. For anisotropic materials, they do not and the vapour permeability becomes a tensor, represented by a (3x3)-matrix.

The technical definition of the vapour permeability is coupled to the formula for the steady-state density of vapour flow through a flat, infinitely extended single layer wall:

$$g = \frac{\delta_p \cdot (p_1 - p_2)}{d} \quad \rightarrow \quad \delta_p = \frac{g \cdot d}{p_1 - p_2} \quad (1.15)$$

with $p_1 - p_2$: the vapour pressure difference over the layer

d : thickness of the layer.

The formula says:

"The vapour permeability of a material is the amount of vapour, flowing in steady-state, during 1 s, from one side of a cube of 1 m³ of the material to the other, the vapour pressure difference between both sides being 1 Pa, the other 4 sides being vapour tight"

To get δ_v , $p_1 - p_2$ must in formula (1.15) be replaced by $c_1 - c_2$.

The vapour resistance factor μ is given by the ratio between the vapour permeability of the material and the vapour permeability of stagnant air under identical thermodynamic conditions (same temperature, same pressure). For stagnant air, μ is by definition 1.

μ is a kind of one number description of the pore system and it's relation to the vapour transfer in and through the material.

If in a slab of dry material, all pores are straight on, have a constant section and are parallel to the thickness, the vapour resistance factor becomes:

$$\mu = \frac{1}{\psi_0} \quad (1.16)$$

with ψ_0 : the open porosity of the material.

If the pores are of constant section, straight on but inclined, μ turns to:

$$\mu = \frac{1}{\psi_0 \cdot \cos \alpha} \quad (1.17)$$

with α : the angle between pore and thickness direction.

If the pores are tortuous, of changing direction etc, μ looks like:

$$\mu = \frac{\psi_t}{\psi_0} \quad (1.18)$$

with ψ_t : the tortuosity factor.

Changes in tortuosity in macroscopically identical samples of the same material, have a direct impact on the μ -value. The result is a large scattering in measured values for the same material.

For hygroscopic materials, the diffusion resistance factor is a falling function of the R.H. in the material pores. Reason: the water filling pores, shortens the diffusion path, increasing water transfer.

Very open porous materials, such as mineral wool have a μ -value, close to 1. Materials with a high μ -value (i.e. a very low open porosity) are called vapour retarding or vapour tight. Thin foils or layers of such material are used as vapour retarders or vapour barriers.

H.2.2 VAPOUR DIFFUSION THICKNESS (symbol: μd / units:m)

We call diffusion thickness, the product μd , which is used instead of μ :

- for all material layers with a non constant thickness or a thickness difficult to measure;
- for composite thin layers, like many vapour barriers are;
- for composite layers, such as masonry work;
- to describe vapour transfer through layers with inevitable cracks, joints or an important sensitivity to workmanship. In this case, the property is called "equivalent diffusion thickness".

H.2.3 MOISTURE CONDUCTIVITY (symbol: k_m / units:s)

As exact definition of the moisture conductivity, we have:

"The moisture conductivity in a point of a material is the ratio between the 'density of moisture flow'- vector and the 'suction gradient'-vector in that point. Suction includes capillarity, gravity and external pressure"

For isotropic materials, both vectors coincide and the moisture conductivity is a scalar. For anisotropic materials, they do not and the moisture conductivity becomes a tensor, represented by a (3x3)-matrix.

The moisture conductivity is highly dependent on the suction potential, and through that on the moisture content, in the sense that k_m increases sharply with increasing moisture content. This is a direct consequence of:

- Poiseuille's law of water transfer in capillaries, stating that their water conductivity increases with the square of the diameter;
- the moisture behaviour of open porous materials, where, for low moisture contents, only the very small pores are water filled, while, with a rise in moisture content, wider and wider pores become water filled.

Lacking measured data, an estimation of k_m is possible with the formula:

$$k_m = D_w \cdot \frac{\partial w}{\partial s} = a \cdot \left(\frac{A}{w_c}\right)^2 \cdot \exp\left(\frac{b \cdot w}{w_c}\right) \cdot \frac{\partial w}{\partial s} \quad (1.19)$$

with a and b: material- dependent constants.

$\partial w / \partial s$: the specific moisture capacity.

As a mean value for porous building materials, a is taken 0.00674

b is taken 6.4.

H.2.4 THERMAL DIFFUSION COEFFICIENT (symbol: D_t / units:kg/(m².K.s))

We call thermal diffusion coefficient:

"The ratio, in a point of a material in isosuction conditions, between 'the density of moisture flow'- vector and the 'gradient of temperature'- vector in that point"

In isotropic materials, both vectors coincide and the thermal diffusion coefficient is a scalar. In anisotropic materials, they do not, and the thermal diffusion coefficient becomes a (3x3)-matrix tensor.

For capillary materials, the thermal influence on the moisture transfer is a direct consequence of the temperature dependence of surface tension and viscosity, and of the exponential relation 'saturation pressure- temperature'.

For hygroscopic, non- capillary materials, the thermal influence has its roots in hygroscopicity itself.

H.3.1 MOISTURE DIFFUSIVITY (symbol: D_w / units:m²/s)

The moisture diffusivity is given by the ratio:

$$D_w = \frac{k_m}{(\partial w / \partial s)} \quad (1.20)$$

$\partial w / \partial s$ being the specific moisture capacity.

Combining (1.20) and (1.19), we get as an estimate for the moisture diffusivity:

$$D_w = a \cdot \left(\frac{A}{w_c}\right)^2 \cdot \exp\left(\frac{b \cdot w}{w_c}\right) \quad (1.21)$$

The formula shows that the moisture diffusivity drops quickly with decreasing water absorption coefficient and increasing capillary moisture content:

MATERIAL	A kg/(m ² .s ^{1/2})	w _c kg/m ³	D _w m ² /s
bricks	0.5	300	1.7E-7 .exp(0.021.w)
concrete	0.02	100	2.7E-10 .exp(0.06.w)

H.3.2 WATER SORPTION COEFFICIENT (symbol:A/units: kg/(m².s^{1/2}))

In accordance to the thermal definition of effusivity,
we should call A the quantity:

$$A = \sqrt{k_m \cdot \frac{\partial w}{\partial s} = \frac{\partial w}{\partial s} \cdot \sqrt{D_w}} \quad (1.22)$$

In practice however, the definition of A remains restricted to a very specific moisture transfer situation: suction by a dry material in contact with a free water surface.

In a [m_c, t^{1/2}]- coordinate pair, the sucked water per unit of surface mostly appears as a straight line, the slope being the water sorption coefficient. So, instead of a moisture content dependent relation, only one value for A is taken as the water sorption coefficient.

AIR PROPERTIESA.1.1 AIR CONTENT (symbol: ψ_a / units: %m³/m³)

We call air content, the volume of air per unit volume of material.

The air content is a function of the water content:

$$\psi_a = \psi_o - \frac{w}{10} \quad (1.24)$$

In some closed cell porous materials, instead of air, another mixture of gasses may be present. If the pore system is not gas tight, a slow diffusion 'gas out-air in' takes place and time induced changes in property values can be observed (e.g. The increase in thermal conductivity of aging PUR and EPS- foam).

If interstitial condensation takes place in closed cell materials, which are not vapour tight, the pore air or gasses are slowly compressed, resulting in a swelling of the material. Especially in light PUR foam, this phenomenon may induce worrying dimensional changes.

A.2.1 AIR PERMEABILITY (symbol: k_a /units:s)

We call air permeability:

"The ratio, at a point of a material, between 'the density of air flow'- vector and the 'gradient of pressure'- vector in that point"

In isotropic materials, both vectors coincide and the air permeability is a scalar. In anisotropic materials, they do not and the air permeability becomes a (3x3)-matrix tensor.

As with the vapour conductivity and the vapour resistance factor, the air permeability is a 'poresystem'- parameter, combining information about the total porosity, mean path length, tortuosity and mean section of the pores.

For the same material, there is considerable scatter.

Non porous materials or closed pore materials have an air permeability 0.

A.2.2 AIR PERMEANCE (symbol: K_a /units:s/m)

The air permeance represents the ratio between the density of air flow through and the pressure difference over that layer.

The air permeance is used instead of the air permeability:

- for all materials/ layers with a variable thickness or a thickness difficult to measure;
- for layers, composed of different materials (brick work);

- to describe the air transfer through a layer or system with joints, inevitable cracks, highly sensitive to workmanship...

Measurements show that in most cases K_a can be represented by a function:

$$K_a = a.(\Delta p)^{-b} \quad (1.26)$$

with: $0 < b < 0.5$.

Δp = the pressure difference over the layer.

1.2 STANDARD LISTS

1.2.1 The concept "calculation value"

In most countries, standard lists with material data are available, giving the so called calculation values for some thermal and hygric properties. The motivations to implement, in spite of all inconvenience, these simple data sets and not to wait until everything is known, are:

- the need for data to calculate;
- the notion that indeed all properties depend on the different parameters, discussed above, that these influences may be very complex and interrelated, but that they are not experimentally verifiable over the whole range of their application;
- the fact that material parameters such as density, pore system, pore tortuosity always show a stochastic character, introducing for any material an inevitable scatter in the values for each property. This multiplies further the need for experimental validation until statistically meaningful sets of values have been collected;
- the unavoidable limitation in techniques of experimental validation possibilities, introducing a statistical uncertainty to distribution laws, mean values, standard deviation, 95%- limit...
- the correlation that may exist between measuring method and measured value;
- the limited accuracy of all measuring methods;
- the uncertainty about the time dependent values of temperature and moisture content, that the material will be submitted to, during its life span;
- the fact that, as far as a limited temperature interval is considered, temperature has only a limited influence on the property value;
- etc.

The methodology to arrive at calculation values is not always clear. Sometimes, a list, edited in the grey past, survives all changes in standards, in spite of new data being published, parameter influences being better known..etc. Other lists start from:

- if enough data for a material and property are available, a statistical analysis, proposing as the calculation value the 50% or 95% limit. It is not always clear what concepts of mean value, 95%-limit.. are used in these statistics: the harmonic one, the arithmetical one?
- the use of weight factors, correction terms, class concepts..., all implemented from the measured, so called laboratory data. Also here, the methodology must be handled with care and remain linked to reality. Using for example a correction to the measured thermal conductivity of an insulating material, to compensate for expected bad workmanship on site, may be wrong and give important errors in evaluating the thermal behaviour of the construction part in which the material is used.

In practice, lists of calculation values are useful in preliminary or simplified overall calculations. A more fundamental approach, as put forward in the next chapters, may ask not only for the calculation values but also for their relationships with the important influencing parameters. Searching for these relations, was one of the challenges of this part of the "Energy and condensation" annex work.

1.2.2 Examples of standard lists of calculation values

Given in the catalogue report are:

- Belgium: NBN B62-002 (ref.2);
- the Netherlands: the "stichting bouwresearch" list (ref.3);
- France: the CSTB document Règles Th- K77 (ref.4);
- Germany: DIN 4108 (ref.5);
- Italy: the "Talloncino di aggiornamento N°2 alla UNI 7357 (dic. 1974) (ref.6);
- United Kingdom: part of the standard BS: 5250 (ref.7).

The six lists are given in the national languages. For important remarks concerning units or the way parameter influences are handled, see the introduction to each list in the catalogue.

1.2.3 Discussion

- compared to the survey of 21 hygrothermal properties, all standard lists, except the Dutch SBR- report 17, remain very restrictive:

LIST	NUMBER OF PROPERTIES	WHICH
NBN B62-002 (B)	3	ρ, λ, R
SBR report 17 (NL)	10	$\rho, c, \lambda, e, \alpha, w_H$ $\delta_p, \mu, \epsilon, (E)$
Règles th-77 (F)	3	ρ, λ, R
DIN 4108 (FRG)	3	ρ, λ, μ
UNI 7357 (I)	2	ρ, λ
BS: 5250 (UK)	2	$r, +1/\delta_p$

- only two lists contain information on parameter influences, other than the density:

LIST	PARAMETER INFLUENCES
NBN B62-002 (B)	moisture content: i value for inside use, e value for outside use
SBR report 17 (NL)	id.

a remarkable difference in calculation value between the 6 lists can be seen for some commonly used materials:

MATERIAL	PROPERTY	VALUE					
		B	NL	F	FRG	I	UK
concrete 2400 to 2500 kg/m ³	λ_i	1.7	1.9	1.75	2.1	1.9	1.67
	λ_e	2.2	2.3				
glass 2500 kg/m ³	λ	1	0.8	1.15	0.8	1	1
cellular glass 120 to 200 kg/m ³	λ	0.045	0.05	0.05	0.045	0.055	0.063
		to	to	to	to		
		0.07	0.06	0.06	0.06		

1.2.4 Conclusion

Three conclusions may be drawn from the lists:

- five of the six give poor information on the totality of the hygrothermal properties of building, insulating and finishing materials;
- the lists, except two in a rather elementary way, give no information on the influence of the most important parameters;
- the calculation values given seem at least for some materials subject to discussion...

or, working on a catalogue does not seem to be a lost job!

1.3 EXPERIMENTAL METHODS

1.3.1 Aim

Aim of this paragraph is, not to give an extended description of all measuring methods, but to sketch very shortly the physical principles backing these commonly used.

1.3.2 Methods

DENSITY

Measured by

- weighing, after drying, a well defined volume of the material;
- applying Archimedes law in weighing an arbitrary volume of dry material, saturating it and weighing it again above and under water;

THERMAL PROPERTIES

T.1.1 SPECIFIC HEAT CAPACITY

Measured for a dry material with a calorimeter. The value for a wet material is calculated, using formula (1.1) (mixture law).

T.1.2 VOLUMETRIC HEAT CAPACITY

A calculated quantity.

T.2.1 THERMAL CONDUCTIVITY

Most measuring methods for the thermal conductivity go back to the steady-state flat monolayer theory. In the Poensgen and HFM- methods, a flat sample, thin compared to its sides, is mounted between a warm and a cold plate on different temperatures. Once the steady-state is reached, the heat flow through and the temperature difference over the sample are measured. Knowing the sample thickness d , the thermal conductivity follows from equation (1.3)

In a hot box-cold box apparatus, the same flat monolayer approach is used, with the sample mounted between a warm and cold chamber (air-sample-air).

More unusual, but applied, are non-steady-state methods, deriving the thermal conductivity from a measurement of the thermal diffusivity.

T.2.2 THERMAL RESISTANCE

See thermal conductivity.

T.3.1 THERMAL DIFFUSIVITY

Can be derived from a non-steady-state measurement in a HFM-apparatus using two samples between the hot and the cold plate, and measuring the contact temperatures samples - plates and sample - sample.

T.3.2 THERMAL EFFUSIVITY

A calculated quantity, e.g. coupled to a non-steady-state (measuring the diffusivity) and a steady-state (measuring the thermal conductivity) test in a HFM-apparatus, using the formula:

$$b = \frac{\lambda}{\sqrt{a}}$$

HYGRIC PROPERTIES

H.1.1 MOISTURE CONTENT

The different methods, used to measure or evaluate the moisture content of a material are:

- electrical, coupling the change in electrical resistivity or dielectric constant to the moisture content in the porous material. The problem with these electrical methods is that the change in resistivity or dielectric constant is not only coupled to the moisture but also to the salt content. Also, for each material, a calibration is needed;

- gravimetric, weighing the sample before and after drying;
- chemical, registering the change in pressure in a pressure bottle as a result of a water-carbide reaction, giving acetylene-gas;
- gamma ray intensity attenuation, based on the relation between the wet density and the gamma ray transmissivity of the material;
- MNR- scanning, measuring the change in H⁺-electron spin under a strong magnetic field.

Of these, the gravimetric procedure is the reference.

H.2.1 VAPOUR PERMEABILITY, VAPOUR RESISTANCE FACTOR, DIFFUSION THICKNESS

The dry and wet cup method is used to measure these properties: a sample of the material is mounted on a vapourtight cup, partly filled with distilled water, a saturated salt solution or a desiccant, held in a climatic chamber at constant temperature and relative humidity, and weighed every 2 days to every week. The result is, at first a non linear transient weight change, followed by a linear relation <weight increase or decrease, time>. From the slope of this line, the vapour permeability, vapour resistance factor or diffusion thickness can be calculated.

For complex systems such as masonry, roof coverings etc., the (equivalent) diffusion thickness is derived from an interstitial condensation test.

For finishing materials and isotropic, homogeneous hygroscopic building materials, the diffusion thickness may be derived from a time-logged hygroscopic moisture uptake, coupled to a small increase in RH.

H.2.3 MOISTURE CONDUCTIVITY

This requires the measurement of the suction curve and the moisture diffusivity. The suction curve can be calculated using the hygroscopic curve of the material and the results of pressure plate tests, sand-bed tests and mercury porosimetry. The moisture diffusivity follows from a space-time scanned change in moisture content during a 1-dimensional capillary uptake or drying test.

H.2.4 THERMAL DIFFUSION COEFFICIENT

This can be calculated from a space-time scanned moisture transfer test under a steady-state temperature difference.

H.3.1 MOISTURE DIFFUSIVITY

See moisture conductivity

H.3.2 WATER SORPTION COEFFICIENT

The water sorption coefficient results from a capillary suction test, scanning the weight increase as function of time. Redrawing the results in a $\langle q_m - t \rangle$ -curve (q_m in kg/m^2 ; t in s) normally gives a system of 2 straight lines, the slope of the first being the water sorption coefficient (fig.1.3).

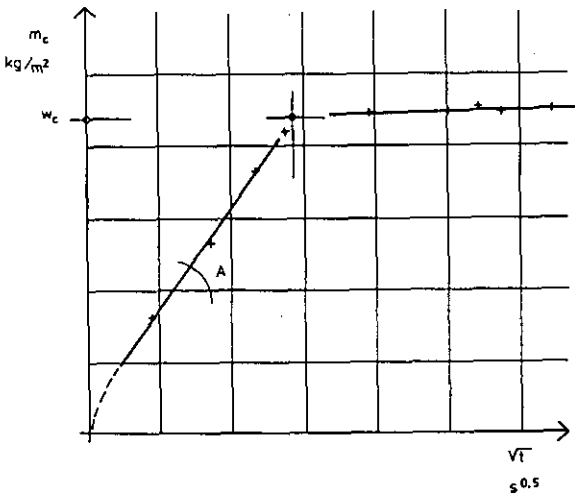


figure 1.3 The capillary suction test: $m_c (\sqrt{t})$ - representation

AIR PROPERTIES

A.1.1 AIR CONTENT

For most porous materials, the air content is given by the total porosity. This property is measured by vacuum saturation of the material.

A.2.1/ A.2.2 AIR PERMEABILITY, AIR PERMEANCE

Both properties are measured with a sample of the material or a layer fixed against an underpressure box, correlating the pressure difference with the airflow through the material or material layer. For air-open, porous materials, this correlation $\langle \text{airflow} - \text{pressure difference} \rangle$ is a straight line, the slope being proportional to the air permeability. For material layers, the correlation fits very well with an exponential function, the air permeance per m^2 being the derivative of this function.

1.3.3 Standards

The measurement of properties supposes conformity with and the use of standardised methods. Otherwise, tests could be performed with different parameter values, with non reliable techniques or with the implicit goal to use such a combination of influencing parameters, that the result obtained is as positive as possible. However, until now, national or/and international measuring method standards exist for only some material properties.

THERMAL CONDUCTIVITY, THERMAL RESISTANCE

In most countries, a standard is accepted for the guarded hot plate, the heat flow meter method and the guarded or calibrated hot box. In some countries also a non-steady-state method is standardised. Also ISO- standards exist:

COUNTRY	GHP	HFM	GHB	CHB	NSS
B	B62-201	B62-203	-	B62-204	B62-202
FRG	DIN 52612	-	-	-	-
I	UNI 7745	UNI 7891	-	-	-
NL	NEN 7043	-	-	-	-
UK	BS 874,2.1	-	BS 874,3.1	BS 874,3.2	-
ISO	DIS 8302	DIS 8301	DIS 8990	DIS 8990	-

GHP: guarded hot plate; HFM: heat flow meter; GHB: guarded hot box
CHB: calibrated hot box; NSS: non-steady-state

VAPOUR PERMEABILITY, VAPOUR RESISTANCE FACTOR, DIFFUSION THICKNESS

Only some countries have a standard, describing the dry cup- wet cup diffusion test. Also, an ISO- standard exist:

dry cup - wet cup		capillary suction	
COUNTRY	STANDARD	COUNTRY	STANDARD
B	-	B	B 05-201
FRG	DIN 52615	FRG	DIN 52617
I	-	I	-
NL	-	NL	-
UK	BSI DD146	UK	-
ISO	ISO/R1663	ISO	-

WATER SORPTION COEFFICIENT

Again, only some countries have a standard for the capillary suction test. No ISO- standard exist:

1.4 EXPERIMENTAL RESULTS

1.4.1 Materials and components tested

In the frame of Annex 14, properties have been measured of:

b: BUILDING MATERIALS

- b1 concrete
- b2 light-weight concrete
- b3 cellular concrete
- b4 polystyrene concrete
- b5 mortars
- b6 bricks
- b7 sand-lime stone
- b8 masonry: bricks
- b9 masonry: concrete blocks
- b10 masonry: sand-lime stone
- b11 masonry: cellular concrete
- b12 gypsum plaster
- b13 outside rendering
- b14 timber
- b15 particle board
- b16 plywood
- b17 woodwool-cement board
- b18 fibre-cement

i: INSULATING MATERIALS

- i1 cork
- i2 cellular glass
- i3 glass- wool
- i4 rockwool
- i5 expanded polystyrene
- i6 extruded polystyrene
- i7 polyurethane foam/ polyisocyanurate foam
- i8 perlite board

f: FINISHING MATERIALS

- f1 wallpaper
- f2 wallpaint
- f3 carpet
- f4 timber slabs

v: VAPOUR RETARDERS

c: COMPONENTS

- c1 gypsum board

o: OTHERS

- o1 newspaper
- o2 periodicals

1.4.2 Analysis of the data

As far as is possible and meaningful, all data for each material or material family have been related, by graphical, analytical and/or statistical means, to the influencing parameters.

Functional relationships used:

T.2.1 THERMAL CONDUCTIVITY

- density : linear or exponential
- temperature : linear
- moisture content : linear

H.1.1 MOISTURE CONTENT

- relative humidity (hygroscopic moisture content):
- the sorption and desorption curves have been fitted with a function

$$w_h = \frac{\phi}{A_1 \cdot \phi^2 + A_2 \cdot \phi + A_3}$$

H.2.1 DIFFUSION RESISTANCE NUMBER

- density: linear or exponential
- relative humidity: for most materials, except wood and wood linked ones:

$$\mu = \frac{1}{B_1 \cdot \phi^n + B_2}$$

For wood and the wood linked ones, an exponential relation is taken:

$$1/\mu = C_1 \cdot \exp(C_2 \cdot \phi)$$

H.3.1 MOISTURE DIFFUSIVITY

Is, as far as the water sorption coefficient and the capillary moisture content are known, calculated with the formula:

$$D_w = 0.006738 \cdot (A/w_c)^2 \cdot \exp(6.4 \cdot w/w_c)$$

ALL OTHER PROPERTIES

have only randomly been linked to one or another parameter (mostly the density)

All relations are, because of too few results or, too narrow limits of variation or, no variation of influencing parameters or, the guess of functional dependence, by definition incomplete. If more information becomes available, further refinements may be necessary.

1.4.3 Database

The results are summarized in the 'Catalogue of Material Properties'- database [2]. The database concerns 'measured values, without any correction for practice purposes'.

1.5 REFERENCES AND LITERATURE

1. Hens H., Kataloog van hygrothermische eigenschappen van bouw- en isolatiematerialen (Catalogue of hygrothermal properties of building and insulating materials), RD- Energie, Technisch Eindrapport 1.1, 1984
2. IEA-Annex 14, Condensation and Energy, Catalogue of Material Properties, Acco, Leuven, 1991
3. NBN B62-002, Berekening van warmtedoorgangscoefficienten van wanden van gebouwen/ Calcul des coefficients de transmission thermique des parois des bâtiments, BIN-IBN, 1986
4. Stichting bouwresearch, Rapport 9: Eigenschappen van Bouw- en Isolatiematerialen, 2e gewijzigde druk, Samson Uitgeverij, Alphen a.d.Rijn, 1974
5. DTU, Règles Th- K77, Cahiers du CSTB, cahier 1478, 1977
6. DIN 4108, Wärmeschutz im Hochbau, Wärme- und Feuchteschutz, technische Kenwerte, 1981
7. UNI 7357, Talloncino di aggiornamento n° 2
8. BS 5250, 'List of material properties'
9. NBN B62- 201, Bepaling in droge toestand van de thermische geleidbaarheid of van de thermische permeantie van de bouwmaterialen door de methode van de verwarmingsplaat met schutsring / Détermination à l'état sec de la conductivité thermique ou de la perméance thermique des matériaux de construction par la méthode de la plaque chauffante à anneau de garde, 1977
10. NBN B62-203, Bepaling van de thermische geleidbaarheid of de thermische permeantie van bouw- en isolatiematerialen met de methode van de warmtestroommeter/ détermination de la conductivité thermique ou de la perméance thermique des matériaux de construction et des matériaux isolants par la méthode du fluxmètre, 1977
11. NBN B62-204, Bepaling van de thermische geleidbaarheid van homogene bouwmaterialen met de parallelsonde/ Détermination de la conductivité thermique des matériaux de construction avec la sonde parallèle, 1977
12. NBN B62-204, Bepaling van de warmtetransmissiecoëfficiënt van bouwdelen/ Détermination du coefficient de transmission thermique des éléments de construction, 1979
13. DIN 52 611, Bestimmung des Wärmedurchlasswiderstandes von Wänden und Decken

- 14 DIN 52 612, Bestimmung der Wärmeleitfähigkeit mit dem Plattengerät
- 15 UNI 7745, Determinazione della conduttività termica con il metodo della piastra calda con anello di guardia
- 16 UNI 7891, Determinazione della conduttività termica con il metodo dei termoflussimetri
- 17 NEN 7043, Platen van hard Polystyreenschuim voor thermische isolatie. Eisen en beproevingsmethoden.
- 18 BS 874, Determining thermal insulation properties. Part 1. Introduction, definitions and principles of measurement. Part 2, section 2.1, Guarded hot plate method. Part 2, section 2.2, Guarded hot box method. Part 2, section 2.3, Calibrated hot box method., 1986- 1987.
- 19 ISO DIS 8302, Thermal insulation- Determination of steady-state areal thermal resistance and related properties- Guarded hot plate apparatus, 1987
- 20 ISO DIS 8301, Thermal insulation- Determination of steady-state areal thermal resistance and related properties- Heat flow meter method, 1987
- 21 ISO DIS 8990, Thermal insulation- Determination of steady-state thermal transmission properties- Calibrated and guarded hot box, 1987
- 22 DIN 52 615, Bestimmung der Wasserdampfdurchlässigkeit von Bau- und Dämmstoffen. Teil 1: Versuchsdurchführung und Versuchsauswertung, 1973
- 23 UNI 9233, Determinazione delle proprietà di trasmissione del vapore acqueo di materiali da costruzione ed isolanti termici, 1986
- 24 BSI DD146, Methods of test for water vapour transmission resistance of sheet materials used in buildings, 1986
- 25 (ISO R1663), Determination of vapour permeability of building and insulating materials, project
- 26 B 05-201, Proeven op bouwmaterialen: vorstbestendigheid, wateropsloppingsvermogen door capillariteit/ Essais des matériaux de construction: Gélivité, capacité d'impregnation d'eau par capillarité, 1976
- 27 DIN 52 617, Bestimmung der kapillaren Wasseraufnahme von Baustoffen und Beschichtungen. Versuchsdurchführung und Versuchsauswertung, 1979
- 28 Knapen M., Hygroskopisch vochtgehalte van bouwmaterialen, Kapillaire potentiaal in functie van het vochtgehalte, poriënverdeling in bouwmaterialen (Hygroscopic moisture content of building materials, suction potential as function of the moisture content, pore distribution in building materials), KU- Leuven 1987
- 29 Hansen K., Sorptionsisotermer. Programme- og brugerdokumentation for programmerne Dataind, Sorpf, Desorpf og Udtegn fra disketten Sorption, , Technical University of Denmark, Department of civil engineering, Building Materials Laboratory, Teknisk rapport 163/ 86

- 30 Hansen K, Sorption Isotherms, a catalogue. Technical University of Denmark, Department of civil engineering, Building Materials Laboratory, Teknisk rapport 162/ 86
- 31 Carpentier G., De hygrotermische eigenschappen van bouw- en isolatiematerialen en het grensgedrag in aanwezigheid van vocht (The hygrothermal properties of building and insulating materials and the limit state behaviour in the presence of moisture), tekst Kursus ' Termische Isolatie en Vochtproblemen in gebouwen', TI-KVIV, 1976-1985
- 32 CNR, Repertorio delle caratteristiche termofisiche dei componenti edilizi opachi e trasparenti, Roma, 1982
- 33 Ruscica G, Vaglio M., Sulla conduttività termica dei calcestruzzi alleggeriti, Condizionamento dell'aria, Riscaldamento, Refrigerazione, 1986/6
- 34 Ruscica G, Vaglio M., Vannelli G., Caratteristiche termiche di componenti edilizi, Condizionamento dell'aria, Riscaldamento, Refrigerazione, 1984/3
- 35 ISO/TC 163/ SC1 N 142 E, Thermal insulation- Moisture effects on heat transfer- Determination of hygrothermal transmissivity, 1988
- 36 ISO/TC 163/ SC 2 N 114 E, Design thermal properties of materials and products
- 37 CIBSE-GUIDE A3, Thermal properties of building structures, 1980
- 38 Prangnell R.D., The water vapour resistivity of building materials: A literature survey, Matériaux et Constructions, 1971/24
- 39 BDA dakboekje 1988 (Roof booklet 1988)
- 40 Rijksgebouwendienst, Rekenwaarden voor de warmtegeleidingscoëfficiënt van isolatiematerialen, Rapport 1209.03, 1209.06, 1985- 1986
- 41 PBNA, polytechnisch zakboekje, 39e druk
- 42 TU Delft, Bouwfysisch Tabellarium, 1987
- 43 Uyttenbroeck J., Carpentier G., Waterdampgeleidingscoëfficiënt en diffusieweerstandsgetal van bouwmaterialen, WTCB, 1982
- 44 Becker R., Katz A., Effect of moisture movement on tested thermal conductivity of moist materials, ASCE Journal on Building materials in Civil Engineering.
- 45 Bomberg M., Klarsfeld S., Semi empirical model of heat transfer in dry mineral fiber insulations, Journal of Thermal Insulation, 1983/6
- 46 KU- Leuven, Laboratorium Bouwfysica, Measuring reports, 1975-1990 All experimental data, gathered between 1975 and 1990 are compiled in a handwritten database and in Lotus 123 spreadsheet files. These files form the base of the catalogue.

Chapter 2

MOULD

Authors:

C. Hunter
BUILDING RESEARCH ESTABLISHMENT
Garston, Watford, United Kingdom

and

C. Sanders
BUILDING RESEARCH ESTABLISHMENT, Scottish Laboratory
Kelvin Road, East Kilbride, Glasgow G75 ORZ, United Kingdom

2.0 INTRODUCTION

As stipulated in the summary, condensation occurs when humid air is cooled below its dew point, depositing liquid water as a mist in the air or as a film of droplets on surfaces such as windows. Although the condensed water can in itself be a nuisance at times, the most significant cause of distress to occupants is, with high relative humidities, the promotion of the germination and growth of moulds on wall surfaces and on furnishing or clothing. Surfaces are disfigured causing psychological distress to the occupants as the house appears 'dirty'; unpleasant 'musty' odours are noticed; questions are raised as to health hazards from spores released by the moulds.

The moulds that grow in houses are normally members of the Deuteromycetes subgroup of fungi, one of the major divisions of the natural world. To establish limiting conditions for growth and identify successful control strategies, we need to understand the basic biology of the organisms. As hundreds of thousands of different species of fungi are known to exist, this could be an almost impossible task. However the more important groups that occur in housing are represented by only a few tens of species on which research has been concentrated.

A number of conditions have to be met for the successful germination and growth of moulds:

- Fungal spores must be present
- Oxygen
- Suitable temperatures
- A nutrient substrate
- Water

The first four of these are readily available in housing; spores are always available from the outdoor air; oxygen is obviously present; temperatures between 10 and 30°C, typical 'room' temperatures, are suitable for mould growth; even the cleanest house has an adequate nutrient supply. The key factor therefore is the presence or absence of available water.

This chapter summarises the relevant microbiology of the fungi and discusses the important species, the conditions for their growth and possible control strategies in the light of recent research. In recent years three aspects have received particular attention:

1. The traditional view that actual condensation, with the deposition of liquid water, has to occur to promote mould growth has been shown to be untrue.

The concept of water activity (a_w) of surfaces has been introduced by microbiologists to quantify the water available to the organisms. It can in steady-state conditions be thought of as the relative humidity at the surface divided by 100.

Experiments have shown that important moulds can germinate and grow at water activities significantly below one, as low as 0.8 in some cases. This obviously imposes a more stringent constraint on internal climates than the need to avoid saturation at the surface.

2. It has become apparent that great care must be taken when aerial sampling is carried out, to obtain spore counts representative of long term conditions within the house. In fact it appears that at any moment in time the number and type of spores in the air depend as much, if not more, on the degree of activity in the rooms, than on the amount of mould growth on the walls. It is unlikely that a single visit will produce representative

data; repeated visits with careful note being taken of household characteristics and recent activities are essential.

- Increasing concern is being expressed as to the health problems that may result from long term exposure to moulds. Except in the case of atopic individuals, who are unusually sensitive to allergies, there is little definite evidence linking mould growth to specific health problems. However, it is certainly right to accept that the widespread growth of moulds on the interior surfaces of our houses is unacceptable in today's world.

2.1 MICROBIOLOGY OF MOULDS

Moulds are characterised by a distinctive, filamentous vegetative structure known as the mycelium. This consists of a branching system of walled tubes, the hyphae, which extend by apical growth and lateral branching; growing over the substrate from which they extract nourishment. After a period of growth, reproduction occurs with the formation of spores, uni- or multi-cellular bodies that become detached from the parent and give rise to new individuals.

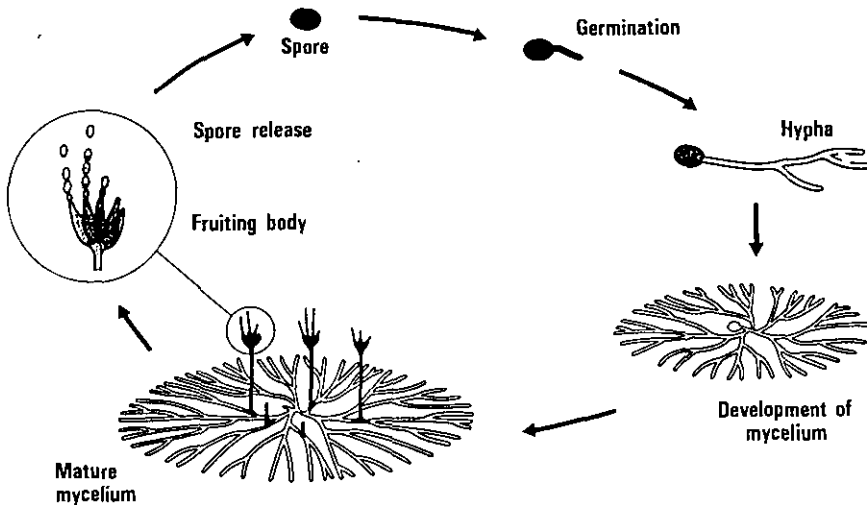


Figure 2.1: The live cycle of a mould fungus

Mould spores are liberated from the parent either passively with the required energy provided by an external source such as wind or by active discharge with the necessary energy provided by the organism [55].

Numerically, fungal spores commonly dominate the air spora, probably outnumbering pollen and bacteria. This predominance is related to several factors which many fungi exhibit, primarily their enormous spore production. A colony of Penicillium, 2.5 cm in diameter, may bear 4×10^9 conidia [55] and sporulation of Cladosporium cladosporioides is estimated to reach 2.5×10^4 spores mg^{-1} dry mycelium under moist conditions [47]. Other important factors are the ability of spores to retain the power to germinate over a wide range of temperatures, relative humidities and light energies, to resist dessication and the ease of spore liberation.

Moulds are present at all times out of doors on dead and decaying organic matter and in the soil. However Gregory [44] considered that the majority of outdoor airborne spores originate from vegetation above ground level. Typically levels of mould spores outdoors during summer are 50000 m^{-3} of air. While the numbers decline during the winter to several hundred m^{-3} [54] because of the normal air exchange between outdoors and indoors, for example through open doors and windows, a source of mould spores is always present in the air of all dwellings. Spores which have settled on to surfaces, along with dust particles, can be resuspended via household activity and also the popularity of houseplants especially in countries like The Netherlands has produced a possible source of infection indoors.

REQUIREMENTS FOR GROWTH

Apart from a source of spores, which as mentioned previously are always present in the air, the main requirements for the growth of moulds are:

- Oxygen
- Suitable temperature
- Nutrients
- Moisture

Oxygen

Most filamentous fungi are obligate aerobes, i.e. they are unable to grow in the complete absence of oxygen, although a very minute amount is often sufficient. For example Pencillium roqueforti can grow at an oxygen concentration of less than 0.14% [72]. Certainly the oxygen level at nearly all surfaces in dwellings is sufficient to permit the growth of moulds.

Temperature requirements

In general, moulds can exist over a very wide range of temperatures. Individual moulds obviously have an optimum temperature range which assists in broadly classifying moulds according to their temperature requirements - psychophilic, mesophilic and thermophilic. For practical purposes, while growth of moulds is retarded by sub-optimal temperatures, they will tolerate temperatures likely to be encountered at wall surfaces during the winter in problem dwellings.

Nutrients

Due to their lack of chlorophyll, fungi cannot carry out the complex process of photosynthesis and hence they obtain their food either as saprophytes or parasites. Their ability to utilise a wide range of carbon compounds is remarkable. Normally in nature, the organic material in the substrate would usually furnish the nitrogen for growth of fungi. However, most imperfect fungi are able to utilise inorganic nitrogen in the form of nitrates or ammonium as sources of nitrogen. Similarly naturally occurring organic compounds often furnish all the inorganic salts necessary for growth. The level of these nutrients required is minimal and perfectly well satisfied by normal levels of dust and other deposits even in well cleaned and maintained homes. This is also the reason why moulds often occur on materials containing no organic substances, such as stone, mortars and plasters [20].

Moisture

The availability of sufficient moisture is probably the most important criterion for mould growth. The mycelium presents a relatively large surface area per unit volume which permits rapid absorption of nutrients and water under favourable conditions but is very susceptible to adverse environmental pressure.

Absorption of moisture from the environment occurs chiefly via osmosis (passive transport) but the cell can also take up water and other molecules against a diffusion gradient (active transport) using enzymes in the cell membrane at the expenditure of a large amount of energy. A mould can also absorb water molecules from the atmosphere in this manner, if the relative humidity is sufficiently high. Beside absorbing water from the surrounding environment, the cell also produces water itself via energy-metabolism, for example the breakdown of carbohydrates and fats releases water [2].

2.2 SAMPLING TECHNIQUES

2.2.1 Air sampling

The basic strategy of air sampling is to collect micro-organisms, by optimum means, and demonstrate their presence by appropriate methods. This has resulted in a large number of devices being produced as discussed by Davis [32], Gregory [44], Chatigny et al. [27] and Beaumont [10] among others. The various methods can be divided into three groups:

- non viable spore samplers
- viable samplers
- immunological analysis.

Immunological detection is a fairly new technique which is rather expensive, requiring sophisticated laboratory apparatus. However, it is probably of use in determining which particular mould species induces allergy in mould sensitive asthmatics. Non viable sampling relies upon the presence of distinct characteristics on the spores enabling detection among the background inorganic particles. Aspergillus, Penicillium and other small spored genera are virtually indistinguishable using this method from background dust particles. Because these genera tend to predominate indoors (see 2.3), sampling for viable micro-organisms is the best means of determining the level and range of moulds present in the air of dwellings.

The oldest and most common viable sampling technique is the "Settle Plate" method which may be considered a useful technique for giving a semi-quantitative impression of moulds indoors [112] but is no longer the method of choice for detailed analysis [23,106]. Most other sampling devices draw a known volume of air through an orifice by means of a vacuum pump, accelerating the air to a

point where spores are impacted onto an agar surface or into liquid. The major drawback of this method is that it relies on short sampling periods, therefore the duration time and location of sampling are all important in determining the final result and should be carefully selected to obtain representative spore counts. This has been demonstrated by Hunter et al. [54] during extensive studies in the UK which revealed that while spot air samples, i.e. single visits to dwellings, provide some information, this is only of limited value in building up a comprehensive picture of the domestic air spora which requires sequential sampling over several weeks.

The actual length of the sampling period varies from house to house depending upon the conditions: in dry clean houses the sample time will be longer than in damp mouldy homes, sample periods of up to a few minutes are commonly used. Of course the duration of sampling will also depend on the selected apparatus.

Verhoeff et al. [112] noted a difference between samples taken in the morning and afternoon, and it is recommended that sampling in individual dwellings should be carried out at approximately the same time each week. The number of spores collected at different heights within a room can also differ [95], therefore the level of the sampler should be held constant over the sampling programme, a convenient table or box can be used as a support.

In a comprehensive comparison of air samplers and culture media [112] it was found that malt extract agar (MXA) and dichloran glycerol 18 agar (DG-18) gave the highest yield in terms of numbers and range of moulds isolated. MXA is widely used in aerobiological studies, [10,14,15,25,54,68,112] allowing comparisons to be made, and for this reason and its apparent usefulness as a broad spectrum collection media, the use of MXA is recommended.

As will be discussed in Section 2.3 it appears that the number of spores in the atmosphere depends upon the level of activity in the room as well as the extent of mould on the walls. Therefore careful records must be kept of the usage of the room, number of occupants, state of cleanliness, number and type of pets and houseplants etc to help understand and explain level of counts and any variations.

2.2.2 Surface sampling

Sampling of surface mould growth is normally achieved by rubbing sterile cotton buds or culture swabs over a specified area [54,68]. The spores are resuspended in a suitable dilutant and aliquots plated out onto media (for example MXA) from a subsequently prepared serial dilution. Pressing adhesive tape [2,68] or specialised agar plates [83] against the wall surface has also been used to demonstrate mould growth on wall surfaces. The resultant colonies on agar will usually be a mixed population of micro-organisms, which require subculturing on to fresh agar to provide pure cultures for identification.

Microscopic examination of the adhesive tapes for fungal hyphae or hyphal fragments will give an indication of whether or not the mould is growing. However confirmation by the use of swabbing and culturing spores on agar is needed to ensure that hyphae were not missed (because of the small sample area of adhesive tape) or that the mould was growing beneath the surface.

2.2.3 Identification

Identification of fungi is normally based upon the spores only or upon sporing structure. To initiate sporulation some may require incubation under near UV light ('blacklight', emission about 310 nm), while others require diffuse daylight and the majority can grow and sporulate under complete darkness.

Appendix 2.a gives details of the manuals used by Lombardi et al. [68] and Verhoeff et al. [112] for the identification of moulds. However there is a wide range of suitable manuals and monographs available such as Onions et al. [84]. Comparison of isolates with isolates obtained from natural culture collections can also help with identification.

2.3 IMPORTANT SPECIES IN HOUSING

2.3.1 Mould spore levels in dwellings

Although levels of spores approaching 450 000 colony forming units (cfu) m⁻³ have been reported in the domestic atmosphere [54], the levels normally recorded have been much lower. Maxima's of approximately 6000 have been reported by

several authors [60,61,76,104], while others have recorded levels of between 13000 and 20000 spores m^{-3} [12,17,52,105,112]. However Hunter et al. [54] also noted counts in several dwellings of approximately 20 000-116 000 indicating that large numbers of spores may be present in the air at certain times. These indoor levels of airborne spores can be seen in perspective when compared with levels obtainable in the work environment. Kolmodin-Hedman et al. [57] recorded 10^6 cfu m^{-3} in the basement of a museum where mouldy books were stored, while both Lacey [63] and Ström and Blomquist [108] found the concentration of spores in factories where mouldy products were being handled sometimes exceeded 10^8 m^{-3} . Also outdoors during the summertime counts of >30 000 spores were frequently recorded [66] and up to 100 000 Cladosporium spores m^{-3} in the UK are possible [45].

While the air spora indoors is often considered to be a reflection of that outdoors (but at a reduced level) during the spring to autumn period [1,67], the airborne spore count within dwellings during the winter is normally greater than outdoors [11,12,54,79,105]

For example Solomon [104] reported counts from >10 to 20 000 in homes in the midwestern states of America while the outside counts never exceeded 230 cfu m^{-3} . The counts outdoors in Canada were reported to be negligible whilst those indoors were >1000 cfu m^{-3} [79].

The wide variation observed in the numbers of spores in the indoor atmosphere (Figs 2.2 and 2.3), both between and within individual dwellings [54,68,112] indicates little can be deduced from single air samples. Verhoeff et al. [112] found that even plates from successive samples showed a degree of variation in the number of colonies appearing, but this might have been due to the short sampling time. This variation can also be attributable to the extent of visible mould growth and to the nature and extent of any disturbances in the dwelling. Routine monitoring of dwellings in the UK revealed that there was an increased chance of the spore concentration exceeding 5000 m^{-3} when there was mould growth on any surface in the room in which the air sample was collected [54]. Holmberg [52] earlier reported that spore counts during still periods in "mould-free" dwellings were 6 to 2200 spores m^{-3} , whilst totals of 10 000 to 15 000 were likely where there was surface mould growth.

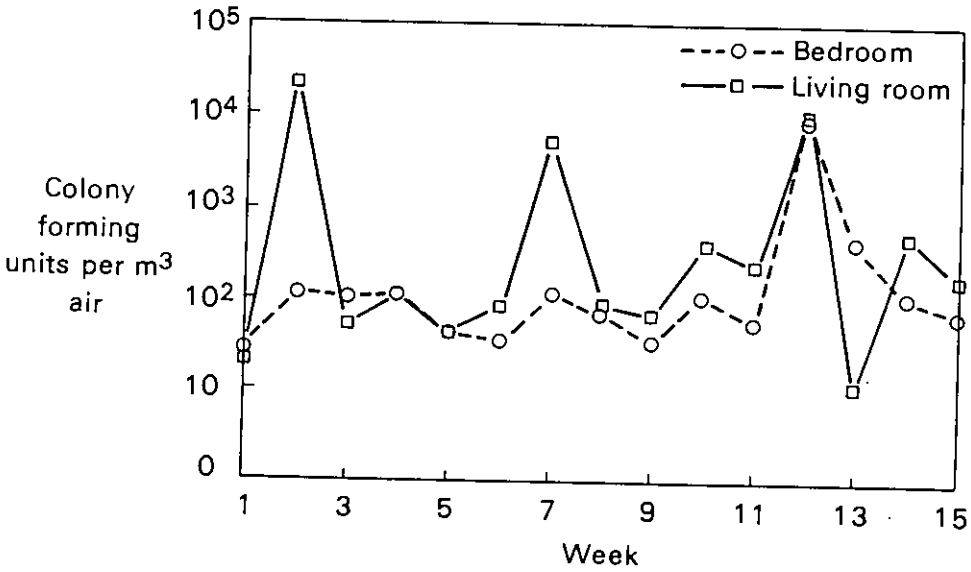
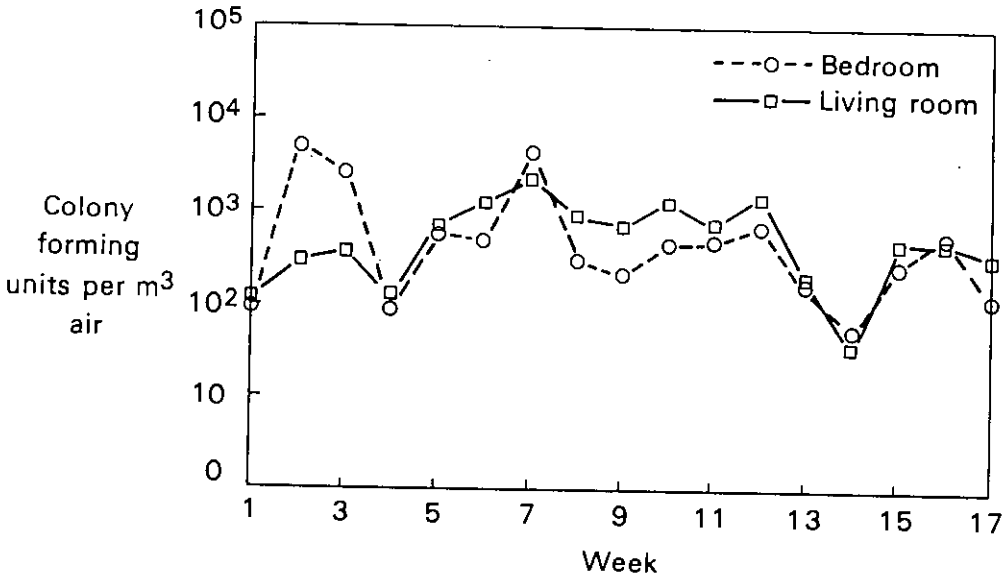


Figure 2.2 and 2.3

Number of colony-forming units in air samples taken weekly in two dwellings (after Hunter et al)

Large temporal fluctuations in concentration can occur, for example, when furniture is moved or a vacuum cleaner is used. Swaebly and Christensen [109] and Maunsell [75] demonstrated that dust-raising activities such as shaking bedding and sweeping carpets or floors could increase counts on settle plates up to 14-fold. Some measurements have also been made on the extent and duration of spore release following physical disturbance by hand brushing of an area of mixed mould growth [54]. Counts 0.3 m from the wall increased by a factor of approximately 400 to nearly 900 000 cfu m⁻³ immediately after brushing. Away from the wall the maximum count was recorded after five minutes and was less than one-fifth of that at 0.3 m. Subsequently the counts at both sampling points decreased with time but even after 90 minutes levels were still very high. Physical dislodgment of spores, for example by cleaning or occupants accidentally brushing against surfaces, would therefore appear to have an important role in distributing spores and boosting the count in the atmosphere.

Examination of data from 26 published aerobiological surveys of the indoor air, mainly from Europe and North America (Table 2.1) revealed that Penicillium, Aspergillus and Cladosporium were isolated in the most number of surveys. Fungi in the genera Penicillium and Aspergillus are generally held to be particularly characteristic of the indoor air spora [1,13,104].

This was also reflected in the recent studies [54,68,112], whose work has been submitted to IEA, where 36 Penicillium species were identified, the largest number of species assigned to one genus, 15 species of Aspergillus were recorded (including Eurotium spp. now considered synonyms of Aspergillus) [8]. However only Aspergillus versicolor and four penicillia (P.brevicompectum, P.chrysogenum, P.corylophilum and P.nigricans) were recorded by all three groups.

Apart from the previously mentioned aspergilli and penicillia only six species were recorded from air samples by the three groups, these were: Acremonium strictum, Alternaria alternata, Aureobasidium pullulans, Cladosporium cladosporioides, C.sphaerospermum and Stachybotrys atra.

Table 2.1: FREQUENCY OF OCCURRENCE OF COMMON MOULDS IN AIR SAMPLES TAKEN FROM 26 PUBLISHED STUDIES

	(%)		(%)
Penicillium	100	Geotrichum	38
Aspergillus	92	Helminthosporium	38
Cladosporium	92	Monilia	35
Alternaria	85	Scopulariopsis	35
Aureobasidium	81	Stemphylium	31
Fusarium	73	Verticillium	31
Mucor	69	Curvularia	27
Phoma	65	Nigrospora	27
Epicoccum	62	Stachybotrys	27
Rhizopus	58	Torula	27
Trichoderma	50	Trichothecium	27
Botrytis	46	Gliocladium	23
Acremonium	42	Oospora	19
Paecilomyces	42	Ulocladium	19
Chaetomium	38		

Data derived from: Ackermann et al. (1969); Burge et al. (1980); Chen & Chuang (1975); Fergusson et al. (1984); Flensburg & Samsøe Jensen (1950); Fradkin et al. (1987); Gravesen (1972); Hirsch & Sosman (1976); Hunter et al. (1988); Kozak et al. (1980); Levetin & Hurewitz (1978); Lombardi et al. (1988); Lumpkins & Corbit (1976); Lumpkins et al. (1973); Maunsell (1952); Popescu & Capetti (1971); Richards (1954); Ripe (1962); Rogers (1983); Schaffer et al. (1953); Sneller & Roby (1979); Solomon (1975); Van der Werff (1958); Verhoeff et al. (1988); Wallace et al. (1988); Wallace et al. (1950); Wray & O'Steen (1975).

Table 2.2: FREQUENCY OF OCCURRENCE OF COMMON MOULDS ON WALL SURFACES TAKEN FROM 14 PUBLISHED STUDIES

	(%)		(%)
Aspergillus	93	Phoma	36
Penicillium	85	Ulocladium	36
Cladosporium	71	Acremonium	29
Aureobasidium	64	Paecilomyces	29
Alternaria	57	Stachybotrys	29
Scopulariopsis	43	Fusarium	21
Mucor	36		

Data derived from: Adan & Weersink (1988); Barry (1978); Burr et al. (1988); Erhorn (1988); Fergusson et al. (1984); Hirsch & Sosman (1976); Hunter et al. (1988); Kozak et al. (1980); Lombardi et al. (1988); Miller & Holland (1981); Richards (1954); Senave (1988a); Van der Werff (1958); Wray & O'Steen (1975).

2.3.2 Prevalence of moulds on surfaces

Aspergillus, Penicillium and Cladosporium were again the most commonly isolated genera in surveys of indoor surfaces (Table 2.2) and samples of house dust. (Table 2.3). The general trend in the frequency of occurrence of the other fungal genera on surfaces was also similar to that from air samples (Table 2.1).

As occurred with data provided from air samples by IEA Annex XIV participants

A.versicolor, P.brevicompactum and P.chrysogenum were again the most common aspergilli and penicillia from surface samples taken in Belgium [100], Italy [68], The Netherlands [2], Germany [35] and the UK [54].

Cladosporium species were isolated from surfaces in four countries and found in dust samples in the fifth (The Netherlands). Most species of Aspergillus and Penicillium are considered to be xerophilic, i.e. capable of growth at an a_w of 0.85 or below [88], and species of Cladosporium can also grow at levels below 0.85 [41]. Another xerophile, Wallemia was predominant in samples taken by Adan and Weersink [2]. This may explain why these genera are frequently isolated from dwellings.

A relationship between the occurrence of a fungus on a mouldy surface and its appearance on sample plates was observed by Lombardi et al. [68]. They identified Cladosporium sphaerospermum from mouldy wallpaper and paint which comprised >85% of the cfu's identified, while on settle plates the species accounted for 67% of colonies. This was also noted by Hunter et al. [54]; when Stachybotrys atra was predominant in mould growths it occurred in 86% of the air samples and spore counts up to 17 900 of this species were recorded. Senave [100] isolated a larger number of species from wallpapered (13 species) than from painted surfaces (8) and the frequency of occurrence was higher (Table 2.4), although samples were taken from different rooms and therefore conditions to which the mould growth was exposed would differ. In contrast Lombardi et al. [68] in the same room found 12782 cfu from a painted surface but only 96 from a similar area of "mouldy" wallpaper. This they suggested was the result of the differing nutrient sources. However C.sphaerospermum was the dominant organism at both sites and one must assume that other physiochemical factors on the painted surface were also more amenable to growth of micro-organisms.

Colonisation of a surface is dynamic, responding to and being influenced by the immediate environmental conditions; during the early part of the winter when the surface was still relatively dry Grant et al. [41] reported xerophilic organisms

Table 2.3: FREQUENCY OF OCCURRENCE OF COMMON MOULDS IN DUST SAMPLES TAKEN FROM 6 PUBLISHED STUDIES

	(%)		(%)
Aspergillus	83	Alternaria	50
Cladosporium	83	Mucor	50
Penicillium	83	Rhizopus	50
Aureobasidium	50	Trichoderma	50

Data derived from: Adan & Weersink (1988); Gravesen (1978); Schaffer et al. (1953); Van der Werff (1958); Wallace et al. (1950); Wray & O'Steen (1975).

Table 2.4: THE FREQUENCY OF OCCURRENCE OF MOULD SPECIES ISOLATED FROM WALLS IN FOUR DWELLINGS (after [99])

	(a) On wallpapered surfaces (%)	(b) On painted surfaces (%)
<u>Alternaria alternata</u>	50	-
<u>Aspergillus fumigatus</u>	75	25
<u>A.niger</u>	25	-
<u>Aureobasidium pullulans</u>	-	25
<u>Cladosporium cladosporioides</u>	50	75
<u>C.herbarum</u>	50	-
<u>Geotrichum candidum</u>	25	25
<u>Mucor sp.</u>	75	25
<u>Paecilomyces variotii</u>	25	-
<u>Penicillium brevicompactum</u>	50	-
<u>P.cyclopium</u>	75	25
<u>P.funiculosum</u>	75	-
<u>Scopulariopsis brevicaulis</u>	25	25
<u>Ulocladium consortiale</u>	75	75

(Penicillium spp. and Aspergillus versicolor) were predominant but as the winter progressed and conditions became very wet Ulocladium and Stachybotrys atra were dominant.

Other authors suggest that decay increases the water availability to moulds [34] or that "conditioning" of the surface by moulds has to occur prior to colonisation by perhaps more demanding species [87,118]

2.4 LIMITING CONDITIONS FOR GROWTH

Although the factors influencing growth are discussed separately, rarely (if ever) do they act independently and are also subject to fluctuation. The reader should bear in mind that along with other factors not discussed such as pH or competitive effects of other moulds they will influence the effect each factor exerts on the colonisation of surfaces by moulds.

2.4.1 Temperature

Below 0°C, fungal cells may survive but rarely grow, and above 40°C most cells stop growing and soon die, but between these temperatures fungal activities increase and decrease [33] probably due to the effect of temperature on enzymes involved in growth. While most moulds have minimal temperatures of 0-5°C, some isolated from domestic dwellings (such as Cladosporium herbarum and Penicillium expansum) can grow readily on meat at freezing point and even a few degrees below [21] and a yeast has been reported as growing at -34°C [53]. Six mould species selected because they were commonly isolated from air and surface samples of dwellings grew to a certain extent at 5°C on agar, emulsion painted wallpaper and emulsion painted plaster [41]. Senave [99] reported that Penicillium cyclopium was able to grow at 30°C on all nine combinations of plaster and surface finishes examined. The reaction of various species to temperature has also been examined by Waubke and Wallnöfer [115].

2.4.2 Water activity of the surface

The susceptibility of different substrates in dwellings to mould mainly depends upon the water activity (a_w) in the particular substrate. Water activity is a measure of the availability of water to micro-organisms and is determined from the ratio of the vapour pressure of the water in the substrate to that of pure water at the same temperature and pressure. This ratio is in steady-state conditions numerically equal to the equilibrium relative humidity (ERH) of the air except that the latter is commonly expressed as a percentage. When a substrate is placed in an atmosphere of fixed RH it will absorb and/or lose moisture until it comes into equilibrium with the atmosphere. At this point the water activity of the substrate is the same as that of the controlling solution producing the atmosphere.

Much work has been done on determining the minimum a_w for germination, growth and sporulation of moulds on artificial media (Table 2.5). From published data it can be seen that germination of fungal species occurs at an a_w below that to sustain linear growth and likewise the minimum a_w value for sporulation of a particular species is often higher than that required for linear growth.

Table 2.5: MINIMUM WATER ACTIVITIES NOTED IN THE LITERATURE

	(a) germination	(b) growth	(c) sporulation
<i>Alternaria alternata</i>	0.85(H,J)	0.85(M);0.88(H)	0.90(H,M)
<i>Aspergillus versicolor</i>	0.74(N);0.75(J) 0.76(H)	0.75(M);0.78(C,H)	0.80(H,M)
<i>Cladosporium cladosporioides</i>	0.85(E,K);0.86(H) 0.90(D)	0.88(H)	0.90(H)
<i>Mucor plumbeus</i>	0.93(O)	0.93(C,M)	0.93(M)
<i>Penicillium brevicompactum</i>	0.78(G);0.80(H) 0.81(K)	0.81(C);0.82(H)	0.85(H)
<i>Penicillium chrysogenum</i>	0.79(A);0.78(G) 0.81(F,I);0.84(L)	0.79(C);0.85(L)	0.86(M)
<i>Stachybotrys atra</i>	0.85(B);0.90(D)	0.94(B,C)	0.96(J)

KEY:	A Armolik & Dickson (1965)	I Mislivec & Tuite (1970)
	B Ayerst (1969)	J Panasenko (1967)
	C Christian (1980)	K Pelhate (1968)
	D Galloway (1934)	L Pitt & Christian (1968)
	E Grant et al. (1989)	M Reiss (1986)
	F Groom & Panissett (1933)	N Smith & Hill (1982)
	G Hocking & Pitt (1979)	O Snow (1949)
	H Magan & Lacey (1984)	

Studies have also been carried out on the a_w requirements of moulds isolated from the air and surfaces of domestic dwellings [41,49,99] using different substrates, chosen to be representative of those found in dwellings. These substrates were inoculated with spores of various moulds either as a pure culture [41] or as a mixed population [49,99] and incubated over saturated salt solutions known to maintain constant RH, in the case of Herbak [49] the RH was controlled mechanically. Senave [99] found that mould growth was not seen on any samples cultured at 86% RH over a ten week period. At higher RH the rate of

appearance of mould on the substrates was related to the RH, i.e. mould was noted after five weeks at 92% but after only two weeks at 99% RH. The appearance of mould was also influenced by the hygroscopic nature of the finish and nutritional status. Examining the growth of selected fungi on woodchip wallpaper at a temperature considered representative of wall surfaces in problem dwellings during the winter (12°C), Grant et al. [41] noted the a_w minimum for the most xerotolerant species examined (Aspergillus versicolor and Penicillium chrysogenum) to be 0.83. This was also observed by Herbak [49], who reported that the minimum RH for growth was 83% (the lowest RH examined). Herbak [49] introduced the concept of a "mean growth factor" (MGF) that combined the proportion of replicates covered and the degree of development of the moulds. The average MGF over six substrates examined were 1.1% at 83% RH, 2.2% at 90% RH and 16.7% at 97% RH.

Over a range of temperatures between 5-25°C, Grant et al. [41] also noted a general trend of increasing temperatures permitting growth at lower a_w (Fig 2.4). Others [64,73,80,101,110] have also noted this phenomenon, namely that at temperatures distant from optimum conditions the range of water activities permitting germination and growth is reduced.

Although there are differences in the minimum a_w for growth between the information derived [41,49,99] (which may be a result of cultural conditions, isolates or nutrient availability) it appears that susceptible surfaces are in danger of developing mould growth if their surface a_w rises above 0.80. This has to be for a sustained period as it takes several days for spore germination to occur.

2.4.3 Air humidity

The air humidity of a dwelling depends not only, by outside air ventilation, on the outside humidity, but also on the moisture production as a result of normal family life. It has been estimated that a family of four during a 24 hour period releases some 7- 14 litres of water into the air as a result of breathing, cooking, bathing and washing and drying of clothes indoors [22]. Hence the air humidity will fluctuate throughout the day and this will be reflected in the surface humidity (or water availability), not only at the site of production but also in other rooms.

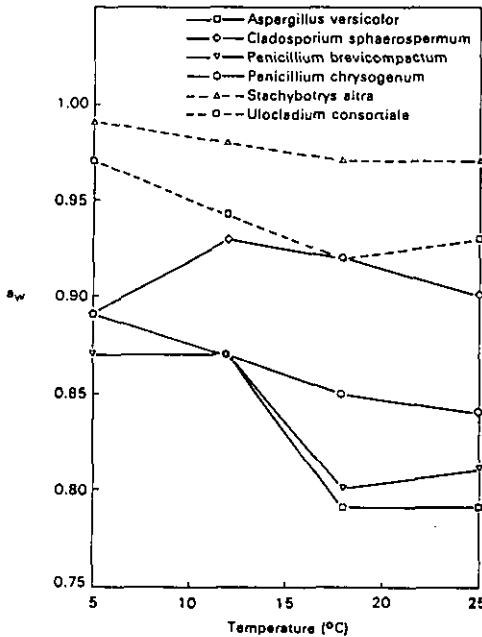


Figure 2.4 Effect of temperature on minimum a_w for growth on woodchip paper (after Grant et al, 1989)

2.4.4. Nutrient availability and substrate

Both Senave [99] and Grant et al [41] have shown that the availability of nutrients plays an important part in the ability of moulds to colonise a surface at reduced a_w [41,99]. On woodchip wallpaper, in general, the addition of a carbon source in the form of carboxymethyl cellulose (CMC) or emulsion paint caused a reduction in the minimum a_w required for growth of moulds tested [41]. Indeed under the most optimum conditions when both emulsion paint and CMC were available to the fungus, the minimum a_w for growth of *Aspergillus versicolor* and certain penicillia was the same as that reported on agar. Senave [99] noted that wallpaper and wood fibre paper are most susceptible to mould growth, whereas mould growth only occurred freely on vinyl paper at 99% RH.

The incorporation of polyvinyl acetate into plaster can encourage mould growth by acting as a nutrient source [82], by increasing the capillar condensation within the plaster and the rate of carbonation of the plaster. The extent of carbonation of plaster also influences any mould growth on subsequently applied wallpaper. Waubke [114] also observed that mould growth was influenced by the level of carbon dioxide and cigarette smoke deposits. The use, by Herbak, of an artificial pollutant (lactic acid) to simulate soiling [49], resulted in greater

growth occurring on test panels compared to corresponding panels free from pollution: the mean growth factors rose from 1.1% to 1.7% at 83% RH, from 2.2% to 11.9% at 90% RH and from 16.7% to 30.1% at 97% RH.

2.5 HEALTH HAZARDS

Mould growth occurs in houses which, for the reasons discussed previously, are actually damp and frequently cold. Alone, these conditions are not conducive to good health and cold air is known to aggravate asthma [59].

Also respiratory problems can be caused by non biological material, chiefly high concentrations of nitrogen dioxide, carbon monoxide and formaldehyde [6]. These environmental conditions are important in affecting the health of occupants and should be borne in mind when considering the possible health hazards of moulds.

2.5.1 Mycotoxins and organic volatiles

Although toxic compounds are known to be present in fungal spores [4] and mycotoxioses (the ingestion of toxic metabolites) does occur [56], relatively little has been published regarding the possible health hazards of inhaling fungal mycotoxins. In reviewing mycotoxins in the air, Flannigan [37] reported a number of medical cases, both in the domestic and work environment where the symptoms could be attributable to inhalation of mycotoxins by the patient. For example, Croft et al. [31] reported that the long term inhalation of *Stachybotrys atra* spores could have caused the chronic health problems in members of a family. Symptoms consistent with trichothecene toxicosis were observed and several macrocyclic trichothecenes were isolated from the spores of the fungi both found in the air and growing on surfaces in the dwelling.

Both Samson [97] and Jorde et al. [56] suggested that volatiles from fungal spores, mainly short chain alcohols and aldehydes such as methyl-1-butanol, 2-hexanone, 2-heptanone [79] and 1-octen-3-ol [97], can affect the health of occupants. Complaints resulting from exposure to these volatiles include headaches, eye, nose, throat irritation or fatigue. However the actual number of people who may be affected by mouldy odours is unknown, for the response of individuals range from no reaction to becoming quite ill [97].

2.5.2 Mould spores

The major health risk arising from exposure to fungal spores is one of allergy. In some cases sensitization occurs upon exposure to an allergen resulting in the production of specific antibodies so that subsequent exposure causes allergic symptoms. There are two major patterns of respiratory allergic response: the so-called type I or anaphylactic reaction and the type III or toxic-complex syndrome. However type IV (cell-mediated) reactions are also considered to participate in type III diseases [6,62].

Type I allergy tends to be hereditary [6] and involves only a small number of particularly sensitive (atopic) individuals, but type III allergies can be induced by exposure. Although normally this is to exceedingly high concentrations of spores, for example 500 to 3000 x 10⁶ m⁻³ [18] which is many times higher than the maximum of 449 800 cfu m⁻³ recorded in problem dwellings [54].

In addition to spores, other particles which can elicit a response when inhaled are pollen grains, animal dander, bacteria, coal dust etc. The size of a particle determines how far it penetrates into the respiratory system and hence where it would cause a response. Fungal spores involved in type I allergy are generally greater than 5 µm and these include commonly occurring species such as Alternaria alternata, Botrytis cinerea, Cladosporium herbarum, C. macrocarpum, Drechslera spp. and Epicoccum purpurascens (E. nigrum) [30].

The spores smaller than 5 µm for example those of Aspergillus and Penicillium spp. penetrate to the alveoli, where they may cause alveolitis [65]. However it is the spores of bacteria (actinomycetes) which are the causative agent of the best known type III condition - Farmer's Lung.

Type I allergic diseases (rhinitis and asthma) are the most common in the UK [74] with type III (extrinsic allergic alveolitis or hypersensitivity pneumonitis) being extremely rare and are normally occupational [62,65]

While spores can induce allergies, there is no definite evidence correlating the level of spores occurring in dwellings with the induction of allergic diseases. However exposure to Penicillium spores may be a contributory factor to the disease in some asthmatic patients [26], since antibodies to Penicillium are identified more often among asthmatics than non-asthmatics.

Cases of individual mould allergies have also been documented. Kozak et al. [61] described one 12 year-old patient highly sensitive to Alternaria, in who's home the counts of this fungus were higher than any other species and 20 times higher than in the control house. Another child was identified with a strongly positive immunological response to Stachybotrys atra, found growing on wet carpets in his room. Earlier Samsoc-Jensen [96] reported two cases of allergy to Cladosporium fulvum.

2.5.3 Mites

The role of the mite Dermatophagoides pteronyssinus in house-dust allergy is now accepted and a relationship established between the level of airborne mite allergen and the severity of patients symptoms [90].

Other species occur in dust samples and some have been shown to illicit allergic responses [7,16]. The major source of allergen is the feed pellet but the pellicles of these mites can also be allergenic [111]. The optimum growth conditions for house dust mites occur at 75-80% RH [74], conditions in damp dwellings which are also conducive to mould growth. Certainly allergy to both mould and mites is common in asthmatics [48,107] and there may be an association between mites and xerophilic moulds. Lustgraaf [71] reported colonisation of human skin scales by Aspergillus penicilloides was related to an increase in the numbers of D. pteronyssinus.

2.6 SOME ELEMENTARY CONTROL STRATEGIES

There is no doubt that the primary control strategy for mould growth, and that most likely to give sustained success, is to reduce the risks of high RH against or condensation on the surfaces of the building fabric [18,19,22,58]. Such measures are often costly and are sometimes difficult to achieve because of structural constraints or the life style of the occupants. Where there are major cost constraints or factors which preclude alternative action, fungicidal methods of controlling moulds may be considered. Fungicidal washes are useful for cleaning down operations and sterilising infected surfaces, and fungicidal paints can be used for redecoration. The composition of surface coatings/treatments inhibiting fungal growth is discussed by Meinhardt [77].

Results have shown that fungicidal washes are capable of initial sterilisation of wall and ceiling surfaces but most of those examined do not provide protection lasting more than a few weeks without reapplication [19]. Several fungistatic substances have been used [91] to prevent mould growth on polyvinyl acetate dispersions and films. While fungicidal paints cost almost twice as much as conventional products, service trials in the UK of proprietary fungicidal paints in occupied dwellings, selected for their past history of mould problems, have shown that mould growth has not recurred in the longest of those trials which extends so far to 2.5 years [19].

2.6.1 Fungicidal strategy

The strategy recommended by Bravery et al. [19] and control of moulds using fungicidal remedies is:

- a. Identify and, where practicable, deal with the source(s) of moisture. If it is due to high RH or surface condensation, take steps to cure the causes. Wherever practicable, improvements in insulation, ventilation and heating of the dwelling should be considered. These actions must be accompanied with a fungicidal remedy.
- b. Ventilate the affected room(s) during the removal of mould growths, to encourage drying and reduction of concentrations of mould spores.
- c. Employ an approved fungicidal wash to remove mould growths from surfaces using safe handling procedures as specified by the manufacturers / suppliers. It is prudent to avoid inhalation of mould spores which can induce allergic reactions, particularly in people prone to respiratory problems, the elderly and the very young.
- d. Remove badly affected paints and wall coverings.
- e. Clean down the area with a further application of fungicidal wash and leave the surface to dry before attempting redecoration.

- f. Redecorate with fungicidal paint; note that such paints are rendered ineffective if papered over and cannot protect applied papers. Wallpapers will require fungicidal protection if very high RH or condensation persists but under very damp conditions are likely to become detached from surfaces due to breakdown of the paste by moisture. Fungicidal pastes are not intended to resist mould growth under damp conditions once the normal drying time of the paste is extended.

2.7 REFERENCES

1. Ackermann H, Schmidt B and Lenk V (1969). Mycological studies of the outdoor and indoor air in Berlin. *Mykosen* 12, 309-320.
2. Adan O C G and Weersink A M S (1987). Sampling and analysis of mould growth in buildings - Preliminary study in three dwellings. Paper CIB-W40 presented at Lund, Sweden.
3. Armolik N and Dickson J G (1965). Minimum humidity requirements for germination of conidia of fungi associated with storage of grain. *Phytopathology* 46, 462-465.
4. Austwick P K C (1966). The role of spores in the allergies and mycoses of man and animals. In *The fungus Spore* (ed. Madelin M F) Colston Paper No 18, Butterworth, London.
5. Ayerst G (1969). The effect of moisture on growth and spore germination in some fungi. *Journal of Stored Products Research* 5, 127-141
6. Anon (1981 a). *Indoor Pollutants*. National Academy Press, Washington DC.
7. Anon (1981 b). *Biology and control of mites*. In *Pest Infestation Control Laboratory Report 1977-79*. HMSO, London.
8. Anon (1988). *Catalogue of the Culture Collection of C.A.B International Mycological Institute*, C.A.B international, Kew (9th edition).
9. Barry S (1980). Comparative field and laboratory testing of fungicidal emulsion paints for interior use. In *Biodeterioration* (ed Oxley T A, Becker G and Allsopp D). Pitman, London.
10. Beaumont F (1985). *Aerobiological and clinical studies in mould allergy*. University of Groningen, Groningen. Cited in Verhoeff et al. (1988).
11. Beaumont F, Kauffman H F, Sluiter H J and De Vries K (1984). A volumetric-aerobiologic study of seasonal fungus prevalence inside and outside dwellings of asthmatic patients living in North-East Netherlands. *Annals of Allergy* 53, 486-492.

12. Beaumont F, Kauffman H F, Sluiter H J and De Vries K (1985). Sequential sampling of fungal air spores inside and outside the homes of mould-sensitive, asthmatic patients: a search for a relationship to obstructive reactions. *Annals of Allergy* 55, 740-746.
13. Benson F B, Henderson J J and Caldwell D E, (1972). *Indoor-Outdoor Air Pollution Relationships: A Literature Review*. U.S. Environmental Protection Agency, National Environmental Research Center Publication No. AP-112. U.S. Government Printing Office, Washington, D.c.
14. Blomquist G, Strom G and Stromquist L, G, (1984 a). Sampling of high concentrations of airborne fungi. *Scandinavian Journal of Work and Environmental Health* 10, 109-113.
15. Blomquist G, Palmgren V and Strom G, (1984 b). Improved techniques for sampling airborne fungal particles in highly contaminated environments. *Scandinavian Journal of Work and Environmental Health* 10, 253-258.
16. Blythe M E (1976). Some aspects of the ecological study of the house dust mites. *British Journal of Diseases of the Chest* 70, 3-31.
17. Botzenhart K, Altenhoff K and Leithold T (1984). Moulds in the air of greenhouses. In *Indoor Air, Vol 3. Sensory and Hyperreactivity Reactions to Sick Buildings* (ed. Berglund B, Lindvall T and Sundell J), Swedish Council for Building Research, Stockholm.
18. Bravery A F (1980). Origin and nature of mould fungi in buildings. In *Mould Growth in Buildings. Proceedings of a joint BRE/Paint Research Association Seminar*. Building Research Establishment, Princes Risborough, Bucks.
19. Bravery A F, Grant C and Sanders C H (1987). Controlling mould growth in housing. Paper presented at *Unhealthy Housing Prevention and Remedies Conference*, Warwick, December 1987.
20. Bronswijk, J van (1971). Cited in Adan and Weersink (1987).
21. Brooks F T and Hansford C G (1923). Mould growth upon cold-store meats. *Transactions of the British Mycological Society* VIII, 113-141.
22. Building Research Establishment (1985). *Digest 297: Surface condensation and mould growth in traditionally-built dwellings*. BRE, Garton, Herts.
23. Burge H A (1985). Indoor sources for airborne microbes. In *Indoor Air and Human Health* (ed. Gammage R B and Kaye S V). Lewis Publishers, Chelsea, Michigan.
24. Burge H A, Solomon W R and Williams P (1980). Microbial prevalence in domestic humidifiers. *Applied and Environmental Microbiology* 39, 840-844.
25. Burge H P, Solomon W R and Boise J R (1977). Comparative merits of eight popular media in aerometric studies of fungi. *Journal of Allergy and Clinical Immunology* 60, 199-203.
26. Burr M L, Mullins J, Merrett T G and Stott N C H (1988). Indoor moulds and asthma. *Journal of Royal Society of Health* 3, 99-101.

27. Chatigny M A, Wolochow H and Hinton D O (1983). Sampling aeroallergens. In Air sampling Instruments for Evaluation of Atmospheric Contaminants 6th ed. (ed. Liou P J and Liou M J Y). American Conference of Governmental Industrial Hygienists, Cincinnati.
28. Chen C and Chuang C (1975). Fungi isolated from asthmatic homes in the Taipei area. Chinese Journal of Microbiology 8, 253-258.
29. Christian J H B (1980) Reduced water activity. In Microbial Ecology of Foods I. Factors Affecting Life and Death of Microorganisms Academic Press, London
30. Cole G T and Samson R A (1984). The conidia. In Mould Allergy (ed. Al-Doory Y and Domson J F), Lea and Febiger, Philadelphia.
31. Croft W A, Jarvis B B and Yatawara C S (1986). Airborne outbreak of trichothecene toxicosis. Atmospheric environment 20, 549-552.
32. Davis R R (1971). Air sampling for fungi, pollen and bacteria. In Methods in Microbiology, Vol 4 (ed. Booth C), Academic Press, London.
33. Deverall B J (1965). The physical environment for fungal growth. 1. Temperature. In The Fungi An Advanced Treatise, Vol 1, The Fungal Cell (ed. Ainsworth G C and Sussman A S). Academic Press, London.
34. Dix N J (1985). Changes in the relationship between water content and water potential after decay and its significance for fungal successions. Transactions of the British Mycological Society 85, 649-653.
35. Erhorn H (1988). National Status Report - Germany. IEA Annex XIV Report, Glasgow Meeting, April 1988
36. Fergusson, R J Milne L J R and Crompton G K (1984). Penicillium allergic alveolitis: faulty installation of central heating. Thorax 39, 294-298.
37. Flannigan B (1987). Comment: Mycotoxins in the air. International Biodeterioration 23, 73-78.
38. Flensburg E W and Samsøe-Jensen T (1950). Studies in mold allergy: 3. Mould spore counts in Copenhagen. Acta Allergologica III, 49-65.
39. Fradkin A, Tobin R S, Tarlo S M, Tuccic-Porretta M and Mallock D (1987). Species identification of airborne moulds and its significance for the detection of indoor pollution. Journal of Air Pollution Control Association 37, 51-53.
40. Galloway L D (1934). The moisture requirements of mould fungi, with special reference to mildew in textiles. Shirley Institute Memoirs 13, 27-33.
41. Grant C, Hunter C A, Flannigan B and Bravery A F (1989). The moisture requirements of moulds isolated from domestic dwellings. International Biodeterioration, 25, 259-284.

42. Gravesen S (1972). Identification and quantification of indoor airborne micro-fungi during 12 months from 44 Danish homes. *Acta Allergologica* 27, 337-354.
43. Gravesen S (1978). Identification and prevalence of culturable mesophilic microfungi in house dust from 100 Danish homes. Comparison between airborne and dust-bound fungi. *Allergy* 33, 268-272.
44. Gregory P H (1973). *Microbiology of the Atmosphere*, (2nd ed.), Leonard Hill, Aylesbury.
45. Gregory P H and Sreeramulu T (1958). Air spora of an estuary. *Transactions of the British Mycological Society* 41, 145-156.
46. Groom P and Panisset T (1933). Studies on *Penicillium chrysogenum* Thom in relation to temperature and relative humidity of the air. *Annals of Applied Biology* 20, 633-660.
47. Harvey R (1970). Spore productivity in *Cladosporium*. *Mycopathologia et Mycologia Applicata* 41, 251-256.
48. Hendrick D J, Davis R J, D'Souza M F and Pepys J (1975). An analysis of skin prick test reaction in 656 asthmatic patients. *Thorax* 30, 2-8.
49. Herbak Z (1989). Experimental investigations of mould growth on building components surfaces. *Personnel communications*.
50. Hirsch S R and Sosman J A (1976). A one-year survey of mould growth inside twelve homes. *Annals of Allergy* 36, 30-38.
51. Hocking A D and Pitt J I (1979). Water relations of some *Penicillium* species at 25°C *Transactions of the British Mycological Society* 73, 141-145.
52. Holmberg K (1984). Mould growth inside buildings. In *Indoor Air, Vol 3. Sensory and Hyperreactivity Reactions to Sick Buildings* (ed. Berglund B, Lindvall T and Sundell J.) Swedish Council for Building Research, Stockholm.
53. Hudson H J (1980). *Fungal Saprophytism*, (2nd ed.). The Institute of Biology's Studies in Biology No.32. Edward Arnold, London.
54. Hunter C A, Grant C, Flannigan B and Bravery A F (1988). Mould in buildings: the air spore of domestic dwellings. *International Biodeterioration* 24, 81-101.
55. Ingold C T (1971). *Fungus Spores: Their Liberation and Dispersal*. Oxford University Press (Clarendon), London.
56. Jorde W, Schata M and Linskens H F (1987). Health risks from moulds in buildings. Keynote Address presented at IEA Annex XIV, Stuttgart Meeting, October 1987.

57. Kolmodin-Hedman B, Blonquist G and Sikström E (1986). Mould exposure in museum personnel. *International Archives of Occupational and Environmental Health* 57,321-323.
58. Köneke M and Köneke R (1987). *Schimmelpilze in Gebäuden*. Hammonia-Verlage, Hamburg.
59. Korsgaard J (1988). Demands of the allergic and hypersensitive population. In *Healthy Buildings '88*, Vol 1. State of the art reviews (ed. Berglund B and Lindvalt T). Swedish Council for Building Research, Stockholm.
60. Kozak P P, Gallup J, Cummins L H and Gillman S A (1979). Factors of importance in determining the prevalence of indoor moulds. *Annals of Allergy* 43, 88-94.
61. Kozak P P, Gallup J, Cummins L H and Gillman S A (1980). Currently available methods for home mould surveys. II. Examples of problem homes surveyed. *Annals of Allergy* 45, 167-176.
62. Kurups V P, Barboriak J I and Fink J N (1984). Hypersensitivity pneumonitis. In *Mould Allergy*, (ed. Al-Doory Y and Domson J F), Lea and Febiger, Philadelphia.
63. Lacey J (1973). The air spora of a Portuguese cork factory. *Annals of Occupational Hygiene* 16, 223-230.
64. Lacey J, Hill S T and Edwards M A (1980). Micro-organisms in stored grains: their enumeration and significance. *Tropical Stored Products Information* 39, 19-33.
65. Lacey J, Pepys J and Cross T (1972). Actinomycetes and fungus spores in air as respiratory allergens. In *Safety in Microbiology* (ed. Shapton D A and Board R G), Academic Press, London.
66. Lacey M E (1962). The summer air-spora of two contrasting adjacent rural sites. *Journal of General Microbiology* 29, 485-501.
67. Levetin E and Hurewitz D (1978). A one-year survey of the airborne moulds of Tulsa, Oklahoma. II. Indoor survey. *Annals of Allergy* 41, 25-27.
68. Lombardi G, Aghemo C, Bongiovanni L, Girard M, Sampo S, Bertin A and Mannino M (1988). Case study 2. IACP Torino. IEA Annex XIV Report I-T7-02/1988. Glasgow Meeting, April 1988.
69. Lumpkins E D and Corbit S L (1976). Airborne fungi survey. II. Culture plate survey of the home environment. *Annals of Allergy* 36, 40-44.
70. Lumpkins E D, Corbit S L and Tideman G M (1973). Airborne fungi survey. I. Culture plate survey of the home environment. *Annals of Allergy* 31, 361-370.
71. Lustgraaf B van der (1978). Seasonal abundance of xerophilic fungi and house-dust mites in mattress dust. *Oecologia* 36, 81-91.

72. Magan N (1982). Studies on the microflora of wheat grain: ecology of the fungi and effects of fungicides Ph. D Thesis, University of Reading.
73. Magan N and Lacey J (1984). Effect of temperature and pH on water relations of field and storage fungi. Transactions of the British Mycological Society 82, 71-78.
74. Mant D C and Muir Gray J A (1986). Building Regulations and Health. Building Research Establishment, Garston, Herts.
75. Maunsell K (1952). Air-borne fungal spores before and after raising dust. International Archives of Allergy and applied Immunology 3, 93-103.
76. Maunsell K (1954). Concentrations of airborne spores in dwellings under normal conditions and under repair. International Archives of Allergy and Applied Immunology 5, 373-376.
77. Meinhardt S (1984). Möglichkeiten der Oberflächenausbildung und Nachbehandlung zur Verhinderung bzw. Beseitigung von Mikroorganismen im Wohnungsbau. Internal Report, Fraunhofer Institut für Bauphysik, Stuttgart.
78. Miller J D and Holland H (1981). Biodeteriogenic fungi in two Canadian historical houses subjected to different environmental controls. International Biodeterioration Bulletin 17, 39-45.
79. Millar J D, Laflamme A D, Sobol Y, Lafontaine P and Greenhalgh R (1988). Fungi and fungal products in some Canadian houses. International Biodeterioration 24, 103-120.
80. Mislivec P B, Dieter C T and Bruce V R (1975). Effect of temperature and relative humidity on spore germination of mycotoxic species of *Aspergillus* and *Penicillium*. Mycologia, 67, 1187-1189.
81. Mislivec P B and Tuite J (1970) Temperature and relative humidity requirements of species of *Penicillium* isolated from yellow dent corn. Mycologia 62, 75-88.
82. Morgenstern J (1982). Einfluss von Polyrinylacetat-Zusätzen in Putzmörtel auf die Schimmelbildung. Material and Organismen 17, 241-251.
83. Morton L H G, Mitchell A F and Vaughan F (1987). Microbial investigation of hard surfacing materials. In Biodeterioration of Constructional Materials (ed. Morton L H G). Biodeterioration Society Occasion Publication No 3. Lancashire Polytechnic, England.
84. Onions A H S, Allsopp D and Eggins H O W (1981). Smith's Introduction to Industrial Mycology (7th ed.). Edward Arnold, London.
85. Panasenko V T (1967). Ecology of microfungi. Botanical Review 33, 189-215.
86. Pelhate J (1968) Determination of water requirements in grain storage fungi. Mycopathologia et Mycologia applicata 36, 117-128
87. Pendleton D E, O'Neill T B and Drisko R W (1987). Field performance of EPA approved mildewcides. In The Impact of Regulations and Litigations on

- Protective Coatings. Proceedings of the Steel Structures Painting Council 5th Technical symposium, New Orleans.
88. Pitt J I (1975). Xerophilic fungi and spoilage of foods of plant origin. In Water Relations of Foods (ed. Duckworth R B), Academic Press, New York.
 89. Pitt J I and Christian J H B (1968). Water relations of xerophilic fungi isolated from prunes. Applied Microbiology 16, 1853-1858.
 90. Platts-Mills T A E, Tovey E R, Chapman M D and Wilkins S R (1983). Airborne allergen exposure, allergen avoidance and bronchial hyper-reactivity. Asthma 18, 297-314.
 91. Pöge W (1961). über den schimmelbefall and Polyvinylazetat - dispersionen und sein verhütung. Phaste and kautschuk 8, 74-76.
 91. Popescu I G and Capetti E (1971). Study of mold spores in the homes of asthmatics. Revue Roumaine de Medicine Interne 8, 357-361.
 92. Reiss J (1986). Schimmelpilze. Springer-Verlag, Berlin.
 93. Richards M (1954). Atmospheric mold spores in and out of doors. Journal of Allergy 25, 429-439.
 94. Ripe E (1962). Mould allergy.I. An investigation of the airborne fungal spores in Stockholm, Sweden. Acta Allergologica 17, 130-159.
 95. Rogers S A (1983). A comparison of commercially available mold survey service. Annals of Allergy 50, 37-40.
 96. Samsoe-Jensen T (1955). Mould allergy. Sensitization by special exposure illustrated by two cases of allergy to Cladosporium fulvum. Acta Allergologica 9, 38-44.
 97. Samson R A (1985). Occurrence of moulds in modern living and working environments. European Journal of Epidemiology 1, 54-61.
 98. Schaffer N, Seidmon E E and Buskin S (1953). The clinical evaluation of airborne and house dust fungi in New Jersey. The Journals of Allergy 24, 348-354.
 99. Senave E (1988 a). Summary of mould research at the laboratory of building physics of the K.U., Leuven. IEA Annex XIV Report OA/B-T2-05/1988 Glasgow Meeting, April 1988.
 100. Senave E (1988 b). Mould research in the Zolder housing estate. IEA Annex XIV Report OA/B-T7-15/1988 Glasgow Meeting, April 1988.
 101. Smith S L and Hill S T (1982). Influence of temperature and water activity on germination and growth of Aspergillus restrictus and A.versicolor. Transactions of the British Mycological Society 79, 558-559.
 102. Sneller M R and Roby R R (1979). Incidence of fungal spores at the homes of allergic patients in an agricultural community. I. A 12-month study in and out of doors. Annals of Allergy 43, 225-228.

103. Snow D (1949). The germination of mould spores at controlled humidities. *Annals of Applied Biology* 36, 1-13.
104. Solomon W R (1975). Assessing fungus prevalence in domestic interiors. *Journal of Allergy and Clinical Immunology* 56, 235-242.
105. Solomon W R (1976). A volumetric study of winter fungus prevalence in the air of midwestern homes. *Journal of Allergy and Clinical Immunology* 57, 46-55.
106. Solomon W R (1984). Sampling techniques for airborne fungi. in *Mould Allergy* (ed. Al-Doory Y and Domson J F), Lea and Febiger, Philadelphia.
107. Solomon W R and Mathews P P (1978). Aerobiology and inhalant allergens. In *Allergy, Principles and Practice* (ed. Middleton E), C V Mosby, St Louis.
108. Ström G and Blomquist G (1986). Airborne spores from mouldy citrus fruit - a potential occupational health hazard. *Annals of Occupational Hygiene* 30, 455-460.
109. Swaebly M A and Christensen G M (1952). Moulds in house dust, furniture stuffing and in the air within homes. *Journal of Allergy* 23, 370-374.
110. Tomkins R G (1929). Studies on the growth of moulds - I. *Proceedings of the Royal Society of London. Series B. Biological Sciences* 105, 375-401.
111. Torey E R, Chapman M D, Wells G W and Platts-Mills T A E (1981). The distribution of dust mite allergen in the houses of patients with asthma. *American Review of Respiratory Diseases* 124, 630-635.
112. Verhoeff A P, van Wijnen J H, Attwood P, Versloot P, Boley J S M, van Reeman-Hoekstra E S and Samson R A (1988). Quantification and qualification of airborne fungi in houses. A comparison of measurement techniques. *Municipal Health Service, Amsterdam*.
113. Wallace M E, Weaver R H and Scherago M (1950). A weekly mold survey of air and dust in Lexington, Kentucky. *Annals of Allergy* 8 202-211.
114. Waubke N V (1987). Schimmelbefall in Wohnugen-Hygienische und Stoffliche Aspekte. *Bauphysik* 5, 163-168.
115. Waubke N V and Wallnöfer P (1984). Pilzbefall kunststoffgebundenor Putze und Spachtelmassen des Bauwesens. Internal Report, Hochschule der Bundeswehr, Neubiberg.
116. Wray B B and O'Steen K G (1975). Mycotoxin-producing fungi from house associated with leukaemia. *Archives of Environmental Health* 30, 571-573.
117. Van der Werff (1958). Mould fungi and Bronchila Asthma. *Stenfert Kroese, Leiden*.
118. Zyska, B J Cieplik A T, Kwiatkowska D, Wichary H M and Koztowska R (1988). Fungal colonisation of organic coatings in cotton mills. In *Biodeterioration 7* (ed Houghton D R, Smith R N and Eggins H O W). Elsevier Applied Science, London.

APPENDIX 2.A: IDENTIFICATION OF MOULDS

- Ainsworth G C (1973), Introduction and keys to higher taxa. In The Fungi, Vol 4A (ed. Ainsworth G C, Sparrow F K and Sussman A S). Academic Press, New York.
- Ames L M (1961), A Monograph of the Genus Chaetomium. U.S. Government Printing Office.
- Arx J von (1981), The Genera of Fungi Sporulating in Pure Culture. J. Cramer, Verlag.
- Booth C (1971), The Genus Fusarium. Commonwealth Mycological Institute, Kew.
- Domsch K H, Gams W and Anderson T H (1980), Compendium of Soil Fungi. Vol I and II. Academic Press, London.
- Ellis M B (1971), Dematiaceous Hyphomycetes. Commonwealth Mycological Institute, Kew.
- Ellis M B (1976), More Dematiaceous Hyphomycetes. Commonwealth Mycological Institute, Kew.
- Gams W (1971), Cephalosporium: artige Schimmelpilze (Hyphomycetes). Gustav Fischer, Verlag.
- Gams W, Aa van der H A, Plaats-Niterink van der A J, Samson R A, Stalpers J A (1987). CBS Course of Mycology.
- Mazzucchetti G (1964), Il Genere Chaetomium. Pubblicazioni dell Ente Nazionale per la Cellulosa e per la Carta, Roma.
- Pitt J I (1979), The Genus Penicillium and its teleomorphic states Eupenicillium and Talaromyces. Academic Press, London.
- Ramirez C (1982), A Manual of the Penicillia. Elsevier Biomedical Press, Amsterdam.
- Raper K B and Fennel D I (1965), The Genus Aspergillus. Williams and Wilkins Co, Baltimore.
- Seth H K (1971), A Monograph of the Genus Chaetomium. Van J Cramer, Lebre.
- Vries, G A de (1952), Contribution to the Knowledge of the Genus Cladosporium. Diss. Univ., Utrecht.

Chapter 3

MODELLING: Thermal Aspects

Authors:

C. Lombardi: Part 3.1: Conduction
Polytecnico di Torino, TORINO - Italy

J. Reiß and H. Erhorn: Part 3.2: Convection and radiation
Fraunhofer Institut Fur Bauphysik, STUTTGART - Germany

P. Standaert: Paragraph 3.2.8
Physibel C.V., MALDEGEM - Belgium

3.0 INTRODUCTION

High surface RH and surface condensation are directly linked to the thermal quality of the envelope or envelope parts, condensed in the 'TEMPERATURE RATIO'

$$\tau = \frac{\theta_{si} - \theta_e}{\theta_i - \theta_e}$$

Thermal modelling must create the tools, needed to calculate the temperature ratio. This asks for a sound knowledge of heat transfer by conduction - the fabric part - and heat transfer by convection and radiation - the surface heat transfer part.

The building envelope acts as a three-dimensional composition of walls, connected to one another in such a way as to create rooms, the living space, which must be maintained on thermal comfort conditions [12].

The envelope is crossed by heat flows, caused by the inside-outside temperature differences, by shortwave direct, indirect and reflected solar radiation and by longwave earth, surrounding buildings and sky radiation.

A combined model for heat transfer throughout the entire envelope would be too complex to be solved easily. Therefore it is preferable first to analyze single envelope parts, then to combine to single rooms, and at last to extend to the whole building.

The equations of the model are slightly different for a single wall system or for a 'room+ walls'-combination..

In both cases however, the fundamental law applied is that of energy conservation, called the first law of thermodynamics. In the case of conduction in solids, it sounds:

$$\rho c \cdot \frac{\partial T}{\partial \tau} = -\text{div } q \quad (3.1)$$

This equation must be combined with the Fourier law of conduction of heat (3.2), with Newtons law for convection between the internal air and the wall and the wall and the external air (3.3) and with the Stefan-Boltzmann law for heat exchange by radiation between the wall and the surrounding surfaces (3.4):

$$q = -\lambda \cdot \nabla T \quad (3.2)$$

$$q_c = h_c \cdot (T_s - T_{\text{air}}) \quad (3.3)$$

$$q_r = f \cdot (T_s^4 - T_{s2}^4) \quad (3.4)$$

with T : temperature in K
 λ : thermal conductivity in W/(m.K)
 ρc : the volumic heat capacity in J/(m³.K)
 h_c : convective surface film coefficient in W/(m².K)
 f : a suitable function of the radiative exchange encompassing the effects of geometry, the emissivity of the surfaces and the Stefan-Boltzmann constant
 q : the 'density of heat flow'-vector in the solid,
 q_c, q_r : the density of heat flow exchanged by convection and radiation at the surfaces

3.0.1 Single envelope parts

For envelope parts, not exchanging mass with the environment and having constant material properties, the model equation becomes:

$$\frac{\partial^2 \theta}{\partial x^2} + \frac{\partial^2 \theta}{\partial y^2} + \frac{\partial^2 \theta}{\partial z^2} = \frac{\rho c}{\lambda} \cdot \frac{\partial \theta}{\partial \tau} \quad (3.5)$$

with as boundary conditions: both convection with the air in contact with the wall, and radiation with other surfaces having a different surface temperature:

$$-\lambda \cdot \frac{\partial T}{\partial n} = h_c \cdot (T_s - T_{air}) + \sum_i [f_i \cdot (T_s^4 - T_{si}^4)] \quad (3.6)$$

with n: normal to the surface.

Equation (3.6) applies for the internal and external surfaces.

Introducing as constraint in the envelope part, on each surface between different materials k and l:

$$\lambda_k \cdot \left[\frac{\partial \theta}{\partial n} \right]_k = \lambda_l \cdot \left[\frac{\partial \theta}{\partial n} \right]_l \quad (3.7)$$

the temperature field at any time in the envelope part is found by solving equation (3.5) in combination with the boundary conditions (3.6).

3.0.2 Single room

If the energy balance concerns a room with its envelope, the energy conservation equation for the room air must be added to 3.m equations (3.5) - (3.7), m being the number of envelope parts:

$$\sum_i \Phi_i + \sum_j (\pm \rho_a c_a \cdot \Phi_{aj} \cdot \theta_{aj}) = \rho_a c_a \cdot V_a \cdot \frac{\partial \theta_a}{\partial t} \quad (3.8)$$

where each Φ_i is the heat flow by convection with the i-th wall.

V_a and Φ_{aj} , respectively, are the internal air volume of the room and the outgoing (+) or incoming (-) air flow rate via the j-th opening at temperature θ_{aj} .

The combined solution of the equations (3.5) (3.6) (3.7) (3.8), even for a simple geometry, is complex. Therefore, in most cases, a one-dimensional, steady-state temperature field is assumed in all envelope parts, and the effect of radiation in (3.6) is linearized.

Those simplifications were and are commonly made to calculate heat losses through walls and, by adding, of rooms in wintertime.

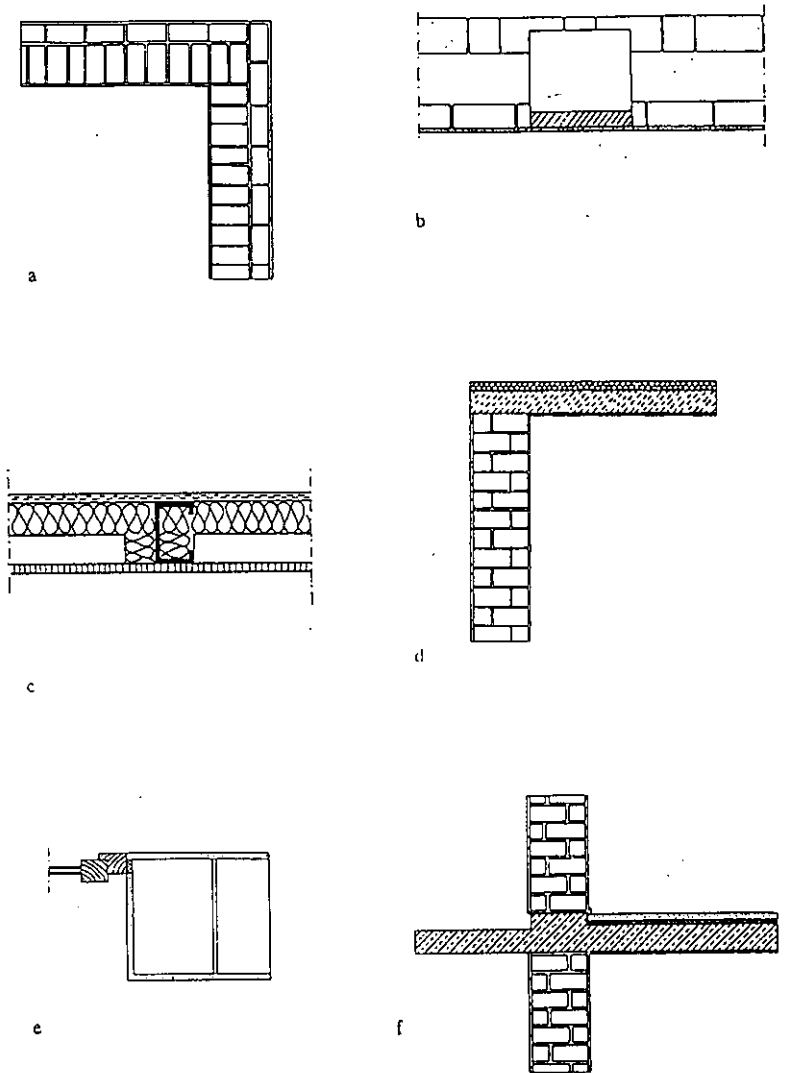


figure 3.1: Thermal bridges: a) corner between walls; b) pillar inside a wall; c) sheet metal frame assembling prefabricated panels; d) roof wall junction; e) window wall junction; f) concrete slab penetrating outer wall.

For years, this way of working was considered satisfactory until, by the increase in thermal insulation, the effects of so-called "thermal bridges" became too evident.

The word "Thermal bridge" is used to define each part of the building envelope where, during wintertime, there is a local increase of heat flow density and a decrease of internal surface temperatures.

Thermal bridges appear in places where the envelope changes its geometry or composition or both [4]: the assumption of a one-dimensional field is no longer valid and solutions must be found for the more complex 2-dimensional (2D) or 3-dimensional (3D) conduction.

In figure 3.1 some common thermal bridges are shown: the corner between two identical external walls is an example of a geometrical change; a column inside the wall is an example of a composition change. Small discontinuities in the wall structure, such as gaps in the insulation layer due to bad workmanship, or sheet metal frames to assemble prefabricated panels, give composition variations. Examples of combined geometrical and composition changes are: windows parapets, balconies and cantilevered floor slabs.

Many thermal bridges modify the one-dimensional field into a two-dimensional one: the heat flux has components along two orthogonal axis. This is the case when the geometry and composition of the cross section along the third axis doesn't change. We call them 2D thermal bridges.

Others give heat flux components along the three axes. This is the case e.g. in corners between two walls and a ceiling. We call them 3D thermal bridges.

Due to their impact on the total heat losses, and the possible presence of inside surface temperatures low enough to cause mould growth and condensation, thermal bridges are no longer negligible.

Therefore it is important to know more precisely the heat fluxes in, and the surface temperatures on thermal bridges, and to have an evaluation tool in the design stage, giving the possibility to check the envelope solution on both (energy and mould risk) and to compare improvements.

The modification in temperature and heat flow in the presence of a thermal bridge, is not only caused by 2D or 3D conduction, but also by the convective and radiative surface film coefficients h_c and h_r , being variable all over the surface.

In fact the convective surface film coefficient is bound to the air flow pattern against the wall, itself depending on the temperature difference between wall and air and on the surface geometry: e.g. the flow pattern will differ from the middle of a flat wall to the edge and corners.

As for the radiative surface film coefficient, it is variable, largely because of changes in the geometry factor.

So, it is necessary to redress the calculation of the three types of heat transfer in order to come to a sufficiently approximate evaluation of thermal bridges.

3.1 CONDUCTION

3.1.1 Theoretical background

3.1.1.1 Conduction law

Heat transfer occurs from higher to lower temperatures. It follows Fourier's law, given by equation 3.2 for homogeneous and isotropic materials. Equation (3.5) is obtained by applying the energy conservation law to a small volume $dx.dy.dz$ of the material and combining it with (3.2).

The hypothesis of homogeneous and isotropic material anyway simplifies the problem: the porosity of the material allows air infiltration, moisture adsorption, capillar condensation, moisture uptake...

This going on, the material is no longer homogeneous and isotropic and the presence of heat sinks and sources and enthalpee flow should be taken into account.

The hypothesis nevertheless remain rather correct if equivalent properties are used (the 'equivalent' thermal conductivity for example).

3.1.1.2 One-dimensional heat flow (steady-state)

For a flat homogeneous wall or a wall composed of several layers of homogeneous and isotropic materials, the heat flux in zones sufficiently far from the edges can be considered 1D, normal to the wall.

In steady-state conditions, with x as axis along the thickness, equation (3.5) becomes for each layer:

$$\frac{\partial^2 \theta}{\partial x^2} = 0 \quad (3.9)$$

Solved, it generates a linear temperature course in the layer. Integration constants follow from the boundary and contact conditions (3.6 and 3.7), the first one simplified to an overall surface film coefficient h_i , combining both convective and radiative heat exchange, multiplied with the difference between surface and reference temperature.

Once the thermal field known, the inside surface temperature and the heat flow rate follow from:

$$\theta_{si} = \theta_i - \frac{U}{h_i} (\theta_i - \theta_e) \quad (3.10)$$

$$\Phi = U.A. (\theta_i - \theta_e) \quad (3.11)$$

where:

$$U = \frac{1}{\frac{1}{h_i} + \sum_{j=1}^n \frac{d_j}{\lambda_j} + \frac{1}{h_e}} \quad (3.12)$$

with:

- d_j and λ_j = thickness and thermal conductivity in the j -th layer
- θ_i and θ_e = inside and outside reference temperature

In many countries, U values for walls, calculated with (3.12), are given, assuming standard values for h_i and h_e : e.g. 8 and 23 W/(m²K), for an outside vertical wall [32].

The inside reference temperature should be defined properly. Some countries take the central air temperature, others the central dry resulting temperature or effective temperature.

As the inside surface temperature and, consequential, the RH and condensation risks are closely dependent on the local surface film coefficient, a correct choice is of great importance, as will be discussed in part 3.2.

3.1.1.3 Two-dimensional heat flow (steady-state)

In the zones of the wall near the edges but sufficiently far from the corners, the steady-state thermal flux has components in 2 directions. The temperature field in each homogeneous layer is defined by the 2D-Laplace equation:

$$\frac{\partial^2 \theta}{\partial x^2} + \frac{\partial^2 \theta}{\partial y^2} = 0 \quad (3.13)$$

which can only be solved in an analytical way for simple geometries and simple boundary conditions [33].

Anyway, the precision with which the material properties are known makes an exact solution impossible. Therefore, approximate solving methods, analogue and numerical, may be used. Thanks to the computer, the numerical methods now prevail.

For quick and easy calculations of 2D thermal bridges, also simplified procedures have been developed, giving the heat flux, by using printout parameters and simple algorithms and, in some cases, the lowest inside surface temperature. Such methods, calibrated with the aforesaid numerical methods, cover only part of the thermal bridges typology, and allow only a few verifications of improvements.

This can also be said of the thermal bridge catalogues: they are undoubtedly useful but always incomplete.

3.1.1.4 Three-dimensional heat flow (steady-state)

In the corners and other peculiar places of the envelope, the heat flow gets components along the three axes. The temperature field in each homogeneous layer is then defined by the 3D-Laplace equation:

$$\frac{\partial^2 \theta}{\partial x^2} + \frac{\partial^2 \theta}{\partial y^2} + \frac{\partial^2 \theta}{\partial z^2} = 0 \quad (3.14)$$

whose solution can be found by using the numerical methods mentioned in 3.1.2.2.

3.1.1.5 Non-steady-state flow

In non-steady-state, the partial time differentiation of the temperature appears in the equations. A solution can be found by using the same numerical methods, giving the temperature field at each time step.

Besides, it must be mentioned that among non-steady-state phenomena, by using the Fourier or Laplace transforms of (3.5) and (3.7), sinusoidal and/or periodic phenomena can be processed as stationary ones.

3.1.2 Calculation methods

3.1.2.1 Analytical solutions

Analytical solutions of 2D and 3D heat conduction with boundary conditions of the type needed in thermal bridge calculations (The Neumann boundary condition) are not mentioned in literature [33].

3.1.2.2 Numerical methods

Two numerical methods are used :

- the finite element method (FEM)
- the energy balance technique or control-volume method (CVM)[40].

The finite difference method (FDM), although often used to solve thermal problems, is not advisable in cases where materials with great differences in thermal conductivity are present (as in thermal bridges).

In FEM, mathematical theorems apply to convert the solution of the differential equation with its boundary conditions into the solution of a system of linear equations with a limited number of unknown field variables. These are normally the temperatures in the nodes, generated by an appropriate domain subdivision in elements. Using Fourier's law, the heat flux is then determined.

The CVM uses the same physical laws, which generated the differential equation, on finite subdivisions of the object. This procedure leads to a system of linear equations in the temperatures in characteristic subdivision points. Some basic rules are forwarded to assure the consistency of the solution of this system with the physical reality: overall balance must be matched and even in the case of coarse grid, the solution must have a physically realistic behaviour. Further steps are identical as in the FE method.

Following rules concern both methods:

- a limited number of assumptions has to be made. Differences in these cause multiple variations in results;
- the boundary conditions have to be implemented. Differences in their mathematical treatment cause differences in the methods application and in results;
- different rules are applied to create the subdivisions (e.g. in regard of the material limits positions), resulting again in differences in method application and results.

In order to give an understanding of the basic concepts of the two methods, an example is given of a bi-dimensional problem, using both.

Finite elements method

The physical problem to be solved, is the steady-state bi-dimensional conduction in a R domain of a homogeneous material, where dl is a boundary element. Therefore, one must find the solution of the equation:

$$\frac{\partial^2 \theta}{\partial x^2} + \frac{\partial^2 \theta}{\partial y^2} = 0 \quad (3.15)$$

with boundary conditions:

$$\lambda \cdot \left[\frac{\partial \theta}{\partial x} \right] \cdot n_x + \lambda \cdot \left[\frac{\partial \theta}{\partial y} \right] \cdot n_y + h \cdot (\theta_s - \theta_{ref}) = 0 \quad (3.16)$$

where n_x and n_y are the direction cosines between the perpendicular on the boundary line C and the Cartesian axis.

These equations are the same as (3.5) and (3.6), assuming stationary conditions and linearizing the effect of radiation. Solving equation (3.15) with its boundary conditions is done by an integral method [9] [31]. The variational principle states that by finding θ , for which the functional $J(\theta)$, given by:

$$J(\theta) = \iint_R \left(\lambda \cdot \left[\frac{\partial \theta}{\partial x} \right]^2 + \lambda \cdot \left[\frac{\partial \theta}{\partial y} \right]^2 \right) dx \cdot dy + \int_C h \cdot (\theta_s - \theta_{ref}) \cdot dl = 0 \quad (3.17)$$

reaches a minimum:

$$\partial \{ J(\theta) \} = 0 \quad (3.18)$$

is equivalent to finding the solution of the equation (3.15) together with (3.16).

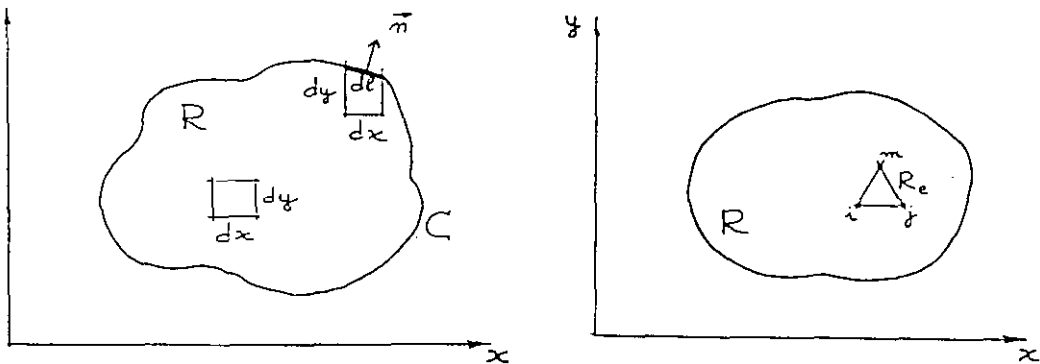


Figure 3.2 R domain with a boundary element dl

Figure 3.3 Example of subregion R_e for thermal field solution using the FEM.

The finite element method divides the R region in many subregions R_e , called "finite elements" (for instance small triangles) (fig 3.3) and assumes that in each element the temperature is a known function of the space coordinates. If linear:

$$\theta = a_1 + a_2x + a_3y \tag{3.19}$$

Writing this equation for the three nodes (i,j,m) of the triangle, θ can, after some elaborations, be related to the nodes temperatures:

$$\theta = N_i \theta_i + N_j \theta_j + N_m \theta_m \tag{3.20}$$

with the N coefficients called "shape functions". They only depend on the space coordinates and their value varies between 0 and 1 (1 in the node to which they refer and 0 in all other nodes).

The full representation of θ in R is obtained by putting together the partial representations, following (3.11). Fig.3.4 shows that concept in a graphical way. In order to find the temperature field, equation (3.20) is introduced in (3.18) giving following equations for the e-element:

$$J_e = J_e(\theta_i, \theta_j, \theta_m) \tag{3.21}$$

$$\delta\{J_e\} = \frac{\partial J_e}{\partial \theta_i} \delta\theta_i + \frac{\partial J_e}{\partial \theta_j} \delta\theta_j + \frac{\partial J_e}{\partial \theta_m} \delta\theta_m \tag{3.22}$$

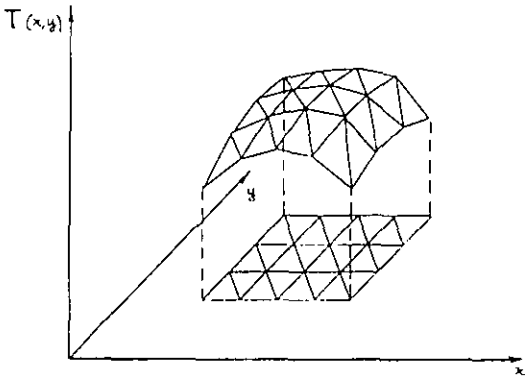


Figure 3.4 Graphical representation of the thermal field solution using the FEM

So, the problem is reduced to finding the solution of N equations of the form (so many as the nodes are):

$$\frac{\partial J}{\partial \theta_i} = \sum \frac{\partial J_e}{\partial \theta_i} \quad i = 1 \dots N \quad (3.23)$$

By making these equations explicit, it is shown that getting $\partial[J(\theta)] = 0$ means solving a system of linear equations in so many temperatures as there are nodes.

The temperature in any other point is obtained with (3.20). The heat flow through the boundary contour follows from:

$$\Phi_C = \oint_C h \cdot (\theta_s - \theta_{ref}) \cdot dl \quad (3.24)$$

where θ_s is the mean temperature on dl .

With the finite element method, the temperature field is more correctly known if the finite elements are smaller. Smaller elements are necessary in zones with higher gradients.

The method can also be used to solve 3D problems and to study non-steady-state conditions.

Remarks:

No restrictions exist concerning the shape of the finite elements (normally triangular or rectangular). Their dimensions can be changed in the different zones giving the possibility to locate element boundaries on the surfaces of separation. Similarly, discontinuities in the boundary conditions can be handled conveniently to avoid discontinuities within a boundary element. This simplifies the calculation algorithms when composite parts with space-variable boundary conditions are studied, such as thermal bridges.

Control-volume method

To solve a bi-dimensional thermal field with the perimeter on steady-state boundary conditions, one divides the field into a grid of square or rectangular meshes with their sides parallel to 2 Cartesian coordinate axis [35],[20],[40].

The mesh determines N nodes, each of the nodes being representative for a square or a rectangle having Δx and Δy as sides, with the node in the centre. For a node with i and j as indexes (the first referred to the column and the second to the line of the node), the thermal balance tells that the sum of heat flows to the node equals zero in steady-state conditions:

$$\begin{aligned} & \lambda \cdot \frac{\Delta y}{\Delta x} \cdot (\theta_{i-1,j} - \theta_{i,j}) + \lambda \cdot \frac{\Delta y}{\Delta x} \cdot (\theta_{i+1,j} - \theta_{i,j}) \\ & + \lambda \cdot \frac{\Delta x}{\Delta y} \cdot (\theta_{i,j-1} - \theta_{i,j}) + \lambda \cdot \frac{\Delta x}{\Delta y} \cdot (\theta_{i,j+1} - \theta_{i,j}) = 0 \end{aligned} \quad (3.25)$$

When $\Delta x = \Delta y$, the equation is simplified to:

$$\theta_{i-1,j} + \theta_{i+1,j} + \theta_{i,j-1} + \theta_{i,j+1} - 4\theta_{i,j} = 0 \quad (3.26)$$

The implementation of boundary conditions is done in different ways to obtain one equation, valid for the considered boundary node.

For example, for a node on a curved profile (node no.2 in figure 6), one gets:

$$\begin{aligned} & \frac{b}{\sqrt{a^2+b^2}} \cdot \theta_1 + \frac{b}{\sqrt{c^2+1}} \cdot \theta_3 + \frac{a+1}{b} \cdot \theta_{1,j} + \frac{h \cdot \delta}{\lambda} \cdot (\sqrt{c^2+1} + \sqrt{a^2+b^2}) \cdot \theta_e \\ & - \left[\frac{b}{\sqrt{a^2+b^2}} + \frac{b}{\sqrt{c^2+1}} + \frac{a+1}{b} + \frac{h \cdot \delta}{\lambda} \cdot (\sqrt{c^2+1} + \sqrt{a^2+b^2}) \right] \cdot \theta_2 = 0 \end{aligned} \quad (3.27)$$

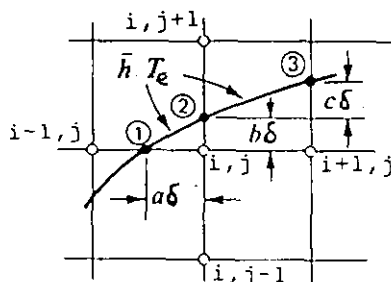
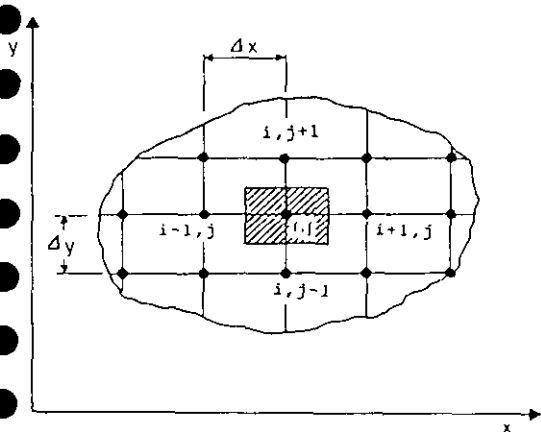


Figure 3.5 Subdivision of a bi-dimensional field in a grid formed by rectangular meshes.

Figure 3.6 Node on the contour with convection and radiation boundary conditions.

Also here the problem is reduced to solving a system of N linear equations in N temperatures.

Remarks:

With the CVM- approach, different dimensions of the control volume in the different layers are possible, giving the same advantages as the finite element method.

Requirements for both numerical methods

A rich bibliography exists about the errors resulting from the discretization process [30] [34] [36] [40].

It is important to point out that a converging solution can be achieved by a numerical method only if for an increasing number of subdivisions the solution converges to the exact one. The convergence could be proved by a "convergence table", showing the temperatures in the characteristic points of a "standard problem" as function of the number of nodes.

In Appendix A a table of available PC Programmes is given with their main characteristics.

Requirements for the use of numerical methods

Once a numerical method is adopted, a correct solution is achieved (e.g. the temperature distribution is calculated) if:

1. the problem is "well posed".

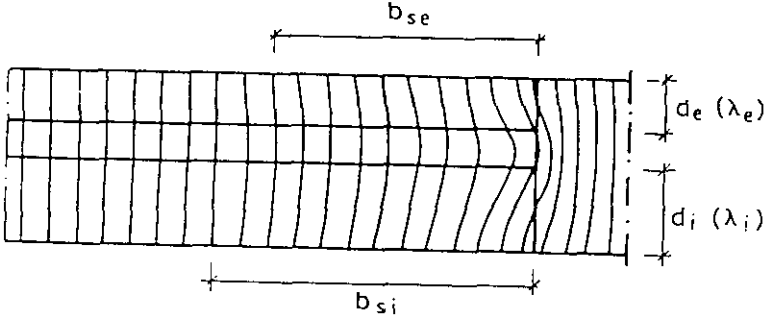


Figure 3.7 Width of the zone of influence on each side of a thermal bridge: b_s is different for the inner and the outer leaf

i.e. the exact boundary conditions are defined. This means that the correct values of h_i and h_e along the internal and external surfaces must be given and that no heat flux may cross the other sides of the thermal bridge calculation field (adiabatic conditions). To be sure that the last condition is achieved, it is necessary to take a suitable dimension of the geometrical model of the thermal bridge under examination; a 2D thermal bridge must have for instance a width b_s :

$$b_s = \max \left[2 \cdot \sqrt{\frac{\lambda_i \cdot d_i}{h_i}}, 2 \cdot \sqrt{\frac{\lambda_e \cdot d_e}{h_e}} \right] \quad (3.28)$$

as demonstrated in [8]; the meaning of the symbols are explained in fig.3.7;

2. the minimum number of subdivisions necessary to guarantee a certain degree of accuracy is defined.

The error is defined as:

$$e_i = |\theta_i - \hat{\theta}_i| \quad (3.29)$$

where $\hat{\theta}_i$ is the approximate temperature at nodal point i
 θ_i is the exact temperature.

For FEM, Cali [26] uses a formula given by Babuska and others [36], allowing an upward evaluation of the error, expressed in %. For the thermal bridge of figure 3.8 for example, the relative error is given as a function of the number of nodes. So a criterion is defined to ensure a maximum error less than $x\%$.

More empirically, Standaert suggests [19] for CVM that the largest difference between two temperatures, obtained with the same numerical method respectively with n and $2n$ equations, in the same characteristic points, should be less than $x\%$ of X , X being the largest temperature difference in the thermal bridge. He proposes a value of $x = 0,5\%$ of X .

It is good to remember that the limited accuracy in actual values of many parameters (such as the thermal conductivity and the surface film coefficients) makes it senseless to maintain the error within very narrow limits, because a long and heavy work in solving very large systems of equations doesn't result in better accuracy.

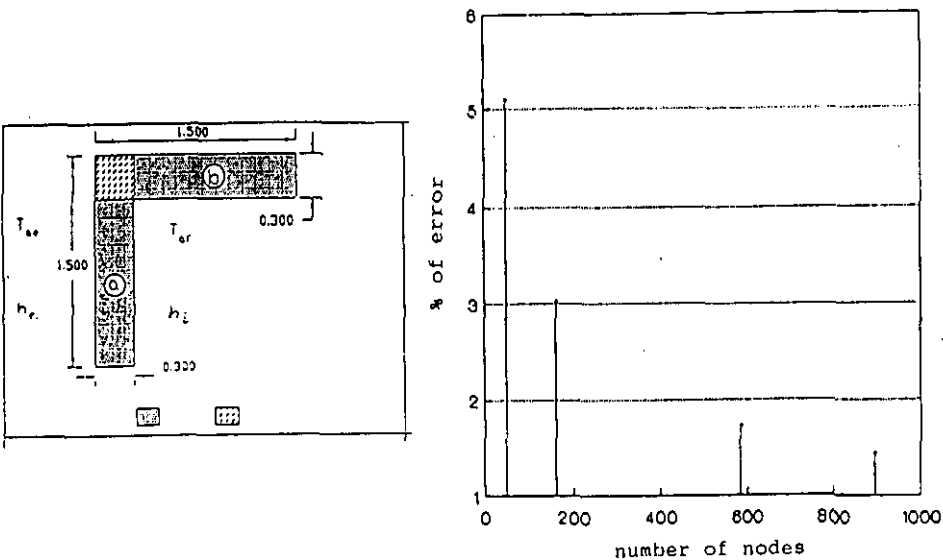


figure 3.8 Corner configuration and % of error in the evaluation of the temperature in the nodes versus the number of nodes.

3.1.2.3 Simplified methods

General considerations

All simplified methods provide correction factors for the additional heat loss through a thermal bridge. Only few of them make it possible to calculate inside surface temperatures, giving the possibility to judge the condensation and mould growth risks. These are treated here.

The minimum inside surface temperature at a thermal bridge is generally given as a dimensionless parameter: the "temperature-ratio or -factor":

$$\tau_{hi} = \frac{\theta_{si} - \theta_a}{\theta_i - \theta_o} \quad (3.30)$$

representing the temperature difference between the inside surface and the external air for a unit temperature difference between in- and outside and a specific value of the inside surface heat coefficient.

The additional heat loss through a 2D thermal bridge per unit length and for 1°C of temperature difference is represented by U_1 [W/(mK)], the linear thermal transmittance. The additional heat loss through a 3D thermal bridge for 1°C of the inside - outside temperature difference is given by U_p [W/(mK)]: the punctual thermal transmittance.

τ , U_1 or U_p are found, or by shaping a simplified model of the thermal bridge and solving the relevant equations, or by some formulae, calibrated with a FEM or CVM approach and valid for a specific class of thermal bridges.

Simplified modelling

In 1983 the Swedish Standards Association published a working draft [2] giving a method for the calculation of the thermal transmittance of metal constructions having thermal bridges. This method was generalised in 1986 by Staelens [8], while working at the Lund Institute of Technology, and includes:

- thermal bridges in heavy constructions
- corners and thermal bridges in corners
- steel constructions

It may be defined as a semi-analytical method, based on the electrical analogy.

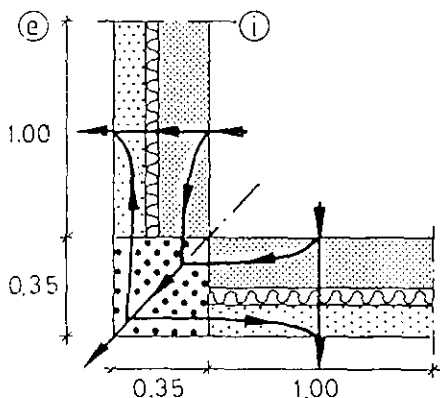


Figure 3.9 Main flow paths for a corner construction

Following physical considerations the heat flow through a zone including the thermal bridge is divided into flow paths (transversal and lateral paths) (fig 3.9).

The thermal resistance for each flow path is analytically derived. These resistances are combined into a network. By calculating the network resistance the thermal resistance of the construction and the heat flow through the zone is obtained. A manual is included, containing general networks and the formulae necessary to calculate thermal resistances of flow paths. The calculation also gives the temperatures in the network nodes. These in fact are not the real temperatures at that point, but a mean temperature over an area. In some simple cases the minimum inside surface temperature is approximated.

The results of the method were compared with numerical calculations. The relative difference in U-value was smaller than 10%. The degree of approximation for the temperatures is not mentioned. The method may give an insight in the location of the weak points in thermal resistance in a structure, but, it requires a good knowledge of physics to design a good equivalent circuit.

Other methods:

1) ISO DP.6946/2.1

An ISO group published in 1983 [3] a draft proposal with simplified calculation methods for beam-shaped thermal bridges in flat structures to determine:

- the lowest surface temperature on the thermal bridge;
- the thermal transmittance of a structure containing the thermal bridge.

The lowest internal surface temperature θ_{tb} is calculated with:

$$\theta_{tb} = \theta_e + r_{hi} \cdot (\theta_i - \theta_e) \quad (3.31)$$

r_{hi} is expressed as a simple function of the thermal transmittance of the plain wall and the thermal transmittance at the location of the thermal bridge:

$$r_{hi} = 1 - \frac{1}{h_i} \cdot (U_o + \eta(U_{tb} - U_o)) \quad (3.32)$$

where:

- U_o = thermal transmittance in locations other than thermal bridges
- U_{tb} = thermal transmittance at the location of the thermal bridge
- η is a characteristic of the thermal bridge.

In a similar way, the areal thermal transmittance of a structure including a thermal bridge is given by adding to the mean thermal transmittance a term including a factor χ characteristic of the thermal bridge.

The approximate formulae to calculate η and χ for six basic types of beam-shaped thermal bridges are tabulated as a function of the geometry and the thermal conductivity of the different materials. Specific assumptions are made for the surface film resistances $1/h_i$ and $1/h_e$. These two values can be changed only slightly.

The formulae were calibrated by several computer runs of a numerical model. They give the thermal transmittance with an estimated accuracy of 5%. The minimum temperature is obtained within 10%.

From the U value, a linear thermal transmittance U_1 can be derived (depending of the assumptions!):

$$U = \frac{(A - A_{tb}) \cdot U_o + U_1 \cdot L}{A} \quad \text{or} \quad U = \frac{A \cdot U_o + U_1 \cdot L}{A} \quad (3.33)$$

where:

- A is the surface area of the wall in m^2
- A_{tb} is the surface area of the thermal bridge in m^2
- L is the length of the 2D thermal bridge in m

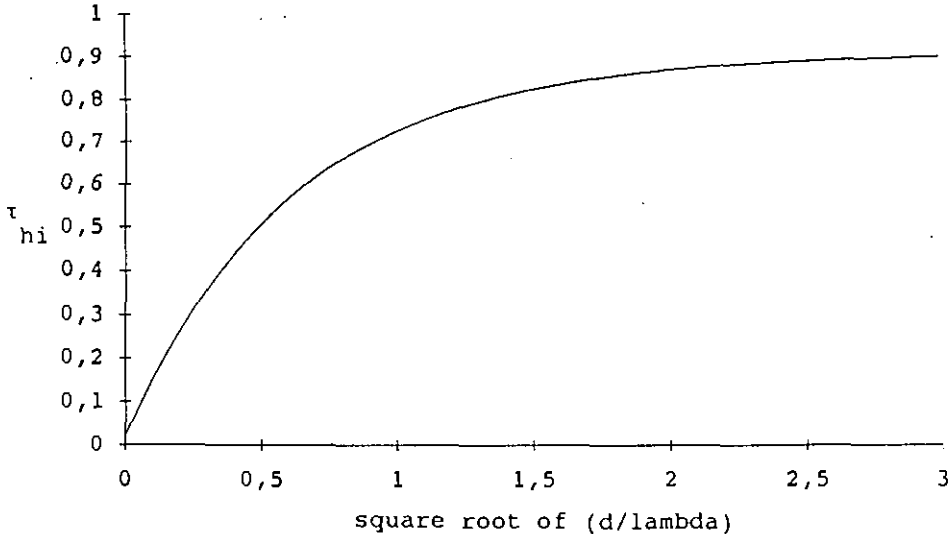


Figure 3.10 Non-dimensional surface temperature in monolithic corners versus different thermal exchange parameters.

2) Giergia [25]

While working at the Fraunhofer Institut für Bauphysik, Giergia studied symmetric corners in single and multilayer walls.

In his report a curve $(1-\tau_{6.5})$ versus d/λ is given for single walls:

$$\tau_{6.5} = 0.91 - 0.89 \cdot \exp(-1.59 d/\lambda) \quad (3.34)$$

As all the calculations were done with $h_i = 6.5$ [W/(m²K)],

a correction factor is provided for other h_i :

$$\tau(h_i) = C(h_i) \cdot \tau_{6.5} + [1 - C(h_i)] \quad (3.35)$$

where:

$$C(h_i) = 1.368 - 0.057 h_i \quad (3.36)$$

$\tau_{6.5}$ was also obtained for multilayer insulated walls:

$$\tau_{6.5} = 0.97 - \exp(-1.55 c \cdot R) \quad (3.37)$$

where:

$c = 0.87$ for outside insulation

$c = 1.00$ for cavity filling

$c = 1.25$ for inside insulation

R is the thermal resistance of the wall ($0.5 \leq R \leq 4$ m²K/W)

Further, easy-to-use formulae are given to calculate U_i for corners.

Temperature evaluation is within $\pm 0.01^\circ\text{C}$ and U_i within ± 0.05 W/(mK).

3.1.2.4 Thermal bridges catalogues

To help designers, some countries produced catalogues [14],[41],[42],[44] of common thermal bridge constructions. These catalogues contain drawings and descriptions of building details, surface temperatures profiles or τ_{hi} values for the critical points and heat loss data. The data are obtained from numerical calculations, assuming standard thermal conductivities and constant surface film coefficients, the value being different from catalogue to catalogue.

In theory, a thermal bridge catalogue provides a rapid, easy (no computing is required) method of assessing a particular case and sometimes gives informations on improvements. However, in practice, the catalogues rarely give the specific thermal bridge, a designer is aiming to judge.

3.1.3 Experimental investigations

Experimental investigations on thermal bridges are done following two different methods:

- Hot-box/cold box measurements;
- Analogue models.

3.1.3.1 Investigations using the hot box / cold box apparatus.

This system uses two boxes, one on outside and the other on inside climate. The tested configuration separates the two climates. For the surface temperature measurement, thermocouples or thermoresistors are located along the thermal bridge cross - section contour (see e.g. fig. 3.11)

To measure the heat flow [37,38], a third, smaller box is inserted in the hot box , facing the central part of the tested configuration; the heat released in this third box is measured, the zone between the hot box and the smaller box being the guarding environment, on the same temperature as the measuring box. This configuration is called the guarded hot box. An alternative, easier to use for thermal bridge research, is the calibrated hot box.

The measurement of the heat flow through the wall without and with the thermal bridge, allows to calculate the U_1 - or U_p - value.

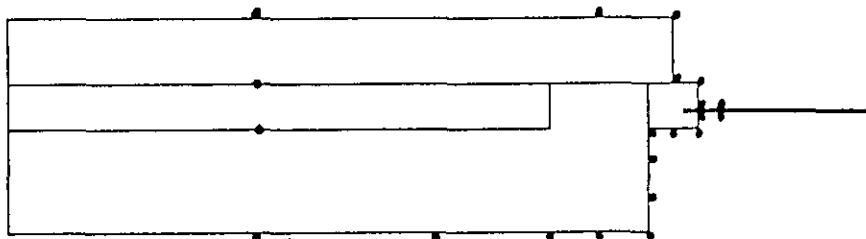


figure 3.11 Horizontal cross section of a wall - window junction. The dots indicate the thermocouple position [17].

3.1.3.1 Experiments using analogue models.

Analogue models are based on the fact that electric or mass transport obey identical laws as the Fourier equation. So an analogue model of the thermal problem can be built. Let us think of the electric analogy.

Ohm's law states that:

$$dI = -\lambda_e \cdot (\nabla V \cdot n) \cdot dS \quad (3.38)$$

where:

- λ_e = electric conductivity of the material
- V = electric potential
- dI = charge flow through an element with surface dS
- n = the normal to the surface dS

Ohm's law is formally equal to (3.9). The V - field satisfies the equation:

$$\frac{\partial^2 V}{\partial x^2} + \frac{\partial^2 V}{\partial y^2} + \frac{\partial^2 V}{\partial z^2} = \frac{C_e}{\lambda_e} \frac{\partial V}{\partial t} \quad (3.39)$$

where C_e is the volumic electric capacity of the material. The analogy links tension to temperature, charge flow to heat flow, the electric resistance to the thermal resistance and volumic electrical capacity to the volumic heat capacity.

Author		2D ENVELOPE CORNERS	WINDOWS	FINS	IN BETWEEN FLOOR	INSIDE WALL - ENVELOPE	STRUCTURAL T.B.	ROOFS - ENVELOPE JUNCTION/	3D ENVELOPE CORNERS
Baum 1980	o			T/W			T/W		
Brun- ner e.s. 1985	x	T/W	T/W	T/W	T/W				
Erhorn/ Gertis 1984	x		W						
Erhorn/ Tammes 1985	o						T/W		
Erhorn e.s. 1988	x		W						
Heindl e.s. 1987	x	T/W	T/W	T/W	T/W	T/W	T/W	T/W	T/W
Johann- sen 1968	*						T/W		
Kasper e.s. 1984	x		T/W						
Küntel 1961	o	T/W							
Kupke 1980	x	T/W		T/W				T/W	
Malinka/ Paschen 1986	x	T/W	T/W	T/W	T/W	T/W	T/W	T/W	T/W
RECLES Frankr. 1975	o	W	W	W	W	W	W	W	
Stae- lens 1986	o	W				W	W		
Sten- daert 1984	*	T/W	T/W		T/W	T/W	T/W	T/W	T/W
Wölt- gens 1986	o	T/W	T/W	T/W	T/W	T/W	T/W		

x thermal bridges catalogue o simplified method * numerical method

T temperatures

W heat flows

Table 3.1 *Field literature - Details concerning different thermal bridges examined by the authors according to the results calculation and representation.*

In practice, a model, geometrically similar to the thermal bridge under examination is built by using layers with known electric conductivities or lumped electric resistances. By measuring the current, it is possible to evaluate the heat flow, while temperature differences are proportional to the voltage differences.

3.1.4 Applications

3.1.4.1 Introduction

By using one of the above methods, different types of thermal bridges have been studied, searching general correlations for at least a class of them. Table 3.1 [25] gives a list of researchers, the types of thermal bridges examined, the evaluation method used and the results obtained, updated until 1988. Since, many others contributed [22-29].

Some interesting results are discussed below, first looking to the sensitivity and then showing the kind of information one gets.

3.1.4.2 Sensitivity

In many papers the sensitivity of the calculated temperature ratio to uncertainties in parameters like the inside surface film coefficient, the thermal conductivity of the materials or to the choice of numerical method and grid spacing are reported. Typical limits of accuracy are summarised in following table [43].

VARIABLE	UNCERTAINTY ON τ
Solution method	< 0.01
Grid spacing	< 0.01
Thermal conductivity (± 0.1 W/(m K))	< 0.05
Outside surface film coefficient (16.7 to 33.3 W/(m ² K))	< 0.01
Inside surface film coefficients (4 to 8 W/(m ² K))	< 0.1
Variation in local surface film coefficients (4 to 8 W/(m ² K))	< 0.05
Solar radiation (0 to 50 W/m ²)	< 0.05

The inside surface film coefficient is the most important parameter, followed by the thermal conductivities and the incident solar radiation. So, the in situ values of τ may show differences of as much as 0.13 compared to the modelled ones. This means that, with an inside-outside temperature difference of 20°C, the inside surface temperature can only be approximated within $\pm 2.6^\circ\text{C}$, a great uncertainty to assess mould and condensation risks. For that reason, and in order to avoid misunderstandings, h_i must be added as subscript to τ , every time a value is given.

3.1.4.3 Two-dimensional thermal bridges in steady-state conditions

Fin-type thermal bridges

A theoretical analysis by P. Cooper [23] states that balconies and other cantilevered parts in the envelope, considered as severe thermal bridges, in many cases do not increase the heat flow nor make the inside surface temperature decrease, compared to the absence of the cantilevered part. The author employs, in his analysis, an analytical solution for the one-dimensional heat flow through a thin fin. He underlines the fact that the fin behaves according to the outer surface coefficient: the ratio between the thermal permeance of the fin root area with (P_f) and without fin (P_o) increases when the outside surface film coefficient decreases.

In most cases $P_f/P_o < 1$ (see fig. 3.12).

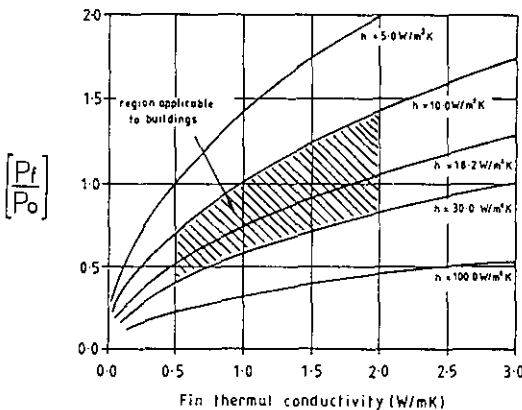


Figure 3.12 Ratio of thermal permeance of a fin to that of a flat surface. Fin dimensions: height $b = 0.2$ m, width $a = 10.0$ m, length $l = 0.5$ m.

He also developed a one-dimensional model to predict the lowest inside surface temperature on a fin-type thermal bridge.

In situations similar to fig.3.13, he assumed a one-dimensional two-fins model, both fins extending perpendicularly to the building envelope, the one as inside floor slab, the other as balcony (see fig.3.14).

The difference between the temperature factors of the plain wall $r_{hi,w}$ and the thermal bridge $r_{hi,tb}$ can be estimated as:

$$r_{hi,w} - r_{hi,tb} = \frac{R_f}{R_{f1} + R_w + R_{f2}} - \frac{h_i^{-1}}{h_i^{-1} \cdot (d/\lambda_w) + h_o^{-1}} \quad (3.40)$$

where:

d = wall thickness in m

λ_w = equivalent thermal conductivity of the wall.

The formula overestimates the thermal bridging effect. Nevertheless, it is a relatively accurate estimation, with an inherent safety margin regarding mould and condensation. The uncertainty in r -evaluation is < 0.03 .

Predicted r_{hi} -values for several walls with and without a balcony fin are compared in [43]. The balcony slightly increases r_{hi} except for a wall with inside insulation. Interesting is that with outside insulation and the fin not insulated, the r_{hi} value increases, [43,18]. This suggests a retrofitting possibility with external cladding, leaving the balconies uninsulated (fig 3.15).

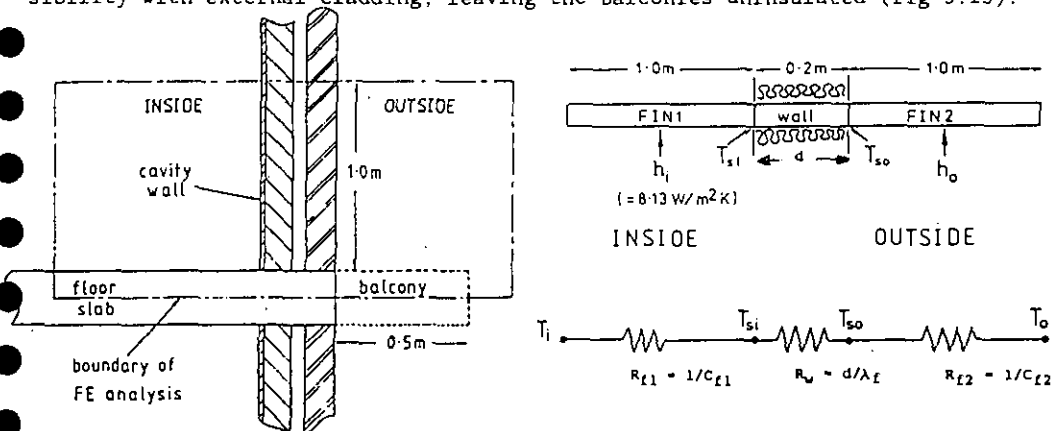


Figure 3.13 Concrete slab, bridging a cavity wall.

Figure 3.14 Fin model of extended thermal bridge: fin arrangement and temperature/thermal resistance circuit. λ_f is the floor conductivity.

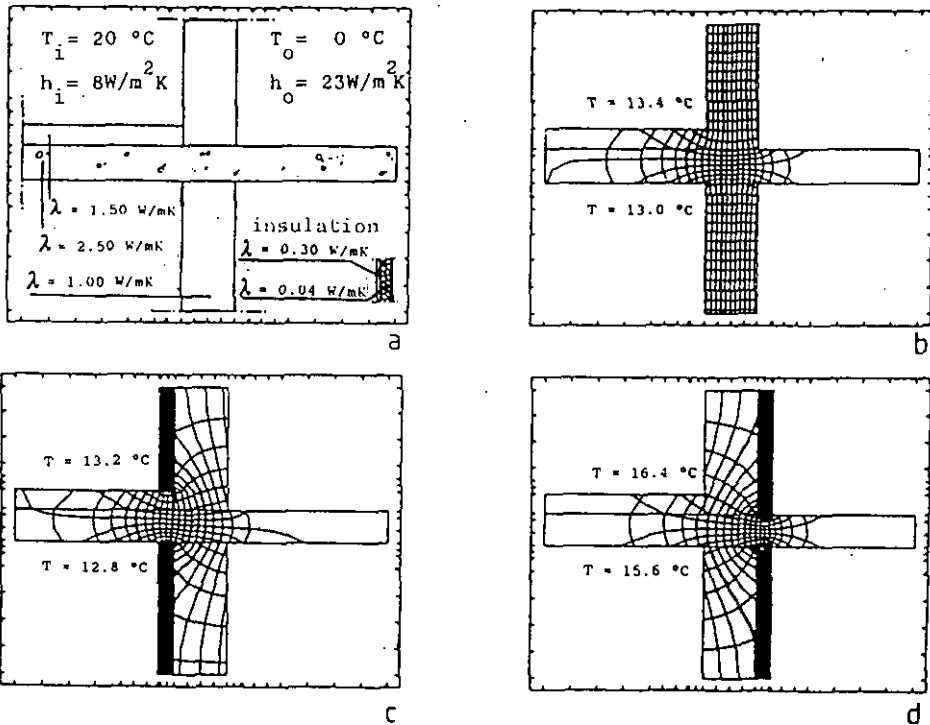


figure 3.15 Vertical section of a concrete slab, penetrating the outer wall. (a) Geometry, thermal conductivities and boundary conditions; isotherms and streamlines with (b) no insulation, (c) inner insulation, and (d) outer insulation.

Thermal bridges in cavity walls

Standaert [18] studied a number of traditional thermal bridges in cavity walls. He concluded that, if possible, they must be avoided by making the cavity insulation continuous, with correct thermal cuts. Although the energy savings are lower than predicted one-dimensionally without thermal bridges, cavity insulation remains efficient to thermally improve existing buildings, if at least the inside relative humidity is not too high.

The same considerations are found in [43] with the warning not to add insulation along partition walls (floors, internal walls) when the envelope is cavity filled: r_{hi} decreases.

To show how these and other conclusions can be drawn from an numerical analysis, a thermal bridge of the case-study "Alexanderpolder Building" was examined with a FEM programme: it concerns the junction between the floor and an external wall. The results are shown in fig. 3.16 (outside temperature: 0°C, inside temperature: 20°C). The temperature difference between isotherms is 2°C.

Conclusions:

1. The junction gives the lowest inside surface temperature on the underside of the floor;
2. Inside insulation gives a minimum surface temperature lower than a non insulated wall;
3. A higher inside surface temperature and a lower heat flow not always coincide: an inside insulation is to prefer if a heat flow reduction is the main aim, cavity insulation is better if higher surface temperatures are wished;
4. The best solution for both is, as Standaert states, outside insulation.

In an other paper [17] Standaert discusses the improvement of window reveals in cavity walls. He underlines the importance of a thermal cut between the inner and outer leaf along the reveal. Analogous results are obtained with a FEM programme studying 7 solutions (fig. 3.17) for the horizontal cross-section of the window-cavity wall junction in the case-study "IACP Torino":

- 3.17 a) external leaf, no cavity insulation, single glazing
- 3.17 b) external leaf, 4 cm cavity insulation, single glazing
- 3.17 c) external leaf, 4 cm continuous cavity insulation, single glazing
- 3.17 d) internal leaf, no cavity insulation, single glazing
- 3.17 e) internal leaf, 4 cm cavity insulation, single glazing
- 3.17 f) internal leaf, 4 cm cavity and reveal insulation single glazing
- 3.17 g) external leaf, 4 cm continuous cavity insulation, double glazing

Conclusions:

1. Without any other improvement, looking to the temperature factor, the window-internal leaf junction is the best solution. From the heat loss point of view it is the worst solution. Condensation risks are not real.

2. If the window is connected to the inside leaf, cavity insulation, also covering the reveal, doesn't increase the lowest inside surface temperature, compared to cavity insulation, not covering the reveal. On the other hand, the decrease in thermal flow through the reveal by cavity insulation without reveal covering, is minimal. In any case a thermal bridge effect cannot be avoided.
3. With cavity insulation, connecting the window to the outside leaf is the best: it can give up to 5°C increase in inside surface temperature.
4. It is clear that a thermal cut between inner and outer leaf along the reveal is a conclusive improvement. The best solution is g) where the insulation layer is continuous and double glazing is used.

Thermal bridges in massive walls.

Massive brick walls with a thickness of 20-30 cm (European buildings constructed before 1940) didn't show important thermal bridging because of the general lack of thermal resistance. Insulating them can be done at the inside or at the outside. This introduces thermal bridges at the discontinuities in the thermal insulation. An example was already shown in fig. 3.15a [18]: a vertical section through a balcony. The isotherms and heat flow lines were determined for three cases: no insulation (fig. 3.15b), inner insulation (fig. 3.15c), outer insulation (fig. 3.15d). The calculated thermal bridge characteristics are:

- no insulation	: $U_1 = 0.3 \text{ W/(m.K)}$	$\tau_8 = 0.65$
- inner insulation	: $U_1 = 0.8 \text{ W/(m.K)}$	$\tau_8 = 0.64$
- outer insulation	: $U_1 = 0.8 \text{ W/(m.K)}$	$\tau_8 = 0.78$

Window reveals are one of the few thermal bridges that can get substantially worse by insulating the wall, unless it is done at the outside. (fig. 3.18).

Thermal bridges in prefabricated buildings

A general study of thermal bridges in prefabricated buildings is, because of the very great variety in geometry and materials, an impossible task. However, important extra heat losses and low temperature factors may occur, if in concrete or metallic parts, discontinuities in the thermal insulation exist. Therefore, a thermal bridge analysis must be part of the development work.

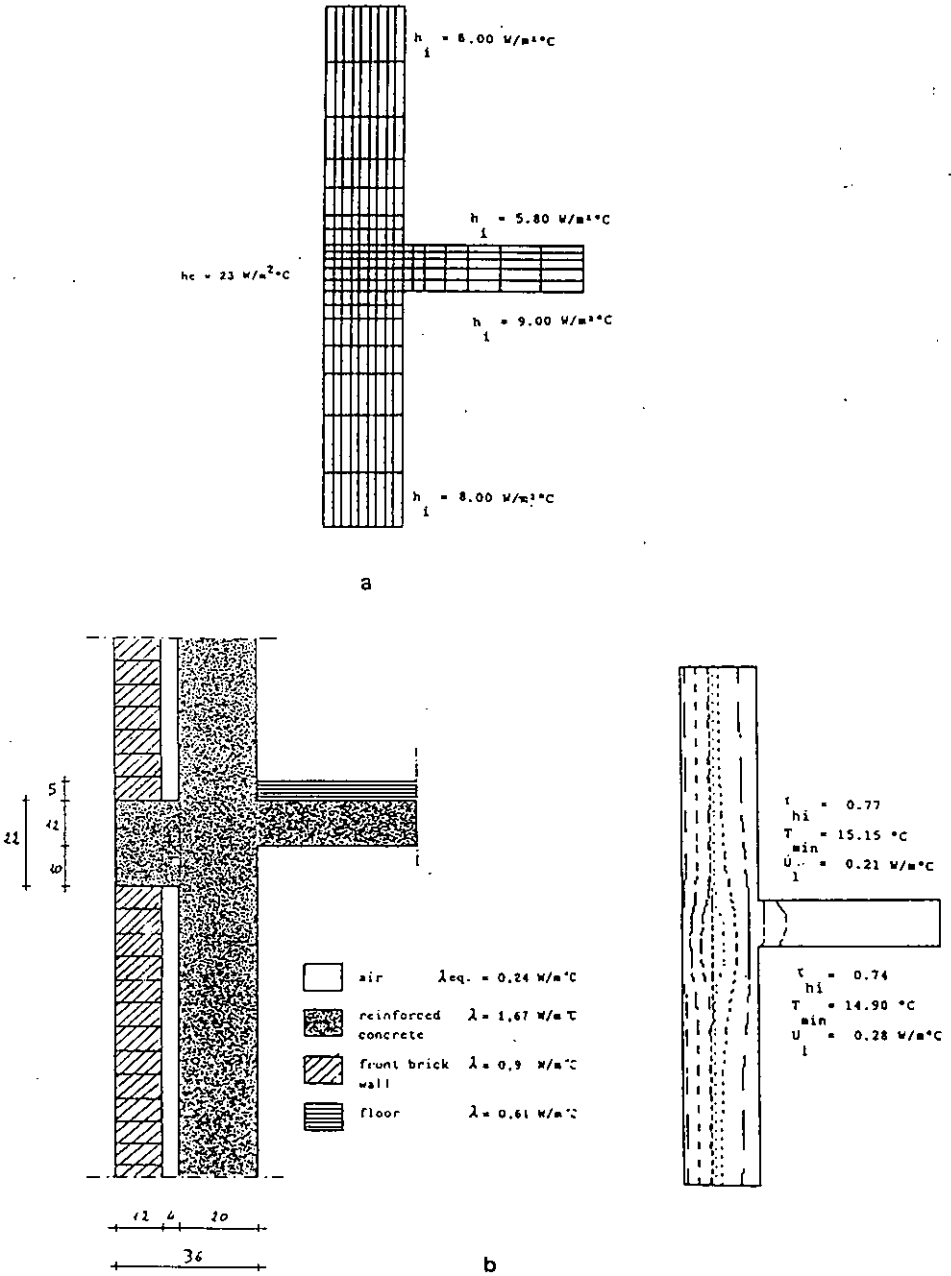
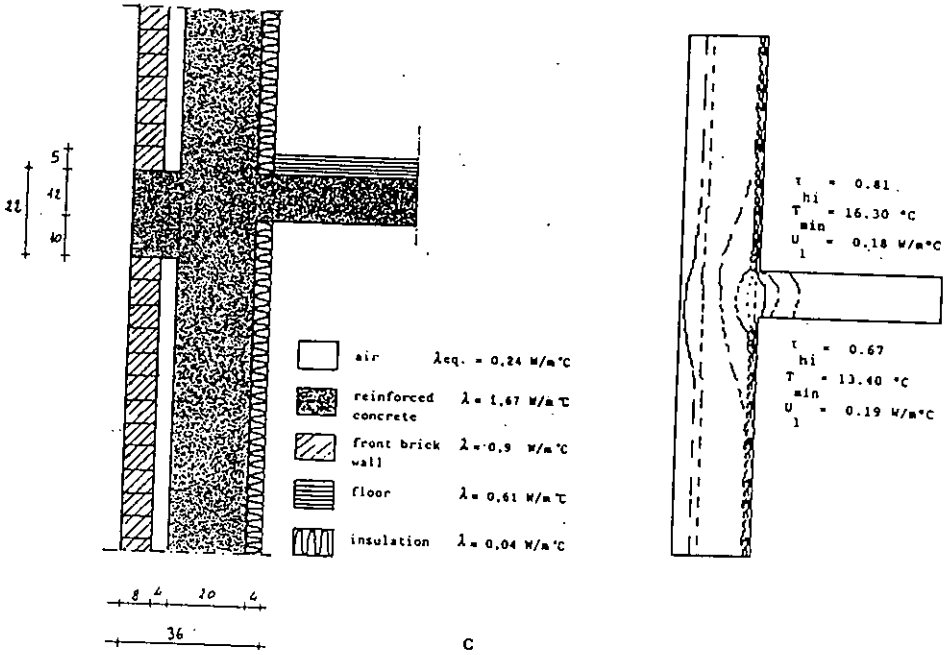
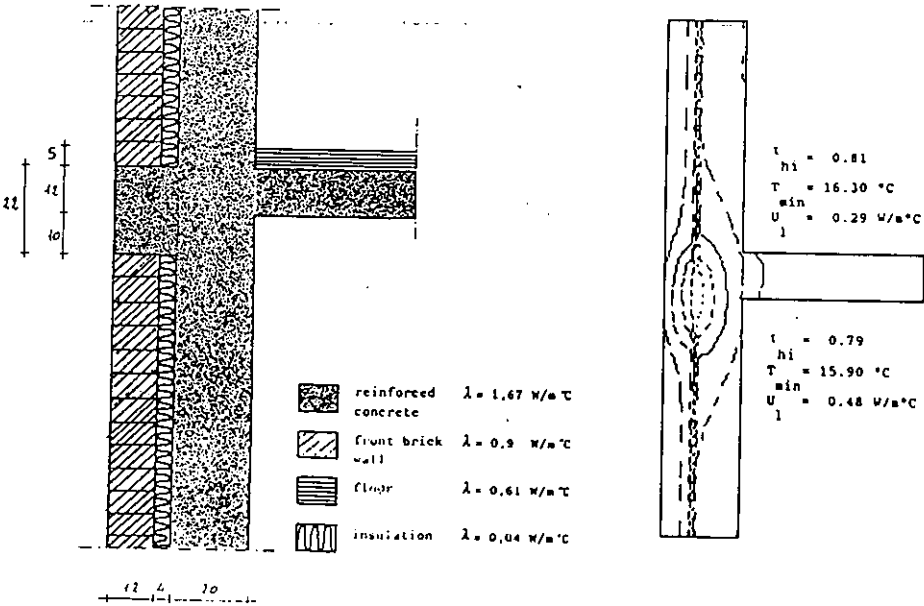


Figure 3.16 Vertical cross section of a floor-external wall junction: a) mesh, b) no insulation



c



d

figure 3.16 Vertical cross section of a floor-external wall junction: c) inside insulation, d) cavity insulation,

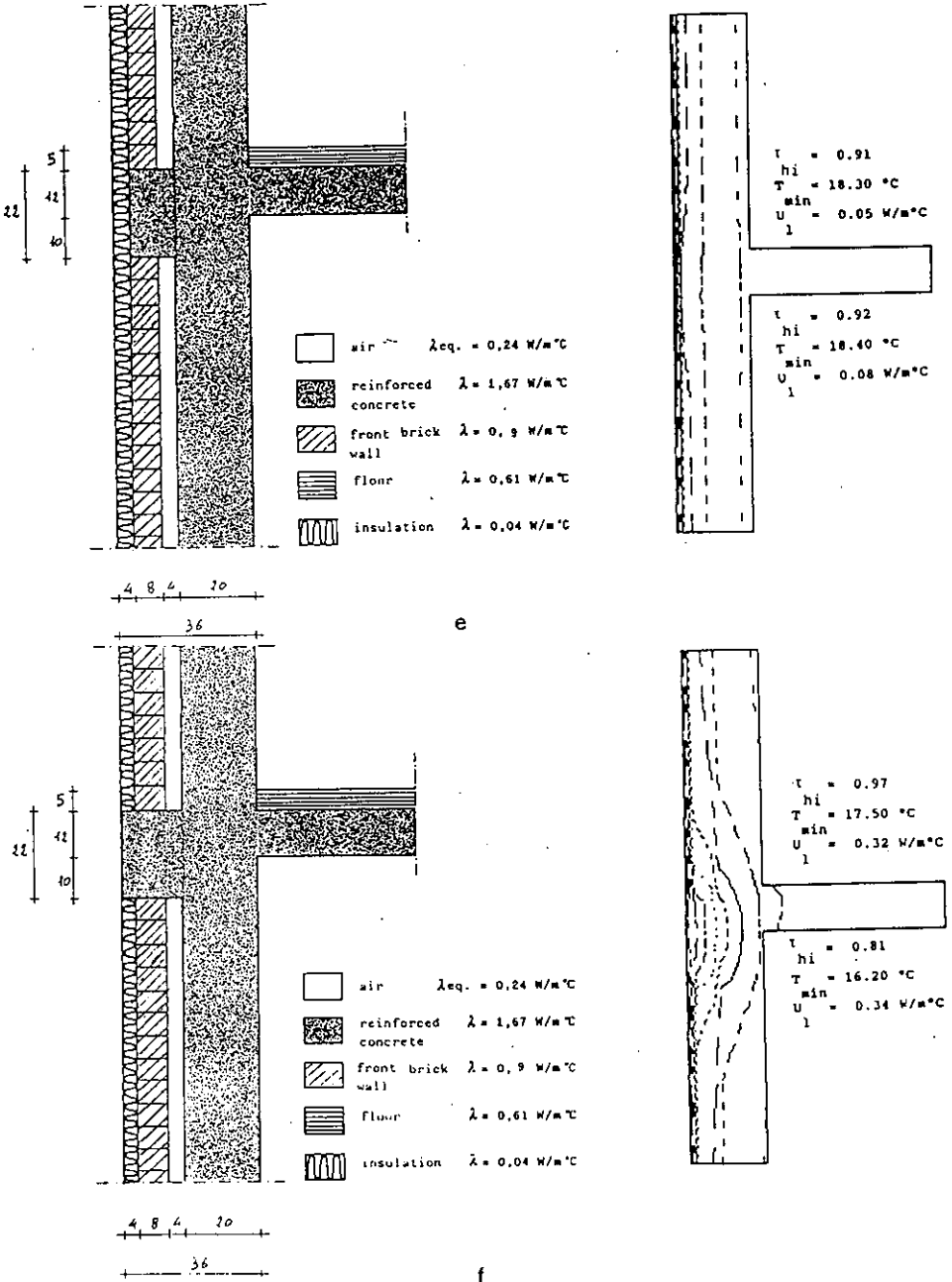
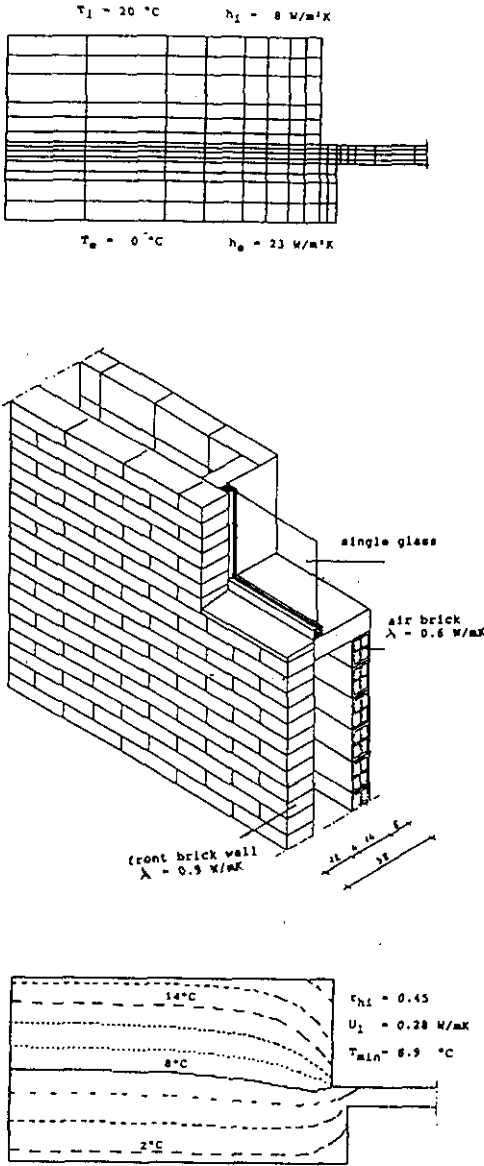


figure 3.16 Vertical cross section of a floor-external wall junction: e) and f) outside insulation.



a

figure 3.17 Horizontal cross section of a window - cavity wall junction.
 a) external leaf, no cavity insulation, single glazing

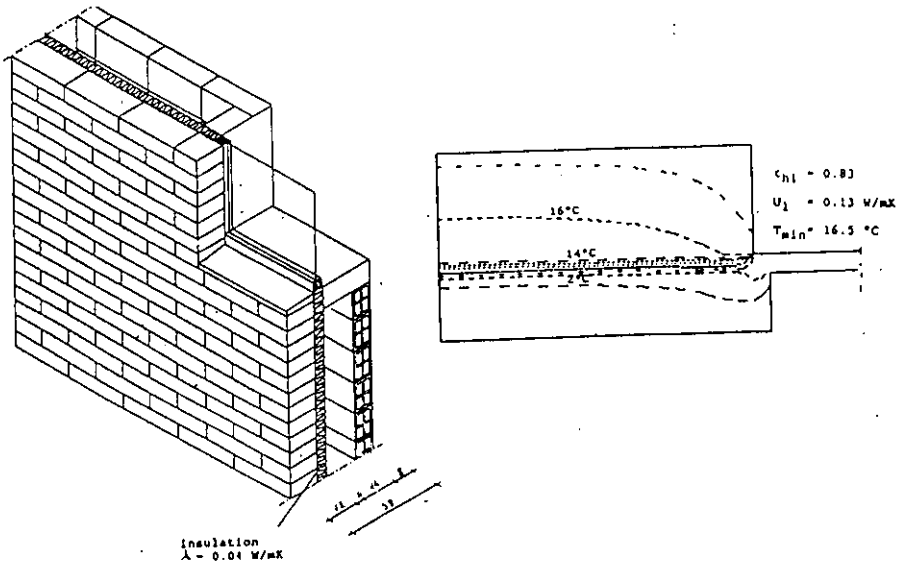
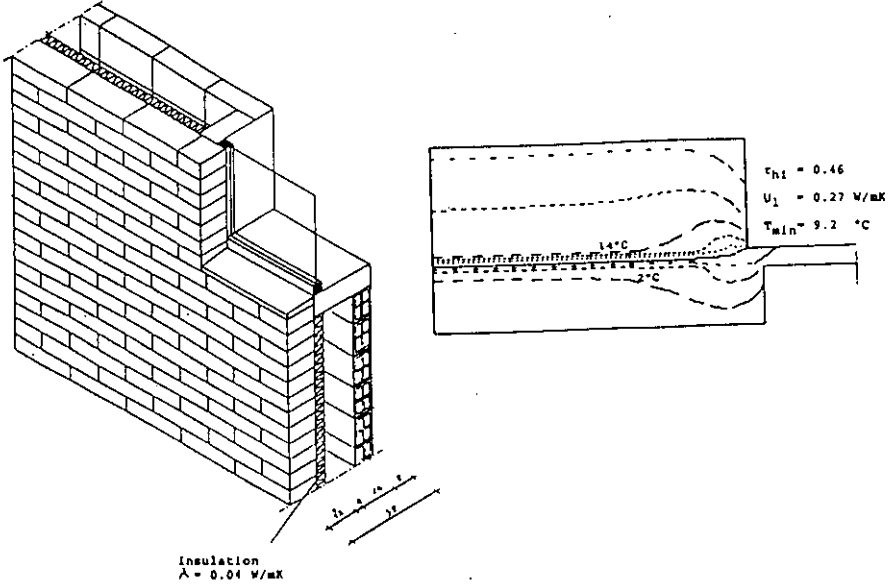
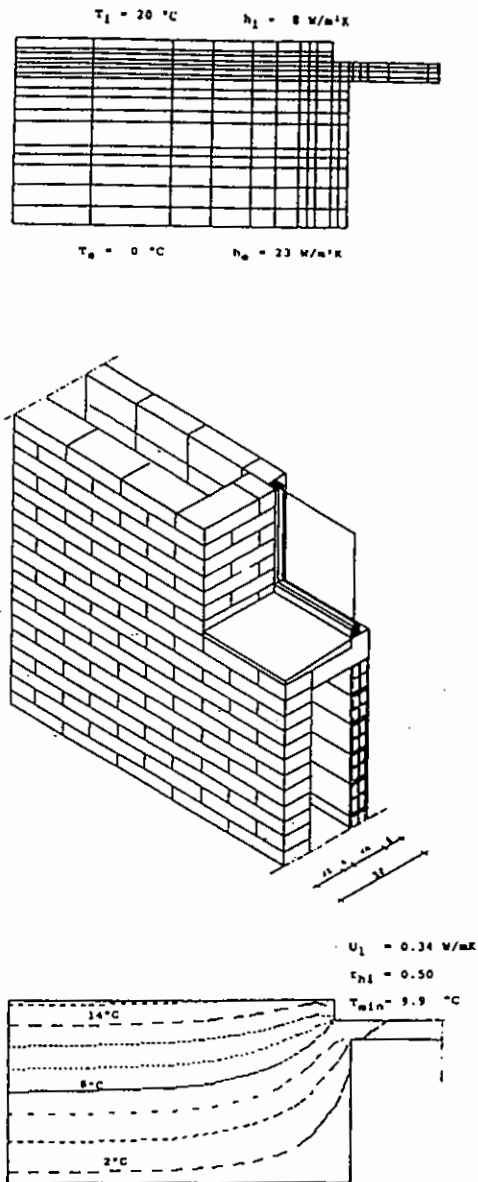
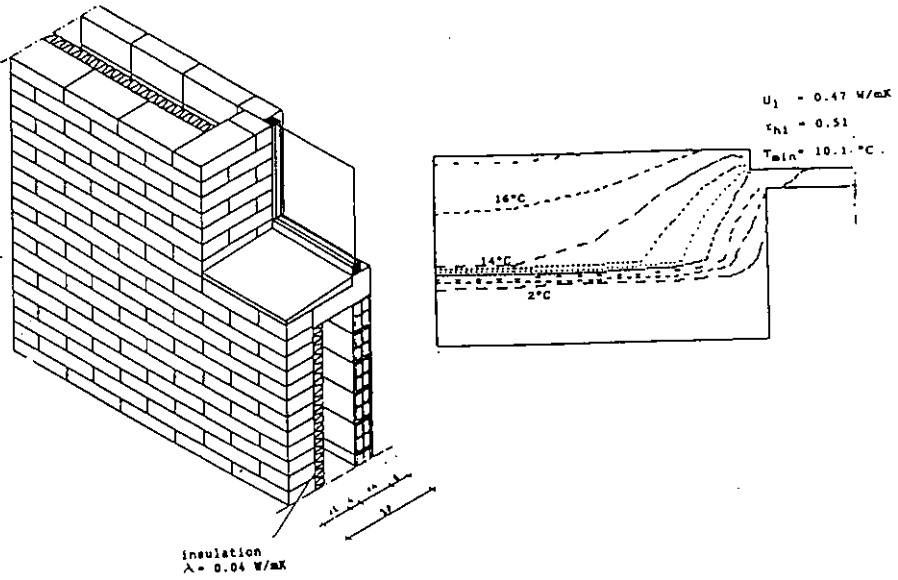


figure 3.17 Horizontal cross section of a window - cavity wall junction.
 b) external leaf, 4 cm cavity insulation, single glazing
 c) external leaf, 4 cm continuous cavity insulation, single glazing

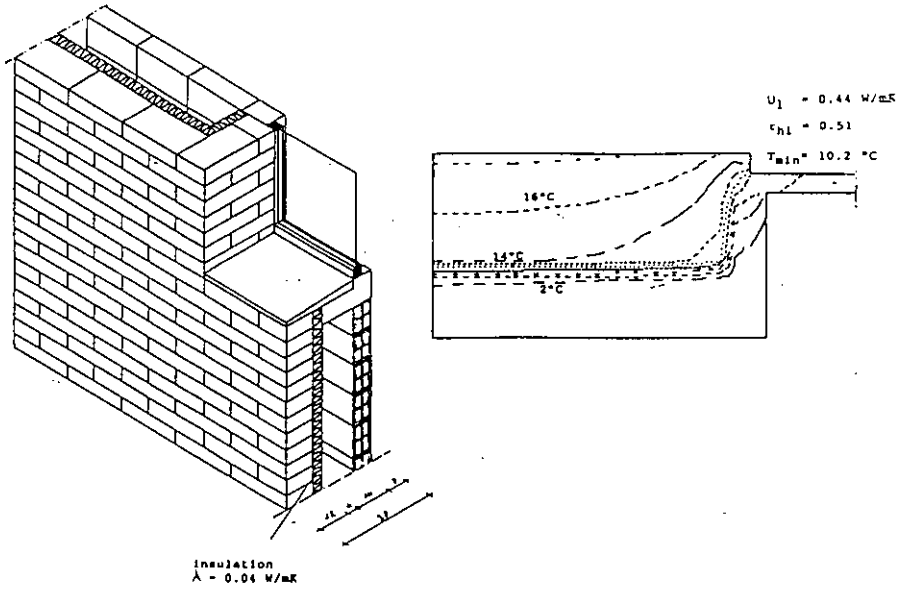


d

figure 3.17 Horizontal cross section of a window - cavity wall junction.
 d) internal leaf, no cavity insulation, single glazing



e



f

figure 3.17 Horizontal cross section of a window - cavity wall junction.
 e) internal leaf, 4 cm cavity insulation, single glazing
 f) internal leaf, 4 cm cavity and reveal insulation single glazing

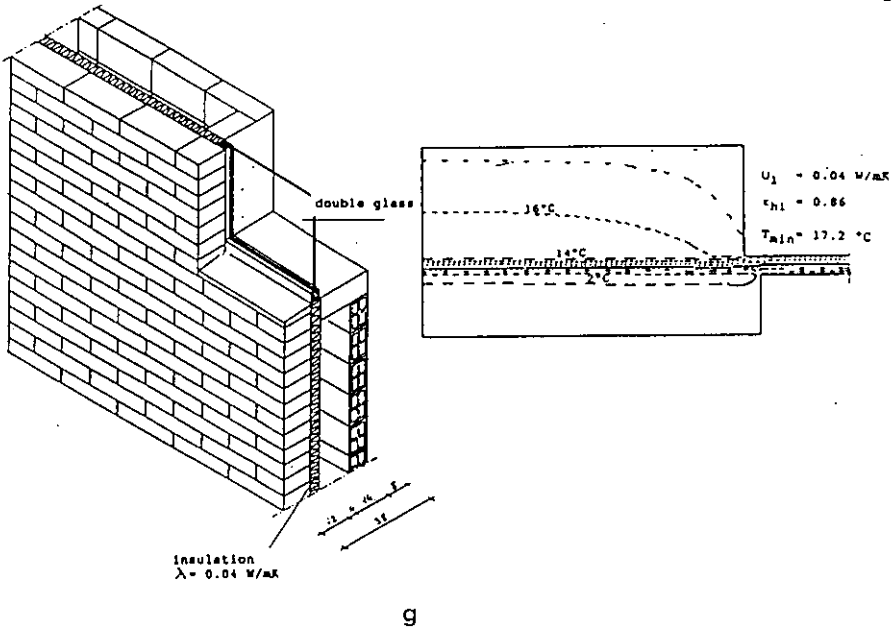


figure 3.17 Horizontal cross section of a window - cavity wall junction.
 g) external leaf, 4 cm continuous cavity insulation, double glazing

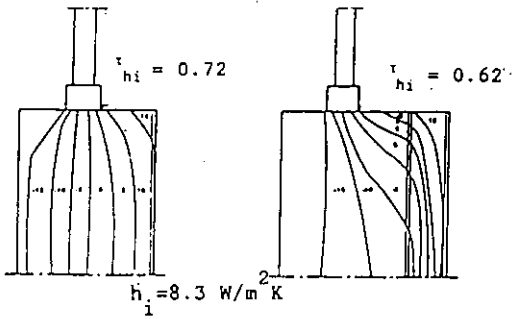


figure 3.18 Temperature contours at a window splay in a 38 cm brick wall, plus 10 cm insulation.

3.1.4.4 Three-dimensional thermal bridges (Steady-state)

Some examples of three-dimensional thermal bridge calculations are reported in literature. The analysis of 3D details is more complex and much more time consuming than a 2D calculation, so approximate methods to calculate the 3D temperature factor from the results of a 2D analysis may be useful [43,45]. In [45], the basic idea is that when $\tau_{hi}^{2D} < \tau_{hi}^{1D}$, one may write:

$$\frac{1}{\tau_{hi}^{2D}} = \frac{1}{\tau_{hi}^{1D}} + \frac{1}{\tau'} \quad (3.41)$$

For a 3D thermal bridge where in fact 3 2D thermal bridges join, three contributions of the type $1/\tau'$ must be added to τ_{hi}^{1D} . Comparative calculations have finally lead to the following equation:

$$\frac{1}{\tau_{hi}^{3D}} = \frac{1}{\tau_{hi,x}^{2D}} + \frac{1}{\tau_{hi,y}^{2D}} + \frac{1}{\tau_{hi,z}^{2D}} - \frac{2}{\tau_{hi}^{1D}} \quad (3.43)$$

where $\tau_{hi,x}^{2D}$, $\tau_{hi,y}^{2D}$ and $\tau_{hi,z}^{2D}$ are the 2D temperature factor of the 2D thermal bridges along the x, y and z- axis (fig. 3.19). τ_{hi}^{1D} is the mean value of 1D τ_{hi} - values of the three walls, shaping the 3D thermal bridge.

As approximate method, its application is restricted to 3D thermal bridges, where the thermal resistance of the three walls and the τ_{hi} values of each 2D thermal bridge obey certain conditions.

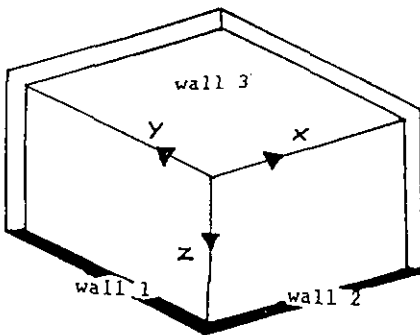


figure 3.19 Three-dimensional corner and reference axis.

3.1.4.5 Influence of non-steady-state conditions

In [18] and [22] solutions for the non-steady-state temperature field in thermal bridges are given, showing that there isn't a pronounced transient effect on the heat losses. On the other hand, the results show that the greater the heat capacity of the thermal bridge composing structural parts, the more important are the inertia in inside surface temperature oscillations.

3.1.5 Conclusions

Predicting the inside surface temperatures on the building envelope is of primary importance to assess mould and condensation risks. This requires, even in steady-state, the solution of the 2D or 3D conduction equation to get the thermal field in some peculiar zones of the envelope, called "thermal bridges". Sophisticated numerical methods are available. The time needed to prepare the input for the computer programmes, still inspires researchers to try simplified methods, able to give the surface temperature with good accuracy at least for a class of thermal bridges. To help the designer, others produced catalogues of thermal bridges.

Not all simplified methods give an insight in the physics involved. Owing to that, they don't help for advising possible improvements. Catalogues are not always useful, when a designer wants to develop new ideas.

For these reasons numerical methods seem to be, at least for the 2D problems, the best approach. Their utility in choosing good construction details was proved with some examples. Nevertheless, the quantitative results, i.e. the inside surface temperatures found, may be quite diverging from the in situ values, even though the qualitative importance of the instrument is out of doubt. This is mainly due to the uncertainty in data input, especially the inside surface film coefficient. The user of numerical methods must be aware of the fact that the input of non realistic data gives wrong results even although the calculation method assures good accuracy. The standardised h_i - and h_o - values, adopted to calculate heat losses, are not precise enough to assure a correct surface temperature evaluation. Especially h_i must have its real value at the thermal bridge.

For 3D problems, solving them with numerical methods is heavy. A good guess can be obtained from 2D results, combined with approximating formulas.

The solution of 2D and 3D problems in non-steady-state conditions learns that, because of the thermal capacity of the structure, high relative humidities or surface condensation may be present for a certain period of time, although it doesn't appear in steady-state. The significance and the importance of this result cannot be fully understood without knowledge of the response of mould growth to dynamic conditions.

3.2 CONVECTIVE AND RADIATIVE HEAT TRANSFER

3.2.1 Introduction

The inside thermal surface film or surface heat transfer coefficient strongly influences mould growth and condensation in dwellings. It consists of a convective and a radiative part. Radiation and convection being two different thermal phenomena, they should be considered separately. In most cases, the theory of surface film coefficients has been restricted to flat, undisturbed wall surfaces. There is only scarce literature on surface heat transfer coefficients in corners or at walls behind furniture. This precisely concern the investigations, conducted within the frame of IEA-Annex XIV.

The influence of the exterior surface film coefficient (h_a) on the U- value of a wall is shown in figure 3.20. Obviously, the impact is small in cases of U-values, used today in buildings. Therefore, the description of convective and radiative heat transfer at exterior surfaces is not included..

3.2.2 Radiative heat transfer

If two surfaces at different temperatures face each other, a radiative heat transfer in the range 0.8 to 800 μm takes place. The energy emitted depends on the surface temperature and material. The maximum radiation at any temperature is emitted by black surfaces. Planck's radiation law states that the radiation exitance distribution depends on temperature and wavelength [46]:

$$E_b(\lambda, T) = \frac{C_1 \cdot \lambda^{-5}}{\exp(C_2/\lambda T) - 1} \quad (\text{W}/(\text{m}^2 \cdot \text{m})) \quad (3.43)$$

with E_b : the spectral exitance ($\text{W}/(\text{m}^2 \cdot \text{m})$)
 $C_1 = 0.374 \cdot 10^{-16}$ (W/m^2)
 $C_2 = 1.439 \cdot 10^{-2}$ ($\text{K} \cdot \text{m}$)
 λ : wavelength (m)
 T : absolute temperature (K)

The total amount of energy per m^2 or exitance E_b (W/m^2) emitted by a black surface, related to its temperature, is found by integrating (3.43)

$$E_b(T) = \int_{\lambda=0}^{\infty} \frac{C_1 \cdot \lambda^{-5}}{\exp(C_2/\lambda T) - 1} d\lambda = \sigma \cdot T^4 \quad (\text{W}/\text{m}^2) \quad (3.44)$$

with $\sigma = 5.67 \cdot 10^{-8} \text{ W}/(\text{m}^2 \cdot \text{K}^4)$ (= Stephan-Boltzmann constant)

The exitance E_b is the radiation, emitted into a hemisphere. Radiation in a specified direction is expressed by Lambert's cosine law [3.45].

$$I_{b,\beta} = I_{b,n} \cdot \cos \beta \quad (\text{W}/(\text{m}^2 \cdot \text{rad})) \quad (3.45)$$

with $I_{b,n}$: radiation intensity in the normal direction (W/m^2)
 $I_{b,\beta}$: radiation intensity in the direction β (W/m^2)
 β : angle between the radiation direction and the normal direction (-)

By integrating (3.45) over the hemisphere, the following equation is obtained [3.45]:

$$E_b(T) = \pi \cdot I_{b,n} \quad (\text{W}/\text{m}^2) \quad (3.46)$$

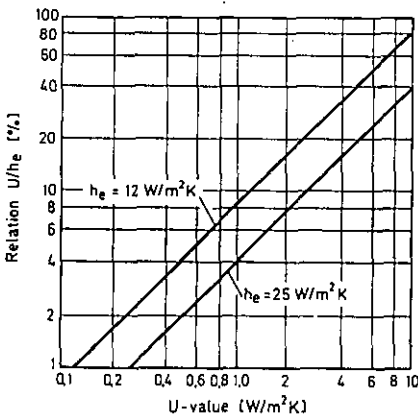


Figure 3.20: Relationship between the exterior surface film coefficient h_e and the thermal transmittance U of an external wall.

Surfaces in buildings differ from an idealised black body. The emissivity ϵ is defined as the ratio of the exitance of the real surface to the exitance of the black surface at a specified temperature. Hence, the exitance of a real (grey) surface is:

$$E(T) = \epsilon E_b(T) = \epsilon \sigma T^4 \quad (\text{W/m}^2) \quad (3.47)$$

Strictly speaking, Lambert's cosine law only applies to black surfaces. For irregular building material surfaces the reflection is more complex. According to Kirchhoff, the ratio of emissivity ϵ to absorption a at a given temperature is 1 for all bodies. a and ϵ are a function of temperature [3.46]

$$\epsilon = a = f(T) \quad (3.48)$$

with ϵ : emissivity (-)
 a : absorptivity (-)

The heat transferred by radiation from a surface A_1 to a surface A_2 depends on the size, orientation, temperature and emissivity of both surfaces. If two equal surfaces A are parallel and their area is large compared to their distance, the radiation heat flow is given by the following formula:

$$\Phi_{12} = \frac{A \cdot \sigma \cdot (T_1^4 - T_2^4)}{1/\epsilon_1 + 1/\epsilon_2 - 1} \quad (\text{W}) \quad (3.49)$$

with Φ_{12} : radiation heat flow (W)
 A : surface (m^2)
 ϵ_1, ϵ_2 : emissivity of the surfaces 1 and 2
 T_1, T_2 : temperature of the surfaces 1 and 2 in K

For the calculation of the radiation heat flow between arbitrary surfaces, the shape factors have to be known. They are defined as:

$$F_{ij} = \frac{1}{A_i} \cdot \int_{A_i} \int_{A_j} \frac{\cos \beta_1 \cdot \cos \beta_j}{\pi \cdot r_{ij}^2} \cdot dA_i \cdot dA_j \quad (3.50)$$

with β_1 : angle between r_{ij} and the normal direction of dA_i (-)
 β_j : angle between r_{ij} and the normal direction of dA_j (-)
 r_{ij} : distance of the centre points of dA_i and dA_j respectively (m)

F_{ij} represents the fraction of the radiation heat flow from surface A_i being intercepted by surface A_j (fig 3.21)

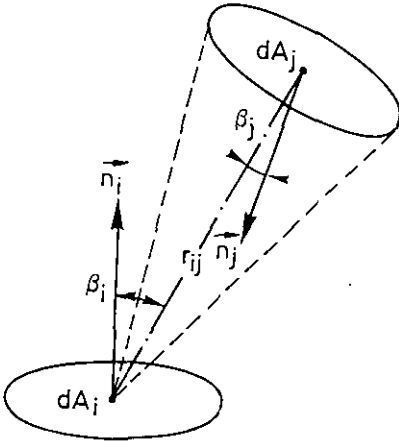


figure 3.21 Radiative heat transfer between two surface elements i and j

The fraction emitted by A_j and intercepted by A_i is expressed by the inverse shape factor:

$$F_{ji} = \frac{1}{A_j} \int_{A_i} \int_{A_j} \frac{\cos \beta_i \cdot \cos \beta_j}{\pi \cdot r_{ij}^2} \cdot dA_i \cdot dA_j \quad (3.51)$$

For the shape factor relations to be true, the surfaces are assumed diffuse and isothermal. By combining integrals (3.50) and (3.51), the reciprocity relation is obtained:

$$A_i F_{ij} = A_j F_{ji} \quad (m^2) \quad (3.52)$$

For the surfaces of an enclosed space, the summation rule applies:

$$\sum_{j=1}^N F_{ij} = 1 \quad (3.53)$$

This means that the total radiation emitted by surface i is intercepted by all other surfaces.

To calculate the radiation heat transfer within a room with N surfaces, N^2 shape factors are necessary. Not all have to be calculated directly however. By using (3.52) and (3.53), only $N(N-1)/2$ factors remain to be computed by solving the double integrals (3.50) or (3.51). Solutions for various geometries and surface orientations are found in literature [49-53].

With the shape factors, the radiation transferred between 2 black surfaces i and j may be expressed as:

$$Q_{12} = A_1 \cdot F_{1j} \cdot \sigma \cdot (T_1^4 - T_j^4) \quad (W) \quad (3.54)$$

If the radiation transfer takes place between surface i and N others, the radiation absorbed or emitted by surface i is:

$$\sum_{j=1}^N A_1 \cdot F_{1j} \cdot \sigma \cdot (T_1^4 - T_j^4) \quad (W) \quad (3.55)$$

Equation (3.55) is as simple only for black surfaces. They however do not exist. Multiple reflection makes the computation more complicated.

With following assumptions:

- the surface temperature is constant;
- emissivity, absorption and reflection are independent of wavelength and direction;
- all surfaces are diffuse emitters and reflectors;
- $\sum F_{1j} = 1$;

it is possible to calculate the density of heat flow rate at surface i due to radiation to the other room enclosing surfaces with equation [54]:

$$q_i = \epsilon_i \cdot \sigma \cdot T_{si}^4 - \epsilon_i \cdot \sigma \cdot \sum_{j=1}^N (F_{ij} \cdot T_{sj}^4) + \epsilon_i \cdot \sum_{j=1}^N (F_{ij} \cdot \frac{1 - \epsilon_j}{\epsilon_j} q_j) \quad (W/m^2) \quad (3.56)$$

If we write the equation for all N walls of a room, a linear system with N unknown densities of heat flow rate $q_1 \dots q_N$ results. The system may be solved either by matrix inversion or by iteration.

Dropping the third term in (3.56), gives as approximation:

$$q_i = \epsilon_i \cdot \sigma \cdot (T_{si}^4 - \sum_{j=1}^N F_{ij} \cdot T_{sj}^4) \quad (W/m^2) \quad (3.57)$$

In [55] however, it is stated that in certain cases (3.57) may give wrong results.

Radiation within a room becomes simple to describe when transforming it in a two surfaces system: an external wall, surface A_w , emissivity ϵ_w , surface temperature T_w , and the remaining five surfaces (ceiling, floor, interior walls), total surface A_1 , identical emissivity ϵ_1 , transposed to a

planparallel surface at mean surface temperature T_R . The radiative heat exchange between the external wall and the planparallel interior surface follows from:

$$\Phi_{wi} = \frac{\sigma \cdot (T_w^4 - T_R^4)}{(1 - \epsilon_w) / (\epsilon_w \cdot A_w) + 1 / (A_w \cdot F_{wi}) + (1 - \epsilon_i) / (\epsilon_i \cdot A_i)} \quad (W) \quad (3.58)$$

Example

Consider a cubic space with:

$$\begin{aligned} A_w &= 10 \text{ m}^2, & \Sigma A_i &= 50 \text{ m}^2 \\ \epsilon_w &= 0.90, & \epsilon_i &= 0.93 \\ T_w &= 288\text{K}, & T_R &= 293\text{K} \end{aligned}$$

The radiation flow from the internal walls to the external one, is 246.9 W. By definition, the radiative surface film coefficient now is given by:

$$h_r = \frac{\Phi_{wi}}{A_w \cdot (\theta_i - \theta_w)} \quad (W/(m^2 \cdot K)) \quad (3.59)$$

h_r becomes: 4.9 W/(m²·K).

This value of the radiative surface film coefficient h_r , is a mean for the wall. In corners, where external wall and internal surfaces meet, h_r is lower (see 3.2.6).

3.2.3 Convective heat transfer

Heat transfer between the air and a wall takes place by convection. The density of heat flow rate is proportional to the temperature difference between the air and the surface:

$$q_{ci} = h_c \cdot (\theta_i - \theta_s) \quad (W/m^2) \quad (3.60)$$

with q_{ci} : density of convective heat flow rate (W/m²)
 h_c : convective surface film coefficient (W/(m²·K))
 θ_i : indoor air temperature (°C)
 θ_s : surface temperature (°C)

The convective surface film coefficient h_c depends on the flow pattern of the air, the temperature of the wall and the temperature of the air.

A distinction is made between forced and free convection. Free convection is important when considering inside surfaces. It is caused by temperature induced differences in air density. If the air flow is exactly parallel to the wall surface, one has laminar flow. In the case of air, whirling against the wall surface, one has turbulent air flow. Independent of the air flow, there remains always a laminar surface air layer against the wall. In this surface layer, heat transfer takes place by conduction, perpendicular to the wall.

$$h_c \cdot (\theta_1 - \theta_s) = -\lambda \cdot (\partial\theta/\partial n)_s \quad (\text{W/m}^2) \quad (3.61)$$

with λ : thermal conductivity of the air near the wall (W/(m.K))
 $(\partial\theta/\partial n)_s$: temperature gradient of the air against the wall (K/m)

Convective heat transfer can be described by a system of differential equations. [56-58]. Solving the system however, is only possible for some very simple cases.

Nusselt's similarity theory allows to determine similarity criteria. As dimensionless parameters are found:

$$\text{Nusselt number: } Nu = \frac{h_c \cdot l}{\lambda} \quad (3.62)$$

$$\text{Grasshof number: } Gr = \frac{\beta \cdot g \cdot l^3}{\nu^2} \cdot \Delta\theta \quad (3.63)$$

$$\text{Prandtl number: } Pr = \frac{\nu}{a} \quad (3.64)$$

$$\text{Reynolds number: } Re = \frac{v \cdot l}{\nu} \quad (3.65)$$

with l : length (m)
 λ : thermal conductivity of the air (W/(m²K))
 β : coefficient of thermal expansion (K⁻¹)
 g : gravitational acceleration (m/s²)
 ν : cinematic viscosity (m²/s)
 a : thermal diffusivity coefficient (m²/s)
 v : velocity (m/s)
 $\Delta\theta$: temperature difference between the surface and the fluid (K)

The following functional equation is valid for the convective heat transfer between the air and an inside wall [56]:

$$Nu = C \cdot (Gr \cdot Pr)^n \quad (3.66)$$

C and n are constants. They depend on whether the flow is laminar or turbulent. According to [56], the change from laminar to turbulent takes place

at approximately $Gr.Pr = 10^9$. For the flow range $10^8 < Gr.Pr < 10^{12}$, various equations are given in literature. One often finds [59]:

$$Nu = 0,13. (Gr.Pr)^{1/3} \quad (3.67)$$

Additional algorithms for other ranges and geometries are tabulated in 3.3.

Relations (3.67) and (3.62) allow to calculate h_c :

$$h_c = (\lambda/l).Nu \quad (W/(m^2.K)) \quad (3.68)$$

$$\text{or } h_c = 0,13 \lambda. (\beta.g/(\nu.a))^{1/3} .\Delta\theta^{1/3} \quad (W/(m^2.K)) \quad (3.69)$$

The characteristic length l does not appear in equation (3.69). This means that h_c is independent of the geometry of the wall surface.

GEOMETRY	FORMULA	APPLICABLE RANGE
Vertical plate (L=height)	$Nu = 0.59 (Gr.Pr)^{1/4}$	$10^4 < Gr.Pr \leq 10^9$
	$Nu = 0.129 (Gr.Pr)^{1/3}$	$10^9 < Gr.Pr < 10^{12}$
Horizontal plate (L = mean of dimensions)		
A. Upper surface of warm plate or lower surface of cool plate	$Nu = 0.54 (Gr.Pr)^{1/4}$	$10^5 < Gr.Pr \leq 2.10^7$
	$Nu = 0.14 (Gr.Pr)^{1/3}$	$2.10^7 < Gr.Pr < 3.10^{10}$
B. Upper surface of cool plate or lower surface of warm plate	$Nu = 0.44 (Gr.Pr)^{1/5}$	$10^5 < Gr.Pr < 2.10^7$
Vertical enclosed space (L = height, d = width, L/d > 3)	$Nu = 0.18 Gr^{1/4}(L/d)^{-1/9}$	$2.10^4 < Gr \leq 2.10^5$
	$Nu = 0.065 Gr^{1/3}(L/d)^{-1/9}$	$2.10^5 < Gr < 10^7$
Horizontal enclosed space (L = height)		
A. Lower surface warmer	$Nu = 0.195 Gr^{1/4}$	$10^4 < Gr \leq 4.10^5$
	$Nu = 0.068 Gr^{1/3}$	$4.10^5 < Gr < 4.10^8$
B. Upper surface warmer	$Nu = 1$	

Table 3.3: Free convection algorithms according to [67]

For instance, at an air temperature θ_i of 20°C, a wall surface temperature θ_s of 16°C and the temperature dependent constants $\lambda = 0.026 \text{ W/(m.K)}$,

$\beta = 3.43 \cdot 10^{-3} \text{ K}^{-1}$, $\nu = 15.1 \cdot 10^{-6} \text{ m}^2/\text{s}$, the surface heat transfer coefficient turns to:

$$h_c = 1.57 \cdot \Delta\theta^{1/3} \approx 2.5 \text{ W/(m}^2\text{.K)} \quad (3.70)$$

At the air temperature θ_i and wall surface temperature θ_s usually recorded in rooms, the value 1.57 changes only slightly. So for building applications, equation (3.69) may by definition be simplified to:

$$h_c = 1.57 \cdot \Delta\theta^{1/3} \quad (\text{W/(m}^2\text{.K)}) \quad (3.71)$$

In [61] and in a more recent study [55], as constant C in (3.66) is given: 0.10. (3.69) then becomes:

$$h_c = 1.21 \cdot \Delta\theta^{1/3} \quad (\text{W/(m}^2\text{.K)}) \quad (3.72)$$

In [62] and [63], the following relation is found:

$$h_c = 2.03 \cdot (\Delta\theta/H)^{1/3} \quad (\text{W/(m}^2\text{.K)}) \quad (3.73)$$

with H: wall height (m)

The equation was obtained experimentally: in an enclosure convective heat transfer from a heated vertical wall to the cooled opposite vertical wall was studied.

In the 1981 ASHRAE handbook [64], the convective surface film coefficient is given by:

$$h_c = 1.31 \cdot \Delta\theta^{1/3} \quad (\text{W/(m}^2\text{.K)}) \quad (3.74)$$

In fig. 3.22 the formulas (3.72), (3.73), (3.74) are shown as a function of the temperature difference $\Delta\theta$, for a wall height of 2.50 m.

From the figure it can be deduced that (3.72), (3.73) and (3.74) differ less than 0.5 W/(m².K) for temperature differences $\Delta\theta$ below 5K and agree still better in the higher temperature difference range.

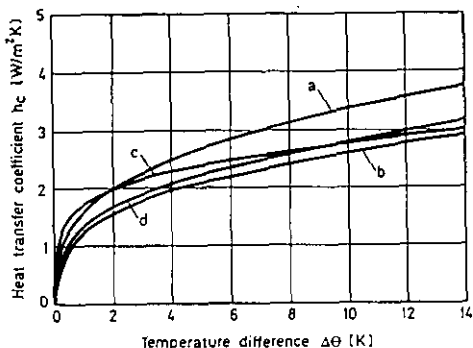


Figure 3.22 Convective surface film coefficient h_c dependent on the temperature difference $\Delta\theta$ between indoor air and wall surface for some examples taken from literature.

- a: $h_c = 1.57 \cdot \Delta\theta^{1/3}$ according to [59]
- b: $h_c = 1.21 \cdot \Delta\theta^{1/3}$ according to [55, 61]
- c: $h_c = 2.03 \cdot (\Delta\theta/H)^{1/3}$ according to [62, 63]
- d: $h_c = 1.31 \cdot \Delta\theta^{1/3}$ according to [64]

3.2.4 Total surface film coefficient

The total surface film coefficient consists of a convective and a radiative part:

$$h_i = \frac{q_c + q_r}{\theta_i - \theta_{si}} \quad (\text{W}/(\text{m}^2 \cdot \text{K})) \quad (3.75)$$

- with h_i total surface film coefficient
- q_c convective heat flow rate
- q_r radiative heat flow rate
- θ_i inside reference temperature
- θ_{si} surface temperature

3.2.5 Influence of the reference temperature on the surface film coefficient

In a heated room, a distinction has to be made between the air temperature and the effective or resulting temperature. The air temperature denotes the gas temperature of the air. It is measured with a radiation-protected temperature sensor. In general, the air temperature is a function of place. Its stratification largely depends on the heating system. The effective or resulting

Ceiling and floor are provided with an additional thermal insulation of 6 and 8 cm respectively, giving U-values $0.45 \text{ W}/(\text{m}^2\cdot\text{K})$ and $0.38 \text{ W}/(\text{m}^2\cdot\text{K})$. The room is heated with a convector on constant power, installed against an internal wall near the ceiling. A protection prevents radiative heat exchange with the external walls. In- and outside air temperature and surface temperatures are measured at various heights with thermocouples. During the measuring period, the air temperature in the climate simulator and the room are set at 0 and 21°C respectively.

3.2.6.2 Measurement results

Figure 24 gives the vertical air temperature profile, measured at the centre of the room. A pronounced temperature stratification is observed: the air temperature increases from 17.6°C near the floor to 22.4°C near the ceiling. The mean indoor air temperature in the middle is 19.6°C .

The measured surface temperatures and the material and envelope part data were used to calculate the densities of heat flow rate with a 3D steady and non-steady-state computer programme [66]. The total surface film coefficient found in edges and corners, given by the ratio $q/(\theta_{\text{ref}} - \theta_s)$, is shown in fig. 3.25, on the left related to the mean air temperature at the level of measurement, on the right to the central air temperature at a height of 1.70 m. Left, the minimum surface film coefficient in the edge is below $6 \text{ W}/(\text{m}^2\text{K})$. From edge to centre of the wall, the coefficient increases exponentially to a maximum value of nearly $8 \text{ W}/(\text{m}^2\text{K})$.

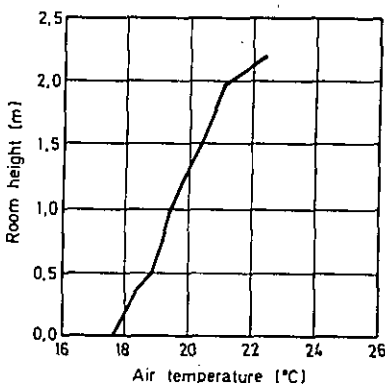


Figure 3.24 Air temperature distribution measured at the centre of the test room

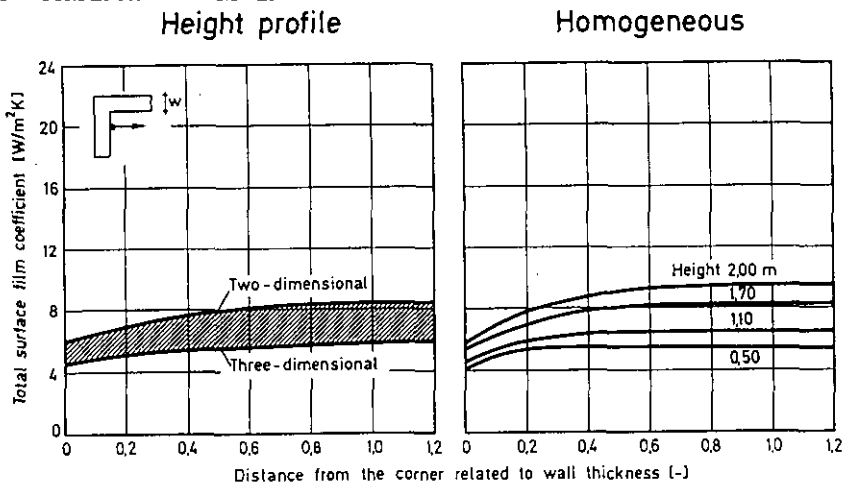


Figure 3.25 The total film coefficient, measured in a massive external walls edge, as a function of the distance from the edge (given by the distance - wall thickness ratio) for various heights.
 θ_{ref} : mean inside air temperature at each height
 two-dimensional : θ_i at mean room height
 three-dimensional: θ_i directly under the ceiling
 θ_{ref} : inside air temperature at the centre of the room, at a height of 1.7m

The length of influence of monolithic edges can be assumed equal to the wall thickness. In formula:

$$h_{i,x} = h_i \cdot [1 - (1 - \frac{h_{i,edge}}{h_i}) \cdot \exp(-3 \cdot x/s)] \quad (W/(m^2.K)) \quad (3.77)$$

with $h_{i,x}$ Total surface film coefficient at a distance x from the edge
 h_i Total surface film coefficient in the centre of the wall
 $h_{i,edge}$ Total surface film coefficient in the edge
 x distance from the corner (m)
 s wall thickness (m)

In the corner, the surface film coefficient is lower with a minimum h_i of $\pm 4.5 W/(m^2.K)$. From corner to edge, the value raises to $6 W/(m^2.K)$. The hatched section shows the surface film coefficient when passing from an edge to a corner.

However, in the calculation models in use for the heat demand or the thermal and energy performance buildings, a constant indoor air temperature is generally assumed. At the right, fig. 3.25 therefore shows for several heights on the external wall the corresponding values of the surface film coefficient in relation to the central air temperature at 1.70 m. A wider range of values results. At a height of 2.00 m, h_i is above $6 W/(m^2.K)$, and

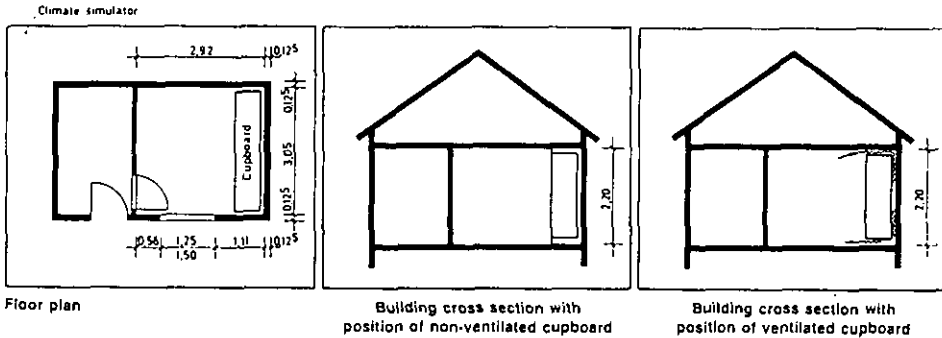


Figure 3.26 Model room for the determination by way of measurements of the surface film coefficient for various heating systems and cupboard positions.

increases to $10 \text{ W}/(\text{m}^2.\text{K})$ in the centre of the wall. This illustrates the scatter in values by linking h_i to a constant central air temperature, when in reality the air temperature is height-related. At all heights, the profile again is an exponential function from the type (3.77).

3.2.7 Influence of furniture and the heating system on the surface film coefficient.

The inside surface film coefficient at external walls depends also on the heating system and the arrangement of furniture. A cupboard placed before an external wall in fact influences the radiative and the convective exchanges with the room and acts as extra inside thermal resistance. For built-in cupboard without backside ventilation, the convective exchange for example is particularly small. Floor heating, radiator heating and air heating, the most common systems in use, differ in location, number, size and temperature of heat-emitting surfaces. Heat transfer by radiation now is largely determined by those parameters. They also have an impact on the inside air flow and thus on the convective heat transfer.

3.2.7.1 The tests

A second test building was constructed in the climate simulator, with ground plan and section as given in figure 3.26. The room considered has three external walls, a floor of $3.05 \times 2.92 \text{ m}^2$ and a height of 2.20 m. One external wall has a double glazed window of 1.90 m^2 . The three remaining walls separate interior zones. The external walls are made of cellular concrete, $d = 0.125 \text{ m}$, thermal resistance $R = 0.9 \text{ (m}^2\text{.K)/W}$. The room is heated by floor-, radiator- or air heating. The heated air inlet is located in the floor under the window. There is also the radiator. The heating systems have a set-point such that a central air temperature of $20\text{--}21^\circ\text{C}$ at 1.70 m is maintained in the test room. The temperature in the adjoining rooms is kept at 20°C , the outside temperature at -10°C . The location of the cupboard is shown in fig. 3.26: in the middle a built-in cupboard, on the right a back-ventilated cupboard on feet (150mm). The distance to the ceiling is 50 mm, to the exterior walls 25 mm. With the built-in cupboard, these gaps are closed.

The surface film coefficient behind the cupboard, is determined at specified locations by measuring the heat flow rate through and the surface temperatures on the external wall. The reference air temperature is logged in the centre of the room, either at the same height of the specified location, or at 1.70 m. Air and surface temperatures are measured with thermocouples. The air-temperature ones are radiation protected. The densities of heat flow rates are recorded with heat flow meters.

3.2.7.2 Measurement results

For all heating systems, the surface film coefficient is measured on an unobstructed external wall and on an external wall behind the back of the vented and the built-in cupboard.

Temperature distribution

The temperature distribution in a heated room largely depends on the heating system. The central air temperature recorded as a function of height, is shown in figure 3.27. In case of floor heating, the value first decreases, then remains nearly constant between 0.8 and 1.70 m, and rises again near the ceiling. This increase is due to the ceiling surface

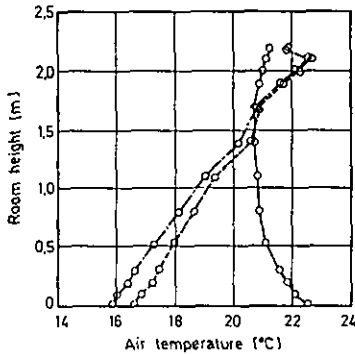


Figure 3.27 Air temperature distribution measurements for different heating systems when determining the surface coefficient of heat transfer behind cupboards

- Floor heating
- - - Radiator heating
- · · Air heating

temperature: higher than the indoor air temperature because of radiative exchanges with the floor. The temperature profiles for radiator and air heating are nearly identical. However, the gradient is the largest for air heating.

Heat transfer at an unobstructed external wall

The surface film coefficients for the different heating systems at an unobstructed external wall are given in fig.3.28. The values were measured at the centre of the wall at 6 different heights: 0.10, 0.30, 1.10, 1.90, 2.0 and 2.10 m above floor level. Hence, they are located outside the edges wall-floor and wall-ceiling. On the left, the central air temperature at the respective height is the reference, on the right, the central air temperature at 1.7 m is the reference. On the left, the surface film coefficient at 1.1 m is nearly $8 \text{ W}/(\text{m}^2.\text{K})$ for floor heating, approximately $7 \text{ W}/(\text{m}^2.\text{K})$ for radiator heating and a little less than $7 \text{ W}/(\text{m}^2.\text{K})$ for air heating. Towards the ceiling, the values decrease for the 3 heating systems. Near the floor, slightly higher values are recorded for radiator and air heating.

If h_i is related to the central indoor air temperature at 1.70 m (see figure on the right), an entirely different profile results, reflecting the

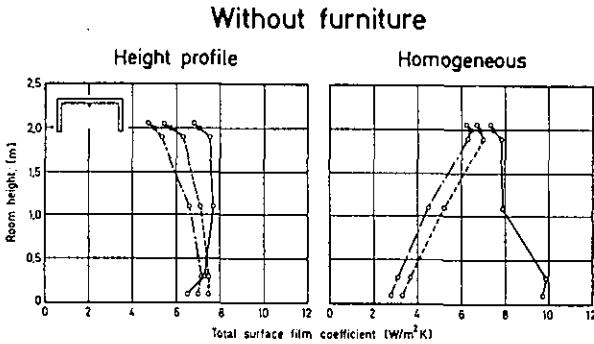


Figure 3.28 Total surface film coefficient measured at a monolithic external wall for different heating systems and various room heights: no furniture against the wall.

— Floor heating
 - - - - Radiator heating
 ····· Air heating

temperature stratification. For air heating, the lowest surface heat transfer coefficient, $3 W/(m^2K)$, is measured at 0.10 m above the floor.

Heat transfer at an external wall with cupboard on feet (ventilated cupboard)
 Heat transfer is impaired by a cupboard placed against the external wall. Figure 3.29 shows the values of h_1 at the centre of the wall at various heights, dependent on the heating system (floor heating, radiator heating, air heating), for an empty cupboard and a cupboard filled with clothes. The distance between the back of the cupboard and the wall is 50 mm. In addition, for floor and radiator heating, the surface film coefficients are also given for a distance of 20 mm. The surface film coefficient of a unobstructed wall is used as reference. Related to the indoor air temperature at 1.70 m, the values at 1.10 m decrease for floor heating (diagram above, right), from $8 W/(m^2.K)$ (unobstructed) to $3 - 3.5 W/(m^2.K)$ for a full and an empty cupboard respectively. With the cavity between wall and cupboard reduced to 20 mm, a value of $2.5 W/(m^2.K)$ is found for an empty cupboard. Reason: less convection by the increased flow resistance.

In the case of radiator heating, the values decrease from $5 W/(m^2K)$ (unobstructed) to $3 W/(m^2.K)$ (empty and full cupboard), which is slightly

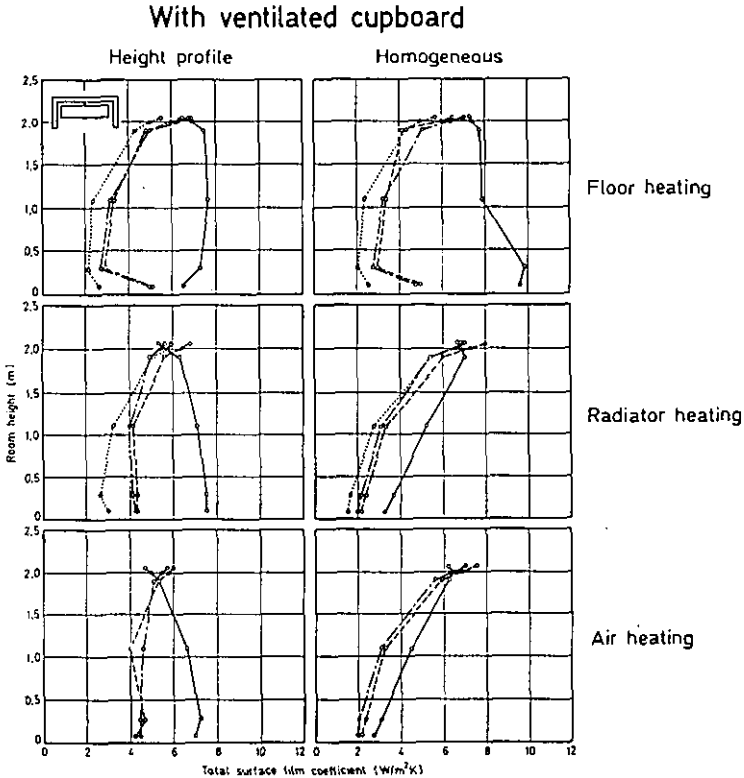


Figure 3.29 Total surface film coefficient, measured on a massive external wall for floor-, radiator- and air heating, as a function of height. Against the wall stands ventilated cupboard with feet. Height profile: related to the indoor air temperature in the centre at the height considered. Homogeneous: related to indoor air temperature in the centre at 1.70 m height.

- without furniture
- - - - - cupboard empty, distance 50 mm
- · · · · with clothes, distance 50 mm
- · - · - cupboard empty, distance 20 mm.

below those for floor heating.

The values for air heating correspond to radiator heating (see diagram below, right). h_i as a function of the room height, with as reference the central air temperature at the same height, resembles the results with as reference the central air temperature at 1.70 m. However, the profile noticeably differs from the values without furniture. The distance wall-cupboard has a strong influence on the h_i -value near the floor and at the wall centre (fig. 3.29).

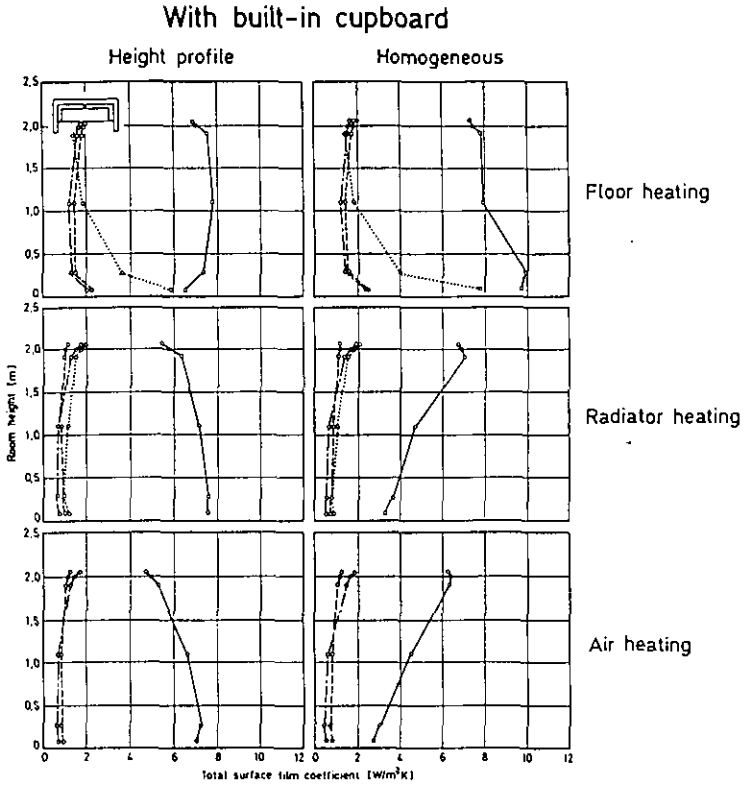


Figure 3.30 Total surface film coefficient measured at a massive external wall for floor-, radiator- and air heating, as a function of the height. In front of the wall stands a built-in cupboard. Height profile: related to the indoor air temperature in the centre at the height considered. Homogeneous: related to indoor air temperature in the centre at 1.70 m height.

- without furniture
- cupboard empty, distance 50 mm
- with clothes, distance 50 mm
- cupboard empty, distance 20 mm.

Heat transfer at an external wall with a built-in cupboard

Heat transfer at an external wall is even more impaired by a built-in cupboard. The surface film coefficient at various heights for the different heating systems, cupboard fillings and distances is shown in fig. 3.30.

With the indoor air temperature at 1.70 m as reference, the surface film coefficient at 1.10 m with floor heating decreases from 8 W/(m².K) (unobstructed) to 1.5 W/(m².K). However, for a distance of 20 mm, the value

increases to 2 W/(m²K). The values for radiator- and air heating are approximately identical. The lowest h_i of about 0.5 W/(m²K), was recorded for air heating with a filled cupboard and a wall distance of 50 mm (see fig. 3.30, on the right below).

3.2.7.3 Recommendations

Assuming a constant surface film coefficient with as reference temperature an indoor air temperature at specific height, is not sufficient to obtain correct wall surface temperatures.

External walls must not be obstructed by built-in cupboards. Due to the very low surface film coefficient in this case, the wall surface temperature may be below the indoor air dew point, even for walls with a high level of thermal insulation. If cupboards against an external wall cannot be avoided, some venting is necessary: distance between cupboard and wall and cupboard and ceiling at least 50 mm, the cupboard itself on feet of at least 100 to 150 mm high. To calculate the wall surface temperature behind the cupboard and to dimension the thermal resistance needed for avoiding mould growth, the surface film coefficient should be taken 2 W/(m²K).

3.2.8. Practical method to define the surface heat transfer in surface temperature calculations.

3.2.8.1. Introduction

For calculation of inside surface temperatures θ_s in 1D steady-state thermal conditions, the following formula applies:

$$\theta_s = \theta_i - \frac{U_{si-e}}{h_i + U_{si-e}} \cdot (\theta_i - \theta_e) \quad (^\circ\text{C}) \quad (3.78)$$

with θ_s : surface temperature (°C)
 θ_e : outside temperature (°C)
 θ_i : room temperature (°C)
 h_i : wall (internal) surface film coefficient (W/(m²K))
 U_{si-e} : wall thermal transmittance from the internal surface to the external environment, i.e. inclusive the outside surface film coefficient and exclusive the inside surface film coefficient; (W/(m²K))

The formula shows that beside the wall (characterised by its thermal transmittance U_{s_i-a}), the inside boundary conditions (characterised by the set (h, θ)) have to be known.

In the case of two- (2D) and three-dimensional (3D) heat transfer, numerical methods are used (see chapter on Modelling, thermal aspects, conduction). Beside the geometrical description and material properties (thermal conductivities), these methods normally require the inside boundary conditions in the form of a set (h, θ) . (I)

Because the mean (h, θ) , used in heat loss calculations, e.g. $(h = 8 \text{ W}/(\text{m}^2\text{K})$, $\theta_i =$ central dry resultant temperature), provide in most cases too high surface temperatures, appropriate (h, θ) - sets for thermal bridge evaluation are needed. This closing paragraph provides a method to define more realistic (h, θ) - sets.

3.2.8.2. Principles and assumptions.

- the goal of the method is to determine a safe but realistic inside boundary condition, suitable in the current calculation techniques.
- to model the convective heat transfer between a surface part and the inside environment, a constant convective surface film coefficient is introduced, coupled to the adjacent air temperature (out of the convective boundary layer). Only a vertical, constant air temperature gradient is assumed. Therefore a choice of a value for the convective surface film coefficient and a formula for the air temperature gradient suffice to model convection.
- to model the radiative heat transfer between a surface and all other surfaces (heating surfaces included), a constant radiative surface film

(I) Remark: they don't, provided that the numerical method integrates both the conduction in the geometry and the radiation and convection to the room. Until today, such methods are only rarely used in practice, mostly because a large amount of data is required. Results of such method can be found in [14].

coefficient is taken, coupled to a central radiation temperature (which is the viewfactor weighted mean surface temperature). For edges and corners, the value of the radiative heat transfer is reduced, assuming that part of the visible surfaces and the surface considered are at the same temperature. Therefore a choice of a value for the radiative surface film coefficient and a formula for the central radiant temperature suffice to model radiation.

- although the method could be adapted to define the course of the set (h, θ) along the surface, the one proposed defines a set (h, θ) which is constant in a limited zone and representative for the most critical point of the surface part considered (the corner point, the edge point). It means that the method uses only one (h, θ) set in thermal bridge calculations: the set derived for the critical point.
- although the method could be adapted for several room reference temperatures, the air temperature in the centre of the room at a height of 1.7 m is taken as reference. An assumption which was made to simplify the formulas, without affecting the results in an important way, is that this reference temperature and the air temperature in the centre of the room at half height, have the same value, denoted further as $\theta_{a,y=0}$.
- The reference temperature being defined, the purpose of the following is to derive a value for the corresponding surface film coefficient $h_{a,y=0}$.

3.2.8.3. Dimensionless temperatures.

Dimensionless temperatures are used. It means that each temperature is scaled to an outside temperature of 0°C and a reference temperature (being the central air temperature) of 1°C .

The temperature factor of a thermal bridge, defined as

$$\tau_{hi} = \frac{\theta_s - \theta_e}{\theta_{a,y=0} - \theta_e} \quad (3.80)$$

is such a dimensionless temperature. To denote dimensionless temperatures, the symbol τ is generally used:

$\tau_{a,y}$: dimensionless air temperature at a level of y m above the reference level.

τ_r : dimensionless central radiant temperature.

3.2.8.4. The air temperature gradient.

In [68] a formula, based on the analysis of several laboratory tests, is proposed for the vertical air temperature gradient. The formula expresses that the gradient is proportional to the amount of convective heat exchanged, divided by the total surface of the room walls. As shown in [69] the formula can be transformed to the following upper limit relation:

$$r_{a,y} = 1 + C_a \cdot p_c \cdot y \cdot U_m \quad (3.81)$$

with $r_{a,y}$ cfr. above.
 C_a a constant, = 0.2 m²K/W
 U_m the wall-surface weighted mean U-value (thermal transmittance) of all room walls (W/(m².K)). Surface weighted means: each U-value multiplied with the ratio between the parts surface and the sum of all parts surfaces. For inner walls the U-values are multiplied with the ratio 'difference in reference air temperature between both rooms to the difference in reference air temperature in the room considered and the outside temperature'; (inner room walls between two rooms at the same reference air temperature have a zero weighted U-value).

Remark: to calculate the U-values, standard 'heat loss' surface film coefficients may be used.
 p_c the proportion of the convective heat power to the total heat power dissipated by the heating system ($0.3 \leq p_c \leq 1$).

Possible values for p_c are:

- $p_c = 1.0$ for air heating systems
- $p_c = 0.9$ for convectors and shielded (e.g. by furniture) radiators
- $p_c = 0.4 - 0.8$ for radiators
- $p_c = 0.3 - 0.4$ for floor heating systems.

Interpretation of the formula: for poorly insulated rooms and convective heating systems, larger air temperature gradients are found, while for well insulated rooms and radiative heating systems smaller air temperature gradients are present.

3.2.8.5. The central radiant temperature.

Starting from theoretical considerations, fitted to the results of numerical simulations of combined conduction - convection - radiation in rooms, the following formula is proposed in [69]:

$$r_r = \frac{h_c}{h_c + \frac{p_c - 0.4}{0.6} \cdot U_m} \quad (3.82)$$

with τ_r dimensionless central radiant temperature.
 h_c convective heat transfer coefficient ($W/(m^2.K)$). A value of 2.5 $W/(m^2.K)$ is used (This value is justified by applying equation (3.22) of paragraph 3.2.2.2 for a temperature difference of 2.5°C. This can be considered as a minimum difference in the case of problematic thermal bridges)

Interpretation: normally the central radiant temperature is lower than the central air temperature (only for $p_c < 0.4$ (mainly radiant systems) τ_r becomes higher). The lowest values are present for poorly insulated rooms and convective heating systems, while for well insulated rooms and radiative heating systems, the central radiant temperature will be higher.

3.2.8.6. Compilation.

Applying the definition of the surface film coefficient and the principles and assumptions mentioned above, the convective and radiative heat exchange at an internal surface part (at height y), coupled to the reference temperature can be written as:

$$h_{a,y=0} \cdot (\tau_{a,y=0} - \tau_{hi}) = h_c \cdot (\tau_{ay} - \tau_{hi}) + h_r \cdot (\tau_r - \tau_{hi}) \quad (3.83)$$

Because $\tau_{a,y=0} = 1$, this equation is rewritten as:

$$h_{a,y=0} = \frac{h_c \cdot (\tau_{ay} - \tau_{hi}) + h_r \cdot (\tau_r - \tau_{hi})}{(1 - \tau_{hi})} \quad (W/(m^2K)) \quad (3.84)$$

To apply the formula:

- $h_c = 2.5 W/(m^2K)$.
- τ_{ay} is calculated according to formula (3.81).
- τ_r is calculated according to formula (3.82).
- $h_r = 5.0 W/(m^2K)$ for surfaces away from corners and edges.
 3.0 $W/(m^2K)$ for surfaces near edges (2D).
 2.0 $W/(m^2K)$ for surfaces near corners (3D).

Because the temperature factor τ_{hi} is unknown (it is the result of the surface temperature calculation itself) one of the following procedures is proposed to apply formula (3.84):

- 1) Direct approach: in the numerical method used for 2D/3D heat transfer, equation (3.84) can be implemented. It means that no value of $h_{a,y=0}$ is

required, but that 2 sets of (h, θ) ($\{h_c, \tau_{ay}\}$ for the convective part, $\{h_r, \tau_r\}$ for the radiative part) have to be given as input.

- 2) Graphical approach: several (e.g. 3 to 4) 2D/3D numerical calculations of the building element considered are performed using different values of $h_{a,y=0}$. This leads to a relation between τ_{hi} and $h_{a,y=0}$. The intersection with relation (3.84) leads to the value of $h_{a,y=0}$. Figure 3.31 shows the points of intersection of a 3D thermal bridge and two curves representing formula (3.84) for an upper and a lower corner. From the intersections, both the value of the temperature factor τ_{hi} and the value of the surface coefficient $h_{a,y=0}$ can be read.

An alternative convenient graphical representation, using other quantities for the axes, is given in figure 3.32.

The quantities used are:

$$R_i = \frac{1}{h_{a,y=0}} \quad (W/(m^2K)) \quad R_{eq} = \frac{\tau_{hi}}{1 - \tau_{hi}} \cdot R_i \quad (W/(m^2K)) \quad (3.85)$$

Using these definitions, the equivalent of expression (3.84) is:

$$R_i = \frac{1 + p \cdot R_{eq}}{h_c + h_r - p} \quad (W/(m^2K)) \quad (3.86)$$

$$p = h_c \cdot (1 - \tau_{ay}) + h_r \cdot (1 - \tau_r) \quad (W/(m^2K)) \quad (3.87)$$

Figure 3.32 shows that the room conditions given with the formulas (3.86) and (3.87) are straight lines (p is a parameter representing the room conditions). Again the points of intersection between the (almost) straight line representing the thermal bridge and the straight lines with the parameter p , define the values of R_i , being the inverse $1/h_{a,y=0}$. Both representations are fully equivalent.

3.2.8.7. Cupboard against an outside wall.

Cupboards against an outside wall are simulated by an overall surface film coefficient:

$$h_{a,y=0} = h_i = 2 \text{ W}/(m^2.K)$$

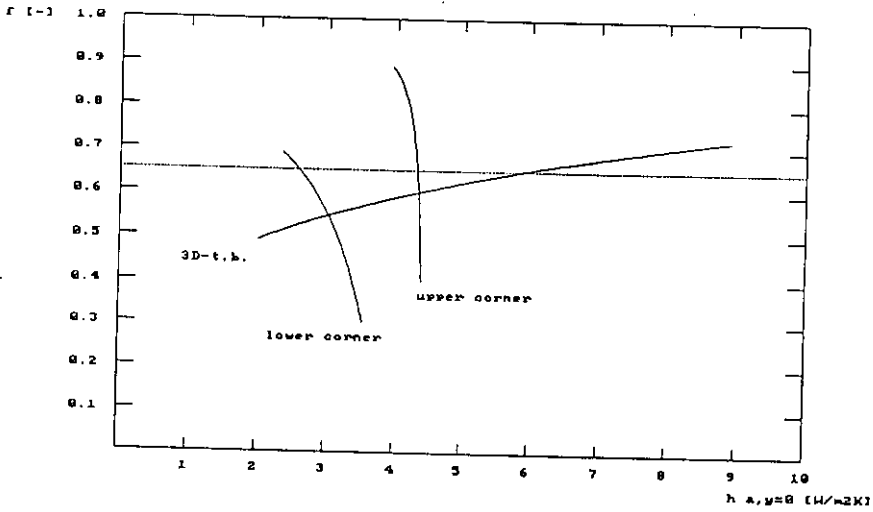


Figure 3.31 Graphical approach example

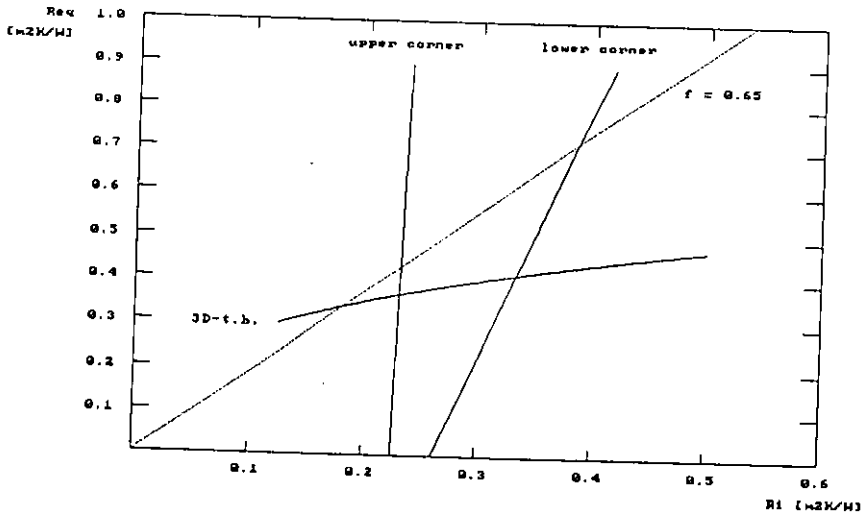


Figure 3.32 Alternative graphical approach example

3.2.8.8. Simplified approach.

To apply the method explained, the room parameters (U_m , p_c) have to be known.

The aim of this paragraph is to give safe values of $h_{a,y=0}$ based on (safe)

estimated room parameters, i.e. $U_m = 0.5 \text{ W/(m}^2\text{K)}$, $p_c = 0.9$.

Using these values, formulas (3.81) and (3.82) give:

$$r_{a,y=1} = 1.094$$

$$r_{a,y=0} = 1$$

$$r_{a,y=-1.7} = 0.847$$

$$r_x = 0.857$$

Assuming a temperature factor $r_{hi} = 0.65$ (safe target temperature factor), the method above was applied for 9 situations (1D/ 2D/ 3D combined with $y = 1\text{m}$ (ceiling) / $y = 0\text{m}$ / $y = -1.7\text{m}$ (floor)).

Results:

$h_{a,y=0}$ (W/(m ² .K))	1D	2D	3D
$y = 1.0 \text{ m}$	6.1	4.9	4.3
$y = 0.0 \text{ m}$	5.5	4.3	3.7
$y = -1.7 \text{ m}$	4.4	3.2	2.6

These values were calculated using formula (3.83) and represent the intersections of the curves with the horizontal line $r_{hi} = 0.65$ in figure 3.31.

For thermal bridges, these values can be used as safe (but not always realistic) if no room information is available and if several thermal bridge calculations (with different h-values) are not desirable.

3.3 REFERENCES

1. NBN B 62-002 " Calcul des coefficients de transmission thermique des parois " Inst. Belge de Normalisation.
2. SIS Thermal insulation - Sheet metal constructions with thermal bridges - Calculation of thermal transmittance" The Swedish Standard Association.
3. ISO DP.6946/2.1 "Thermal Insulation. Calculation rules - Part 2: Beam shaped thermal bridges in plain structures."
4. ISO DP 10211 "Thermal insulation - Thermal bridges - General principles"
5. Progetto di norma: CTI-1-2A-02. 1/88 - "Calcolo termico di pareti con disomogeneita di forma e di materiale" - Agosto 1988
6. Cahiers Du Centre Scientifique et Technique Du Batiment, No184, Novembre 1977 - Cahier 1478
7. Progetto di norma CTI 1/27 E02.01.027.0 - "Trasmittanza unitaria di pareti non uniformi contenenti punti singolari" - Settembre 1986
8. Peter Staelens " Thermal bridges: a non computerized calculation procedure " Lund Inst. of Technology - Report TVBH - 3011 ,1986
9. M. Cali - V. Ferro - M. Masoero " Campi termici' bidimensionali delle strutture edilizie " Condizionamento dell'aria - Riscaldamento - Refrigerazione " 8-9 1978
10. Hans Erhorn und Eltjo Tammes - "Eine einfache Methode zum Abschätzen balkenformiger Wärmebrücken in Bauteilen mit planparallelen Oberflächen" BAUPHYSIK (1985) - H1, S7-11
11. ir. G.L.M. Augenbroe - "Finite elements in building physics" Bouwfysica P 7801 - Delft, January 1978
12. M. Cali - "Thermal Modelling In Buildings" - Torino Ottobre 1988
13. M. Cali & A. Capetti - "Proposta di norma di un codice per il calcolo di riferimento dei ponti termici" Politecnico di Torino - Settembre 1986
14. G. - W. Mainka / H. Paschen - "Wärmebrücken katalog: Tafeln mit Temperaturverläufen, Isothermen und Angaben über zusätzliche Wärmeverluste" - B. G. Teubner Stuttgart 1986
15. Verhoeven - "Simplified formulae to calculate thermal bridges in plain structures" - in "Comportement thermique dynamique des batiments" - Conseil International de la langue française - Paris 1986
16. Standaert, P. - "Twee- en driedimensionale warmteoverdracht: numerieke methoden, experimentele studie en bouwfysische toepassingen" - Doktoraal proefschrift - Katholieke Universiteit Leuven - 1984

17. Knapen, M & Standaert, P - "Experimental research on thermal bridges in different outer-wall systems", Katholieke Universiteit Leuven -CIB-W40, Holzkirchen meeting, Sept. 85.
18. Standaert, P. - "Thermal Bridges: A Two - Dimensional And Three - Dimensional Analysis" - ASHRAE/DOE/BTECC conference "Thermal Performance of the Exterior Envelopes of Buildings III" - December 2 - 5 1985, Clearwater Beach, Usa
19. Standaert, P. - "Proposal For A Definition Of Numerical Methods For Solving Two - Dimensional And Three - Dimensional Heat Transfer In Building Elements" - Report 890402 CEN TC89 WGI 11 April 1989
20. Standaert, P. - "Operation Of The Heat Balance Technique For Solving Steady-state Heat Conduction" - Report 890411 CEN TC89 WGI 11 April 1989
21. C. Kupke "Temperatur - und Wärmestromverhältnisse bei Eckausbildungen und auskragenden Bauteilen", Gesundheits-Ingenieur 101.Jahrgang (1980) - Heft 4 Seite 88-95
22. U. Wolfseher - "Rechnerische Ermittlung mehrdimensionaler Temperaturfelder unter stationären Bedingungen. Rechnensystem und bauphysikalische Anwendung" - Doktorarbeit Universität Essen 1978
23. Cooper, P. " Fin-type cold bridges: Heat loss and surface temperature " Building Services Engineering Research and Technology 8 1987 21-27
24. T Oreszczyn - "Cold bridging at corners: Surface temperature and condensation risk" London: Building Serv. Eng. Res. Technol. 9 (4) 167-175 (1988)
25. M. Giergia - "Handrechenverfahren zur Beurteilung baublicher Wärmebrücken" - Diplomarbeit Universität Stuttgart, 29 Juli 1988
26. M. Cali - R. Borchellini - "Commenti su una proposta di normativa per il calcolo termico dei nodi strutturali e dei ponti termici" - Condizionamento dell'aria Riscaldamento, Refrigerazione n.3 - Marzo 1989 - 323-335
27. Oliveti - Sabato - "Correlazioni di calcolo per la valutazione della potenza perduta attraverso pavimenti poggiati sul terreno" - In the 43rd National Meeting ATI (Associazione Termotecnica Italiana) - 20-23 Settembre 1988
28. Zanello - Nonino - "Visualizzazione delle dispersioni termiche in strutture a contatto col terreno" - In the 44th National Meeting ATI (Associazione Termotecnica Italiana) - 12- 15 Settembre 1989
29. Pagliarini - Piva - "Analisi numerica di campi termici tridimensionali in pannelli di tamponamento prefabbricati" - In the 44th National Meeting ATI (Associazione Termotecnica Italiana) - 12-15 Settembre 1989

30. Babuska - Miller - "The post-processing approach in the finite element method - part 3: A posteriori error estimates and adaptive mesh selection" - Int. J. Num. Meth. Engng. vol 20 - 2311-2324 - 1984
31. O. C. Zienkiewicz - "The finite element method in engineering science" - McGraw Hill - London 1971
32. UNI-CTI 7357-74 "Calcolo del fabbisogno termico per il riscaldamento degli edifici"
33. H. S. Carslaw, J. C. Jaeger - "Conduction of heat in solids" - Clarendon Press - 1965 - Oxford
34. W. J. Minkowycz - E.M. Sparrow - G. E. Schneider - R. Fletcher - "Handbook of numerical heat transfer" - Wiley - New York - 88
35. F. Kreith - "Principles of heat transfer" - second edition - Harper - New York 1973
36. D.W. Kelly - J.P. DES. R. Gayo - O. C. Zienkiewicz - L. Babuska - "A posteriori error analysis and adaptive processes in the finite element method: part 1 - Error analysis" - Int. J. Num. Meth. Eng. vol.19 pp. 1593-1619 - 1983
37. ASTM Standard test method for thermal performances of building assemblies by means of a calibrated hot box - 1985 Annual Book of ASTM Standards - vol. 04.06 ASTM C976-82 - pp.660-683
38. ASTM Standard test method for thermal performances of building assemblies by means of a guarded hot box - 1985 Annual Book of ASTM Standards - vol. 04.06 ASTM C236-80 - pp.81-92
39. M. Necati, Ozisik - " Heat conduction " - Wiley - New York- 80.
40. Suhas V. Patankar - " Numerical heat transfer and fluid flow " - Hemisphere Publishing Corporation - USA - 1980
41. Brunner C. U., Nanni J. " Warmebrucken " Nationaler Energie - forschungsfonds NEFF 262.1 - Schweiz - 1985
42. Heindl, Krec, Panzhauser, Sigmund " Warmebrucken " Springer Verlag - Wien - 1987
43. Oreszczyn T., Littler J. " Cold bridging and mould growth " SERC Final Report - Polytechnic of Central London - 1989
44. CSTC - " Problemes d'humidite dans les batiments. Note d'information technique 153 - maggio-giugno 1984
45. Ontwerp NPR 1074 "Simplified method for the calculation of the temperature factor at the inner surface" - Normcommissie 351 74 "Klimaatbeheersing in gebouwen" - The Netherlands - 1990

46. Plank M., The theory of heat radiatory. Dover Publications, New York 1959.
47. Gluck B., Strahlungsheizung - Theorie und praxis. Verlag C.F. Muller, Karlsruhe, 1982.
48. Kreith, F. and Bohn, M.S.: Principles of heat transfer. Harper International, Fourth edition, 1986.
49. Incorpera F.P., De Witt D.P., Fundamentals of Heat and Mass Transfer
50. Hamilton D.C. and Morgan W.R., Radiant interchange configuration factors. National advisory committee for aeronautics. Technical note 2836, 1952.
51. Eckert E.R.G., radiation: relations and properties. In: M. Rohsenow and J.P. Harnett, Eds., Handbook of heat transfer, 2nd ed., McGraw-Hill, New York, 1973.
52. Siegel R. and Howell J.R., Thermal radiation heat transfer. McGraw-Hill, New York, 1973.
53. Howell J.R., A catalog of radiation configuration factors, McGraw-Hill, New York, 1981.
54. Wolfseher U., Der warmetransport an Bauteiloberflächen unter besonderer Berücksichtigung des langwelligen Strahlungsaustauschs. Gesundheitsingenieur, H.4, S.184-200, 1981.
55. Heidt F.D. und Streppel H.J., Die Warmebilanz and Wandoberflächen in Raumen mit und ohne Sonneneinstrahlung, Gesundheitsingenieur, H.2, S.61-67, 1988
56. Michejew, Grundlagen der Wärmeübertragung. VEB Verlag Technik, 2.Aufl., Berlin, 1963.
57. Grober, Erk, Grigul: Wärmeübertragung 2. Aufl. Springer Verlag, Berlin, 1963.
58. Elsner, Grundlagen der technischen Thermodynamik, 2.Aufl. Akademie Verlag, Berlin, 1974.
59. Hell, Grundlagen der Wärmeübertragung, 3. Aufl. VDI Verlag, Dusseldorf, 1982.
60. Verein Deutscher Ingenieure, VDI Wärmeatlas: Berechnungsblatt für den Wärmeübergang, 4.Aufl., VDI Verlag, Dusseldorf.
61. Saunders, O.A., Natural convection in liquid, Proc. royal Society, London (A), 1939, pp.55-71.
62. Nansteel M., and Greif R., Natural Convection in Undivided and Partially Divided Rectangular Enclosures. Transactions of ASME, Journal of Heat Transfer, 103, Nov. 1981, pp.623-629.

63. Bauman F., Gadgil A., Kammerud R. and Greif R., Buoyancy driven convection in rectangular enclosures: Experimental results and numerical calculations (ASME paper No. 80-HT-66, presented at the 19th National Heat Transfer Conference, 27-30 July 1980, Orlando, FL; also issued as Lawrence Berkeley Laboratory Report LBL-10257, 1980)
64. Handbook of fundamentals. ASHRAE, New York, 1981.
65. DIN 4108, Wärmeschutz im Hochbau. Beuth Verlag, Berlin. August 1981.
66. Wolfseher U., Rechnerische Ermittlung mehrdimensionaler Temperaturfelder unter stationären und instationären Bedingungen. Rechensystemen und Bauphysikalische Anwendung. Dissertation, Universität Essen, 1978.
67. IEA, Task VIII, Passive and hybrid solar low energy buildings, simulation model validation using test cell data. Thermal Insulation Laboratory, Technical University of Denmark, 1986.
68. LEBRUN J., 1972, "La climatisation par corps de chauffe statique", Chaleur et Climat, 438 & 439.
69. STANDAERT P., LICHTVELD W., "Determination of the inside surface boundary conditions in surface temperature calculations", Proceedings of "Energy, moisture, climate in Buildings", September 1990, Rotterdam.

APPENDIX 3.A: LIST OF AVAILABLE HEAT TRANSFER PC PROGRAMS

APPENDIX A - LIST OF AVAILABLE HEAT TRANSFER PC PROGRAMS

	LIBRA	COSMOS-M	MICROCOMPACT	IMAGES-THERMAL	mTAB-HEAT
VENDOR	Intercept Sw. (408)377-4998	SILAC (213)452-2158	Innovative Research (612)559-6067	Celestial Sw. (415)420-0300	Structural Analysis (512)444-0555
PREPROCESSOR ⁴	line ed.	(MODSTAR) line ed. (GEOSTAR) graphics	FORTRAN subroutine	line ed.	(mTAB/Pre) graphics
POSTPROCESSOR ⁵	full	(PLOTSTAR) full	(MICROGRAPHICS) basic	basic	(mTAB/Post) full
INDIVIDUAL H.T. MODULE	no	yes	no	yes	yes
TRANSIENT	yes	yes	no	no	yes
OPTIONAL FLUID FLOW MODULE	no	yes	included	no	no
3-D	yes	yes	no (3-D model input OK)	yes	yes
VAR. PROPERTIES	yes	yes	yes	no	yes
TYPES OF LOAD CONDITIONS	T,q,conv,rad	T,q,conv,rad,heat gen	most types, user definable	T,q,conv	T,q,conv,rad
NUMBER OF NODES	4000	10000(386)	4000	2000(Sept)	2000
OPTIMIZED FOR 386 PC'S	no	yes	no	no	no
CAD INTERFACES	LIBRA mainframe	ANSYS NASTRAN AUTOCAD CADKEY	from CAD to post only	ANSYS NASTRAN AUTOCAD CADKEY etc.	ANSYS NASTRAN STARDYNE MSC/Pat2
VERIFICATION MANUAL	no	yes	yes, Dr. Patankar's textbook	yes	no

	GIFTS	MSC/CAL	SCADA	ANSYS	THERMOSAP
VENDOR	CASA (602)795-3884	MSC (213)259-3888	American Comp. & Eng (213)820-8998	Swanson Anal. Sys. (412)746-3304	Algor Interactive Sys. (412)661-2100
PREPROCESSOR	line ed. (digitizer)	(MSC/MOD) graphics	(SEDFIT) line ed.	(PC/SOLID 4.3)	(VIZICAD) graphics; (digitizer) (PARAGEN) parametric
POSTPROCESSOR	basic	full	(SEDFIT) basic	PC/Solid 4.3) full	(VIZICAD) full
INDIVIDUAL I.I.T. MODULE	no	yes	yes	yes	yes
TRANSIENT	yes	yes	yes	yes	yes
OPTIONAL FLUID FLOW MODULE	no	no	yes	included	no
3-D	yes	yes	yes	yes	yes
VAR. PROPERTIES	no	yes	yes	yes	yes
TYPES OF LOAD CONDITIONS	T,conv	T,q,conv	T,q,conv,rad,heat gen	T,q,conv,rad,heat gen	T,q,conv,rad
NUMBER OF NODES	no limit	2000	no limit	no limit	no limit
OPTIMIZED FOR 386 PCS	yes	yes	no	PC/THERMAL 4.3 no., special 4.4 (full ANSYS) yes	yes, with HYPERSAP
CAD INTERFACES	AOINA NASTRAN	MSC/NASTRAN	none	AUTOCAO VERSACAD	AUTOCAD VERSACAD CV CADKEY IGES
VERIFICATION MANUAL	yes	no	yes	yes	yes

	NISA II		KOBRU86	TRISCO
VENDOR	EMRC (313)649-9380	Vendor	Physibel Heirweg 21 B-9990 MALDEGEM Tel (+32)50711432 Fax (+32)50717842	Physibel Heirweg 21 B-9990 MALDEGEM Tel (+32)50711432 Fax (+32)50717842
PREPROCESSOR	(DISPLAY II) graphics			
POSTPROCESSOR	(DISPLAY II) full	Preprocessor	included	included
INDIVIDUAL H.T. MODULE	yes	Postprocessor	included	included
TRANSIENT	yes	Individual h.t. module	yes	yes
OPTIONAL FLUID FLOW MODULE	yes	Transient	no	no
3-D	yes	Optional fluid flow module	no	no
VAR. PROPERTIES	yes	3-D	no (2-D)	yes
TYPES OF LOAD CONDITIONS	T,q,conv,rad,heat gen	Var. properties	no	no
NUMBER OF NODES	10000	Types of load conditions	T,q,conv,rad, heat gen.	T,q,conv,rad, heat gen.
OPTIMIZED FOR 386 PC'S	yes	Number of nodes	4,761	65,535
CAD INTERFACES	CAEDS SUPERTAB and mc others shown	Optimized for 386 PC's	yes	yes
VERIFICATION MANUAL	yes	CAD interfaces	no	no
		Verification manual	yes	yes
		Demo package	no	no

Chapter 4

MODELLING: hygric aspects

Author:

H. Hens
LABORATORY FOR BUILDING PHYSICS
Celestijnenlaan 131, B-3001 LEUVEN (Heverlee)
Belgium

4.1. Introduction

In the previous chapter, the heat transfer aspects were discussed. This discussion focused on 2D- and 3D- conduction problems, important in understanding thermal bridges, and on convection and radiation, important in understanding the heat transfer between the inside environment and each inside surface. In this chapter, the hygric aspects are analysed, starting with a recapitulation of psychrometry (vapour in the air), going on to vapour and, more general, moisture in materials and ending with a thorough discussion of the vapour balance in a single zone room/space/enclosure. Multizone problems are handled in chapter 5, after inter-room air transport is introduced.

The chapter is not complete in the sense that the whole theory of vapour in the air and moisture transfer in materials has been treated in depth. Only the most important facts and simplifications are recapitulated. Anyone who likes to know more, is referred to the references.

4.2 VAPOUR IN THE AIR: RECAPITULATION

4.2.1 Water?

Having its triple point within the terrestrial temperature conditions:
 $\theta = 0^{\circ}\text{C}$, $p = 611 \text{ Pa}$, water is always present in 2 or 3 states:

Table 4.1 The saturation vapour pressure as a function of temperature

θ ($^{\circ}\text{C}$) \rightarrow	0.0	0.1	0.2	0.3	0.4	0.5	0.6	0.7	0.8	0.9
- 0	611	606	601	596	591	586	581	576	572	567
- 1	562	558	553	548	544	539	535	530	526	522
- 2	517	513	509	504	500	496	492	488	484	479
- 3	475	471	467	464	460	456	452	448	444	441
- 4	437	433	430	426	422	419	415	412	408	405
- 5	401	398	394	391	388	384	381	378	375	371
- 6	368	365	362	359	356	353	350	347	344	341
- 7	338	335	332	329	326	323	321	318	315	312
- 8	310	307	304	302	299	296	294	291	289	286
- 9	284	281	279	276	274	271	269	267	264	262
- 10	260	257	255	253	251	248	246	244	242	240
- 11	237	235	233	231	229	227	225	223	221	219
- 12	217	215	213	211	209	207	206	204	202	200
- 13	198	196	195	193	191	189	188	186	184	183
- 14	181	179	178	176	174	173	171	170	168	167
- 15	165	164	162	160	159	158	156	155	153	152
- 16	150	149	148	146	145	143	142	141	139	138
- 17	137	136	134	133	132	131	129	128	127	126
- 18	125	123	122	121	120	119	118	116	115	114
- 19	113	112	111	110	109	108	107	106	105	104
- 20	103	102	101	100	99	98	97	96	95	94
- 21	93	92	91	90	90	89	88	87	86	85
- 22	84	84	83	82	81	80	80	79	78	77
- 23	76	76	75	74	73	73	72	71	70	70
- 24	69	68	68	67	66	66	65	64	64	63
- 25	62	62	61	60	60	59	59	58	57	57
- 26	56	56	55	55	54	53	53	52	52	51
- 27	51	50	50	49	49	48	48	47	47	46
- 28	46	45	45	44	44	43	43	42	42	41
- 29	41	41	40	40	39	39	38	38	38	37
- 30	37	36	36	36	35	35	35	34	34	33

Table 4.1 Continuation

θ ($^{\circ}\text{C}$)→	0.0	0.1	0.2	0.3	0.4	0.5	0.6	0.7	0.8	0.9
0	611	615	620	624	629	634	638	643	647	652
1	657	662	666	671	676	681	686	691	696	701
2	706	711	716	721	726	731	736	742	747	752
3	758	763	768	774	779	785	790	796	802	807
4	813	819	824	830	836	842	848	854	860	866
5	872	878	884	890	896	903	909	915	922	928
6	935	941	948	954	961	967	974	981	987	994
7	1001	1008	1015	1022	1029	1036	1043	1050	1057	1065
8	1072	1079	1087	1094	1101	1109	1117	1124	1132	1139
9	1147	1155	1163	1171	1178	1186	1194	1203	1211	1219
10	1227	1235	1243	1252	1260	1269	1277	1286	1294	1303
11	1312	1320	1329	1338	1347	1356	1365	1374	1383	1392
12	1401	1411	1420	1429	1439	1448	1458	1467	1477	1487
13	1497	1506	1516	1526	1536	1546	1556	1566	1577	1587
14	1597	1608	1618	1629	1639	1650	1661	1671	1682	1693
15	1704	1715	1726	1737	1748	1760	1771	1782	1794	1805
16	1817	1829	1840	1852	1864	1876	1888	1900	1912	1924
17	1936	1949	1961	1973	1986	1999	2011	2024	2037	2050
18	2063	2076	2089	2102	2115	2128	2142	2155	2169	2182
19	2196	2210	2224	2237	2251	2265	2280	2294	2308	2322
20	2337	2351	2366	2381	2395	2410	2425	2440	2455	2470
21	2486	2501	2516	2532	2547	2563	2579	2595	2611	2627
22	2643	2659	2675	2691	2708	2724	2741	2758	2774	2791
23	2808	2825	2842	2859	2877	2894	2912	2929	2947	2965
24	2983	3001	3019	3037	3055	3073	3092	3110	3129	3148
25	3166	3185	3204	3224	3243	3262	3281	3301	3321	3340
26	3360	3380	3400	3420	3440	3461	3481	3502	3522	3543
27	3564	3585	3606	3627	3649	3670	3692	3713	3735	3757
28	3779	3801	3823	3845	3868	3890	3913	3935	3958	3981
29	4004	4028	4051	4074	4098	4122	4145	4169	4193	4218
30	4242	4266	4291	4315	4340	4365	4390	4415	4440	4466
31	4491	4517	4543	4569	4595	4621	4647	4673	4700	4727
32	4753	4780	4807	4835	4862	4889	4917	4945	4973	5001
33	5029	5057	5085	5114	5143	5171	5200	5229	5259	5288
34	5318	5347	5377	5407	5437	5467	5498	5528	5559	5590
35	5621	5652	5683	5715	5746	5778	5810	5842	5874	5907
36	5939	5972	6004	6037	6071	6104	6137	6171	6205	6239
37	6273	6307	6341	6376	6410	6445	6480	6516	6551	6587
38	6622	6658	6694	6730	6767	6803	6840	6877	6914	6951
39	6989	7026	7064	7102	7140	7178	7217	7255	7294	7333
40	7372	7412	7451	7491	7531	7571	7611	7652	7692	7733

Table 4.1 Continuation

θ ($^{\circ}\text{C}$)	45	50	55	60	65	70	75	80	85	90	95
	9582	12335	15741	19917	25007	31156	38550	47356	57800	70108	84524

$\theta \leq 0^{\circ}\text{C}$: solid (= ice), gaseous (= vapour), (undercooled liquid)

$\theta \geq 0^{\circ}\text{C}$: liquid (= water), gaseous (= vapour)

The equilibrium (p', θ) , also called the saturation pressure line liquid-vapour and ice-vapour, is approximately given by (or, or):

$-20^{\circ}\text{C} < \theta < 60^{\circ}\text{C}$:

$$p' = \exp(65.8094 - 7066.27/T - 5.976 \cdot \ln(T))$$

$-30^{\circ}\text{C} < \theta \leq 0^{\circ}\text{C}$:

$$p' = 611 \cdot \exp(82.9 \cdot 10^{-3} \cdot \theta - 288.1 \cdot 10^{-6} \cdot \theta^2 + 4.403 \cdot 10^{-6} \cdot \theta^3)$$

$0^{\circ}\text{C} \leq \theta < 40^{\circ}\text{C}$:

$$p' = 611 \cdot \exp(72.5 \cdot 10^{-3} \cdot \theta - 288.1 \cdot 10^{-6} \cdot \theta^2 + 0.79 \cdot 10^{-6} \cdot \theta^3)$$

Numerical values: see table 4.1.

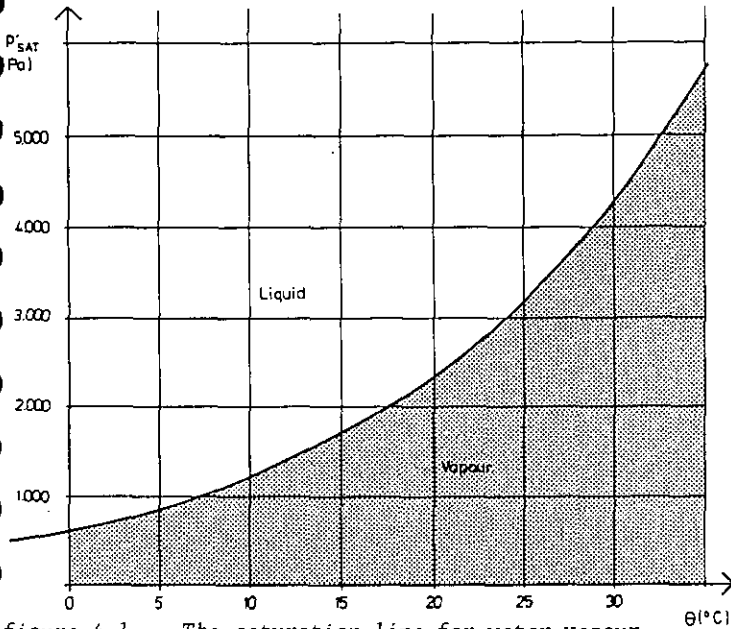


figure 4.1 The saturation line for water vapour

By no means can the vapour pressure in a dry air - water vapour mixture at a temperature θ be higher than the saturation pressure, belonging to that temperature!

4.2.2 Quantities, describing the presence of vapour in the air.

For the mixture dry air- vapour, it is assumed that both gasses behave as if they were ideal and that no chemical interaction exists. So, they obey Gay-Lussac's law:

$$p.V = m.R.T \quad (4.1)$$

with: p the pressure in Pa, V the volume in m^3 , m the amount in kg, T the gas-temperature in K and R the gas constant, 287 J/(kg.K) for dry air and 462 J/(kg.K) for vapour.

Also Dalton's law holds, stating that the total pressure p_t of both gasses in an enclosure equals the sum of the partial pressures:

$$p_t = p_a + p \quad (4.2)$$

Quantities used to describe the presence of vapour in the air are:

QUANTITY	SYMBOL	UNITS
ABSOLUTE Vapour pressure :	p	Pa
Vapour concentration :	c	kg/m ³
Vapour ratio :	x	kg/kg
<i>(in relation to 1 kg of dry air)</i>		
RELATIVE Relative Humidity:	ϕ or RH	%
<i>(= ratio between the vapour pressure and the saturation pressure at the same temperature)</i>		
INDIRECT Dewpoint:	θ_d or T_d	°C or K
<i>(= temperature for which during an isobaric change, the vapour pressure becomes the saturation pressure)</i>		
Wet bulb temperature:	θ_w or T_w	°C or K
<i>(= temperature of the air with vapour ratio x/ vapour concentration c/ pressure p, after an adiabatic saturation)</i>		

4.2.3 Relations between quantities

The state of a dry air - vapour mixture is thermodynamically defined if the temperature and one of the given quantities are known. The one given, allows to calculate all others:

Vapour pressure -> vapour concentration:

$$c = \frac{p}{R \cdot T}$$

Vapour pressure -> vapour ratio:

$$x = 0.621 \cdot \frac{p}{p_t - p}$$

Vapour pressure -> Relative humidity:

$$\phi = 100 \cdot \frac{p}{p'(\theta)}$$

Vapour pressure -> wet bulb temperature:

$$p = p'(\theta_w) - 66.71 \cdot (\theta - \theta_w)$$

4.2.4 Condensation - Evaporation

An easy way to follow the changes in a dry air - vapour mixture is by using a psychrometric chart: the graphical representation of all conditions of moist air within the atmospheric range. An example of such a chart is shown in fig. 4.2. In the figure, the saturation line and the lines of equal RH are drawn as a function of temperature.

Condensation now starts when, during a change of state, the vapour pressure p reaches the saturation or 100% RH- line. Two clear ways exist: either moistening the air without change in temperature, a so called isothermal saturation, represented by a line, parallel to the p -axis, or cooling the air without changing the vapour pressure, a so called isobaric saturation, represented by a line, parallel to the temperature axis. The temperature of

the moist air at the intersection point in a isobaric saturation, is called: the DEWPOINT (see quantities).

Example

Air at 20°C and 60% RH:

vapour pressure: $2340 \cdot 0.6 = 1404$ Pa

vapour concentration: $1404 / (462.293) = 10.3$ g/m³.

vapour ratio: $0.621 \cdot 1404 / (101300 - 1404) = 8.7$ g/kg.

To achieve an isothermal saturation, we have to increase the vapour pressure with $2340 - 2404 = 936$ Pa, this means adding some 7g of vapour per m³ of air or some 5.9 g of vapour pro kg of dry air. In a non ventilated, isothermal room with a volume of 40 m³, that means a vapour production of 280 g.

An isobaric saturation requires cooling of the air to 12°C. 12°C is the dewpoint of moist air at 20°C and 60% RH

In buildings, both ways of saturating moist air are mixed: we have at the same time vapour production and, cooling of the moist air against the inside surfaces of the outside walls. Once laying on the saturation line, i.e., once $p = p'$ or $\theta = \theta_d$, the point, representing the state of the moist air, moves along it, with condensation or evaporation going on. Both are coupled to the

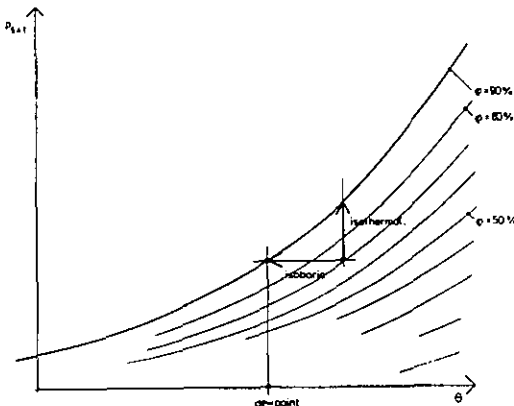


Figure 4.2 The psychrometric chart, isothermal and isobaric changes of state of the 'air-vapour'

release (condensation) or uptake (evaporation) of the LATENT HEAT OF EVAPORATION, approximately $2,5 \cdot 10^6$ J/kg. (table 4.2).

This latent heat introduces a strong coupling between heat transfer and evaporation/condensation.

Table 4.2: The latent heat of evaporation under atmospheric conditions

θ [°C]	0	10	20	30	40	50	60	70	80	90	100
h_{θ} ($\cdot 10^3$ J/kg)	2500	2476	2453	2430	2406	2382	2358	2333	2308	2282	2256

$$\text{regression line: } h_{\theta} = 2.5 \cdot 10^6 - 2430 \cdot \theta \\ r^2 = 0.999$$

4.2.5 Vapour transfer from and to a surface

Vapour flow in the air is directly and \pm totally linked to air flow by convection, diffusion playing only an extremely limited role. An exception is found in the vapour transfer air \rightarrow surrounding surfaces, where the stagnant air boundary layer has to be crossed by diffusion. This is conventionally described by an equation:

$$g = \beta \cdot (p - p_s) \quad (4.3)$$

with β the surface film coefficient for diffusion, p the vapour pressure in the air and p_s the vapour pressure at the surface.

If, instead of the vapour pressure, the vapour concentration is used, the formula becomes:

$$g = \beta_v \cdot (c - c_s) \quad (4.4)$$

Between β and the convective heat surface film coefficient h_c , a relation exists, given by:

$$\beta = \frac{h_c}{c_p \cdot R_a \cdot T \cdot \rho_a} \cdot \left[\frac{c_p \cdot R_a \cdot T \cdot \delta_p}{\lambda_a} \right]^{0.67}$$

This equation can for building applications be simplified to:

$$\beta = \frac{h_c \cdot \delta_p}{\lambda_a} \approx 7.4 \cdot 10^{-9} \cdot h_c \quad (4.5)$$

In both, λ_a is the thermal conductivity, δ_p the vapour permeability, c_p the isobaric specific heat capacity, R_a the gas constant and ρ_a the volumic mass, all related to air.

Formulas (4.3) and (4.5) are used as a tool to calculate the condensation-evaporation quantities. The heat released or absorbed during these processes is:

$$q = g \cdot h_e = \beta \cdot h_e \cdot (p - p_s) \approx 0.0185 \cdot h_c \cdot (p - p_s) \quad (4.6)$$

As long as a non capillary surface is moist, the vapour pressure against it is the saturation value (RH = 100%).

4.3 MOISTURE IN MATERIALS

4.3.1 Hygroscopicity

As vapour diffuses into or out of pores, typical physical phenomena occur in the pore, resulting macroscopical in an increase or decrease of the moisture content of the material. That process is called SUCTION or HYGROSCOPICITY

- hygroscopic materials

Let's start from a dry material and raise the RH in the surrounding air stepwise, each step being maintained long enough to reach an equilibrium situation in the material. As long as, for each step, a difference in vapour pressure exists between the air and the pores in the material, diffusion into the pore system goes on. For very low RH ($0 \leq \text{RH} \leq 20\%$), the incoming water molecules are adsorbed against the large amount of pore wall surface per m^3 of material. A monolayer of watermolecules is build, resulting in a measurable increase in moisture content, given by:

$$w_H = 2,62 \cdot 10^{-6} \cdot A_p \cdot \frac{C \cdot \phi}{1 + C} \quad (4.7)$$

with A_p : the specific pore surface (m^2/m^3)
 C : the energy of adsorption between the water molecule and the porewall: $C = k \cdot \exp[(h_a - h_e)/(R \cdot T)]$
 k : the adsorption constant
 h_a : the heat of adsorption (J/kg).

Once ϕ passes 20%, the monolayer adsorption turns to multilayer:

$$w_H = 2,62 \cdot 10^{-6} \cdot A_p \cdot \frac{1 - (n+1) \cdot (\phi/100)^n + n \cdot (\phi/100)^{n+1}}{1 - (n-1) \cdot (\phi/100)^n - n \cdot (\phi/100)^{n+1}} \quad (4.8)$$

with n : the number of layers.

At $\phi \approx 30\%$, the adsorbed layers in the smallest pores touch one another: water menisci are formed. Once that happens, adsorption turns to CAPILLARY CONDENSATION (fig. 4.3). This phenomenon is governed by Thompsons law:

$$p'' = p' \cdot \exp[-p_c / (R \cdot T_a)] \quad (4.9)$$

with p'' : the saturation pressure above the curved meniscus
 p_c : the capillary suction in the pore, given by:

$$p_c = \frac{\sigma \cdot \cos \theta}{1/r_1 + 1/r_2} \quad (4.10)$$

with σ : the surface tension (N/m)
 θ : the contact angle meniscus - pore wall
 r_1, r_2 : the curvature radii of the meniscus (fig.4.3).

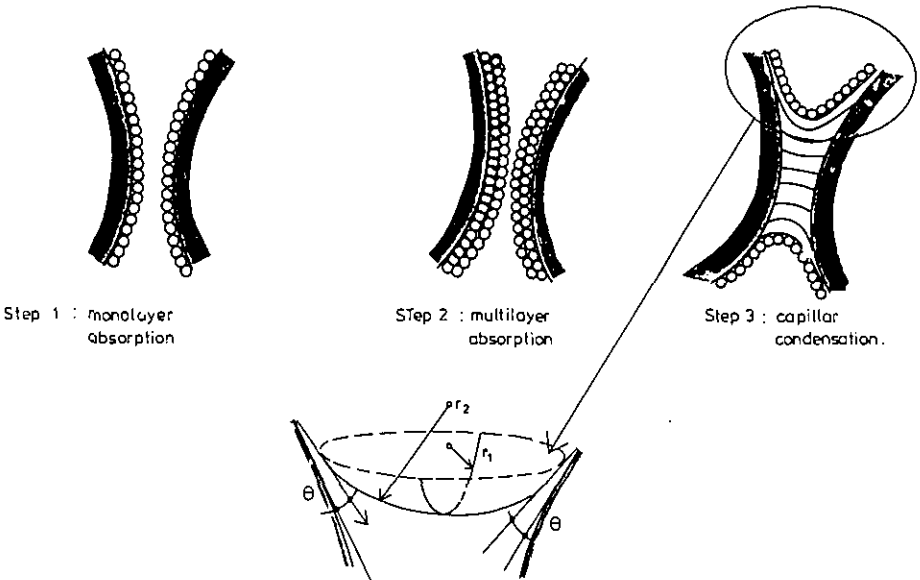


Figure 4.3

With a further rise of the RH, capillary condensation occurs in wider and wider pores, until at 100% the whole pore system should be water filled if no air was entrapped. In practice, this is always the case and saturation is never reached: the moisture content blocks at the capillary one!

The hygroscopic curve, built up in that way, is called the SUCTION ISOTHERM of the material. It is S-shaped (fig.4.4) with:

- a steeper increase at low RH, the higher the porosity and the smaller the pores;
- a slower or steeper, more or less linear increase at higher RH, dependent of the pore distribution in the material.

If we start from a water saturated porous material and lower the RH stepwise, a drying route is found, comparable with the hygroscopic wetting. However, between both routes a hysteresis exists, with, for the same RH, a higher moisture content on the drying than on the wetting suction isotherm.

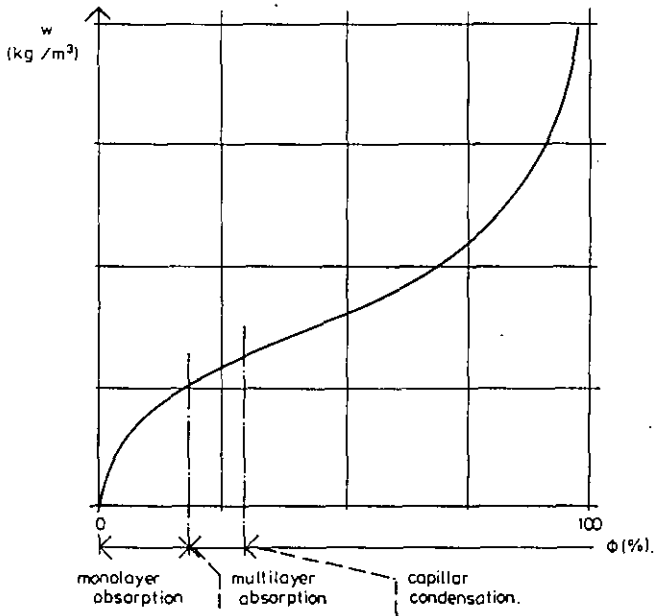


Figure 4.4 The suction isotherm

In literature, different reasons for this hysteresis are given:

- the different moisture conditions in a water saturated sample, compared to a capillary saturated one (influence of entrapped air!);
- other menisci during drying;
- the slowness of the drying processes inducing the danger of taking a state, which is still slowly evolving, as equilibrium;
- thermodynamic equilibrium differences...

The wetting-drying suction isotherm is a fundamental moisture characteristic, specific for a given material, at least as far as the salt content remains restricted. High salt contents may result in a much more pronounced hygroscopicity.

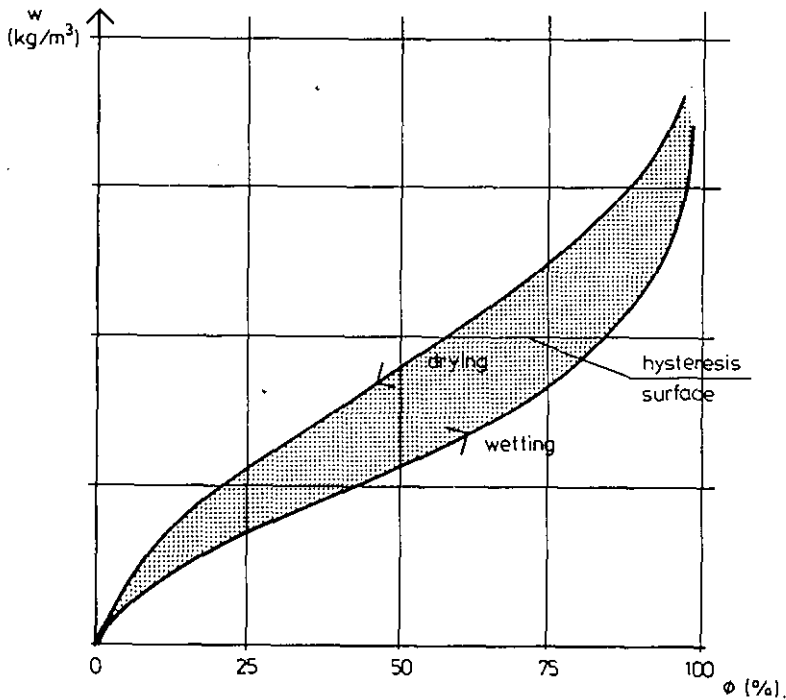


Figure 4.5 The hygroscopic hysteresis

- non- hygroscopic materials

In an ideal non hygroscopic material, the adsorption constant equals 0 and no capillary suction (water repellent layers) exists. So, hygroscopic behaviour should be absent. However, pure non hygroscopic materials do not exist.

- Importance of hygroscopicity

The suction isotherm acts as moisture capacity in all vapour transfer processes in capillary-porous materials. In fact, the vapour transport equation looks like:

$$\operatorname{div}(\delta_p \cdot \operatorname{grad}(p' \cdot \phi)) = \frac{\partial w_H}{\partial \phi} \cdot \frac{\partial \phi}{\partial \tau} \quad (4.11)$$

with $\partial w_H / \partial \phi$: the specific hygroscopic moisture content or capacity c_H
of the material
 δ_p : the vapour conductivity of the material (see diffusion)

For all materials, c_H is a function of RH. Supposing isothermal conditions and simplifying the suction curve to a 0-step/ straight line/ 100%-step function, the specific moisture capacity becomes:

$$c_H = a_H / p' \quad (4.12)$$

with a_H : the slope of the hygroscopic line
 p' : the saturation pressure, coupled to the isothermal condition.

$p' \cdot \delta_p / a_H$ stands for the isothermal vapour diffusivity D_p of the material. For most hygroscopic materials, D_p is only a fraction of the thermal diffusivity. That means that vapour flow and -storage are very slow phenomena, not influenced by short term, non-steady-state, boundary conditions....

Example: Concrete, $\theta = 20$ °C

hygric $a_H / p' = 1,84 \cdot 10^{-2} \text{ kg}/(\text{m}^3 \cdot \text{Pa})$; $\delta_p = 1,85 \cdot 10^{-12} \text{ s}$

thermal $\rho c = 2250000 \text{ J}/(\text{m}^3 \cdot \text{K})$; $\lambda = 2,5 \text{ W}/(\text{m} \cdot \text{K})$

hygric diffusivity $1,0 \text{ E-}9 \text{ m}^2/\text{s}$

thermal diffusivity $1,1 \text{ E-}6 \text{ m}^2/\text{s}$

Or, the hygric diffusivity is 3 orders of magnitude lower than the thermal diffusivity!

4.3.2 Vapour transfer by diffusion

Vapour transfer in and through porous materials is caused by vapour diffusion and convective flow of moist air in and through the pores. As far as microporous materials are concerned, the hydraulic resistance is so big, that convection may be omitted...

- Ficks equations

To describe the diffusion process in the material, Ficks law for the density of vapour flow rate is used:

- for dry materials:

$$g = \delta \cdot c_a \cdot \text{grad}(c/c_a) \quad (4.13a)$$

- for hygroscopically wet materials:

$$g = \delta \cdot [c_a^2 / (c_a - c)] \cdot \text{grad}(c/c_a) \quad (4.13b)$$

Both equations show that diffusion is generated by, and proportional to, the gradient in relative vapour concentration. The quantity δ , part of the proportionality factor, is called the vapour conductivity or permeability of the material. For the 'dry air- vapour'- diffusion in the pores, δ is defined by:

$$\delta = \frac{D_{va}}{\mu} = \frac{2.26173}{\mu \cdot p_a} \cdot \left[\frac{T}{273.16} \right]^{1.81} \quad (4.14)$$

with D_{va} : the binary diffusion coefficient 'dry air- vapour'
 p_a : the atmospheric pressure
 T : the air temperature in K.

The factor μ in the equation is called THE DIFFUSION RESISTANCE RATIO of the material, expressing how much lower the vapour conductivity of the material is, compared to the value for stagnant air under the same pressure and temperature. For stagnant air, μ is 1. This is the lowest value. The highest is ∞ for a vapour tight material.

Vapour retarders are materials with a high to very high μ -value. Especially in the German and Dutch literature, μ replaces δ as material property: it's easier to understand and gives a better feeling of the differences between materials. As number, it describes very concisely the porous system of a

material. Because of this link with porosity and porous system, one may understand the important scattering of μ -values for the same material... For hygroscopic materials, μ , as δ , are explicit functions of the moisture content, or, by the suction curve, of the RH in the material, in the sense that μ lowers and δ increases with raising RH.

- simplifications

For temperatures below 50°C, the equations for the dry and wet material simplify to:

$$g = \frac{\delta}{R.T} \cdot \text{grad } p \quad (4.15)$$

or, with $\delta / RT = \delta_p$:

$$g = \delta_p \cdot \text{grad}(p) \quad (4.16)$$

δ_p can also be written as:

$$\delta_p = \frac{D_{va}}{\mu \cdot R.T} = \frac{1}{\mu \cdot N}$$

with $RT/D_{va} = N$, the diffusion constant, units: s^{-1} .

δ_p and N are, as formula (4.14) shows, explicit functions of temperature and air pressure. However, as far as the narrow temperature differences between in- and outside of cold moderate climates are concerned, the temperature influence is too weak to have a major impact: hand calculations can be done, assuming a constant value: $N = 5.4 \cdot E+9 \text{ s}^{-1}$

In 1D- steady-state conditions (i.e. using long term mean climatological data), equation (4.16) becomes for a single layer wall (fig.4.6)

$$g = (p_1 - p_2) / (N \cdot \mu \cdot d) \quad (4.17)$$

with p_1 and p_2 : the vapour pressures on both sides of the wall.

Theoretically, we should take the vapour pressures at the surface. Practically, compared to the diffusion resistance of the wall, the vapour surface film resistances $1/\beta$ are so small, that p_1 and p_2 apply for the vapour pressure in the air at both sides of the wall.

We call $(N \cdot \mu \cdot d)$ the diffusion resistance of the wall, symbol Z , units m/s . $(\mu \cdot d)$, units m , stands for the diffusion thickness.

For a composite wall, the steady-state vapour transfer equation becomes (fig.4.7):

$$g = (p_1 - p_2) / [N \cdot \Sigma(\mu_i \cdot d_i)] \quad (4.18)$$

with $\Sigma(\mu_i \cdot d_i)$: the diffusion thickness of the composite wall

The diffusion thickness replaces the μ - or δ_p -value for:

- all non homogeneous layers
- layers for which the thickness cannot or is difficult to measure
- layers for which the thickness is so small that the layer has no significant thermal resistance.

Example: The composite facade wall of the Zolder case study dwelling

from the inside to the outside:

gypsum plaster,	d = 1.5 cm	$\mu = 5$
inside leaf in brick masonry work,	d = 18 cm	$\mu = 10$
cavity,	d = 5 to 6 cm	$\mu_{eq} \approx 0.3$
outside leaf in facing bricks,	d = 9cm	$\mu = 10$

Diffusion resistance:

$$Z = 5.4 \text{ E}+9 \cdot (0.015 \cdot 5 + 0.18 \cdot 10 + 0.09 \cdot 10) \approx 1.5 \text{ E}+10 \text{ m/s}$$

Vapour flow density for a yearly mean $(p_i - p_e) = 500 \text{ Pa}$:

$$g = \frac{500}{1.5 \text{ E}+10} = 3.3 \text{ E}-8 \text{ kg}/(\text{m}^2\text{s}) \text{ or } 0.12 \text{ g}/(\text{m}^2\text{h}) \text{ or } 2.9 \text{ g}/(\text{m}^2\text{day})$$

This result shows, as did the hygric diffusivity calculation for concrete, how slow vapour diffusion is: only some $3\text{g}/\text{m}^2$ of vapour passes, for mean boundary conditions, per day, through the cavity wall! Each inhabitant should need 400 m^2 of wall to evacuate his perspiration by diffusion only!!

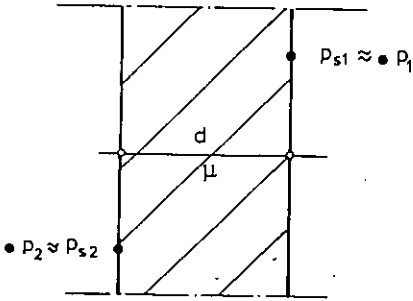


figure 4.6: Single layer wall

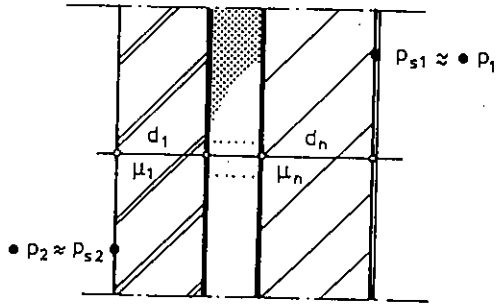


figure 4.7: Composite wall

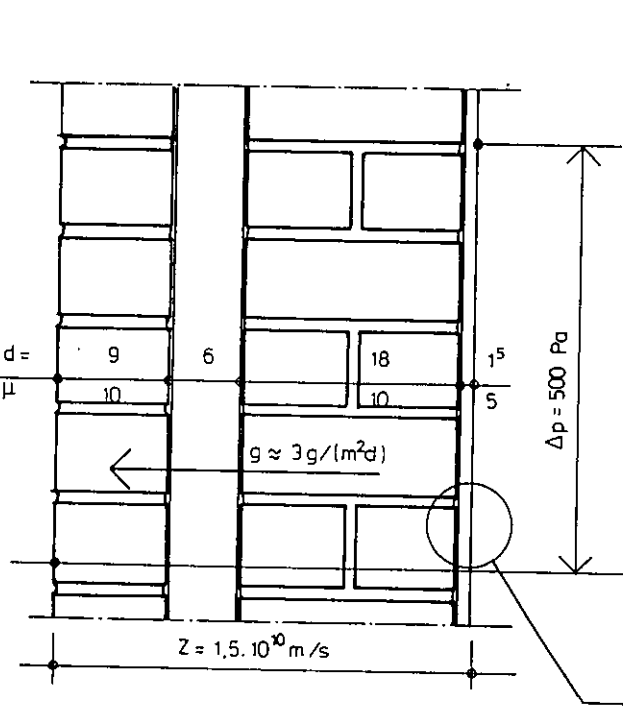


figure 4.8: Example of a steady state diffusion calculation

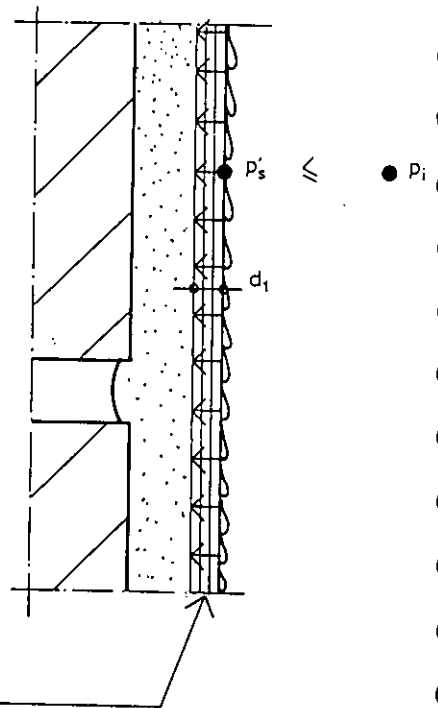


figure 4.9: Wetting by capillarity drying by diffusion

4.3.3 Capillary wetting- drying by diffusion

When condensation starts on a capillary surface, the condensate is sucked and a critical moist surface layer, with thickness d , develops (fig 4.9). As the inside vapour pressure drops below the saturation pressure at the surface, drying begins, starting at the surface but instantaneously shifting into the material: at the critical moisture content, capillary flow to the drying surface in fact is impossible. Because of the increasing diffusion resistance, drying slows down progressively added to the surface film resistance, the more the drying front retires into the surface layer. As a consequence more time is needed for drying, a diffusion phenomenon, then for wetting, a capillary reality!

If condensation and drying alternate with time steps Δt_c and Δt_d , then a first order approximation of the critical wet layer imbalance d is given by:

$$d = \frac{\beta}{(w_{cr} - w_H)} \cdot (p_i - p'_s)_c \cdot \Delta t_c - \frac{1}{N \cdot \mu \cdot \beta} \cdot \left[1 + \frac{2 \cdot \beta^2 \cdot \mu \cdot N}{(w_{cr} - w_H)} \cdot (p'_s - p_i)_d \right]^{0.5} \cdot \Delta t_d \quad (4.19)$$

with w_{cr} : the critical moisture content
 w_H : the hygroscopic moisture content for $\phi \approx 98\%$
 μ : the diffusion resistance ratio of the material (value for high RH!)
 β : the surface film coefficient for diffusion
 p_i : the inside vapour pressure
 p'_s : the saturation pressure at the surface
 index c = "during condensation"
 index d = "during drying".

IF $d \leq 0$, AN EQUILIBRIUM BETWEEN WETTING AND DRYING EXISTS. IF NOT, THE MATERIAL IS SLOWLY WETTED BY SURFACE CONDENSATION AND THE SURFACE RH REMAINS AT 100%...

The slowness of drying, compared to wetting, is not only a capillary reality but also a fact in the hygroscopic region. This strengthens the necessity of a permanent, background ventilation rate, stabilising the inside RH at a mean level, to avoid mould germination. Where that level is, depends on the thermal quality of the building envelope, the inside temperature and the vapour production.

Example: The bathroom of the dwelling of the Zolder case study (fig.4.10)

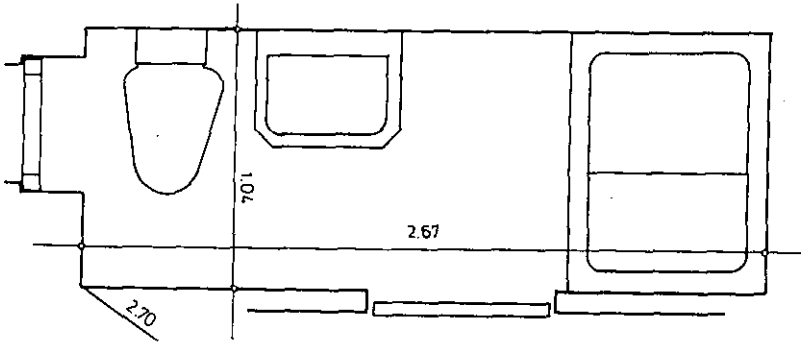


figure 4.10: the bathroom

Suppose the bathroom is in use for two hours a day, 1 hour in the morning and 1 hour in the evening. ($\Delta t_c = 1\text{ h}$; $\Delta t_d = 11\text{ h}$)

When in use, the RH goes to 100% and condensation takes place against every surface, including the colder gypsum plastered ceiling (sleeping rooms not heated). Difference $(p_i - p'_s)_c$: 840 Pa.

Next, during eleven hours the inside temperature drops to 10°C and the mean difference $(p'_s - p_i)_d$ stabilises around 125 Pa ($\phi_i = 90\%$).

For gypsum plaster ($w_{cr} = 320\text{ kg/m}^3$; $w_H = 236\text{ kg/m}^3$; $\mu = 4$) equation (4.19) gives: $d = -2.3\text{ E-4 m}$, or, no moisture accumulation, with as consequence very severe mould growth, has to be expected.

With a more intensive use of the bathroom and/or a lower $(p'_s - p_i)_d$ during the drying period (bad ventilation!), we may realise $d \geq 0$ i.e. a slow moisture accumulation in the plaster and severe mould growth....

4.4 THE HYGRIC BALANCE OF AN ENCLOSURE: A SINGLE-ZONE APPROXIMATION

With the hygric balance, we have a tool to predict the evolution of the vapour pressure, vapour concentration and dewpoint in the inside air. In combination with thermal information, the possibility of surface condensation or too high surface RH can be checked, hygroscopic influences evaluated...etc.

The way the balance is discussed in this chapter in a very systematic one:

- first the most simple case: NO CONDENSATION, NO HYGROSCOPICITY
- then adding: SURFACE CONDENSATION AND SURFACE DRYING
- and finally, introducing: HYGROSCOPICITY

4.4.1 No surface condensation, no hygroscopicity

Starting from the mass balance:

incoming vapour + vapour produced in the zone

=

the outgoing vapour + the vapour stored in the zonal air

and assuming that:

- the inside air is characterised by 1 overall vapour pressure and air temperature (~ideal convective mixing);
- the outside air, entering through leaks, open windows, ventilation devices..., can be represented by 1 outside air vapour pressure;
- all vapour produced in the zone is mixed instantaneously and homogeneously with the zonal air;
- the air and all inside surfaces are at the same temperature, condensation is only possible if the inside RH equals 100%,

we may write:

$$G_p + \frac{n.V.p_e}{462.T_i} = \frac{n.V.p_i}{462.T_i} + \frac{V}{462.T_i} \cdot \frac{d p_i}{d t} \tag{4.20}$$

- with G_p : the vapour production in kg/h
 n : the ventilation rate in h^{-1}
 462 : the gas constant for vapour
 T_i : the inside temperature in K
 V : the zonal volume in m^3 .

Rearranging (4.20) gives:

$$\frac{d p_i}{d t} + n \cdot p_i = n \cdot p_e + \frac{462 \cdot T_i \cdot G_p}{V} \quad (4.21)$$

In equation (4.21), G_p , T_i , n and p_e are time dependent. Hence, exact analytical solutions are only possible for simple cases such as steady-state, sudden change in vapour production or outside vapour pressure (the other parameters remaining constant), periodical vapour production and periodical outside vapour pressure...

4.4.1.1 STEADY-STATE SOLUTIONS

Steady-state stands for: mean values of ventilation rate, vapour production, outside vapour pressure, inside vapour pressure over longer periods (1 week, 1 month, 1 year)...

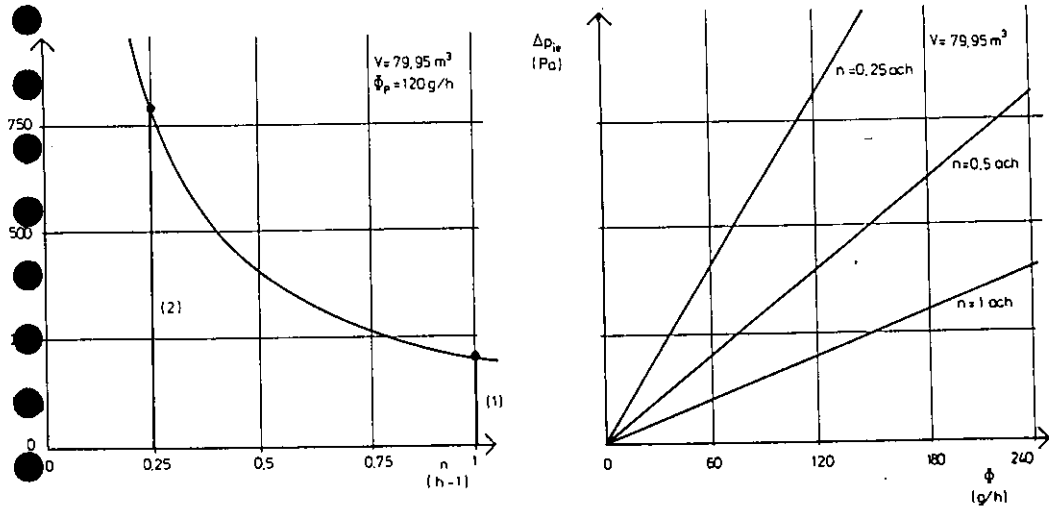
The equation becomes ($dp_i/dt = 0$):

$$p_i = p_e + \frac{462 \cdot T_i \cdot G_p}{n \cdot V} \quad (4.22)$$

stating that:

- the mean inside vapour pressure can never be lower than the mean outside vapour pressure (.....);
- the difference ($p_i - p_e$) increases with higher vapour production or lower ventilation rate ($= P_m/n$). This is illustrated in fig.4.11, the relation [$n, (p_i - p_e)$] being a hyperbolic, the relation [$G_p, (p_i - p_e)$] a linear one. These mean that even for a low vapour production, very low ventilation rates give high differences in inside- outside vapour pressure, but, if a high ventilation rate is already present, still more does not result in a significantly lower ($p_i - p_e$)...
- for a constant ventilation rate and vapour production, the difference ($p_i - p_e$) will be higher, the smaller the zonal volume...

This explains to some extent why more complaints about mould are registered in social dwellings than in middle class houses : the last have a larger volume!



- (1) Zolder case study dwelling before the retrofit.
- (2) Zolder case study dwelling after the retrofit.

figure 4.11 Graphical presentation of the $\Delta p_{1e} = f(n, G_p)$ -relation.

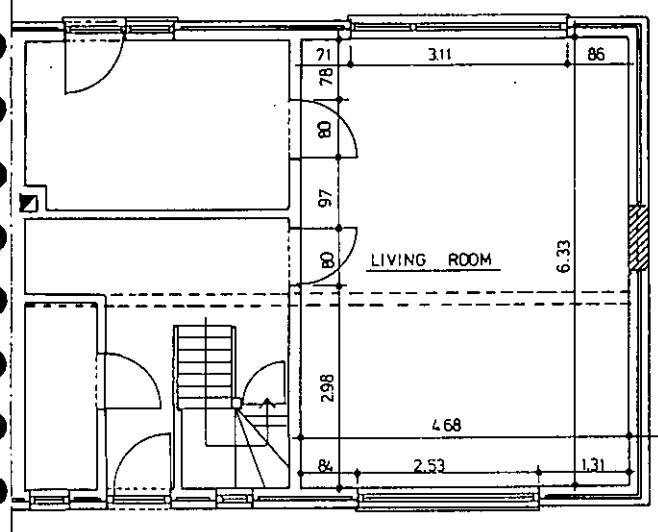


figure 4.12 Living room of the Zolder case study dwelling

Example: The living room of the Zolder case study dwelling:

Before retrofitting of the early eighties, the mean ventilation rate by infiltration and stove heating oscillated around 1 h^{-1} . After, with the replacement of the leaky steel windows by draught stripped PVC- frames and the installation of a gas fired radiator central heating, only some 0.2 to 0.3 h^{-1} were left.

- The mean vapour production did not change: $\approx 120 \text{ g/h}$.
- Mean inside air temperature : 18°C .
- zonal volume : 79.95 m^3
- Difference ($p_i - p_e$) (see fig.4.11):

$$\text{before: } \frac{462 \cdot (273.16 + 18) \cdot 0.120}{79.95} = 202 \text{ Pa}$$

$$\text{after: } \frac{462 \cdot (273.16 + 18) \cdot 0.120}{79.95 \cdot 0.25} = 808 \text{ Pa}$$

- Inside RH ($\theta_i = 18^\circ\text{C}$):

Month	ϕ_i [%]	
	before	after
J	42.6	72.0
F	44.6	73.5
M	49.6	77.3
A	54.6	81.0
O	54.6	81.0
N	48.9	76.7
D	43.9	72.9

Therefore, the poor ventilation reality after retrofitting has an important effect on the inside RH and, through that, on the chance on mould, so widely present in the estate!

4.4.1.2. NON-STEADY-STATE SOLUTIONS

CASE 1

Constant: ventilation rate, inside temperature, outside vapour pressure.
 Inside vapour production starts or changes at $t=0$.

As solution of the balance equation, we get:

$$p_i = p_{i\infty} + (p_{i0} - p_{i\infty}) \cdot \exp(-n \cdot t) \tag{4.23}$$

with $p_{i\infty}$: the inside vapour pressure steady-state value
 p_{i0} : the inside vapour pressure at $t = 0$.

The result shows that in non-steady-state conditions, the hygric inertia of the inside air volume V is relevant, the time constant being the inverse of the ventilation rate: $1/n$. The better the ventilation, the quicker the near steady-state inside vapour pressure $p_{i\infty}$ is reached and the lower it is.

If the moisture production stops at $t = 0$, then (4.23) becomes:

$$p_i = p_e + (p_{i0} - p_e) \cdot \exp(-n \cdot t) \tag{4.24}$$

This equation allows, assuming that no surface condensation took place during the vapour production interval and no hygroscopic inertia exists, an estimate of the ventilation rate to be made from a thermo-hygrograph registration, as shown in fig. 4.13.

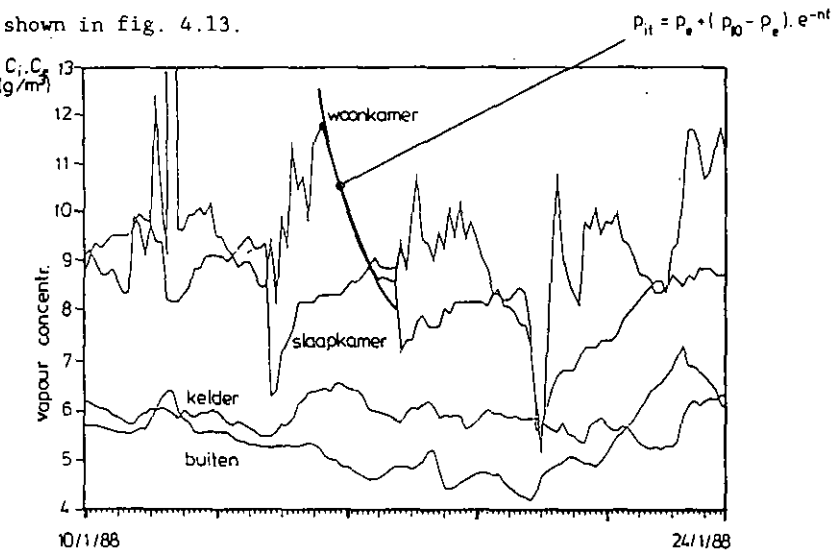


figure 4.13 Guessing the ventilation rate from a hygrothermograph output

Example:

Let's go back to the living room of the Zolder dwelling. The monthly mean vapour production was 120 g/h. Suppose this production starts each day at 8 p.m and goes on at a constant rate until 10 a.m. So, the daily vapour production scheme looks like:

hour	0	1	2	3	4	5	6	7	8	9	10	11	12	13	14	15	16	17	18	19	20	21	22	23
G_p	0	0	0	0	0	0	0	0	0	0	0	<----- 206 g/h ----->										0		

Take a winter day, outside climate: $\theta_o = 0.7^\circ\text{C}$, $\phi_o = 79.5\%$, $p_o = 504 \text{ Pa}$; inside temperature: $\theta_i = 17.9^\circ\text{C}$

Inside vapour pressure and R.H. before and after retrofitting: see fig. 4.14. The figures clearly demonstrate the non-steady-state inertia effect: with $n = 1 \text{ h}^{-1}$, changes go on quickly and the low level p_i and ϕ_i steady-state value and p_o again are reached within 3 h; with $n = 0.25 \text{ h}^{-1}$, after the 14h of vapour production, steady-state is not yet reached and next morning, p_i is still higher than p_o . p_i and ϕ_i also climb to high levels (= an important oscillation in p_i and ϕ_i -value!).

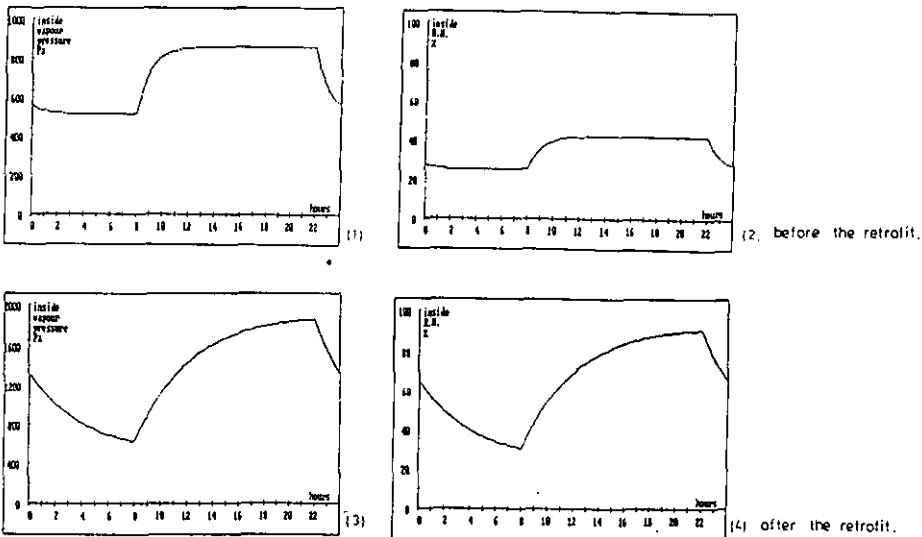


figure 4.14

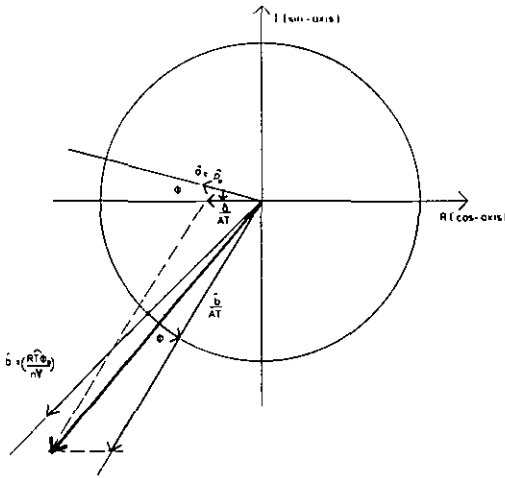


figure 4.15 Solution by vector-calculus

CASE 2

Constant:ventilation rate.
 Outside vapour pressure and inside vapour production oscillate with a period T and amplitude G_p and p_a .

The harmonic solution of the balance equation is:

$$P_i = \bar{P}_i + \sum_{m=1}^{\infty} \hat{P}_{im} \cdot \cos\left(\frac{2 \cdot \pi \cdot t}{T} + \varphi \cdot m + \varphi\right) \quad (4.24)$$

with:

$$\hat{P}_{i(m=1)} = \frac{P_a}{AT} \quad \hat{P}_{i(m=2)} = \frac{R \cdot T \cdot G_p}{n \cdot V \cdot AT}$$

In these, AT stays for the attenuation factor and φ for the phase shift between the p_a and G_p oscillation and the p_i result:

$$AT = 1 + \left[\frac{2 \cdot \pi}{n \cdot T} \right]^2 \quad \varphi = \text{atn}\left(\frac{2 \cdot \pi}{n \cdot T} \right)$$

(4.24) shows that, compared to steady-state, in harmonic mode an amplitude attenuation and a phase shift exists between oscillations in outside vapour pressure or/and inside vapour production and the inside vapour pressure. This attenuation and shift are caused by the air volume inertia, and are totally defined by the harmonic period and the ventilation rate: the shorter the period and the lower the ventilation rate, the larger the attenuation and the phase shift.

Equation (4.24) is easily transposed to vector or complex number calculus: on the goniometric circle, p_e and G_p are vectors with angle φ_1 and φ_2 with the cos-axis. p_e/AT and $(R.T.G_p)/(n.V.AT)$ are also vectors, both shifted over an angle φ compared to p_e and G_p .

p_i is given by the vector sum of p_e/AT and G_p/AT : see fig. 4.15.

Example: The living room of the Zolder case study dwelling.

The outside temperature is 2.7°C , the inside temperature 17.9°C . On a daily basis, the vapour production shows a harmonic course, with a mean value of 120 g/h and an amplitude of 120 g/h, maximum value at 15 h. Also the outside RH changes harmonically with a mean of 84.5% and an amplitude of 5%, maximum value at 11 h. The resulting inside vapour pressure and R.H before and after retrofit are given in fig.4.16.

As attenuation factor and phase shift, we get:

CASE	AT	φ [h]
before retrofit, $n = 1\text{h}^{-1}$	1.03	1
after retrofit, $n = 0.25\text{h}^{-1}$	1.45	3

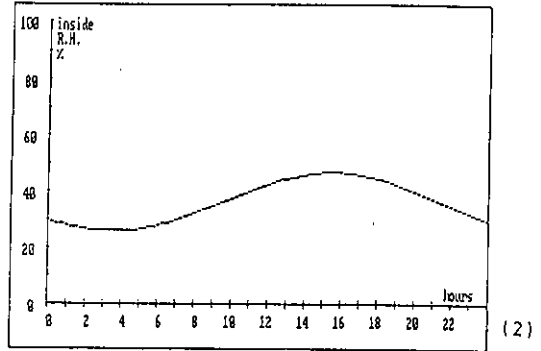
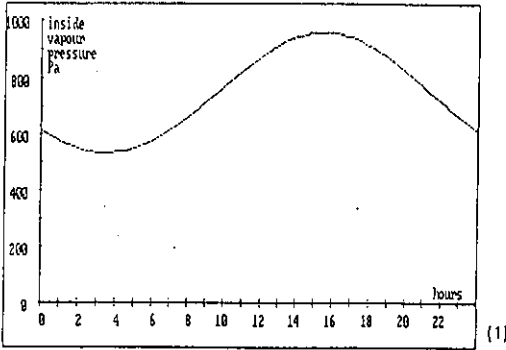
However, in spite of the higher attenuation factor, the inside vapour pressure and RH climb much higher after retrofitting than before:

MAX	AFTER	BEFORE
p_i (Pa)	1920	958
RH (%)	93.5!	46.7

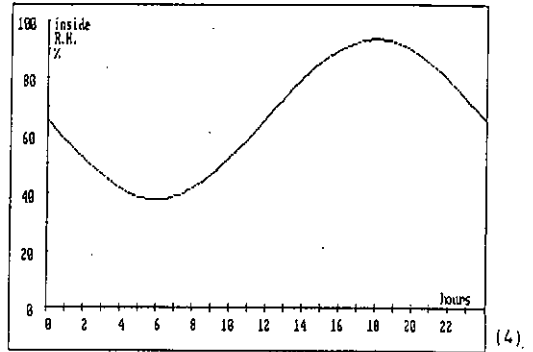
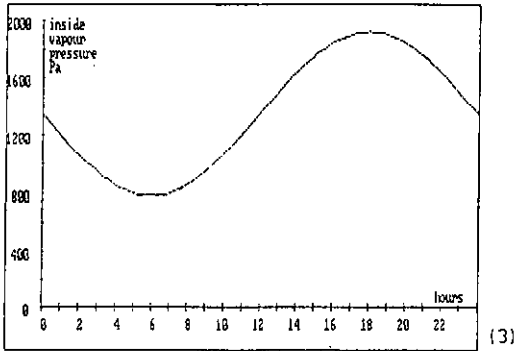
If no air volume inertia interfered, we should find: $AT=1, \varphi=0$ and

MAX	AFTER	BEFORE
p_i (Pa)	= p'_i (2052)	965
RH (%)	= 100.0!	47.0

i.e. after retrofit, condensation occurs everywhere.



Vapour production + outside vapour pressure = harmonic function; before the retrofit.



After the retrofit.

figure 4.16

CASE 3

All parameters variable: outside vapour pressure, ventilation rate, inside temperature, inside vapour production.

An analytical solution is not possible any more: one has to turn to a finite difference approximation. A possibility is the use of a mean differences technique, giving as a solution:

$$P_{i1} = \frac{1}{(1+n \cdot \Delta t/2)} \cdot [(1-n \cdot \Delta t/2) \cdot p_{i0} + n \cdot \Delta t \cdot (p_e + \frac{462 \cdot T_i \cdot G_p}{n \cdot V})] \quad (4.25)$$

with Δt : the time step
 P_{i0} : the inside vapour pressure at the start of the time step
 P_{i1} : the inside vapour pressure at the end of the time step
 P_e, n, G_p, T_i : the mean outside vapour pressure, ventilation rate, inside vapour production and inside temperature (in K!) during the time step.

Equation (4.25) allows us to study the influence of e.g. the aligning of the changes in ventilation rate with the peaks in inside vapour production: more ventilation with increasing, less with decreasing production...

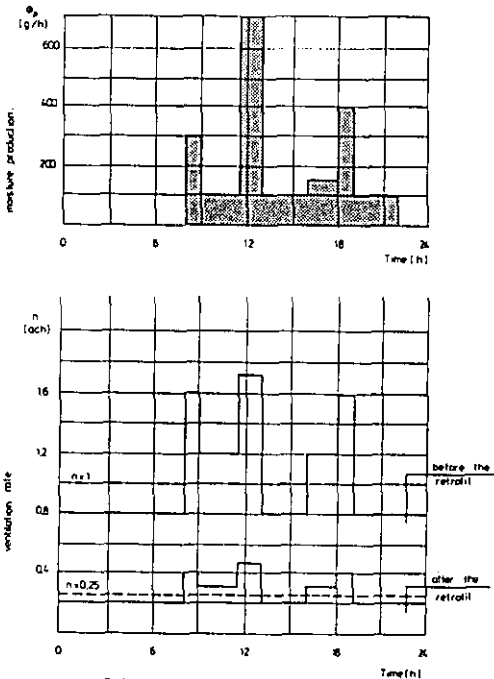


figure 4.17(1) Variable moisture production and ventilation rate

Example: The living room of the Zolder case study dwelling.

As can be seen on the lay-out, this living room is in direct contact with the kitchen, the door between always being open. So the cooking vapour production peaks are directly transmitted to the living space. Suppose before and after retrofitting a vapour production scheme given by (fig.4.17(1)):

h	0	1	2	3	4	5	6	7	8	9	10	11	12	13	14	15	16	17	18	19	20	21	22	23	24
G_p	-----	0	----->		< 100 >		300		< 100 >		700		<--100-->		<150>		400		<--100-->		<--0-->		<--0-->		<--0-->
			(1)		(2)	(3)	(4)		(5)	(6)	(7)	(8)	(9)												

- (1) night, no people in the living room
- (2) breakfast
- (3) a mean of 2 people being present
- (4) noon cooking
- (5) a mean of 2 people being present
- (6) daughter visits: 3 people
- (7) evening cooking
- (8) 2 people television watching
- (9) night

The ventilation rate is either constant or in line with the vapour production:

CONSTANT: before: 1 h^{-1} ;
after: 0.25 h^{-1}

LINED: before:

h	0	1	2	3	4	5	6	7	8	9	10	11	12	13	14	15	16	17	18	19	20	21	22	23	24
n	-----	0.8	----->		< 1.2 >		1.6		< 1.2 >		1.72		<--0.8-->		<1.2>		1.6		<--0.8-->		<--0.8-->		<--0.8-->		<--0.8-->

after:

h	0	1	2	3	4	5	6	7	8	9	10	11	12	13	14	15	16	17	18	19	20	21	22	23	24
n	-----	0.2	----->		< 0.3 >		0.4		< 0.3 >		0.43		<--0.2-->		<0.3>		0.4		<--0.2-->		<--0.2-->		<--0.2-->		<--0.2-->

The low ventilation rate after retrofit, during cooking, is a consequence of the impossibility of the kitchen hood to work well: it creates an underpressure but no effective ventilation...

As hourly mean climatological data, we have (measured with thermohygrographs on 12/2/88):

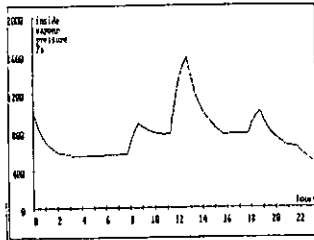
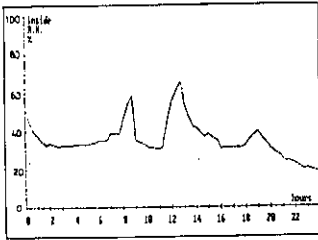
h	θ_a (°C)	ϕ_a (%)	ϕ_i (°C)
1	1.8	74	17.0
2	1.8	76	16.5
3	1.8	77	15.5
4	1.8	78	15.0
5	1.9	78	14.5
6	2.0	79	14.5
7	2.0	80	14.0
8	2.1	80	12.5
9	2.2	80	13.0
10	2.2	81	20.5
11	2.2	81	21.0
12	2.8	81	21.0
13	3.5	81	20.5
14	4.4	74	21.5
15	5.0	70	20.5
16	6.0	56	19.0
17	5.8	57	21.0
18	5.0	59	21.0
19	3.5	60	22.0
20	3.0	61	20.0
21	2.0	62	20.5
22	1.8	64	22.0
23	1.6	65	21.5
24	0.4	66	20.5

The resulting inside vapour pressure and RH_i are drawn in fig.4.17(2). These figures show some interesting features:

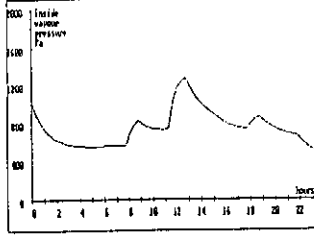
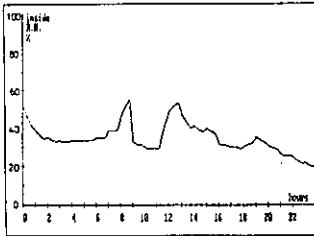
- aligning the ventilation rate with the vapour production results in a clear benefit on maximal inside vapour pressure and inside RH:

n	MAX (at 13h)	AFTER	BEFORE
constant	p_i (Pa)	$= p'_i$ (2412)	1587
	ϕ (%)	$= 100\%$	65.8
lined	p_i (Pa)	2188	1281
	ϕ (%)	90.7	53.1

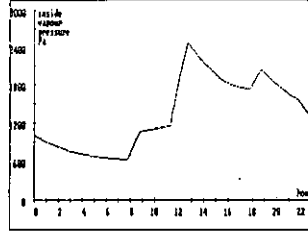
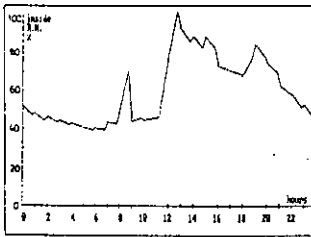
- the low ventilation rate after retrofitting results in a rather slow decrease in vapour pressure after production peaks, the higher value before gives quick changes on much lower p_i - levels;
- the dynamic mean value of inside vapour pressure and RH is very close to the steady-state result on daily mean basis.



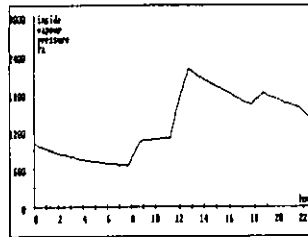
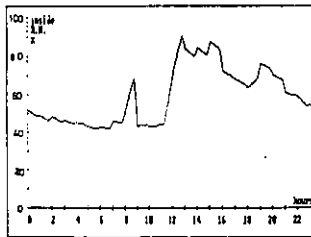
(3) All parameters, except the ventilation rate, variable ($n = 1h^{-1}$) before the retrofit.



(4) All parameters variable, ventilation rate lined with the vapour production before the retrofit.



(1) All parameters, except the ventilation rate, variable ($n = 0.25 h^{-1}$) after the retrofit.



(2) All parameters variable, ventilation rate used with the vapour production after the retrofit.

figure 17(2)

4.4.2 Surface condensation, no hygroscopic influences

Surface condensation is possible as soon as the assumption of a totally isothermal zone (air and all surfaces at the same temperature) is left aside. In practice, this is always the case. With surface condensation or drying, one has to add two extra terms to the mass balance, one to the production side and one to the release side:

$$\begin{array}{c} \text{incoming vapour + vapour produced in the zone} \\ \text{+ THE VAPOUR, DRYING FROM WET SURFACES} \\ - \\ \text{outgoing vapour + the vapour stored in the zonal air} \\ \text{+ THE VAPOUR, CONDENSING ON DIFFERENT SURFACES} \end{array}$$

If the assumptions of ideal mixing of the inside air and 1 outside air vapour pressure are maintained, the balance equation becomes:

$$G_p + \frac{n \cdot V \cdot p_0}{462 \cdot T_i} = \frac{n \cdot V \cdot p_i}{462 \cdot T_i} + \underbrace{\sum_{j=1}^m [\beta_j \cdot A_j \cdot (p_i - p'_{sj})]}_{(1)} + \frac{V}{462 \cdot T_i} \cdot \frac{d p_i}{d t} \quad (4.26)$$

with (1): the condensation / drying term
 β : the diffusion inside surface film coefficient
 A : the surface where condensation / drying takes place
 p'_s : the saturation pressure on that surface.

Rearranging (4.26) gives:

$$\frac{d p_i}{d t} + \left[n + \frac{1}{V} \cdot \sum_{j=1}^m (\beta_j \cdot A_j) \right] \cdot p_i = n \cdot p_0 + \frac{1}{V} \cdot \left[\sum_{j=1}^m (\beta_j \cdot A_j \cdot p'_{sj}) \right] + \frac{462 \cdot T_i \cdot G_p}{V} \quad (4.27)$$

To solve problems of surface condensation / drying, equation (4.27) has to be combined with:

- the condition for surface condensation: inside vapour pressure higher than the saturation pressure on the surface;
- the mass balance at the surface: if M g of water vapour per m^2 have condensed, M g can dry...

If the surface temperature changes from point to point, the Σ in formulae (4.26) and (4.27) has to be replaced by an integral.

In the equations, all parameters except the volume V, are time dependent. That makes exact analytical solutions only possible for simple cases such as steady-state, sudden change in vapour production, harmonic changes, etc.

4.4.2.1 STEADY-STATE SOLUTION

As stated under 4.4.1, steady-state holds for mean situations (1 week, 1 month, 1 year), and mean values for all parameters.

Equation (4.27) turns to ($dp_i/dt = 0$):

$$p_i = \frac{1}{B} \cdot p_e + \frac{462 \cdot T_i}{n \cdot V \cdot B} \cdot G_p + \frac{1}{n \cdot V \cdot B} \cdot \Sigma(\beta_j \cdot A_j \cdot p'_{sj}) \tag{4.28}$$

with $B = (1 + \frac{\Sigma(\beta \cdot A)}{n \cdot V})$

This steady-state solution shows that 4 major influences are relevant to p_i :

- a linear relation with the outside vapour pressure,
- the vapour production
- condensation / drying
- a hyperbolic relation with the ventilation rate.

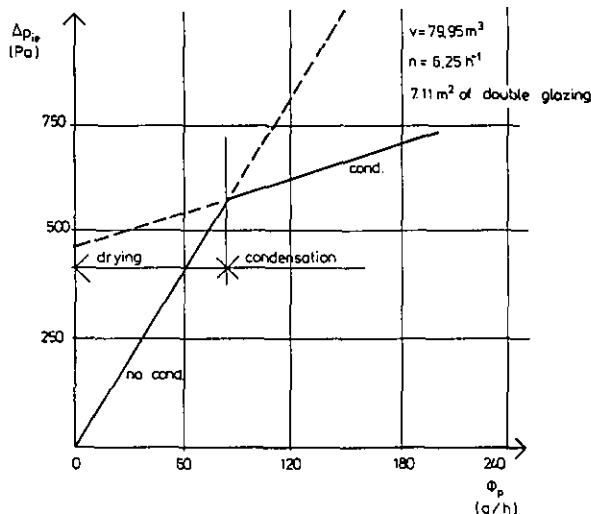


figure 4.18: Influence of condensation-drying on $\Delta p_i = f(G_p)$, G_p being the vapour production

Contrary to the situation with no condensation, after a condensation period, the inside vapour pressure does not equal the outside value in the absence of further vapour production but remains higher. This situation persists, until all condensate has dried.

With condensation, the slope of the line $p_i(G_p)$ is also weaker than without, i.e. vapour production has less influence on the inside vapour pressure than without condensation (fig.4.18):

Example: The living room of the Zolder case study dwelling.

The room has windows on the street and garden sides with total glass surface - 7.11 m². Before retrofitting, both windows were single glazed. During the retrofitting work, they have been replaced by double glazed PVC-frames. Ventilation rate: 1 h⁻¹ before and 0.25 h⁻¹ after retrofitting; inside temperature 18°C; vapour production $G_p = 120$ g/h.

Before retrofitting:

MONTH	θ_c °C	ϕ_e %	SURF.COND. on single glas	P_i Pa	ϕ_i %
J	3.0	89.3	no	881	42.6
F	3.9	90.7	no	936	45.3
M	6.4	92.3	no	1087	52.6
A	9.1	91.3	no	1259	61.0
O	9.1	91.3	no	1259	61.0
N	6.0	92.3	no	1065	51.6
D	3.6	90.2	no	915	44.3

After retrofitting:

MONTH	θ_c °C	ϕ_e %	SURF.COND. on double glas	P_i Pa	ϕ_i %	amount of condens g/m ² day
J	3.0	89.3	yes	1420	68.8	33
F	3.9	90.7	yes	1458	70.6	42
M	6.4	92.3	yes	1562	75.6	66
A	9.1	91.3	yes	1686	81.7	89
O	9.1	91.3	yes	1686	81.7	89
N	6.0	92.3	yes	1547	74.9	62
D	3.6	90.2	yes	1443	69.9	39

or, with $n = 1$ h⁻¹, we have no monthly mean surface condensation on single glazing! That does not mean that, during shorter periods, we may never have some surface condensation, but at least, that condensation and drying of the glazing alternate in such a way that, on a mean basis, dry windows prevail...

After retrofitting however, with $n = 0.25h^{-1}$, we get monthly mean surface condensation on double glazing! The amounts of condensate are substantial: in fact, during the colder half of the year, the glass remains continuously wet, for the inhabitants an annoying situation, in direct contrast to the double glass selling slogan of "no longer wet windows....".

A solution, suggested by some, is to replace a part, or the whole of the double glazing by single glazed panels. Suppose this is done and some to all double glass is omitted. For April, we get as function of the single glass surface (SG = single glazing, DG = double glazing):

SURFACE SG (m ²)	SURF.COND.on the		p _i Pa	φ _i %	amount of condens	
	SG	DG			SG	DG
0.0	-	yes	1686	81.7	-	89
0.3	yes	yes	1677	81.2	936	67
1.0	yes	yes	1653	80.0	702	14
7.1	yes	-	1456	70.5	205	-

with 0.3 m² SG: a ventilation window;

1 m² SG: the openable window single glazed;

7.1 m² SG: the 2 windows single glazed (fig. 4.19).

We can say that:

- replacing part of the double glazing has only a very limited influence on the inside vapour pressure and RH;
- the amounts of condensate per m² on the little surface single glazing at the other hand become awfully high and increase rapidly, with smaller surface (fig. 4.20);
- going back to 'all single glazing' gives a clear benefit in inside vapour pressure and RH, but results in unacceptable wet windows and higher heat losses...

A correct conclusion is that replacing double by single glazing does not give a satisfactory solution; much better is to ameliorate the permanent ventilation (fig. 4.21). Results for April:

VENTILATION RATE h ⁻¹	SURF.COND. on the DG	p _i Pa	φ _i %	amount of condens on the DG	g/(m ² d)
0.1	yes	1764	85.4	263	
0.25	yes	1686	81.6	89	
0.4	no	1561	75.6	0	
0.6	no	1393	67.4	0	
1.0	no	1258	60.9	0	

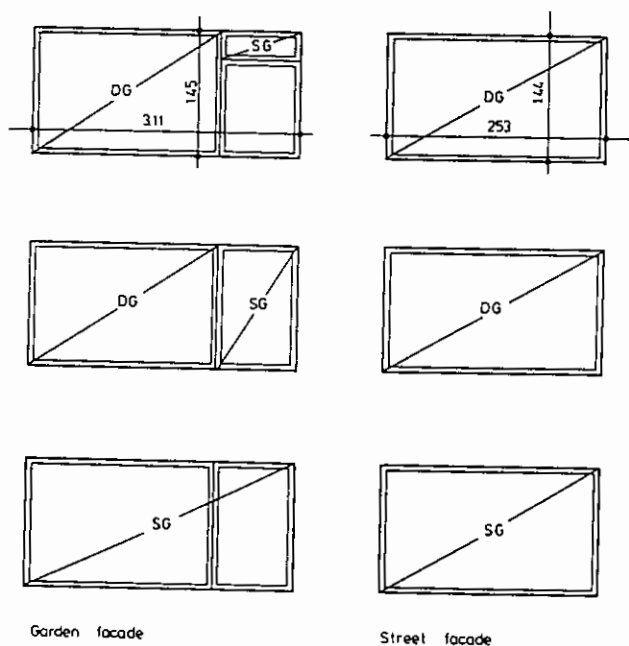


Figure 4.19: windows

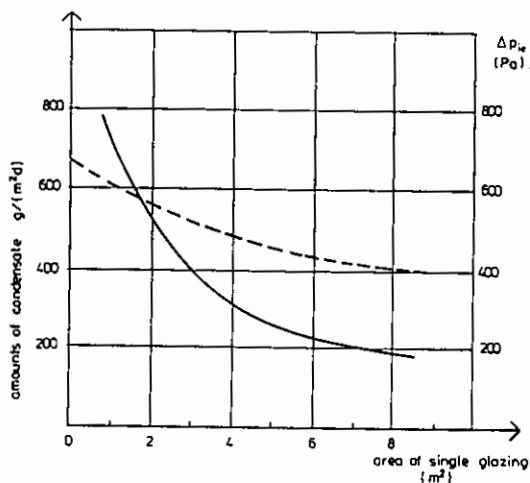


Figure 4.20 Amounts of condensate on lm^2 of single glazing on daily basis

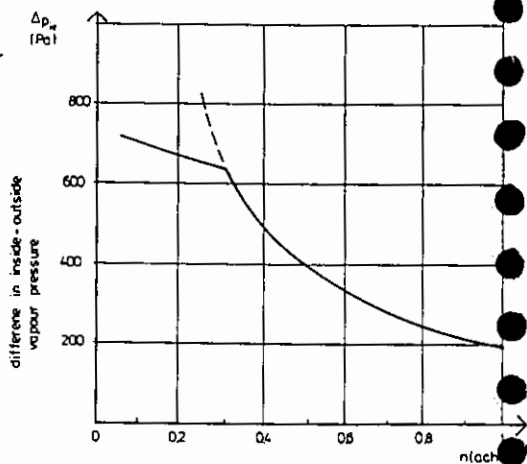


Figure 4.21 Influence of an increased mean ventilation rate on $\Delta p_{i,e}$

4.4.2.2. NON-STEADY-STATE SOLUTIONS

CASE 1

Constant: ventilation rate, inside temperature, outside vapour pressure.
 Inside vapour production starts or changes at $t = 0$, condensation on surface 1 begins at time t_1 .

As the solution of the balance equation when condensation- drying starts, we get:

$$p_i = p_{i\infty 1} + (p'_{s1} - p_{i\infty 1}) \cdot \exp[-a \cdot (t - t_1)] \quad (4.29)$$

with $p_{i\infty 1}$: the steady-state inside vapour pressure value with condensation / drying on surface 1
 p'_{s1} : saturation pressure on 1
 a : the equivalent ventilation rate, given by:

$$a = n \cdot \left[1 + \frac{R \cdot T_i}{n \cdot V} (\beta_i \cdot A_i) \right] \quad (4.30)$$

The solution shows that in non-steady-state conditions, surface condensation and drying are equivalent to a fictitious increase in ventilation rate: the more condensation / drying appears, the quicker the near steady-state inside vapour pressure will be reached.

If the moisture production stops at time t_2 , then (4.29) becomes:

$$p_i = p_{i2\infty 1} + (p_{it2} - p_{i2\infty 1}) \cdot \exp[-a \cdot (t - t_2)] \quad (4.31)$$

with p_{it2} : the outside vapour pressure at the moment the production stops
 $p_{i2\infty 1}$: the steady-state inside vapour pressure given by (4.28) for $G_p = 0$.

(4.31) holds as long as not all the condensate on surface 1 has dried.

For a run on a daily basis, we have to combine the solution for no condensation with the one for condensation, the last to be adapted stepwise, each time condensation starts on another surface with higher temperature ratio than the previous one. During the drying stage, the amounts of condensate remaining on all surfaces have to be monitored. Once a surface dry, it is dropped from the equation.

Example: the step function example with no condensation.

The vapour production in the Zolder living room starts each day at 8 p.m and goes on at a constant rate until 10 a.m, so, the daily vapour production scheme looks like:

hour	0	1	2	3	4	5	6	7	8	9	10	11	12	13	14	15	16	17	18	19	20	21	22	23
G_p	0	0	0	0	0	0	0	0	0	0	0	<----- 206 g/h ----->										0	0	

Before retrofitting, we have: $n = 1 \text{ h}^{-1}$ and 7.11 m^2 of single glazing,
afterwards : $n = 0.25 \text{ h}^{-1}$ and 7.11 m^2 of double glazing.

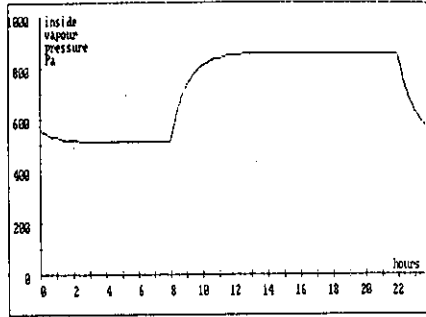
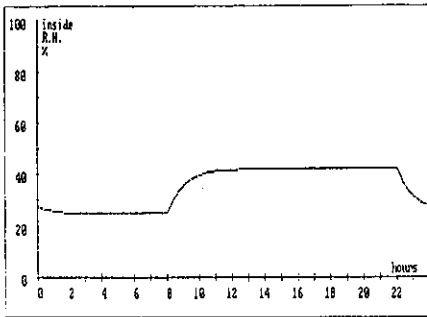
Some years later, the mould complaints led to a reinstallation of 1 m^2 of single glazing. Take a winter day, outside climate: $\theta_e = 0.7^\circ\text{C}$, $\phi_e = 79.5\%$, $p_e = 634 \text{ Pa}$; inside temperature: $\theta_i = 17.9^\circ\text{C}$

Inside vapour pressure and RH before and after retrofitting: see fig. 4.22.

The figures not only show the non-steady-state effects but also the absence of non-steady-state surface condensation on the single glazing before retrofitting, while afterwards, daily condensation on the double glazing is a reality. Putting back a 1 m^2 single glass panel only results in, accumulating condensate on this restricted surface, without eliminating the daily condensation on the double glass. This surface condensation however cuts off the inside vapour pressure peak, spreading the daily moisture production influence on the vapour pressure over all the day (in fact, as long as it is wet, the single and double glazing act as vapour sources) and uncouples the condensation surface RH from the inside value: as long as the surface is wet, one has against it 100% instead of the value:

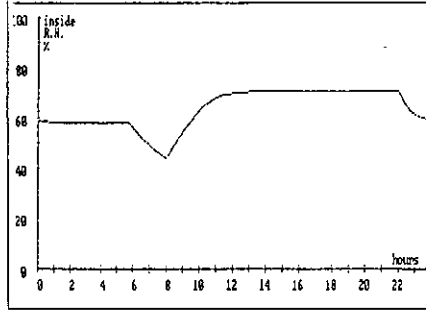
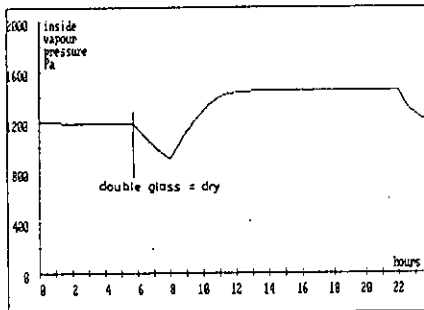
$$\phi_i \cdot p'_i / p'_{s,i}$$

Drying of condensation on a surface with higher temperature ratio, also induces extra condensation against the colder surfaces. Only when the warmer surface is dry, drying of the next colder starts. This may result in long lasting wetting of the coldest spots.



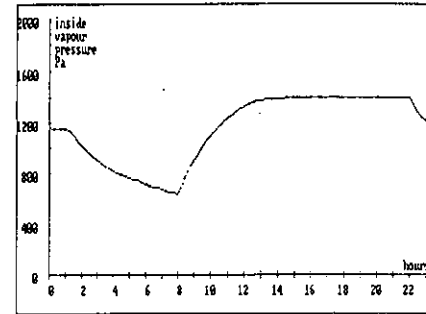
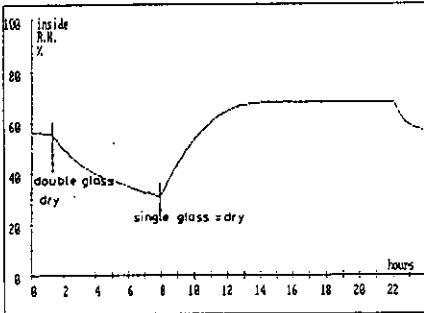
(1)

fig. 4.22: Stepfunction in vapour production before the retrofit: no condensation on single glazing.



(2)

fig. 4.22: Stepfunction in vapour production after the retrofit: condensation on double glazing.



(3)

fig. 4.22: Stepfunction in vapour production 6.1 m² of double glazing, 1 m² of single glazing after the retrofit: condensation on single and double glazing.

figure 4.22

CASE 2

Constant ventilation rate.
Outside vapour pressure and inside vapour production oscillate with a period T and amplitude G_p and p_e .

The use of the harmonic model for the surface condensation case, is only possible if the vapour balance does not jump from condensation/drying to no condensation/ no drying. If so, the solution is easily written by introducing, in the formula 4.24, the equivalent ventilation rate instead of the ventilation rate n .

Example: the Zolder living room

We should have had as attenuation factor and time shift:

CASE	no condensation		condensation	
	AT	φ [h]	AT	φ [h]
A	1.03	1	1.015	0.5
B	1.45	3	1.24	1.8
C			1.24	1.8

A - before retrofit, $n = 1 \text{ h}^{-1}$, 7.11 m^2 of single glass
B - after retrofit, $n = 0.25 \text{ h}^{-1}$, 7.11 m^2 of double glass
C - 6.11 m^2 of double, 1 m^2 of single glass

or, condensation clearly lowers the inertia ...

CASE 3

All parameters variable: outside vapour pressure, ventilation rate, inside temperature, inside vapour production.

In that case, we have to turn to a finite difference approximation, using eg a mean differences technique: (WITH SURFACE CONDENSATION)

$$P_{i1} = \frac{1}{b_1} \cdot \left(a_1 \cdot P_{i0} + a_2 \cdot \left[P_e + \frac{462 \cdot T_1 \cdot G_p}{n \cdot V} + \frac{462 \cdot T_1 \cdot \Sigma(\beta_j \cdot A_j \cdot p'_{sj})}{n \cdot V} \right] \right)$$

$$\text{with } b_1 = 1 + \frac{n \cdot \Delta t}{2} + \frac{462 \cdot T_1 \cdot \Delta t \cdot \Sigma(\beta_j \cdot A_j)}{2 \cdot V}$$

$$a_1 = 1 - \frac{n \cdot \Delta t}{2} - \frac{462 \cdot T_1 \cdot \Delta t \cdot \Sigma(\beta_j \cdot A_j)}{2 \cdot V}$$

$$a_2 = n \cdot \Delta t \quad (4.32)$$

LINED: before:

h 0 1 2 3 4 5 6 7 8 9 10 11 12 13 14 15 16 17 18 19 20 21 22 23 24

n -----0.8-----> | <-1.2> | <--0.8-> | <1.2> | <-----0.8----->
 1.6 1.72 1.6

after:

h 0 1 2 3 4 5 6 7 8 9 10 11 12 13 14 15 16 17 18 19 20 21 22 23 24

n -----0.2-----> | <-0.3> | <--0.2-> | <0.3> | <-----0.2----->
 0.4 0.43 0.4

Possible condensation surfaces:

- before retrofitting: 7.11 m² of single glazing
- after retrofitting : first 7.11 m² of double glazing; then 6.11 m² of double, 1 m² of single glazing.

Hourly mean climatological data, see: no condensation.

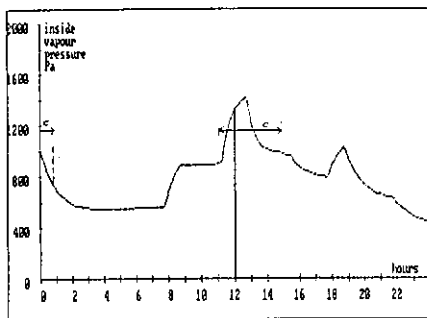
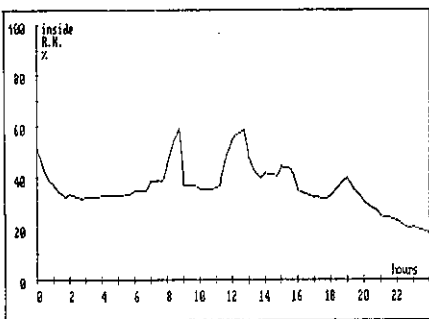
Resulting inside vapour pressure, ϕ_i , surface RH and amounts of condensate before and after retrofitting: fig.4.23.

These figures show, apart from the points discussed in the no condensation / no drying case, some interesting features:

- condensation clearly cuts vapour pressure peaks (see the period when lunch is cooked 1.5 h);
- before retrofitting, some surface condensation appears on the single glazing only during cooking. Drying goes on quickly;
- after retrofitting, condensation on double glazing is abundant and long lasting: the glass is dry only in the morning. The inside outside vapour pressure difference remains positive;
- putting 1 m² of single glazing reduces the condensate on the remaining 6.11 m² double glass. However, the single glass stays awfully wet for the greater part of the day;
- modulation of the ventilation rate with the inside vapour production, reduces the peaks before as well as after retrofitting and gives a somewhat lower mean inside vapour pressure:

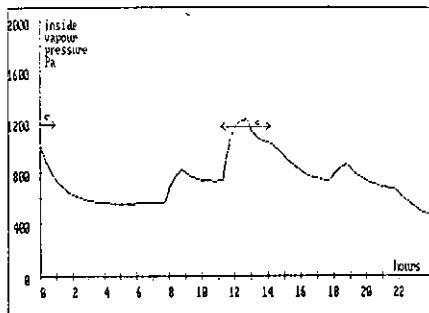
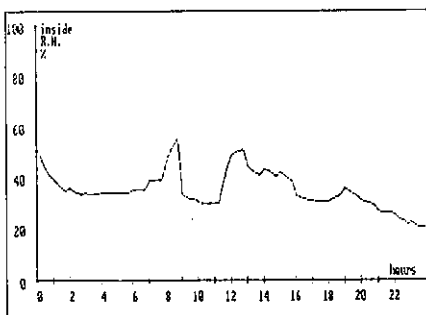
P_{im} (Pa)	before retrofit.	after retrofit.
constant vent.	780.2	1292
modulated vent.	747.1	1256

However, the very low night ventilation 'after' (0.25 h⁻¹) results in permanently wet single glazing.



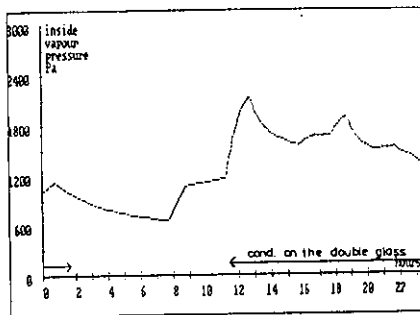
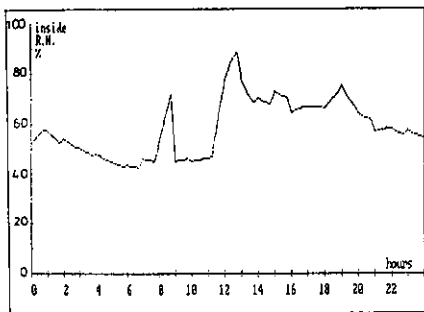
(1)

fig.4.23 : All parameters, except the ventilation rate ($n = 1 \text{ h}^{-1}$) variable, before the retrofit.



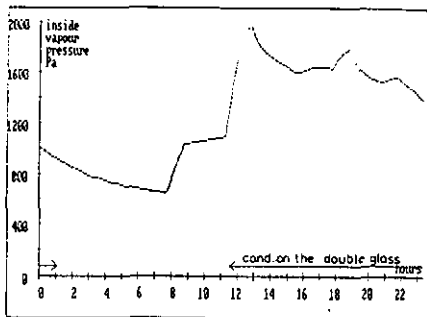
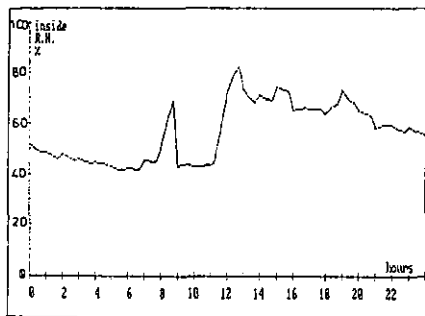
(2)

fig.4.23 : All parameters, variable, ventilation rate lined with the vapour production before the retrofit.

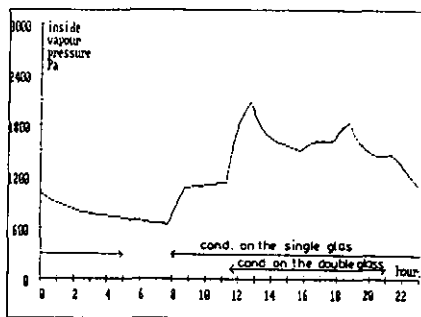
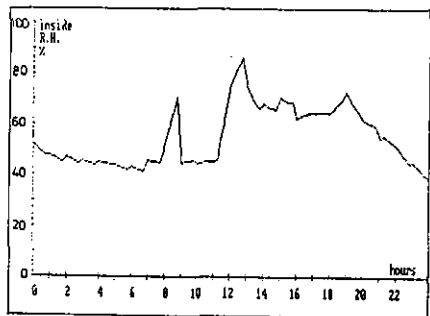


(3)

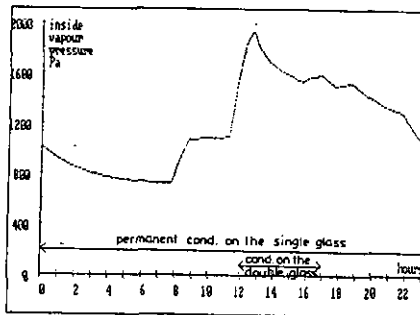
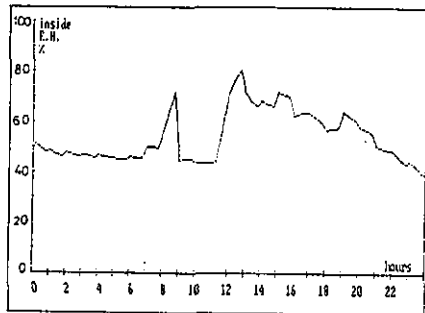
fig.4.23 : All parameters, except the ventilation rate ($n = 0.25 \text{ h}^{-1}$) variable after the retrofit, 7 m^2 of double glazing



(4)
fig. 4.23: All parameters variable, ventilation rate lined with the vapour production after the retrofit, 7,1 m² of double glazing.



(5)
fig. 4.23: All parameters, except the ventilation rate ($n = 0,25 \text{ h}^{-1}$) variable after the retrofit, 6,1 m² of double glazing, 1m² of single glazing.



(6)
fig. 4.23: All parameters variable, the ventilation rate lined with the vapour production after the retrofit, 6,1 m² of double glazing, 1m² of single glazing.

fig.4.23.

ΣG_{sk} stands for the vapour flow at the k different hygroscopic surfaces in the zone. Take hygroscopic surface k . Vapour reaches it by diffusion, the flow in the thin stagnant air layer just against it being given by:

$$G_{sk} = \beta_k \cdot A_k \cdot (p_{sk} - p_i) \quad (4.34)$$

with A_k : the area in m^2 ,
 β_k : the diffusion surface film coefficient,
 p_{sk} : the vapour pressure at the surface.

In wall k , just at the inside surface, the flow can be written as:

$$G_{sk} = \delta_p \cdot (\text{grad } p)_s = \frac{1}{\mu \cdot N} \cdot (\text{grad } p)_s \quad (4.35)$$

The mass balance in the wall looks like:

$$\text{div} (\delta_p \cdot \text{grad } p) = \frac{\partial w_k}{\partial \tau}$$

or, supposing that the flow is one-dimensional:

$$\frac{\partial}{\partial x} (\delta_p \cdot \frac{\partial (p' \cdot \phi)}{\partial x}) = \frac{\partial w_k}{\partial \phi} \cdot \frac{\partial \phi}{\partial \tau} \quad (4.36)$$

Studying suction influences now means: simultaneously solving a system of equations (4.34-4.36), with (4.35-4.36) for each hygroscopic surface. k surfaces results in $2k+1$ equations!

In the system, equation (4.36) is non linear: both the vapour conductivity δ_p and the hygric capacity ($\partial w_k / \partial \phi$) are highly RH-dependent. Because of that, solving the system is only possible with FEM-or FDM-techniques, unless simplifying assumptions are introduced.

4.4.3.2 THEORETICAL APPROACH 1

effective air mass multiplier concept

The most simple concept to represent the moisture storage capacity of a building is the use of the effective air mass multiplier. Several publications deal with this model [16][17]. It assumes the hygroscopic moisture to be stored in an equivalent extra air mass, reducing the system of equations to one:

$$E_m \cdot \frac{d p_i}{d \tau} + n \cdot p_i = n \cdot p_a + \frac{462 \cdot T \cdot G_p}{V} \quad (4.37)$$

with E_m : the air mass multiplier.

This concept virtually moves the storage effects from the solid part to the air. Even short term effects are approximated by this. The multiplier itself depends on the surface to volume ratio, the ventilation rate and the material properties of the walls. The concept is often used in HVAC- simulation programmes. The advantage is that it can be implemented in any existing model with a minimum of difficulty. However, the concept has severe limitations, in particular because of the properties of the building materials not properly defined. Nevertheless, as shown in Annex 13, it can predict the indoor relative humidity with some degree of confidence.

4.4.3.3 THEORETICAL APPROACH 2:

all material properties constant (= linearisation of (4.36)), use of a lumped hygroscopic term (= first order approximation, called the effective penetration depth concept [18])

Lumping is done by using an effective penetration depth d_h . The primary assumption in it is that only a small surface bounded layer of the solid material contributes to the storage process. Temperature and moisture content are assumed to be linear in that layer. With it, (4.35) and (4.36) combine to:

$$\frac{1}{Z_k} \cdot (p_i - p_{sk}) = C_{hk} \cdot \frac{d p_{sk}}{d t} \tag{4.38}$$

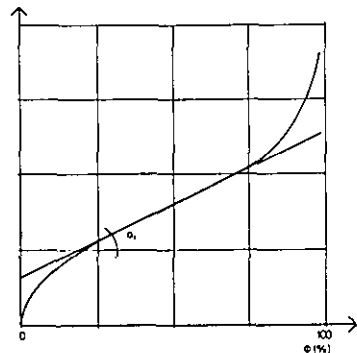
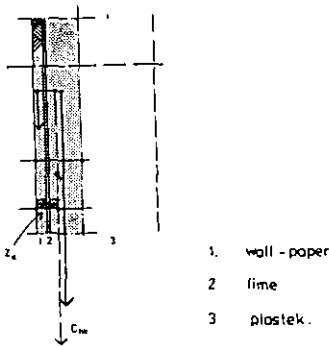


figure 4.24 The effective penetration depth concept

figure 4.25 The specific hygroscopic capacity

Problem in (4.38) is to find reliable values for the effective diffusion resistance Z_k and the storage capacity C_{hk} . A choice as linearised storage capacity over the effective penetration depth, also made in the FAGO- model [19], may be:

$$C_{hk} = \sum_0^{d_h} \left(\frac{a_i \cdot d_i}{p'_{sk}} \right) \quad (4.39)$$

As its diffusion resistance, one may take:

$$Z_k = \frac{1}{\beta_k} + \sum_0^C \left(\frac{1}{\mu_i \cdot N \cdot d_i} \right) \quad (4.40)$$

The sum in C_{hk} has to be taken over all material layers, situated within d_h . In the diffusion resistance Z_k contains all layers between the wall's inside surface and the storage capacity mass centre C of the effective penetration depth (fig. 4.24) (for a 1 layer active thickness situated in the middle of that layer); a_i is the slope of the \pm linear central part of the suction curve of material i (fig 4.25); μ_i is its constant diffusion resistance number.

4.4.3.3.1 CASE 2.1

STEP CHANGE IN VAPOUR PRODUCTION (all other parameters supposed time independent)

We start with the simplest case: 1 hygroscopic surface, no-condensation / no-drying. The system reduces to:

ZONAL HYGRIG BALANCE

$$\left(D + n + \frac{462 \cdot T_i \cdot A_k}{Z_k \cdot V} \right) \cdot p_i - \frac{462 \cdot T_i \cdot A_k}{Z_k \cdot V} \cdot p_{sk} = n \cdot p_e + \frac{462 \cdot T_i \cdot G_p}{V}$$

SURFACE HYGRIG BALANCE

$$- \frac{p'_{sk}}{Z_k \cdot a_k \cdot d_k} \cdot p_i + \left(D + \frac{p'_{sk}}{Z_k \cdot a_k \cdot d_k} \right) \cdot p_{sk} = 0$$

with D : the differentiation operator.

Combining both, reduces the system to a second order differential equation:

$$\left[D^2 + \left(\sum_1^3 \frac{1}{t_i} \right) \cdot D + \frac{1}{t_1} \cdot \frac{1}{t_3} \right] \cdot p_i = \frac{1}{t_3} \cdot \left(\frac{p_a}{t_1} + \frac{462 \cdot T_i \cdot G_p}{V} \right)$$

with the time constants t_1 , t_2 and t_3 given by:

$$\frac{1}{t_1} = n ; \quad \frac{1}{t_2} = \frac{462 \cdot T_i \cdot A_k}{Z_k \cdot V} ; \quad \frac{1}{t_3} = \frac{p'_{sk}}{Z_k \cdot a_k \cdot d_k}$$

Solution of the differential equation:

$$p_i = p_{i\infty} + C_1 \cdot \exp(r_1 \cdot t) + C_2 \cdot \exp(r_2 \cdot t)$$

with $p_{i\infty}$: the steady-state inside vapour pressure value for a vapour production G_p and ventilation rate n .

The roots r_1 and r_2 are:

$$r_1, r_2 = - \frac{1}{2} \cdot \left(\sum_1^3 \frac{1}{t_i} \right) \pm \left[\left(\sum_1^3 \frac{1}{t_i} \right)^2 - \frac{4}{t_1 \cdot t_3} \right]^{0.5}$$

The absolute value of root r_1 (...) normally is so large that $C_1 \cdot \exp(r_1 \cdot T)$ is only important the first moments after the step change. If:

$$\sum_1^3 \frac{1}{t_i} \gg \frac{4}{t_1 \cdot t_3} ,$$

the differential equation turns to first order and root r_2 reduces to:

$$r_2 = \frac{- 1/(t_1 \cdot t_3)}{\sum 1/t_i}$$

The integration constants C_1 and C_2 depend on the starting conditions p_{i0} and p_{sk0} . If both are equal, we get:

$$C_1 = \frac{(r_2 + 1/t_1) \cdot (p_{i\infty} - p_{i0})}{r_1 - r_2} \quad C_2 = \frac{(r_1 + 1/t_1) \cdot (p_{i\infty} - p_{i0})}{r_2 - r_1}$$

Other starting conditions give other integration constants.

With m different hygroscopic surfaces, the differential equation theoretically becomes of m 'th order. In practice, it can be replaced by a first order equation with root r equal to:

$$r = \frac{1/(t_1 \cdot t_3 \cdot t_5 \dots t_{2m+1})}{\sum_1^m (1/t_i)}$$

When condensation and drying on a non porous surface j occurs during the production step, we have to adapt the differential equation:

- p_{i0} becomes the steady-state solution with surface condensation / drying,
- in the time constant $1/\tau = n$, the ventilation rate n must be replaced by the equivalent ventilation rate, defined above.
- the integration constants have to be calculated with either $p_{i0} = p'_{sj}$, the saturation pressure on that condensation surface, or with $p_{i0} = p_{it}$, the inside vapour pressure at the start of drying.

Example

Suppose all walls in the living room of the Zolder dwelling are finished with wall paper, $d = 0.28$ mm. Wall surface: 51 m², from which 36.51 m² outside wall and 13.73 m² inside wall

Paper characteristics: $a \cdot d = 0.0120$ kg/m²; $Z = 29426$ m/s (incl. $1/\beta_1$)

Room volume : 79.9 m³

Ventilation rate : before retrofitting 1 h⁻¹
after retrofitting 0.25 h⁻¹

Inside temperature : 17.9 °C

Starting conditions : $p_{i0} = p_{sk0} = p_e$

The TIME CONSTANTS become:

BEFORE $1/\tau_1 = 1$ h⁻¹ ; $1/\tau_2 = 2.91$ h⁻¹ ; $1/\tau_3 = 5.81$ h⁻¹

AFTER $1/\tau_1 = 0.25$ h⁻¹ ; $1/\tau_2 = 2.91$ h⁻¹ ; $1/\tau_3 = 5.81$ h⁻¹

INSIDE VAPOUR PRESSURE : see fig. 4.26

On the figure, the solution without hygroscopic inertia, no condensation, no drying, is also given. The storage effects are clearly present, leading to a positive difference in inside-outside vapour pressure, over all the day. The effect is more pronounced after retrofitting, with a low ventilation rate, then before.

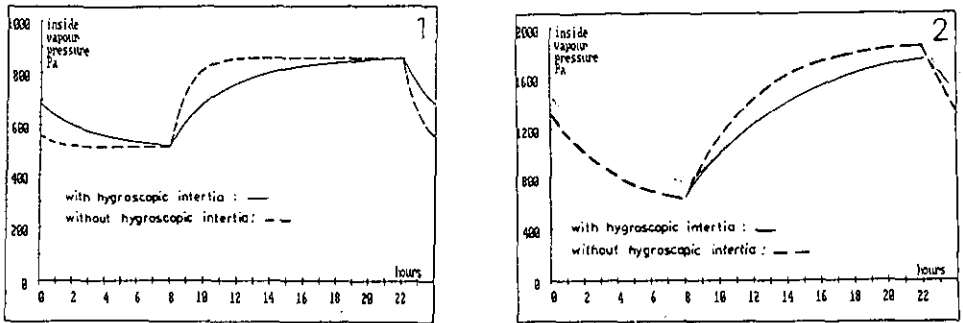


Figure 4.26 Stepfunction in vapour production
Before (1) and after (2) retrofitting, hygroscopic influence

4.4.3.3.2 CASE 2.2

VAPOUR PRODUCTION AND OUTSIDE VAPOUR PRESSURE OSCILLATING WITH PERIOD T
(= HARMONIC SOLUTION)

The harmonic solution gives a good understanding of the hygroscopic inertia by introducing two easy to understand quantities: the attenuation factor AT and time lag φ . With 1 hygroscopic surface, AT and φ are given by:

$$AT = \left[\frac{1}{t_1} \cdot \frac{1}{t_3} \right] / \left[\left[\frac{1}{t_2} \cdot \frac{1}{t_3} - \left(\frac{2 \cdot \pi}{T} \right)^2 \right]^2 + \left(\frac{2 \cdot \pi}{T} \right)^2 \cdot \left(\sum_1^3 \frac{1}{t_i} \right)^2 \right]^{0.5}$$

$$\varphi = \text{atn} \left[\left[\frac{2 \cdot \pi}{T} \cdot \left(\sum_1^3 \frac{1}{t_i} \right) \right] / \left[\frac{1}{t_2} \cdot \frac{1}{t_3} - \left(\frac{2 \cdot \pi}{T} \right)^2 \right] \right]$$

with T: the period

More hygroscopic surfaces complicate the expressions, with for each surface two extra time constants. An analytical solution nevertheless remains possible.

Also between the hygroscopic surfaces themselves and the inside air, we get an attenuation factor and time lag. In formula:

$$AT = 1 + \left(\frac{2 \cdot \pi \cdot t_3}{T} \right)^2 \qquad \varphi = \text{atn} \left(\frac{2 \cdot \pi \cdot t_3}{T} \right)$$

Both uncouple to a (restricted) level the inside RH and the wall surface RH.

Example

Suppose there is an oscillating moisture production in the Zolder dwelling living room, with a mean value and an amplitude of 120 g/h, maximum peak at 15 h. As the daily mean inside temperature, we have 17.9°C. The outside climate is given by: $\theta_o = 0.7^\circ\text{C}$; ϕ_o : mean = 84.5%, ampl = 5.0% peak at 11 h.

The 36.51 m² of outside wall and the 13.73 m² of inside wall are papered, either as described in the step function example or, with a thicker textile, d = 0.8 mm, characteristics: a.d = 0.0312 kg/m²; Z = 84627 m/h. On the floor, there are either tiles or carpet. The tiles are non hygroscopic, the carpet has a pronounced suction activity, with: a.d = 0.3 kg/m²; Z = 21626 m/h

The outside wall has a temperature ratio 0.73.

ATTENUATION FACTOR AND PHASE SHIFT FOR THE INSIDE VAPOUR PRESSURE

	AT	ϕ (h)
before retrofitting (n = 1 h ⁻¹):		
no air inertia	1.00	0.0
no hygroscopic inertia	1.03	1.0
walls papered, tiles	1.13	1.9
walls textiled, tiles	1.67	3.9
walls textiled, carpet	3.08	5.1
after retrofitting (n = 0.25 h ⁻¹):		
no air inertia	1.00	0.0
no hygroscopic inertia	1.45	3.1
walls papered, tiles	2.05	4.0
walls textiled, tiles	3.44	5.1
walls textiled, carpet	9.18	5.9

ATTENUATION FACTOR AND PHASE SHIFT FOR THE VAPOUR PRESSURE AGAINST THE HYGROSCOPIC SURFACES, COMPARED TO THE INSIDE VAPOUR PRESSURE

	AT	ϕ (h)
before and after retrofitting (n = 1 h ⁻¹)		
no hygroscopic inertia	1.00	0.0
walls papered, tiles:		
outside wall	1.00	0.2
inside wall	1.00	0.2
walls textiled, tiles:		
outside wall	1.20	1.6
inside wall	1.11	1.2
walls textiled:		
wall (TF=1)	1.11	1.2
carpet	1.36	2.1

HYGROSCOPIC MOISTURE EXCHANGES (g)

before retrof.

after retrof.

no hygroscopic inertia		0	0
walls papered, tiles	outside wall	112	230
	inside wall	32	64
walls textiled, tiles	outside wall	164	298
	inside wall	50	90
walls textiled,	wall (TF=1)	98	124
	carpet	362	478

INSIDE VAPOUR PRESSURE: fig.4 27

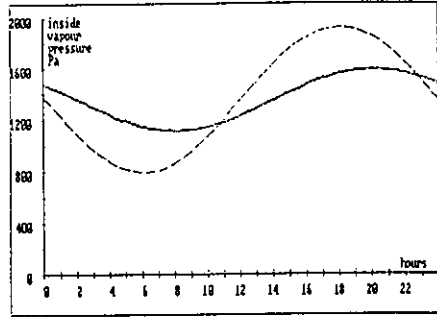
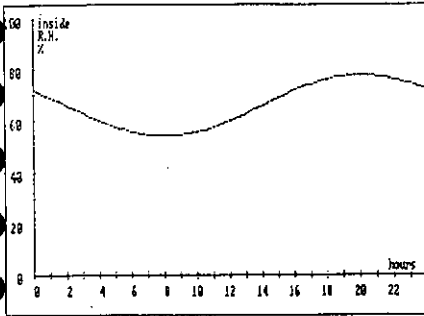


fig. 4.27: Vapour production + outside vapour pressure = harmonic functions after the retrofit.
+ hygroscopic stockage in textile wall finish.

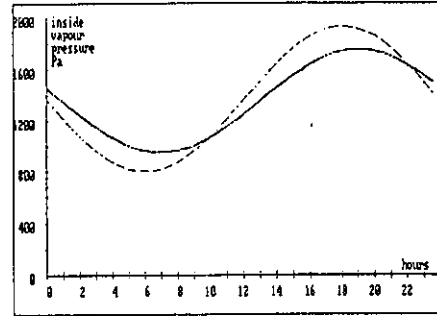
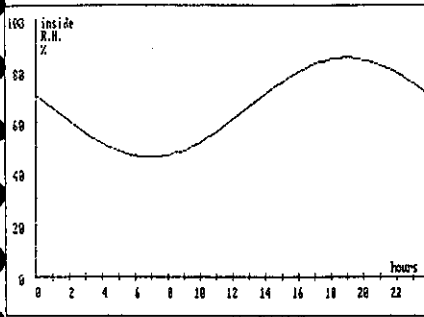


fig. 4.27: Vapour production + outside vapour pressure = harmonic functions after the retrofit.
+ hygroscopic stockage in the wallpaper

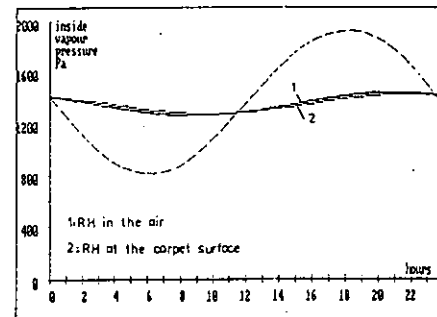
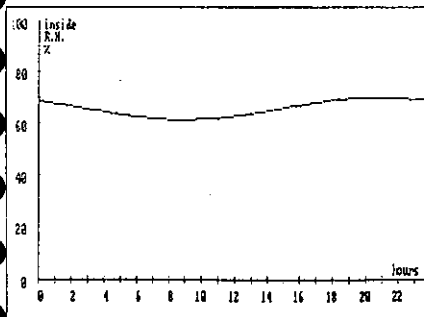


fig 4.27: Vapour production + outside vapour pressure = harmonic functions after the retrofit
+ hygroscopic stockage in textile wall finish + carpet.

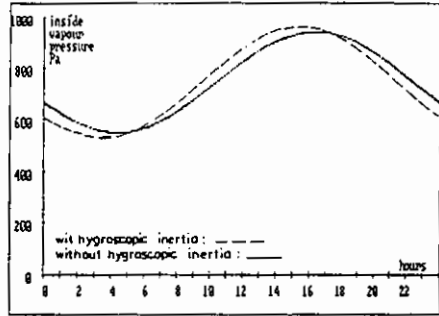
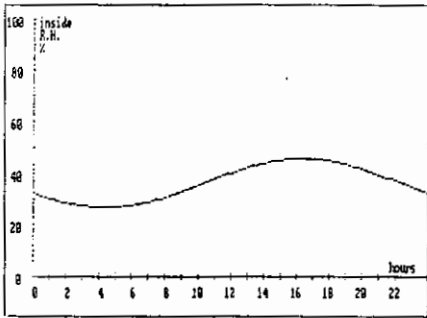


fig. 4.27: Vapour production + outside vapour pressure = harmonic functions
before the retrofit
+ hygroscopic stockage in the wallpaper.

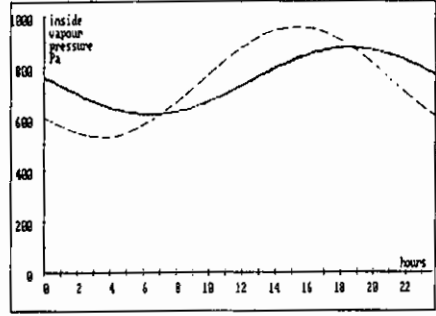
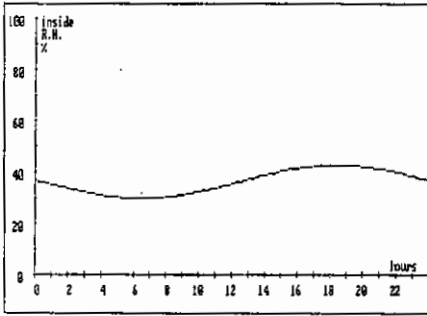


fig. 4.27: Vapour production + outside vapour pressure = harmonic functions
before the retrofit
+ hygroscopic stockage in textile wall - finish.

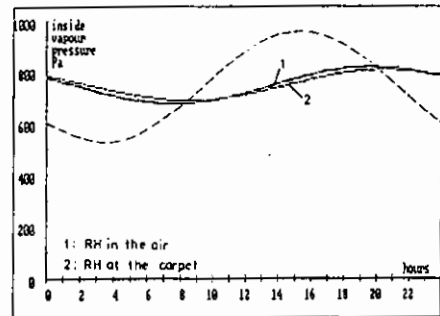
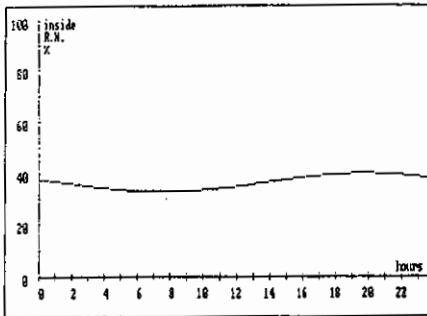


fig. 4.27: Vapour production + outside vapour pressure = harmonic functions
before the retrofit
+ hygroscopic stockage in textile wall finish + carpet.

figure 4.27

The example shows that:

- hygroscopic inertia may become important, with significant amounts of vapour sucked and released by the active surfaces;
- with high hygroscopic load, the zonal reaction shifts more and more to a steady-state response, coupled to the mean values of vapour production and outside vapour pressure;
- very hygroscopic surfaces generate a not unimportant attenuation factor and time shift between the surface RH (ϕ_s) and the air RH (ϕ_i). Through that, the use, on instantaneous basis, of the simple formula

$$\phi_s = \phi_i \cdot (p'_i/p'_s)$$
 with p'_i the inside saturation pressure and p'_s the saturation pressure at the surface turns out to be wrong.

4.4.3.3.3 CASE 2.3

ALL PARAMETERS VARIABLE

All parameters variable means: outside temperature, inside temperature, ventilation rate, vapour production, number of active condensation surfaces, surface temperatures...varying with time.

In thermal non-steady-state conditions, it is much easier to shift from the vapour pressure as the dependent variable to the RH's. To solve the system of 1 zonal hygric and k hygroscopic surface equations, only a FDM- approach is left, e.g. a mean differences solution (Cranck-Nicholson scheme). In that case, one gets per time step a system of pseudo-linear equations, given by (written for 4 hygroscopic surfaces):

$$\begin{bmatrix} A_{11} & -A_{12} & -A_{13} & -A_{14} & -A_{14} \\ -A_{21} & A_{22} & 0 & 0 & 0 \\ -A_{31} & 0 & A_{33} & 0 & 0 \\ -A_{41} & 0 & 0 & A_{44} & 0 \\ -A_{51} & 0 & 0 & 0 & A_{55} \end{bmatrix} \cdot \begin{bmatrix} \phi_1 \\ \phi_{s1} \\ \phi_{s2} \\ \phi_{s3} \\ \phi_{s4} \end{bmatrix} = \begin{bmatrix} B_1 \\ B_2 \\ B_3 \\ B_4 \\ B_5 \end{bmatrix}$$

with (k=2,3,4):

$$A_{11} = \left\{ \left[1 + \frac{n \cdot \Delta t}{2} + \frac{462 \cdot T_i \cdot \Delta t}{2 \cdot V} \cdot \left[\sum_1^4 (\beta \cdot A_j) + \sum (\beta \cdot A_k) \right] \right] \cdot p'_{it} \right\}$$

$$A_{k1} = \left[\frac{462 \cdot T_i \cdot \beta \cdot A_k \cdot p'_{skt} \cdot \Delta t}{2 \cdot V} \right] \quad A_{1k} = \left[\frac{p'_{it} \cdot \Delta t}{2 \cdot Z_k} \right] \quad A_{kk} = \left[\frac{p'_{skt} \cdot \Delta t}{2 \cdot Z_k} + C_{hk} \right]$$

$$\begin{aligned}
 B_1 = & \left(\left[1 - \frac{n \cdot \Delta t}{2} - \frac{462 \cdot T_i \cdot \Delta t}{2 \cdot V} \cdot \left[\sum_1^4 (\beta \cdot A_j) + \Sigma(\beta \cdot A_k) \right] \right] \cdot p'_{i0} \cdot \phi_{i0} \right. \\
 & + \frac{462 \cdot T_i \cdot \Delta t}{V} \cdot \left[\sum_1^4 \left(\frac{\beta \cdot A_k \cdot p'_{sk0} \cdot \phi_{sk0}}{2} \right) + \Sigma(\beta \cdot A_j \cdot p'_{sj}) \right] + n \cdot p_e \cdot \Delta t \\
 & \left. + \frac{462 \cdot T_i \cdot G_p \cdot \Delta t}{V} \right) \\
 B_k = & \left(\left(\frac{p'_{i0} \cdot \phi_{i0} \cdot \Delta t}{2 \cdot Z_k} \right) - \phi_{sk0} \cdot \left(\frac{p'_{sk0} \cdot \Delta t}{2 \cdot Z_k} - C_{hk} \right) \right)
 \end{aligned}$$

In these equations, all quantities, except the RH inside and at the hygroscopic surfaces, are averaged over the time step Δt . The system has to be solved for each time step. Condensation/drying control is coupled to:

Y/N condensation: $p'_{it} < > p'_{sj}$

Y/N drying : amount of condensate on surface $j \geq 0$

4.4.3.4 THEORETICAL APPROACH 3

all material properties constant (= linearisation of (4.36)), the whole wall hygroscopically active (second order approximation)

We restrict the second order approach to the harmonic solution of the hygric balance for thermal steady-state conditions, the vapour production and the outside vapour pressure being periodical functions of time and no surface condensation/drying going on. In that case, the conservation of mass equation on a zonal level can be written, for each harmonic, in complex form (bold - complex number):

$$\frac{462 \cdot T_i \cdot G_p}{V} + n \cdot p_e + \frac{462 \cdot T_i}{V} \cdot \sum_1^k G_{sk} = (n + j \cdot \frac{2 \cdot \pi}{T}) \cdot p_i \quad (4.41)$$

with j : the imaginary unity
 T : the period of the harmonic.

In (4.41), G_{sk} stands for the harmonic component with period T of the vapour flow between the hygroscopic surface k and the zonal air.

On the surface, G_{sk} is given by:

$$G_{sk} = A_k \cdot \left(\frac{p_e}{D_{gk}} - ad_k \cdot p_i \right) \quad (4.42)$$

with D_{sk} : the dynamic diffusion resistance of wall k for the considered harmonic
 ad_k : the vapour admittance of wall k for the considered harmonic

Both complex wall properties follow from the steady-state periodic solution for composite flat walls, of the partial differential equation:

$$\frac{\partial^2 p_i}{\partial t^2} = \frac{a \cdot N \cdot \mu}{p'_i} \cdot \frac{\partial p_i}{\partial t}$$

Merging (4.41) and (4.42) and solving the resulting equation for p_i gives the complex result:

$$p_i \sim \frac{n \cdot p_e + 462 \cdot T_i \cdot G_p / V + 462 \cdot T_i \cdot \Sigma(p_e \cdot A_k / D_{sk}) / V}{n + 462 \cdot T_i \cdot \Sigma(ad_k \cdot A_k) / V + j \cdot 2 \cdot \pi / T}$$

For a period of 1 day, the dynamic diffusion resistance is mostly so high, that $p_e / D_{sk} \approx 0$, reducing the equation to:

$$p_i \sim \frac{n \cdot p_e + 462 \cdot T_i \cdot G_p / V}{n + 462 \cdot T_i \cdot \Sigma(ad_k \cdot A_k) / V + j \cdot 2 \cdot \pi / T} \quad (4.43)$$

On a monthly or yearly basis, the dynamic resistance term is best taken into account.

The vapour pressure against a hygroscopic surface k follows from the combination of (4.42) and:

$$G_{sk} = \beta \cdot A_k \cdot (p_i - p_{sk})$$

In (4.43), the divider stands for the complex attenuation factor, amplitude:

$$AT = \left\{ \left[n + \frac{462 \cdot T_i}{V} \cdot \Sigma(ad_k \cdot A_k \cdot \cos \varphi_{adk}) \right]^2 + \left[\frac{2 \cdot \pi}{T} + \frac{462 \cdot T_i}{V} \cdot \Sigma(ad_k \cdot A_k \cdot \sin \varphi_{adk}) \right]^2 \right\}^{0.5}$$

and phase shift:

$$\varphi = \text{atan} \left[\frac{n + 462 \cdot T_i \cdot \Sigma(ad_k \cdot A_k \cdot \cos \varphi_{adk}) / V}{2 \cdot \pi / T + 462 \cdot T_i \cdot \Sigma(ad_k \cdot A_k \cdot \sin \varphi_{adk}) / V} \right]$$

In the equations, the number of surfaces k is unrestricted.

Example 1

Let's go back to the lumped parameters periodic steady-state Zolder dwelling living room example. All parameters have the same value, except that, only the case of papered inside and outside walls is considered.

The outside wall is composed of (from inside to the outside):

layer	thickness cm	μ -value -	a-value kg/m ³
wallpaper	0.028	80	43
gypsum plaster	1.5	5.5	70.9
brickwork	18.0	15	0.6
cavity	6.0	0.3	0.008
brickwork	8.5	5.5	0.6

The inside wall is composed of (from in- to the other side):

layer	thickness cm	μ -value -	a-value kg/m ³
wallpaper	0.028	80	43
gypsum plaster	1.5	5.5	70.9
brickwork	9.0	15	0.6

ATTENUATION FACTOR AND PHASE SHIFT FOR THE INSIDE VAPOUR PRESSURE

	AT	φ (h)
before retrofitting ($n=1 \text{ h}^{-1}$)		
no air inertia	1.00	0.0
no hygroscopic inertia	1.03	1.0
walls papered, tiles	2.32	1.2
after retrofitting ($n=1 \text{ h}^{-1}$)		
no air inertia	1.00	0.0
no hygroscopic inertia	1.45	3.1
walls papered, tiles	7.10	1.5

HYGROSCOPIC MOISTURE EXCHANGES (g)

	before retrof.	after retrof.
no hygroscopic inertia	0	0
walls papered, tiles		
outside wall	428	559

INSIDE VAPOUR PRESSURE: see fig.4.28

This example shows that the lumped parameter approach, only taking into account the finishing layer, underestimates the hygroscopic attenuation and vapour exchange but overestimates the phase shift.

According to the second order vapour exchange results, the lumped active thickness should have been the wall paper + the inside 1.2 mm of the gypsum

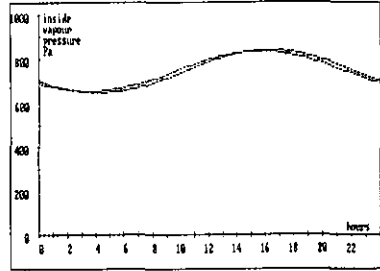
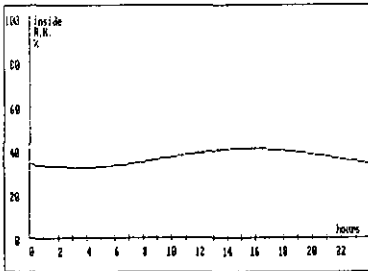


fig.4.28: Vapour production + outside vapour pressure = harmonic functions
before the retrofit
+ hygroscopic stockage second order model.

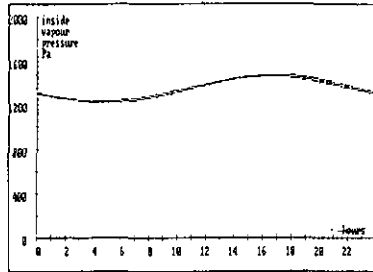
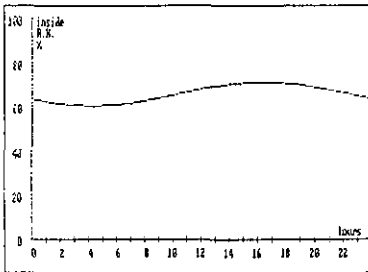


Figure 4.28 Vapour production + outside vapour pressure = harmonic functions
after the retrofit
+ hygroscopic stockage, second order model.

plaster... However, an important conclusion remains that, on a daily basis, only a few inside mm of the wall's thickness act as the active hygroscopic capacity. All layers deeper in the construction have no influence. Statements like 'bricks for the cavity wall give a better inside vapour pressure attenuation than concrete blocks' have nothing to do with reality.

Example 2

The same calculation as above has been redone on a yearly basis, supposing a constant vapour production of 120 g/h, a constant inside temperature and a mean outside vapour pressure of 1100 Pa, with an oscillation amplitude of 430 Pa, maximum value end of July.

ATTENUATION FACTOR AND PHASE SHIFT FOR THE INSIDE VAPOUR PRESSURE

before retrofitting ($n = 1 \text{ h}^{-1}$)	AT	ϕ (h)
no air inertia	1.00	0.0
no hygroscopic inertia	1.00	1.0
walls papered, tiles	1.04	365.3

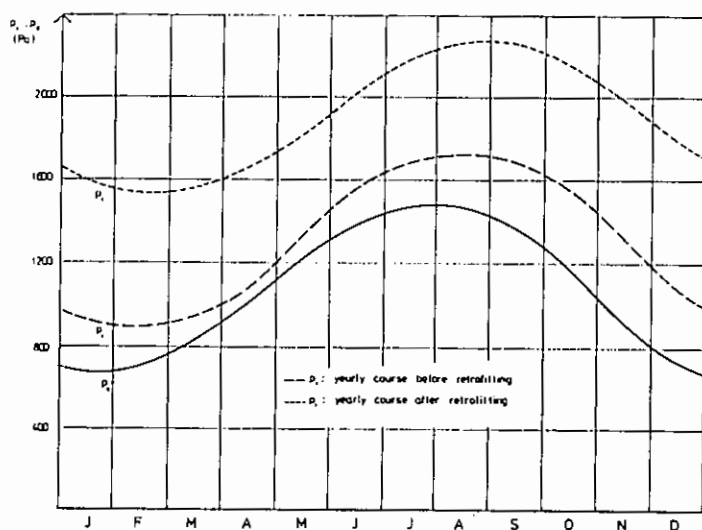


Figure 4.29: Harmonic response on yearly basis

after retrofitting ($n=1 \text{ h}^{-1}$)	AT	φ (h)
no air inertia	1.00	0.0
no hygroscopic inertia	1.00	4.0
walls papered, tiles	1.15	730.0

HYGROSCOPIC MOISTURE EXCHANGES (g)

	before retrof.	after retrof.
no hygroscopic inertia	0	0
walls papered, tiles		
outside wall	36350	32578

INSIDE VAPOUR PRESSURE: see fig.4.29

The high vapour exchange shows that on a yearly basis the whole outside wall acts as hygroscopic capacity, resulting in a time shift of some weeks in poorly ventilated dwellings. That fact may explain why in real world situations the late year period gives more mould and surface condensation problems than the springtime. The phase shift emphasises the inside - outside vapour pressure differences during these autumn months.

4.4.3.5 THEORETICAL APPROACH 4

all material properties variable, the whole wall hygroscopically active (second order approximation)

The solution has to be sought in a FDM- or FEM approximation of the governing 1 zonal and k wall surface differential equations with, for each time step, an iterative solution of the resulting system of non linear algebraic equations.

Possibilities are:

The response factor method [20]

Response factors are pre-calculated values of the hygroscopic response of a construction part, using Z-transfer functions, associated with an inside vapour pressure excitation. However, the factors are depending on moisture content and temperature and have to be defined for each single step in both.

Once calculated, the advantages of using the factors are:

- relatively easy to implement in existing programmes (they are calculated in an independent module);
- valid for any pattern of moisture production.

A frequency response concept [21]

This is similar to the harmonic response, discussed under assumption 3. Because of the non-linearity of the equations, a FEM- or FDM- method has to be used to calculate the admittance and dynamic resistance functions. These depend of the excitation signal.

4.4.3.6 EXPERIMENTAL APPROACH 1

Fraunhofer Institut für Bauphysik, Stuttgart-Germany [10]
(Dipl.-Ing. H.R. Künzel)

Calculations with a single zone hygric model, using 2 approaches for the moisture sorption of furniture and walls, were compared with measurements of the RH-change, induced by a vapour production step, in 2 rooms, one not hygroscopic and one with papered gypsum board walls.

hygroscopic models

In the first model the moisture sorption of furniture and walls is treated as a vapour capacitance in parallel with the air storage, given by:

$$G = (\sum s_k) \cdot \frac{d p_i}{d t} \quad s_k = \frac{l}{462 \cdot T_i} \cdot \frac{A_k}{p'_i} \cdot (a_k \cdot d_k)$$

with G : the total vapour flow
 A_k : the area of hygroscopic surface k,
 a_k : the slope of its suction curve
 d_k : its active thickness.

In the second model the diffusion equation for each wall is linked to the zonal hygric balance in the same way as described in the theory above. The material properties for each wall layer may be RH- dependent.

experimental validation

With both models, the influence on the RH of an injection, during 3.5 h., of 200 g of water vapour, measured in 2 rooms, volume 40 m³, wall area 50 m², the first with walls and ceiling covered with aluminium plates, the second with walls and ceiling finished with gypsum board with textured paper, both with plastic flooring and variable, but monitored ventilation rate, was simulated. Room 1 was used to adjust the ventilation rate in the calculation scheme. With that rate, model 2 gave for the hygroscopic room 2 a calculated RH-course, in good agreement with the measured values.

Model 1 overestimated the inertia effects: see fig.4.30. With model 2, some example calculations were performed on a room with severe moisture production, showing the damping effects, compared to no suction inertia, and the attenuation of the RH against the walls, compared to the air RH: fig.4.31.

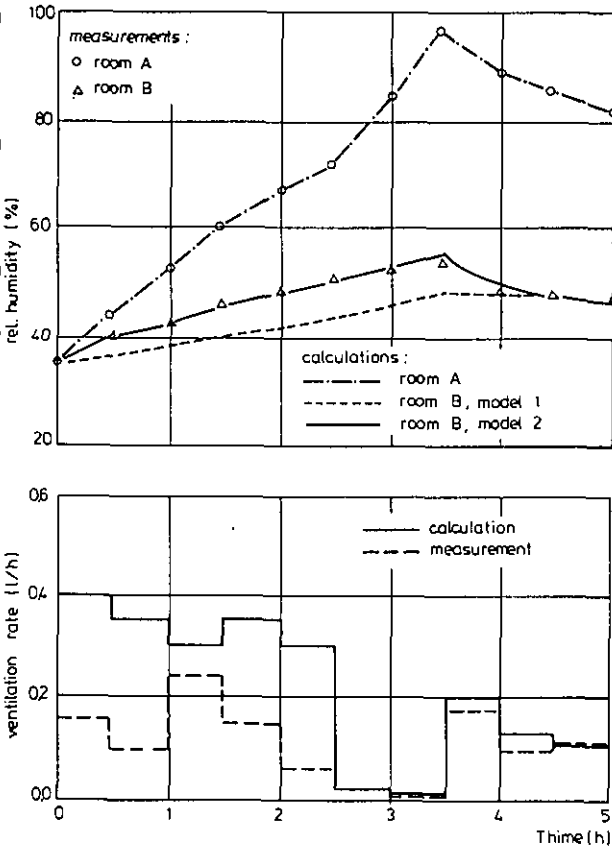


fig. 4.30 : Experimental validation of calculations.

Above: Comparison of the measured and calculated course of relative humidity in a room with aluminium plated walls (room A) and in a room with conventional wall surfaces consisting of ingrain wall paper on gypsum board (room B). Model 1 is referring to equation (2) and model 2 to equation (5)

Below: Comparison of the measured and calculated air change rate in the two rooms. The calculation is a fitting of the ventilation rate in order to ensure a good agreement of the course of humidity between the measurement and the calculation of the room balance without sorption effects in room A.

figure 4.30

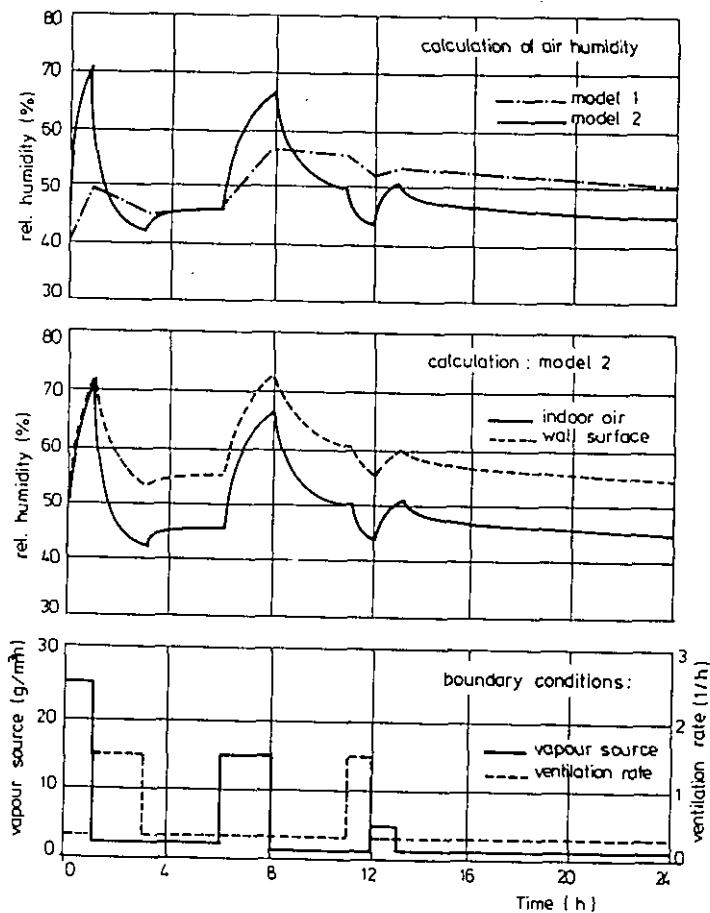


fig. 4.31: Calculations of the moisture behaviour of a bathroom.

Above: Comparison of the course of relative humidity of the air calculated with the aid of sorption model 1 and sorption model 2

Middle: Course of relative humidity of the indoor air and the wall surface calculated with sorption model 2.

Below: Plot of the underlying boundary conditions, vapour production and ventilation rate typical for a bathroom.

figure 4.31

4.4.3.7 EXPERIMENTAL APPROACH 2

Cauberg-Huygen, The Netherlands [11]
ir. J.L.C.L. Boot, ing. A.N.J. Plomp

The influence of an increasing number of hygroscopic active surfaces in a room on the RH-change, coupled to a step in vapour production, was measured.

Test room

An ordinary office room on the 3th floor of an office building, Beemradsingel 70, Rotterdam, floor surface 12 m² and volume 35 m³, was equipped as test room. Three situations were studied:

- empty room: all walls, floor and ceiling covered with plastic foil (70.35 m²)
- finished room: 10.3 m² wool carpet on the floor, 4.2 m² cotton curtains at the windows
- furnished room: the finished room with 1 seat, 4.5 m² of developed surface, 1 chair, 2.1 m² of developed surface and 1 newspaper bag, 0.2 m² of newspaper surface.

Measurements

- heating the room from 18 to 25 °C ($n = 0.07 \text{ h}^{-1}$);
- measuring the course of the RH when going from 40 to 65 % by evaporating some 600 g/h of vapour ($n = 0.07 \text{ h}^{-1}$, no surface condensation);
- evaporating 280 g of vapour ($n = 0.07 \text{ h}^{-1}$, no surface condensation, production flow: 600 g/h).

Measuring results, discussion (See fig.4.32 - fig.4.34)

These figures show the increasing suction influence from empty to furnished, with the greatest step from empty and finished. However, also in the empty situation, with plastic foil all around, we see on the 40% to 65% RH graph a greater hygric inertia than only the air volume. If only that was important, the production time should have been 16.5' instead of 22', proving that non hygroscopic layers (here some 70.35 m² of PE-foil) in fact adsorb water molecules at the surface.

The measurements may be translated into material properties and diffusion surface film resistances.

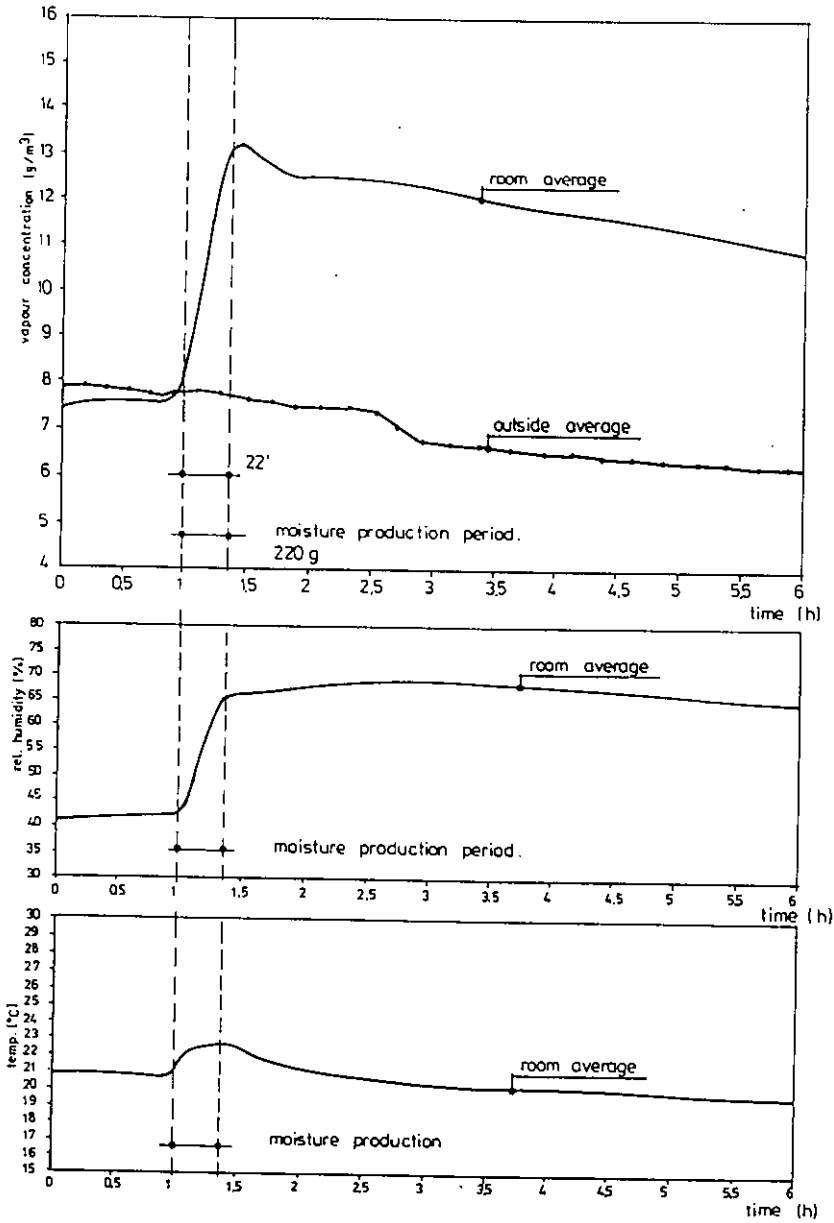


figure 4.32 Empty Room

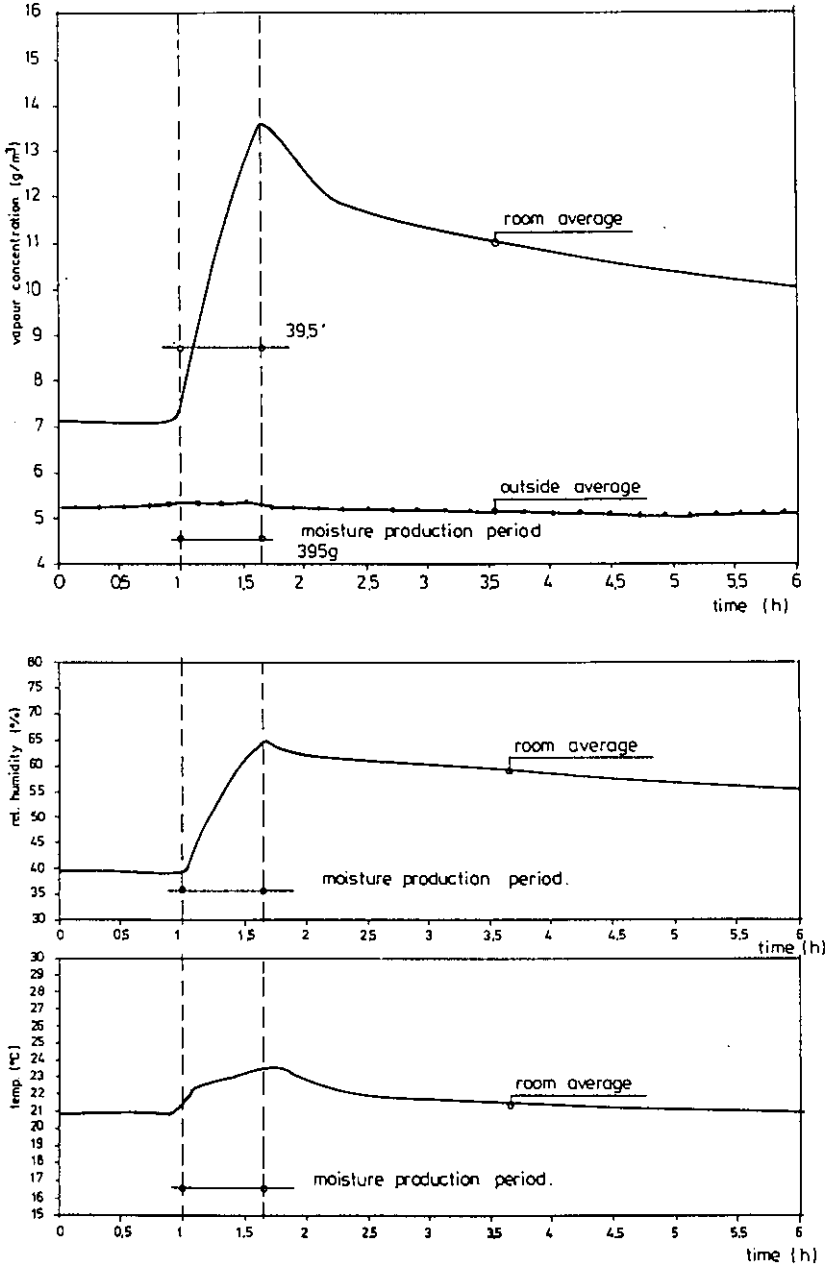


Figure 4.33 Finished Room

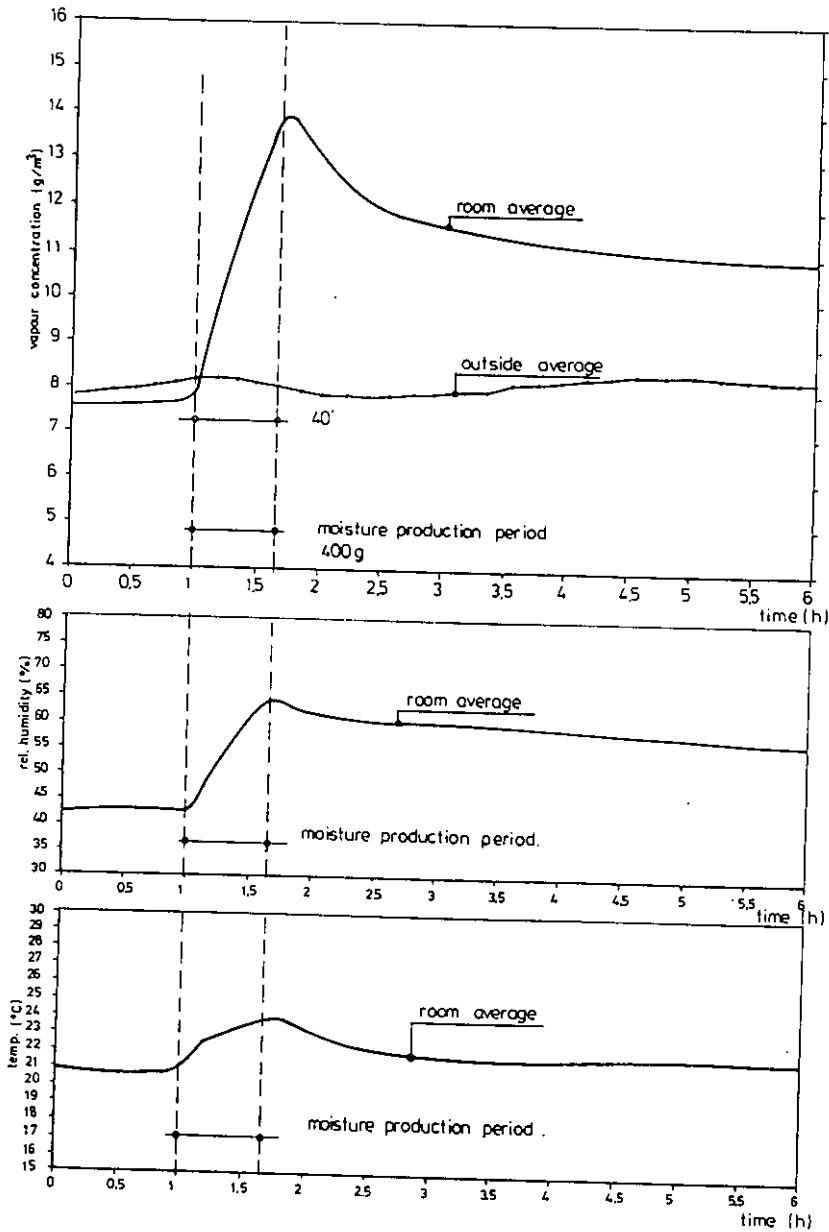


Figure 4.34 Furnished Room

From the respective RH- decreases and the vapour release by the foil, foil + carpet + curtains and foil + carpet + curtains + furniture, we get as a.d-values (a = the slope of the suction curve, d = the active thickness):

	$\Delta\phi$ (%)	Δm (g)	a.d (kg/m ²)
Empty room	17.5	31	.00252
Finished room	12.5	50.4	.0278
Furnished room	10.5	16.5	.0232

Putting these results into the lumped parameter equation for the 40% \Rightarrow 65% RH step measurements, gives as diffusion resistances 'suction surface \Rightarrow room' (Z):

	(time const) (s)	Z-value ($\cdot 10^9$) (m/s)
Empty room	51420 (no suction, $n = 0.07 \text{ h}^{-1}$)	
Empty room	68027	2.24
Finished room	122100	0.37
Furnished room	123760	0.29

While the values, found for carpet, curtains and furniture fit rather well with the diffusion resistance expected ($1/\beta_i + 2/(\mu \cdot d \cdot N)$, $\beta_i = 0,039 \cdot 10^{-9} \text{ a}$ $0,11 \cdot 10^{-9} \text{ s/m}$), for the PE-foil, Z is ± 60 times higher than expected with the water vapour adsorbed at the surface and only the surface diffusion resistance left ($Z = 1/\beta_i \approx 0,0386 \cdot 10^9 \text{ m/s}$). At the other hand, and contrary to the finished and furnished situation, the solution of the lumped equation for a.d for the PE-foil, looks rather insensitive to the Z- value: shifting it from $2.24 \cdot 10^9 \text{ m/s}$ to $0.036 \cdot 10^9 \text{ m/s}$ only changes a.d from 0.00252 to 0.0021 kg/m² but is of major influence on the next two steps.

The a.d-values for the carpet+curtain and for the furniture fit well with the values, found in the KULeuven, Laboratorium Bouwfyca research, described below.

4.4.3.7 EXPERIMENTAL APPROACH 3

TU-Eindhoven, Fago [20]

Test set up and measurements

In the Fago- experiment, the vapour flow into blocks of cellular concrete, due to a sinusoidally varying vapour pressure in a climate room, was measured by continuous weighing the blocks. The results were compared with the theoretically expected moisture uptake/ release, calculated with a method,

very close to the harmonic one described under 'Theoretical approach 3'. Major difference is that the quantities found by the harmonic solution are turned to a capacitance and conductance value, used to feed a first order model. The material properties, needed for the harmonic calculations - the vapour resistance factor μ and the hygroscopic constant a -, were determined from a cup test (86 %- 75%) and a sorption isotherm measurement:

$$\mu = 9.4 \pm 0.4; a = 25 \pm 11 \text{ kg/m}^3$$

Measuring results, discussion (See fig. 4.35)

The figure compares the measured with the calculated mass flows. The calculations were done with two values of the diffusion surface film coefficient: $3,1 \cdot 10^{-9}$ s/m and $6,2 \cdot 10^{-9}$ s/m. The figure shows that the effective diffusion surface film coefficient lies in between, but differs from test to test. It's influence on the mass flow is very important. Or, a better knowledge of β is necessary to come to more accurate predictions.

The same holds for the material properties. Here, a direct measurement of the vapour effusivity, given by $(a/(\mu \cdot N \cdot p'))^{0.5}$, could be an interesting choice.

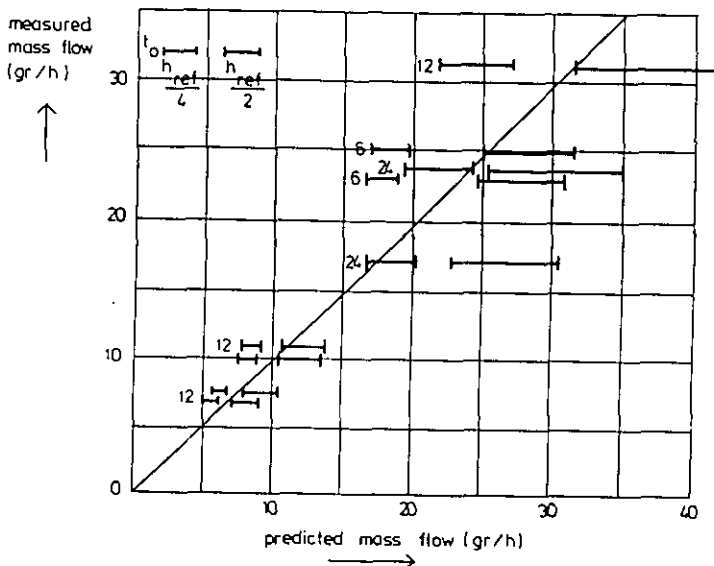


figure 4.35: Comparison of measured and estimated mass flow rates.

4.4.3.8 EXPERIMENTAL APPROACH 4

 KU- Leuven, Laboratorium Bouwfysica [13]

4.4.3.8.1 Introduction

Two programmes have run: measuring the RH in an office room with very high hygroscopic capacity and measuring the lumped parameter approach time constant of wall paper

4.4.3.8.2 RH in a room with high hygroscopic capacity

It concerns a rectangular office room, $V \approx 45 \text{ m}^3$, carpet on the floor, sound absorbing ceiling + 27 m of filled book storage. The room is used by 1 person from 9.00 to 12.30 and from 14.00 to 18.30 h. RH: see fig.4.36.

The RH- course is, in spite of the periodic vapour load, a straight line...

4.4.3.8.3 The lumped parameter approach time constant of 6 types of wall paper.

Measuring method

The time constant is calculated from the hygroscopic moisture uptake when a 0.01 m^2 sample of wallpaper, glued on a vapour tight, non hygroscopic EPS-layer is moved, under isothermal conditions and after suction equilibrium is reached, from a box at RH x to a box at RH y. The weight increase or decrease is measured with an electronic precision balance, accuracy 0.01 g.

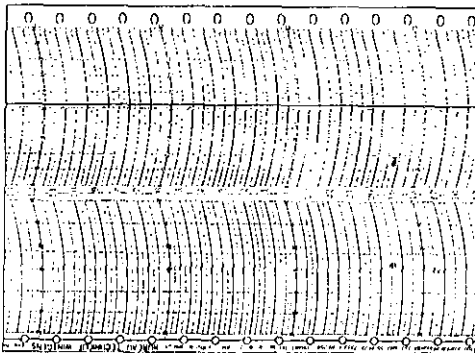


Figure 4.36 Hygrothermograph reading in an office room with high hygroscopic load

Lumped parameter equation

With a ventilation rate 0, the hygric equilibrium in the box and at the wallpaper surface can be written:

$$\begin{array}{l} \text{BOX:} \\ \left(D + \frac{A_s \cdot \beta_s}{V} + \frac{A_h}{Z' \cdot V} \right) \cdot c_b - \frac{c'_h}{Z' \cdot V \cdot a} \cdot m = \frac{A_s \cdot \beta_s}{V} \cdot c_s \end{array} \quad \left| \quad \begin{array}{l} \text{SURFACE:} \\ - \frac{A_h}{Z'} \cdot c_b + \left(D + \frac{c'_h}{Z' \cdot a} \right) \cdot m = 0 \end{array} \right.$$

$\frac{1}{t_1} \quad \frac{1}{t_2} \qquad \qquad \qquad \frac{1}{t_3}$

with A_s : area of the saturated salt surface in the box
 β_s : the diffusion surface film coefficient above the saturated salt solution
 V : the box volume
 A_h : the sample surface
 Z' : the lumped diffusion resistance of the wall paper
 c_b : the vapour concentration in the box
 c_s : the equilibrium vapour concentration of the saturated salt,
 c'_h : the saturation vapour concentration in the wall paper
 m : the mass flow to the wall paper.

It can be proven that, if $1/t_1 \gg 1/t_3$ and $1/t_2 \gg 1/t_3$ - the situation in the tests - the solution of the system for m simplifies to:

$$m = m_y \cdot (1 - \exp(-t/t_3))$$

$$\text{or } \ln[(m_y - m)/m_y] = -t/t_3$$

with m_y : the equilibrium moisture uptake in the box with RH y .

This equation allows the calculation of the time constant from a linear regression analysis on a semi logarithmic plot of 'logged weight increase vs time'.

Results

WALL PAPER RH-step:	TIME CONSTANT $1/t_3$ (s)				
	33⇒54	54⇒75	75⇒85	85⇒98	98⇒85
textile 1	3205	3682	3857	6374	19600
vinyl	3364	4692	4692	4644	21465
textile 2	3625	3585	3714	6020	13914
struct. vinyl	3278	4020	3924	4674	12020
paper 1	2802	2608	2718	4495	16708
paper 2	2664	2694	2599	5554	15257

The results show that:

- between 33% and 85% RH, for the 6 wall papers, $1/t_3$ is rather constant;
- between the 6 kinds of paper, the difference in $1/t_3$ - value is limited;
- drying goes on much slower than wetting: drying from 98% to 85% RH gives a 2 to 4 times higher $1/t_3$ value than wetting from 85% to 98% RH

That last conclusion can have enormous consequences in dwellings with a high mean RH: once moist, they remain moist for a fairly long time..

4.4.4 The effects of steady-state vapour diffusion through the envelope on the hygric balance

In non-steady-state, diffusion has to be counted with the hygroscopic inertia. In steady-state, the hygroscopic capacitance effect reduces to a constant diffusion flow through the envelope. In all steady-state hygric balances discussed, this flow was omitted. That simplification is acceptable if diffusion only represents a minor transfer mode, compared to ventilation and surface condensation. Suppose this is not the case. The exact steady-state mass balance becomes:

$$G_p + \frac{n.V.p_o}{462.V} - \sum_i \left\{ \frac{A_j}{Z_j} \cdot (p_i - p_j) \right\} - \frac{n.V.p_i}{462.V} = 0$$

$$\text{or: } p_i = \frac{p_o + 462.T_i.G_p/(n.V) + 462.T_i.\Sigma(A_j.p_j/Z_j)/(n.V)}{1 + 462.T_i.\Sigma(A_j.p_j/Z_j)/(n.V)}$$

with A_j : the surface of each zonal envelope part.

As far as no interstitial condensation or drying takes place, p_j is the outside vapour pressure for an outside envelope part and the vapour pressure in the adjacent zone for an inside part. Z_j is the diffusion resistance of these parts.

If interstitial condensation or drying goes on, p_j is the saturation pressure in the condensation/drying plane and Z_j the diffusion resistance inside-condensation/drying plane for these parts.

Diffusion influences may become real if:

- the ventilation of the zone is poor;
- the diffusion resistances of the envelope parts are low;
- the outside vapour pressure or the vapour pressures in the adjacent rooms (p_j) are low.

Diffusion has some real influence on the zonal mass balance, only in the rare cases that a very vapour open envelope is constructed.

This means, that the loved concept of breathing walls, putting an active influence of diffusion through the envelope on the zonal hygric balance as granted, has no physical base.

Example: the Zolder case study living room.

Suppose a vapour production of 120 g/h and a ventilation rate of 0.3 h⁻¹. If we take the vapour pressure in all adjacent rooms equal to the living room, as outside wall a cavity wall, surface 36.5 m², diffusion resistance 4,66.10⁶ m/h, no interstitial condensation, then the yearly mean vapour balance becomes ($\theta_e = 9.8$ °C, $p_e = 1100$ Pa, $\theta_i = 20$ °C):

$$p_i = \frac{1100(-p_e) + 679(-G_p\text{-influence.}) + 48.8(-\text{diff.})}{1 + 4,43 \cdot 10^{-2}} = 1750 \text{ Pa}$$

Omitting diffusion, we get $p_i = 1779$ Pa, i.e., a difference of 1.7%.

Let's think the cavity wall replaced by a timber framed construction, without vapour barrier not inside paint. In that case, interstitial condensation seems very likely, and the diffusion resistance from inside to the condensation plane falls to 0,34.10⁶ m/s. Inside vapour pressure: $p_i = 1524$ Pa. Compared to 1779 Pa for diffusion not taken into account, i.e. a difference of 16.7%.

4.4.5 The influence of the latent heat of evaporation

During condensation- evaporation latent heat of evaporation is released or taken up. Through that, as soon as hygroscopic moisture content changes, surface condensation or surface drying starts, the temperature at the surface / in the envelope part changes. This change, a rise during moisture uptake / condensation and a fall during moisture release/drying, influences the heat losses, the moisture flows...etc.

Example

To emphasise the importance, let's compare winter condensation on single and double glazing with and without taking into account the latent heat reality ($\theta_e = 0^\circ\text{C}$, $p_e = 550 \text{ Pa}$ / $\theta_i = 20^\circ\text{C}$, $p_i = 1500 \text{ Pa}$):

	SINGLE GLAZING	DOUBLE GLAZING
no latent heat effects:		
θ_{si} ($^\circ\text{C}$)	5.1	12.4
cond. flow ($\text{g}/(\text{m}^2\text{h})$)	52.1	5.5
heat flow (W/m^2)	119.5	60.8
latent heat effects:		
θ_{si} ($^\circ\text{C}$)	6.7 (+31.4%)	12.6 (+ 1.6%)
cond. flow ($\text{g}/(\text{m}^2\text{h})$)	43.4 (-16.7%)	3.7 (-32.7%)
heat flow (W/m^2)	139.7 (+16.9%)	61.5 (+ 1.2%)

The conclusion is that the effect is not unimportant and should be incorporated in an overall Heat-Air-Moisture (HAM) approach.

4.5 Literature

1. Welty, Wicks, Wilson, Fundamentals of Momentum, Heat and Mass Transfer, John Wiley & Sons, New York, 1969
2. Latta J.K., Walls, Windows and Roofs for the Canadian Climate, NRC, Ottawa, 1973
3. Matsumoto & Fujihana, The moisture Conductivity and Diffusivity of wood for the Estimation of the Room Air Humidity Variation, paper 2.1.1, International Symposium on Moisture Problems in Buildings, Rotterdam, 1974
4. Ahlgren L., Moisture Sorption in Porous Building Materials, paper 2.1.11, International Symposium on Moisture Problems in Buildings, Rotterdam, 1974.
5. Brdlik P.M. & Molchadsky I.S., Calculation of Condensation on Internal Surfaces of Enclosing Structures, paper 2.4.1, International Symposium on Moisture Problems in Buildings, Rotterdam, 1974
6. Bloomfield D., Condensation Risk in Intermittently Heated Rooms, paper 2.4.2, International Symposium on Moisture Problems in Buildings, Rotterdam, 1974
7. Hens H., Bouwfysica 1 & 2 (Building Physics 1 & 2), Acco uitgeverij, Leuven, 1980-1983 (in Dutch)
8. Tammes E, Vos B.H., Warmte en vochttransport in bouwconstructies (Heat and Moisture Transport in Building Constructions), Kluwer Technische Boeken B.V., Deventer- Antwerpen, 1980 (in Dutch)
9. Carslaw H.S., Jaeger J.C., Conduction of Heat in Solids, second edition, Clarendon Press, Oxford, 1986
10. Künzel H.M. Calculation of the indoor moisture behaviour of occupied rooms with the aid of a single-zone-model, IEA-Annex 14, 1989
11. Boot J., Plomp A., Hygroscopische buffering van stoffering en meubilair (Hygroscopic capacitance of finishes and furniture) Caubeg-Huygen, Report 5018-1, IEA-Annex 14, 1989 (in Dutch)
12. Sagelsdorff R., Wasserdampfdiffusion, Grundlagen, Berechnungsverfahren, Diffusionnachweis, SIA- Dokumentation D018. Zürich, 1989 (in German)
13. De Clerck J., De invloed van het hygroscopisch gedrag van oppervlakte-afwerkingsmaterialen op de relatieve vochtigheid binnen (The influence of wall finishing materials on the inside relative humidity), Eindwerk KU-Leuven, 1988

14. Standaert P., Senave E., IEA-Annex 14, Integration Exercise 1, Report OA/B-OR-04/ 1988
15. Hens H., IEA-Annex 14, Integration Exercise 1, Zolder case study, Living House Beukenlaan, 21, Calculation Results, 38 pp, 1988
16. Stehno, Practische Berechnung der instationären Luftzustandsänderungen in Aufenthaltsräumen, Bauphysik 4/1982, pp 128-134
17. Kohonen R., A zone model for room air energy balances, Annex 17, communications between participants, October 1989
18. Kerestecioglu, Theoretical and computational investigation of simultaneous heat and moisture transfer in buildings: "Effective penetration depth" theory, To be published in 1990 ASHRAE Transactions
19. de Wit, M.H., A second order model for the prediction of the indoor humidity, IEA Annex 14, Report NL- T4- o2/1988
20. de Wit M.H., Donze G.J., A model for the prediction of indoor air humidity, Paper for the International CIB W67 Symposium on Energy, Moisture and Climate in Buildings, Rotterdam, 3-6 sept. 1990
21. Duforescel T., Fleury G., The effects of hygroscopicity on the moisture transfers, Paper for the 1989 CIB- congres, Paris 19-23 June 1989
22. Popescu A., Ionescu S, Prévention et lutte contre les moisissures développées sur les bâtiments. Première et seconde partie, INCERC, Bucuresti
23. Freitas V., Etude expérimentale de l'humidité de l'air dans l'intérieur des bâtiments, Paper CIB W40 meeting, Borås, 1987
24. WTCB, Technische Voorlichting 153, Vochthuishouding in gebouwen, (Moisture balance in buildings), Brussel, 1984, 84 pp
25. Becker R., Jaegermann C., The Influence of the Permeability of Materials and Absorption on Condensation in Dwellings, Building and Environment, Vol 17, 2/1982, pp 125- 134
26. Becker R., Condensation and Mould Growth in Dwellings- Parametric and Field Study, Building and Environment, Vol 19, 4/1984, pp 243- 250
27. Becker R., Puterman M., Verhütung von Schimmelbildung in Gebäuden Einfluß der Oberflächenmaterialien, Bauphysik 4/1987 pp 107-110
28. Becker R., Puterman M., Laks J., The effect of Porosity of Emulsion Paints on Mould Growth, Durability of Building Materials, 3/1986, pp 369-380

Chapter 5

MODELLING: combined heat, air and moisture transport

Authors:

J. Oldengarm
TNO-IBBC, DELFT, The Netherlands

C. Pernot, M. de Wit: part 5.8
Working Group FAGO-TNO-TUE, DELFT, The Netherlands

5.1 INTRODUCTION

This chapter is devoted to combined modelling of heat, air and moisture (HAM) transport. Of these three, the thermal and hygric balances have already been discussed separately in chapter 3 and 4.

The importance of HAM- models is obvious: the hygrothermal behaviour of buildings is in fact the result of a complex interaction between the heat balance, the air balance and the moisture balance. A computer model can be a powerful tool to achieve a better understanding of these complicated combined processes, i.e. leading to moisture problems and mould growth in buildings. On the other hand: a thorough knowledge of buildings physics is needed to create these computer models.

The main objective of this chapter is to discuss the capabilities of combined HAM models. The specific objectives are:

- to discuss the need for combined Heat, air and moisture (HAM) modelling in buildings
- to identify the application areas
- to identify the potential users of HAM models

- to introduce a classification of HAM models in order to recognize the different levels of detail in modelling
- to describe (briefly) the HAM transfer mechanisms to be modelled
- to present the state-of-art of HAM modelling
- to review the capabilities of existing building models
- to review input data needed for HAM model calculations
- to review information from field studies in order to identify the most relevant parameters in practice
- to present the analysis of a parameter study in order to identify the most relevant parameters for HAM model studies

5.2 WHY COMBINED HAM MODELLING ?

5.2.1 Building physics and building models.

During the last decades it became increasingly common to develop computerized building models for different purposes. Many aspects of building physics involving Heat, Air and Moisture transport and sometimes lighting are considered in them. Existing building computer models range from simplified calculations to extensive main frame simulation programmes. Most building simulation models address a specific application area of the building physics field. Examples are:

- prediction of indoor climate in association with heating and cooling loads
- prediction of solar gains through windows and other passive solar components
- air infiltration phenomena
- daylighting and artificial lighting
- HVAC system behaviour in relation to other building components
- air flow patterns and ventilation efficiency

Most of the existing building simulation models treat a limited number of these aspects. Because more and more computing power is becoming available at lower costs it is expected that the development of combined modelling, including HAM, will not be hindered any longer by computational constraints.

5.2.2 HAM interactions

Indirect interactions and direct interactions can be distinguished.

Indirect interactions occur because the Heat, Air and Moisture balances in a building are interrelated. For example a change in the ventilation rate will not only affect the indoor air humidity but also the heating demand.

Direct interactions occur when a transfer mechanism of one of the three components in HAM depends on the other. There are several phenomena in which such interactions occur, for example:

- evaporation and condensation of water vapour are related to the heat balance;
- the temperature gradient in a room is one of the driving forces for the air movement;
- temperature differences between different zones will cause buoyancy effects leading to interzonal exchange of heat, air and water vapour;
- material properties are not constant but depend on temperature and moisture content;
- in addition to the suction gradient, the temperature gradient in a solid structure can be a driving potential for moisture transport.

HAM models can be combined in different ways and with different levels of complexity, depending on the purpose and the type of problem.

5.2.3 Combined HAM models and the Annex XIV task

During the Annex XIV study it became clear that several HAM- phenomena can lead to moisture problems in buildings. With respect to moisture behaviour four different type of problems can be distinguished:

- A. Heat, Air and Moisture transport through building structures;
- B. Interaction indoor climate - building structures, in particular with respect to the thermal and hygric inertia;
- C. Air infiltration and interzonal air transport phenomena and, in particular, the accompanying airborne moisture transport;
- D. Air movement and air flow patterns in a single zone and, in particular, the accompanying airborne moisture transport.

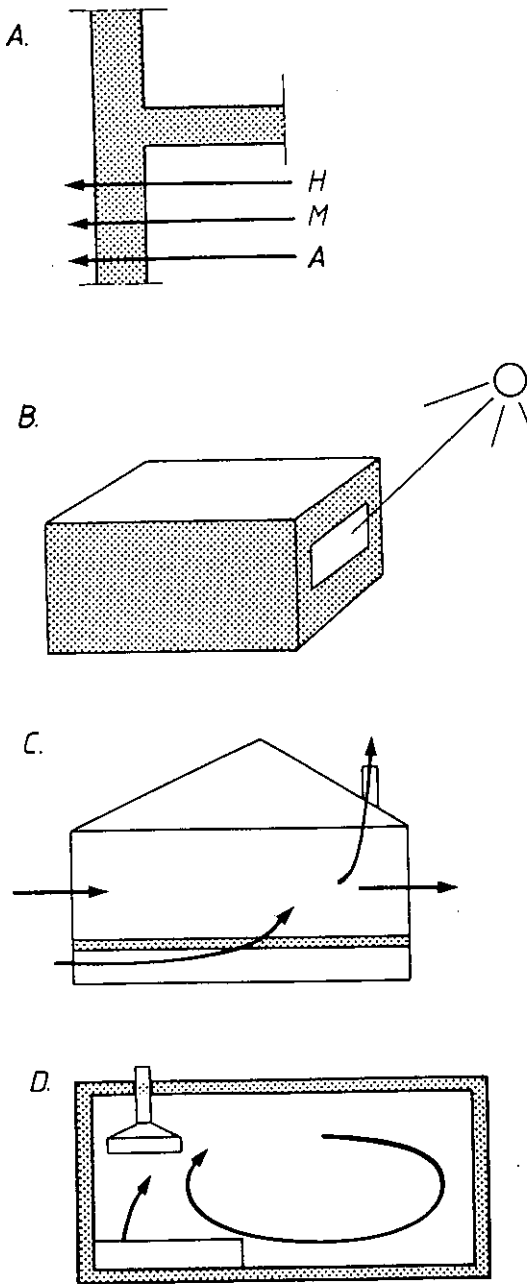


figure 5.1

It will be clear that each of these items requires a different type of model. It is convenient to have this in mind, when considering HAM- modelling. Therefore, to facilitate further discussions, a general classification is introduced.

5.2.4. A general HAM model classification

Based on the four items mentioned and with the Annex objectives in mind, we are able to introduce four model categories. They are visualized in the diagram of figure 5.1. For each category, the general purpose and the Annex XIV specific purposes is formulated (tabel 5.1). Some explanations have to be made here in respect with the air transport component in HAM modelling:

- Model categories B and C assume a complete mixing of the air. Therefore the air mass can be represented by a single parameter for each zone in the HAM- balances. In contrast to this, the model category D uses a grid to compute the air flow pattern.
- Nowadays, some advanced simulation programmes in category B have incorporated some type of air infiltration models from category C. It is expected however that stand alone air infiltration programmes will still find many application areas. It is therefore convenient to consider these models as a separate category.
- To avoid confusion, a clear distinction must be made between a full air infiltration model (C) and the ventilation c.q. air infiltration terms in the heat balance in category B. A full air infiltration model uses a set of non-linear equations to model the combined thermal stack and wind pressure effects.
- One should realize the large difference in detail between C and D category. Category C programmes run on small PC-type computers, category D requires a computer with a large computing power and qualified operators.

MODEL CATEGORIES	GENERAL PURPOSE	ANNEX XIV SPECIFIC PURPOSES
CATEGORY A: BUILDING STRUCTURE MODELS	to predict, evaluate or ana- lyze the hygro- thermal performance of building structures	1. to predict surface condensation on building structures 2. to calculate moisture content of surface layers
CATEGORY B: BUILDING (ENERGY) SIMULATION MODELS	to predict indoor climate in association with heating and cooling loads	1. to predict indoor humidity (regarding thermal and hygric inertia) 2. to calculate surface temperatures
CATEGORY C: AIR INFILTRATION/ VENTILATION MODELS	to predict air exchange rates and interzonal air transport	1. to calculate ventilation rates 2. to predict interzonal airborne moisture transport
CATEGORY D: AIR FLOW MODELS	to predict or analyze air flow patterns and the calculation of the ventilation efficiency	1. to predict or analyze airborne moisture movement in one single zone 2. determine the moisture removal effectiveness

TABEL 5.1: General HAM model classification

5.2.5 Potential users of HAM models

The potential users of HAM models are practitioners and researchers

It is important to realize that the model requirements might be quite different for both groups. The practitioner is directly involved in the building process. His knowledge can be important during the different stages: design, construction and operation & maintenance. For those, there is a need for tools to understand the building physics phenomena he has to handle. In general, such tools should be very simple but accurate enough to make correct and quick decisions. In relation to the 3 stages mentioned, the following categories of tools can be identified: design tools, evaluation tools and diagnostic tools. More specific but still general examples are:

- In early design work one needs tools to select an optimal solution from many options
- In evaluation work one needs tools to check the performance of a design or to test whether it meets standard requirements
- In diagnostic work one needs tools to predict the effectiveness of proposed solutions

In contrast to the practitioner, the researcher needs a higher level of complexity to study the HAM phenomena in more detail. In general much more time and costs are allowed to define the problem and to do the computations. Complex models can be of great help to develop simplified tools for the practitioners. Other purposes for researchers to employ complex HAM- models are:

- the establishment of standards and rules for building codes;
- to achieve a better general understanding of HAM- phenomena;
- to perform parameter studies;
- to generate guidelines with respect to quality control in building and HVAC design;
- research studies in connection with new building concepts (e.g. innovative materials, structures, installations, etc.).

5.3 CLASSIFICATION OF HAM MODELS AND LEVELS OF COMPLEXITY

5.3.1 HAM model categories

It has been noted already that HAM models could be used for quite different purposes. The various application areas are so different that the development of a single, general purpose, HAM simulation model would lead to a very complex thing, that could require an enormous amount of effort. On the other hand, existing building models might be quite capable of solving HAM problems. In some cases, only modifications might be needed to match the requirements for a specific HAM problem. The essential features of the model categories of 5.2.4 are:

A. BUILDING STRUCTURE HAM MODELS.

The general purpose of these models is to evaluate the thermo-hygric performance of the building envelope. Many models are devoted to typical elements such as windows, roofs, cavity walls, ground floor constructions etc. In general, envelope part models could be employed for purposes like the prediction of interstitial condensation or rising damp. Only a few, described in the literature, are true combined HAM models in the sense that they consider all three aspects of Heat, Air and Moisture transport. Most models in this category are not within the scope of Annex XIV report and they will not be considered in further detail here.

B. HAM BUILDING SIMULATION MODELS

The main purpose of building simulation models is to predict the indoor climate and the heating and cooling loads. To achieve this, the thermal characteristics of the building elements are calculated and a term for the air exchange component in the heat balance is included on the level of each zone. Most models are based on hourly calculations and take into account most aspects that influence the heat balance, like solar radiation, internal heat sources, occupant behaviour, etc. In engineering practice, building simulation models are used for the design of HVAC systems and its components. HVAC system simulations have been extensively studied within the framework of IEA Annex X "System Simulations". The HAM capabilities with respect to Annex XIV are considered in more detail in the next paragraphs.

C. VENTILATION / AIR INFILTRATION MODELS.

The main purpose of this category is to predict ventilation rates and air transport between zones in buildings. In general these models are based on solving the air balance equations for a building zone. The essential feature of air infiltration models are the use of air flow rate equations for openings. These equations describe the relation between air flow rate through an opening and the pressure difference over the opening. Wind pressure effects and temperature induced "stack effects" are taken into account. The use of air infiltration with respect to moisture problems is discussed in more detail in 5.4.3.

D. AIR FLOW MODELS

The models in this category are capable of calculating the air flow pattern within a building zone. Such models are based on the numerical solution of the flow equations for two or three-dimensional turbulent, buoyant flows, taking into account the heat exchange with the surrounding walls. Sophisticated software and a large computing power is needed to solve the equations. The capabilities of such a computer programme are shown in one of the next paragraphs.

5.3.2 Levels of detail

Building models can be classified into a very wide range of levels of complexity. An overview is achieved by considering the following aspects:

- modelling the outdoor environment;
- distributed or lumped modelling of heat and mass transfer;
- split or combined surface coefficients;
- 1-D, 2-D or 3-D modelling;
- single zone or multi-zone modelling;
- steady-state, transient (dynamic) or quasi-transient modelling (or in other words: modelling of heat and moisture storage);
- the heat and moisture transfer mechanisms;
- modelling the air exchange or air transport;
- modelling the HVAC system and the interaction with the building;
- modelling HVAC control systems;
- simulation of occupant behaviour;
- the numerical schemes used to solve the HAM equations.

5.3.2.1 Modelling the outdoor environment

The outdoor environment can be described in terms of air temperature, relative humidity, ground temperature, sky temperature, wind velocity, wind direction, solar radiation, etc. Depending on the desired complexity level of the building model, annual, monthly, daily or even hourly climatic data might be needed. Details of terrain and surrounding buildings might be necessary for certain models, for example to compute the solar load or to estimate wind pressure coefficients.

5.3.2.2 Distributed versus lumped equations

Spatially distributed or lumped equations are used to define the HAM-transfer characteristics in solid structures and air. In a distributed calculation, the solid or air domains are discretized into small elements. In a lumped calculation the physical properties are represented by a single parameter or field variable. In most HAM models both concepts will be used simultaneously. For example, in a model for thermal bridge calculations, distributed equations are used for heat transfer by conduction, where indoor and outdoor air temperatures are represented as lumped variables. Many other combinations might be possible. For example one could combine distributed heat transfer calculations with lumped moisture transfer calculations.

It is clear that distributed modelling requires more sophisticated software compared to lumped modelling. On the other hand the necessary input data for lumped model parameters might not always be available. Simulations using distributed modelling can be helpful to find these missing data.

5.3.2.3 Split or combined surface coefficients

Heat transfer by convection and radiation at wall surfaces can be modelled in different ways with different levels of detail. The simplest way is to use a fixed and combined surface heat transfer coefficient. This is generally done in Category A models, where lumped equations for convective and radiative heat transfer are acceptable. Building simulation models in general have the ability to use split surface coefficients, which can be done in different ways:

- a. fixed convective and fixed radiative coefficients
- b. fixed convective coefficients and computation of the radiation balance (e.g. by using view factors and exchange factors)
- c. as b. but using temperature dependent formulae for the convective coefficient
- d. both convective and radiative transfer are computed (this option requires an Air Flow Model)

Options a., b. and c. are widely accepted in building modelling work. Option c. is a sophisticated one, subject of study in IEA Annex XX "Air Flow Patterns". Surface coefficients are of crucial importance for mould and surface condensation computation (see chapter 3, Modelling: thermal aspects). With respect to the diffusion surface film coefficient the situation is less complex. There is only one transfer mechanism: convection.

5.3.2.4 1-D, 2-D or 3-D modelling

Distributed equations can be defined for one- two or three-dimensional HAM transfer phenomena. For envelope calculations (Category A) there is a need for 2-D and 3-D models (e.g. thermal bridges). Building simulation models (Category B) in general use 1-D equations to represent building elements. Air flow calculations require at least 2-D equations, but 3-D is desirable.

5.3.2.5 Single zone or multi-zone

Multi-zone models perform the same calculations for two or more building zones simultaneously. Multi-zone calculations are of interest for the study of HAM-interaction between zones. This is relevant for the B and C model categories. Two kind of multi-zone problems are of importance for Annex XIV: the influence of heated zones on unheated ones (bedrooms) to evaluate temperature levels in the unheated parts with regard to condensation risks and the problem of airborne moisture transport from one zone to another.

5.3.2.6 Steady-state, transient or quasi-transient modelling

In a steady-state calculation all model variables are considered to be constant in time. This implies that heat and moisture storage are neglected.

For many purposes the use of steady-state is satisfactory.

Transient (or dynamic) models are much more complex. Time-dependent equations have to be solved and, in addition, one has to handle much more input and output data. The modelling of heat storage is straightforward and well-known. However, modelling moisture storage is very complex, in particular in combination with heat transfer. Simplified models are needed for different levels of detail: see chapter 4, hygric aspects.

An alternative way to consider storage is the use of quasi-transient modelling. The output of a transient model is then used as an input variable for a steady-state model. An example is given in 5.5.2.1, where the simplified crawl space is described. From an Annex XIV viewpoint, transient models are important because effects of thermal and hygric inertia play an essential role in moisture phenomena.

5.3.2.7 HAM- transport mechanisms

The fundamental heat transport mechanisms are well understood and the mathematical equations straightforward. For the heat balance in a building specific aspects should be considered:

- radiative heat exchange with outdoor environment;
- solar radiation on exterior surfaces;
- solar radiation through windows;
- internal heat sources (people, lighting, apparatus);
- heating and cooling by HVAC systems;
- heat storage in building structures.

See also chapter 3, modelling: thermal aspects.

Moisture transport is much more complex. It occurs both in the air and in solids. In the air domain moisture exists as vapour, and the transport mechanisms are: vapour diffusion and air movement. In solids moisture transport occurs in all three phases. It can be attributed to at least nine different mechanisms, as shown by Kerestecioglu[9]. Generally, in building

physics only three transport mechanisms are considered: vapour diffusion transfer (driving potential: vapour pressure gradient), capillary moisture transfer (driving potential: suction gradient) and airborne moisture transport (driving potential: air pressure gradient)

Other important moisture aspects in combined HAM modelling are: convective vapour transfer at surfaces, condensation-evaporation, hygroscopic moisture storage, moisture sources, control of humidification-dehumidification in HVAC systems. For more information, see chapter 4, modelling: hygric aspects.

5.3.2.8 Combined HAM modelling and HVAC systems

Heating, ventilation and air handling systems can supply or extract Heat, Air and Moisture to or from building zones. In mild climates, heating only is most common, so, modelling HVAC interactions is less relevant. In hot and humid climates, however, humidification and dehumidification are used to control the indoor climate. This is the reason that much work on combined HAM modelling has been done in the USA (9). Combined modelling is also considered within IEA Annex XVII (2).

5.3.2.9 HVAC control

HVAC control modelling becomes relevant if temperature or humidity control is the critical process with respect to mould and condensation phenomena (6).

5.3.2.10 Occupant behaviour

Simplified models concerning the simulation of occupant behaviour are discussed in the chapter on "Boundary conditions".

5.4 STATE OF THE ART OF COMBINED MODELLING

5.4.1 Examples of general purpose models.

Here, some examples of HAM computer models from different categories and with different levels of detail are discussed briefly. The aim is to give information about the state-of-art of HAM models, in particular with respect to mould and condensation problems. Most of the examples refer to work from the Netherlands. This gives a representative overview, because most of development work has been done within the framework of international research programmes. Special efforts were made to collect additional information from Annex XIV participants. For each of the model categories A - D, an example is given and the capabilities with respect to combined HAM modelling or moisture phenomena highlighted.

5.4.1.1 A thermal conduction model with HAM extension

The principles of heat conduction are reported in the chapter 3. Many computer programmes governing these principles have been developed and several are available on a commercial basis. Below a description is given for the model TH3DR, in which some combined HAM features have been implemented.

The TH3DR programme is an extended version of the thermal model TH3D, which was originally developed [33] as a general purpose programme to solve 3D steady-state and transient conduction problems. The main application area has been in the field of thermal bridges. The TH3D belongs to category A, envelope models. The extended version TH3DR however should be considered as a category B model because of its capability of computing indoor climate parameters. To achieve this, some subroutines were added. Using these, an internal space is defined inside a 2D or 3D distributed solid structure. The internal space is confined by the surface elements of the conduction model. Temperature and humidity of the air are considered to be uniform. A subroutine is added to calculate its Heat, Air and Moisture balance.

The heat balance includes:

- radiative heat exchange between surface elements;
- convective heat exchange between each surface element and the internal air;
- heat loss by ventilation;
- latent heat exchange by condensation or evaporation at the surface elements.

The moisture balance includes:

- moisture production;
- condensation or evaporation;
- moisture removal by ventilation;

To solve the combined HAM equations an iterative procedure of two nested iteration steps is followed. In the first step the temperatures in the solid domain are computed. This yields estimated surface temperatures, used in the second step to solve the heat and moisture balance for the internal space. From these equations the air temperature and humidity are computed. The heat fluxes at the surface elements are also computed and used as boundary conditions for the first iteration step. The process is repeated until the desired accuracy is achieved.

5.4.1.2 Application example of the TH3DR model.

The model has been used to study the dynamic hygrothermal behaviour of different types of crawl spaces [33], with the aim to compare the energy and moisture performance. Several technical options were considered, like:

- floor insulation;
- insulation of the foundation elements;
- insulation on the crawl space bottom;
- different types of vapour retarders on the crawl space bottom;
- crawl space ventilation.

Evaluated were: the air humidity in the crawl space, the heat loss through the floor and the thermal bridge effect near to the facade. The study resulted in the development of a simplified crawl space model, described in 5.5.2.1.

TH3DR can be used for other Annex XIV related purposes, for example: combined (dynamic if desired) calculations of indoor climate and thermal bridge interactions or thermal bridge calculations using split (radiative-convective) surface coefficients

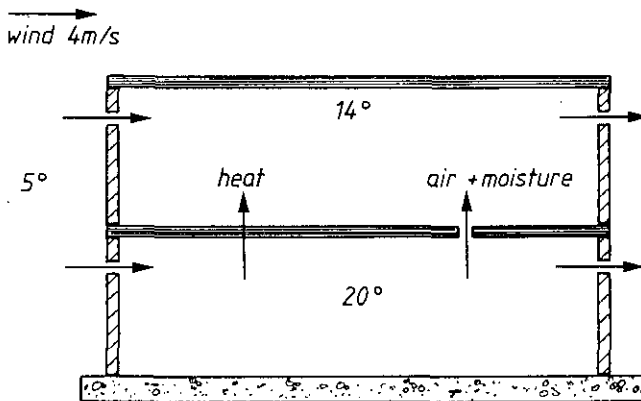


figure 5.2: combined heat and air transport calculations, using a two zone model in VA 114.

5.4.2 Building simulation models (category B).

Numerous building simulation models have been developed, widely used programmes are: ESP, Suncode, BFEP and VAl14. ESP is an energy simulation programme developed at the University of Strathclyde [18], running on mainframes or workstations. It is accepted as a reference tool within the EC passive solar research project. ESP was also used in the parameter study of 5.8. Suncode is a programme to analyze passive solar options. It was used in a HAM parameter study undertaken by the FRG participant in Annex XIV [11]. VAl14 is developed in the Netherlands by TPD-TNO and VABI [32]. It is the updated multi-zone PC-version of the VA32 programme, widely used in the Netherlands during many years. BFEP is a building simulation subroutine set developed at the University of Delft.

5.4.2.1 Application areas for HAM simulation models

HAM building simulation programmes have a very wide application area. In engineering they are used as a tool for energy and indoor climate analysis during the design of buildings and their installations. Some typical applications related to Annex XIV are:

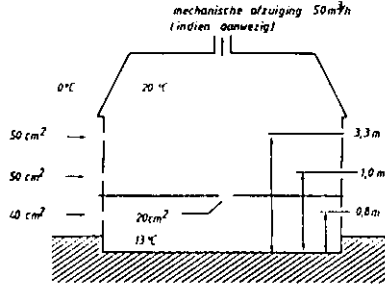
- a. The study of the influence of heated zones on the temperature in unheated zones (bedrooms), with regard to condensation risks. This requires a multi-zone model.

- b. The study of airborne moisture transport from one zone to another in combination with heat transport. The problem is schematically illustrated in figure 5.2. A combined simulation model is required, including air infiltration. The programmes VAL14 and ESP have this capability.
- c. The computation of wall surface temperatures (not on thermal bridges) in dynamic conditions, related to the indoor climate (indoor humidity and temperature). This requires a model with split (radiative and convective) surface film coefficients. The simulation should compute radiative heat exchange between wall surfaces. This is especially important to judge the influence of cold surfaces (like windows).
- d. The study of options in HVAC design with respect to humidity control in relation with aspects mentioned at c. This requires a simulation model that handles HVAC modelling.
- e. The study of the effect of hygroscopic moisture storage in wall surfaces and furniture. This requires a model that considers moisture storage. Various principles are described in the chapter 4 on moisture modelling.

5.4.3 Air infiltration models (category C).

A number of computer models have been developed to calculate air flow rates in buildings. An overview is given by the AIVC [13]. Most of these models are based on a nodal network, in which the nodes represent discrete volumes of air at a certain atmospheric pressure. Internode connections are resistances, representing the distributed air leakage openings. This leads to a system of non linear equations, which can be solved iteratively, when the driving forces are known. The driving force for air transport is a pressure difference, evoked by: mechanical ventilation, wind or/ and temperature differences (buoyancy or stack effect).

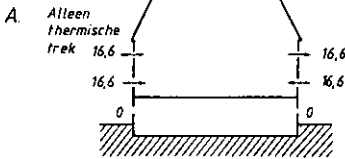
To use an air infiltration model the following input data are required: wind speed data, wind pressure coefficients, air leakage coefficients for building components. The availability of such data is discussed in 5.6. From the viewpoint of Annex XIV, air infiltration models are relevant for the computation of moisture loads in relation to the design and use of ventilation systems and to the airtightness of building components.



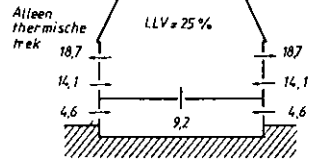
LEKVERDELING
GEVEL :

50/50

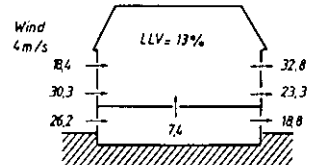
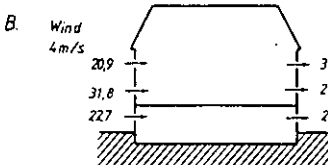
I. Woning met een dichte vloer



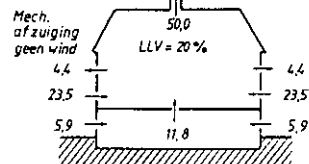
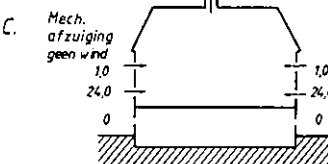
II. Woning met een lekke vloer



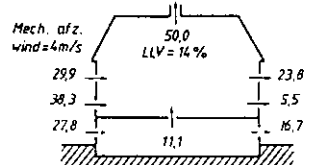
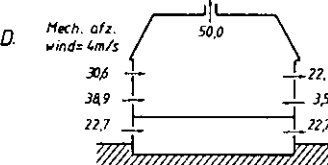
50/50



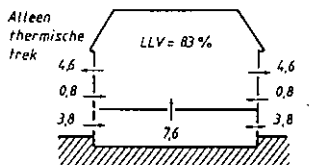
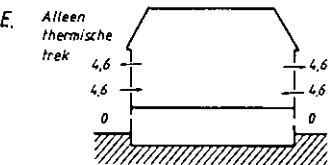
50/50



50/50



90/10



Op tredende luchtstromen in m/h zoals berekend met een computer.
Links een woning met een dichte vloer, rechts een lekke vloer.

Figure 5.3: air infiltration calculations applied to the crawl space moisture infiltration problem

5.4.3.1 Example: moisture infiltration from crawl spaces.

The infiltration of moist air from crawl spaces to the indoor environment is an important cause of moisture problems in Dutch dwellings. A study [22] has been carried out using an air infiltration model. To reduce the number of parameters a two-zone model was used as outlined in figure 5.3. This figure also shows some results. Important conclusions were:

- at normal conditions the moisture load is proportional to the ratio of the airtightness of the ground floor construction to the airtightness of the building envelope (briefly denoted as the "air leakage ratio")
- at certain conditions (for example: no wind and natural ventilation only) the thermal stack effect dominates and, as a result of this, a large amount of fresh air supply will pass through the crawl space, leading to a severe moisture load in the indoor environment.

In general, the air humidity in Dutch crawl spaces is very high because of the presence of ground water: an excess water vapour concentration of 6 g/m^3 with respect to the outdoor air is quite normal during winter conditions. Even small air leakages in the ground floor may then result in moisture loads of the order of 1 to 3 kg water vapour per day.

5.4.3.2 Computation of interzonal moisture transport using an air infiltration model.

A multi-zone ventilation model is able to compute the in- and outgoing air flow rates through the air leakages in the zone boundaries. It will be shown that it takes a simple step to compute the steady-state interzonal moisture transport rates, as long as no condensation takes place. The basic principle of this computation is given for a two-zone example as illustrated in figure 5.4. All incoming air flows should be known. The ventilation model gives the total incoming air flow rate for each zone boundary. Care should be taken not to add the incoming and outgoing flows. For the simplified case of figure 5.4, the water vapour mass balance for zone i can be written as:

$$G_{ae} \cdot x_e + G_{ak} \cdot x_k + G_p = (G_{ae} + G_{ak}) \cdot x_i \quad (5.1)$$

with x_e : air humidity ratio in zone e (outdoor) (g/kg)
 x_i : air humidity ratio in zone i (g/kg)
 x_k : air humidity ratio in zone k (g/kg)
 G_{ae} : incoming air flow rate from zone e to zone i (kg/s)
 G_{ak} : incoming air flow rate from zone k to zone i (kg/s)
 G_p : moisture production in zone i (g/s)

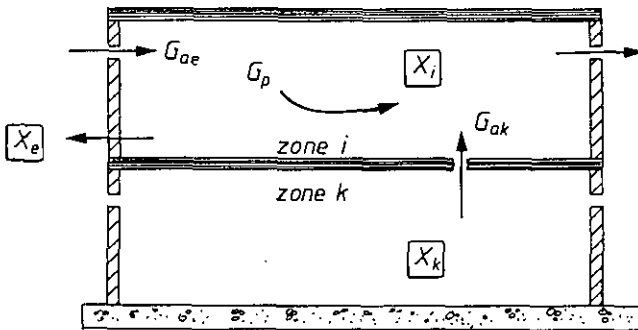


Figure 5.4 The moisture balance between two zones

The computation of x_i is now straightforward:

$$x_i = (G_{ae} \cdot x_e + G_{ak} \cdot x_k) / (G_{ae} + G_{ak}) + G_p / (G_{ae} + G_{ak})$$

This equation expresses the moisture load from zone k to zone i as a result of interzonal air borne moisture transport. It should be clear that more general equations can be used if air transport between more zones is considered. The conclusion is that, as long as surface condensation/ drying and hygroscopic inertia is not considered, it is a simple step to compute the (steady-state) interzonal moisture transport.

5.4.3.3 Combined air infiltration and thermal modelling

An air infiltration model requires zone and outdoor temperatures as input data. For multi zone computations, fixed zone temperatures are then used as boundary conditions. Effects due to interaction with interzonal heat transport are not modelled. However, advanced building simulation programmes are able to combine a full thermal model with a complete air infiltration model (Note: that includes at least thermal stack and wind pressure effects): ESP and VAL14.

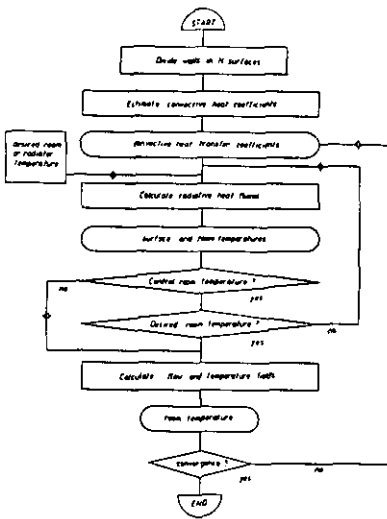


Figure 5.5 Computing flow diagram of WISH-3D Air Flow Simulation model

5.4.4 Air flow simulation models (Category D)

Flow simulation techniques predict air flow patterns within rooms. Such techniques will become increasingly important for the design of HVAC systems. It is expected that in the near future the field of "computational physics" will allow researchers and designers to bypass time-consuming and expensive full scale tests. Flow simulation programmes are available on a commercial basis. PHOENIX and FLUENT are well-known packages. Cooperation between the Technical University of Delft and TPD-TNO resulted in the WISH-3D air flow simulation package [30]. The code is based on the CHAMPION programme. An important feature of WISH-3D is the addition of a thermal radiation model, describing the radiative heat exchange between wall surface elements. The flow diagram in figure 5.5 shows how this has been accomplished.

Flow simulation techniques are based on solving the equations of conservation of mass, momentum and energy. This allows the computation of important indoor climate indicators like the air temperature distribution, the air velocity distribution, contaminant concentration distribution and thermal comfort. One should realize that air flow simulations require large computing powers (WISH-3D runs on a Alliant system) and skilled researchers.

IBBC
BI-89-176

December
1989

page
35

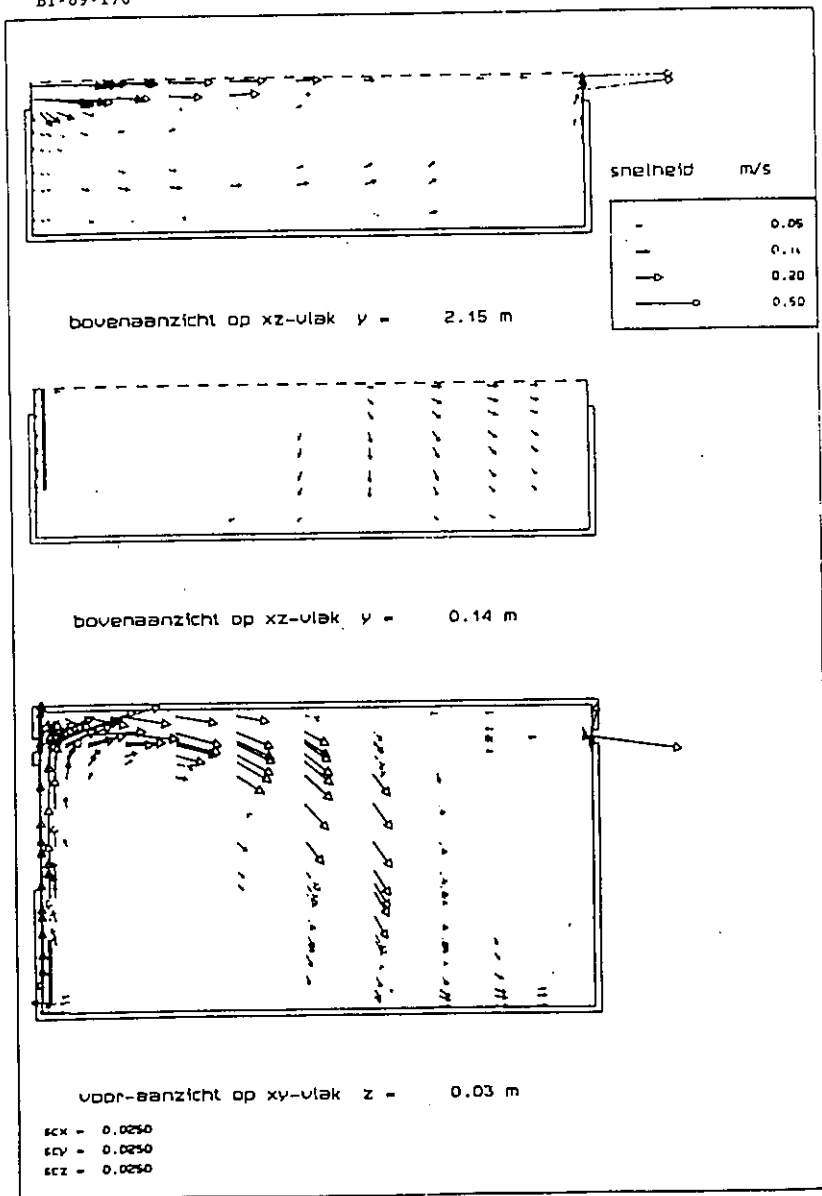


Figure 5.6 3D air flow pattern, calculated with WISH- 3D

5.4.4.1 Application areas of Air Flow Simulations

General application areas for air flow simulation models are:

- smoke transport in buildings
- fire behaviour in building zones
- airborne contaminant transport in clean rooms
- air flow patterns in an atrium with regard to comfort
- displacement ventilation

Development and validation work is done in IEA Annex XX "Air flow patterns" [3]. An example of results, relevant for the Annex XIV work, is given in figure 5.6. It shows the three-dimensional flow pattern in a room due to the combined effect of a heating radiator and the wind pressure induced ventilation of two opposite vent lights.

With respect to the Annex XIV objectives the most relevant capability of air flow simulations are:

- a. the prediction of the moisture removal effectiveness of air exhaust design in relation to room geometry;
- b. the prediction of the water vapour distribution resulting from the airborne moisture spreading in a single zone;

"Ventilation efficiency" is the key term here. Background and definitions of this term are found in an AIVC publication [12]. Much work has already been done in the field of indoor air quality (IAQ), where investigators are concerned with the control and dispersion of contaminants in air. Comparison of numerical simulations and experiments have been reported by [7]. It should be pointed out here that the ultimate goal of air flow simulations is not to calculate reality with all its details. The programmes should be used to evaluate different options under well defined boundary conditions. A comparison can be made with the calculations of thermal bridges. These computations do not fully simulate the real behaviour of thermal bridges, but are made for well defined boundary conditions.

4.5 Special purpose and simplified modelling

4.5.1 Special purpose models

In the literature several special purpose HAM models have been described. The feature of such a model is that it fits its level of detail to a specific problem. This gives less complex calculation compared to solving the problem with a general purpose model. Examples of special purpose models are the crawl space model (see 5.5.2.1) and a swimming pool HAM model [6].

4.5.2 Simplified modelling

There are several strategies in developing simplified models:

- simplified models based on simplified physical assumptions;
- simplified models based on experimental observations in the field (empirical models);
- simplified models based on mathematical reduction of complex models (parameter reduction techniques);
- simplified models based on the results of computer simulations (sometimes denoted as correlation methods; regression equations are used to find the parameters for a simplified model).

Simplification strategies for example could be based on translations from distributed to lumped modelling, from transient to steady-state modelling, from multi zone to single zone, etc.

4.5.3 Simplified crawl space model.

Using simulation results of the extended model TH3DR (introduced in 5.4.1.1) the simplified spreadsheet crawl space model *kruip.wks* [old,1990] has been developed. The purpose of this simplified model is to evaluate different types of measures for the solution of crawl space moisture problems. It allows the evaluation of remedial measures like crawl space ventilation, thermal insulation, vapour retarders on the crawl space bottom and combinations of these. Simplified equations have been used for the Heat, Air and Moisture balances. The simplified model is implemented as a utility on Lotus 123. Comparison between the detailed model (TH3DR) and the simplified model is

outlined in figure 5.7. One of the critical aspects is the modelling of the heat loss to the ground. In the complex model, the ground is divided into a large number of cells for which monthly temperatures and heat flows are computed, taking into account the large thermal inertia of the ground. In the simple model the monthly heat flow through the bottom surface is computed by the equations:

$$q(t) = [h_k(t) - \theta_{gr}(t)] / R_{eq}$$

$$\theta_{gr}(t) = \theta_{ann} + a \cdot [\theta_{ann} - \theta_o(t - t')]$$

- with q : averaged heat flux to the ground (W/m^2)
 θ_k : crawl space air temperature ($^{\circ}C$)
 θ_{gr} : equivalent ground temperature ($^{\circ}C$)
 R_{eq} : equivalent heat resistance of the ground ($m^2.K/W$)
 θ_{ann} : annual mean outdoor temperature ($^{\circ}C$)
 θ_o : monthly mean outdoor temperature ($^{\circ}C$)
 a : damping factor
 t : time (in months)
 t' : time phase shift due to thermal inertia of the ground

In the simplified model the parameters R_{eq} , a , and t' are assumed to be constant. The values are estimated from the results of the detailed model.

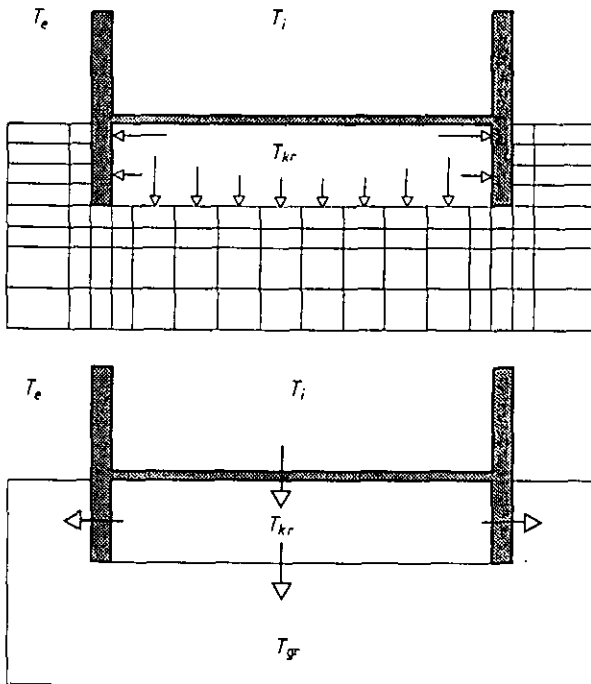


Figure 5.7 Comparison of a complex and a simplified thermal model for HAM calculations on crawl spaces

5.5 CONCEPTS FOR MOISTURE STORAGE MODELLING

Modelling the effect of hygroscopic moisture storage in furniture and building materials is one of the missing features in the HAM models described in the previous paragraphs. Case studies and field experiments, some of them reported in chapter 4, have shown the important influence on the indoor humidity. Modelling of moisture storage is much more complex than heat storage. There are several reasons to be mentioned: the non-linear behaviour of hygroscopic storage, input data for material properties not always available, the hygric inertia of building components being very high, it requires large computing times, in particular in combination with the non linearity.

The third item needs some further explanation. A dynamic model will need initial values for the "capacity nodes". These values are unknown and depend on the input data. In building simulation work this problem is overcome by starting each simulation with "dummy" calculations during a time period that exceeds at least three times the time constant of the building. This principle is based on the assumption that all "capacity nodes" take the proper initial values after the start-up simulation. A building simulation requires about 14 days start-up procedure to achieve a thermal equilibrium. A simulation model in which walls are represented by a complete moisture storage model would require much longer start-up period. Computation time could be reduced by taking larger time steps and by time averaged (e.g. daily averages) indoor and outdoor climate data.

Another consideration should be that the indoor air humidity on the short term (say 24 hours) is influenced only by the moisture stored in a very thin wall surface layer. Moisture stored in the inner wall and furniture is only of importance for long term effects. Consequently, a simplified moisture storage model as described in chapter 4, representing the hygroscopic absorption and desorption in the surface layer is quite acceptable for most HAM simulation problems.

5.6 MODEL AND INPUT DATA REQUIREMENTS

5.6.1 Introduction.

A successful introduction of computer models depends greatly on the amount of effort to make them available to others than the original author. An appropriate model documentation should meet the following requirements:

- A users manual (instructions, description of input and output data, test examples);
- A programme description (programme structure, databases if any, numerical solution methods) ;
- A model description (equations used, defaults, assumptions, limitations, standards used, reference to research reports);

5.6.2 Data requirements

The accuracy and reliability of results from HAM computations are dictated by the quality of input data. Many complex models give very detailed and apparently accurate output data, but the proper interpretation very often relies on the availability of reliable input data. Combined HAM models require different types of data in association with the heat, moisture or air transport component. Input data can be classified into the following categories:

- Climatic data;
- Building design data and terrain conditions;
- Thermal properties of building materials;
- Hygric properties of building materials;
- Air leakage data of building components;
- Wind pressure coefficients;
- HVAC system design data;
- Occupancy profiles;
- Internal sources.

Many computer programmes are provided with databases. In many cases the data rely on common sources of literature or reports (see chapter 1 and chapter 6). Data on wind pressure coefficients and air leakage are documented by the AIVC [15].

5.6.3 Required level of detail

The level of detail in computer models will depend mainly on the nature of the problem. This can be clarified by two extreme examples:

Example 1:

Suppose the problem is to predict the relative humidity in a building to analyze options for a proper hygrothermal design. For this purpose lumped and time averaged equations might be quite useful. For many purposes an analysis on monthly basis would provide the desired information. Even simple hand calculations can be done.

Example 2:

Suppose the problem is to predict the ventilation effectiveness of a ventilation exhaust design in conjunction with room geometry and hygroscopic storage properties of wall surface materials. This problem would require a 3-D air flow simulation programme that also handles surface moisture and indoor air interactions. Simulation of this problem would require a super computer and many man hours of labour.

5.7 CASE STUDIES AND FIELD EXPERIMENTS

5.7.1 The model versus the real world

The ultimate objective of any HAM building model is to predict or analyze physical phenomena in buildings. Modellings, experimentalists and practitioners should cooperate to test the usefulness and correctness of such models. Model development should be accompanied by experiments and experiments should be accompanied by calculations. This may occur at different levels:

- case studies provide information and understanding on what type of problems occur in reality and they provide an idea about the most relevant phenomena;

- full scale field experiments are done to study these phenomena in more detail;

- on a smaller scale laboratory experiments might provide more information under well-controlled conditions.

The statements above refer to the domain of building physics. With respect to the Annex XIV objectives, the situation is much more complicated because of the biological aspects of mould growth. The HAM models discussed in this chapter consider only relative humidity levels and moisture contents. They do not predict mould germination, growth and sporulation.

5.7.2 Feedback from practice to modelling

Annex XIV considers mould growth in buildings. HAM models probably can be helpful to understand and solve the problem. However, the first step should be to examine the problems in practice. Many factors may play a role and each case may differ widely from any other. Two levels of feedback from practice to modelling can be identified: case studies, in which problem cases are examined, which may lead to solutions and the testing of these solutions and field experiments, in which specific phenomena are investigated experimentally in realistic circumstances (but not necessarily in a problem building).

5.7.3 Case studies

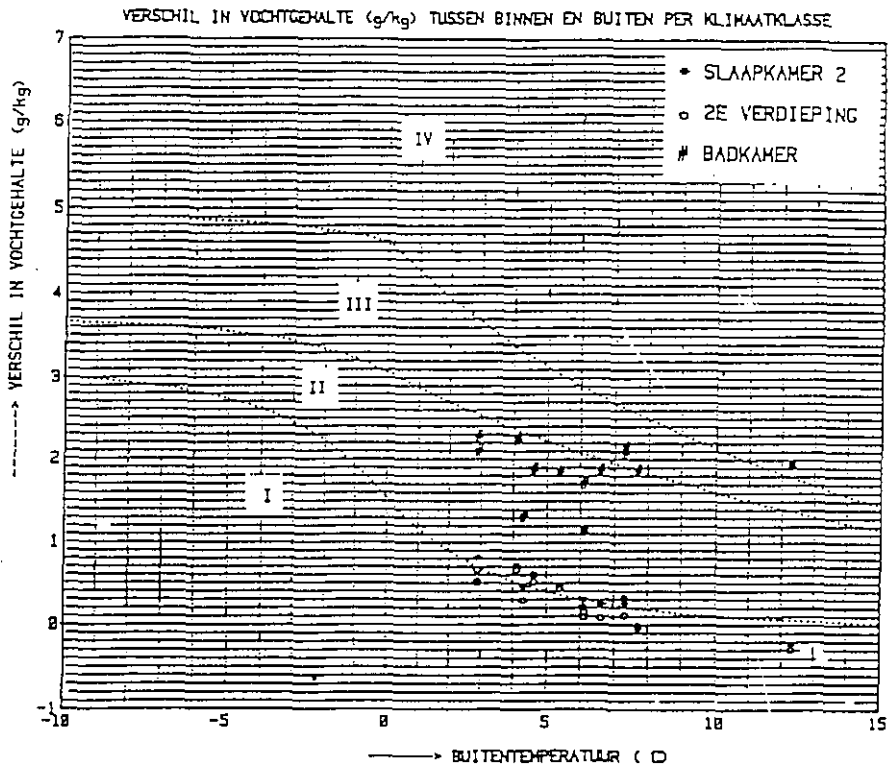
There are two different aspects of the relation between case studies and models:

Aspect 1:

From the viewpoint of an investigator, who is charged to do the case study, the use of (simplified) models might be of interest to analyze the problem and make predictive calculations for the remedial measures, he will propose. Models may also be helpful for interpretation of measured data.

Aspect 2:

From the viewpoint of the modelling the results of a case study are of interest for the further development of his model. He might also adapt his model in order to have a better connection to practical problems. Case studies also may provide useful statistical information for modelling purposes, in particular with respect to aspects related to occupant behaviour. An example is given in figure 5.8, extracted from the Pijnacker case study [5]. It clearly shows the large difference between moisture levels in bedrooms and living rooms.



Climate classification (dutch climate classes); bedroom 2
 (*), landing - loft (o) and bathroom (#)

Figure 5.8 Indoor relative humidity levels, observed in the Pijnacker case study

A number of case studies are summarised in Volume 4 of this Annex XIV final report. Conclusions relevant for HAM modelling:

- An appropriate evaluation of the indoor climate (both for design as for diagnostic purposes) requires a standard reference for indoor climate that refers at least to the indoor temperature, the indoor humidity and the thermal quality of the building envelope.
- For the proper analysis of the indoor climate an insight in hygroscopic storage is needed. Apparently, there is need for HAM models, incorporating that aspect.

5.7.4. Field experiments.

Within the framework of the Dutch participation in the IEA Annex XIV "Condensation" field experiments have been carried out to study airborne moisture transport in realistic circumstances. The experiments were done in an unoccupied 3-story dwelling in Leidschendam. Three institutes (MT-TNO, TPD-TNO and IBBC-TNO) cooperated in this study. The results have been reported in detail in a report [Old,23].

An unoccupied house was chosen to eliminate the disturbing influences of the occupants. To study the airborne moisture transport several experiments were carried out with a precisely defined and controlled moisture production. Three types of moisture generation experiments have been considered:

- a. the cooking experiment (using a moisture generation rate of 800 grams in 30 minutes);
- b. the shower experiment in the bathroom (shower periods of 3 to 15 minutes);
- c. the wash drying experiment in the attic.

In these three experiments two aspects of the airborne moisture transport have been monitored in detail:

1. the interzonal airborne moisture transport
2. the internal airborne moisture movement within a single zone

The experiments were done for various conditions in order to study the effect of the major influencing factors, like open or closed windows, open or closed interior doors and the use of the ventilation system. Sophisticated equipment was installed to collect the experimental data:

- a constant concentration gas tracer (N_2O) technique, to monitor air infiltration of all rooms;
- a constant generation gas tracer (SF_6) technique, to monitor the air transport from the moisture source to the room air and to the other zones;
- a dew-point sensor system to monitor water vapour concentration in all rooms.
- a micro manometer measurement system to monitor air pressure differences at the most relevant locations.

A unique feature in this study was the simultaneous measurement of air transport and airborne moisture transport by using the SF₆ tracer gas and the dew point systems. This feature allowed the study of the moisture storage effects associated with airborne moisture transport. Because SF₆ is an inert non-absorbing gas, the simultaneous measurement of water vapour and SF₆ gas tracer concentration permits to derive quantitative information about the moisture storage effects due to hygroscopic absorption-desorption and condensation-evaporation on wall surfaces.

The results show that moisture storage certainly is an important factor when considering airborne moisture transport. The cooking experiments show the most striking results. If the mechanical ventilation system is not in operation, 56 % of the produced moisture is stored at the wall surfaces within a very short time during the moisture generation period of 30 minutes. 40 % is released to the indoor air and 4 % is removed by natural ventilation. An experiment with the mechanical ventilation switched on, shows that still 39 % is stored at the wall surfaces, 38 % is then released to the indoor air and 22 % is removed by the ventilation system. An overview of the moisture balances for different conditions is shown in figure 5.9. It should be noted that the moisture removal effectiveness, defined as the ratio of the amount of moisture removed by ventilation with respect to the amount of moisture produced, does not exceed 23 % in any case.

During the moisture production large vapour gradients are observed in the living room. Instantaneous differences in water vapour concentration up to 5 g/m³ have been observed between two remote locations in the living room. The water vapour equalization process takes several hours, depending on the ventilation rate. During the equalization period the stored moisture is gradually released again by desorption or evaporation. A more detailed analysis has shown that moisture storage and moisture release occur simultaneously during the equalization period. This can be explained by the phenomenon that wall areas near to the moisture source have been moistened during the production peak, while wall areas remote from the cooking are still dry. Apparently, an equalization process of moisture contents between wall surfaces occurs: moisture from "wet" areas moves to "dry" areas by airborne transport of water vapour.

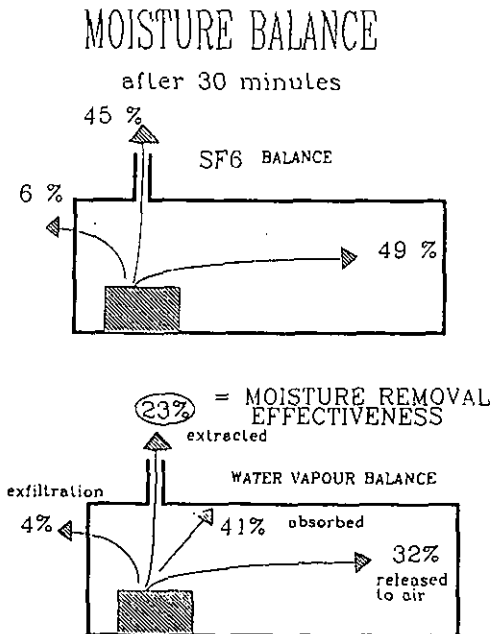


Figure 5.9 Moisture balances, observed in the Leidschendam experiment

The water vapour distribution during and after the cooking experiment was also subject of study. The moisture distribution was monitored at nine measuring positions located in the kitchen and the living room. The internal airborne moisture transport within a single room is not easy to understand. The driving potential of this type of moisture transport is air movement. Water vapour diffusion does not play an important role. Many factors influence the distribution of indoor humidity levels:

- the removal effectiveness of the extract ventilation (if any);
- the amount of dilution by infiltration of outdoor air;
- the process of moisture storage and release at the room surfaces and furniture;
- the air flow patterns in the room and associated mixing process.

The variety of possible air flow patterns makes it very difficult to predict quantitatively the airborne moisture movement within a single zone. The air flow pattern in a room is also influenced by factors as:

- the type and position of heating systems;
- the shape and geometry of the room;
- the thermal quality of the envelopes;
- the way in which air is supplied or extracted.

To understand the experimental results a normalization scheme has been used to present the water vapour distribution. The measured data have been referred to a reference level, being the *maximum room averaged* concentration or the maximum peak level at the ventilation extractor. In this field study it was found that the air humidity peak at the most remote corner from the cooking place was not higher than 30% compared with the magnitude of the humidity peak near to the moisture source.

In all experiments the effect of interzonal air and moisture transport was also analyzed. The results showed that interzonal airborne moisture transport appears to be significant only in cases where internal doors between rooms are kept open during or just after moisture production. An exceptional situation is the wash-drying at the attic. Experiments revealed that this is an important moisture load to other zones in the house.

5.7.5 Discussions with respect to HAM modelling

As shown in the previous paragraph moisture absorption plays a dominant role in the water vapour distribution in real circumstances. However, it is unlikely that the observed phenomena will be predicted by available models, even if they take into account moisture absorption at some level of detail. Models, in which a perfect and uniform mixing is assumed, will give large errors when predicting the indoor humidity level for a given moisture production rate. The problem is that only very detailed modelling could predict the intense absorption rates at wall surfaces near to the moisture source. A more precise prediction can be achieved if the moisture removal effectiveness of the ventilation extractor would be known. Such data are not available however, even not for an order of magnitude.

Air flow simulation models, allowing the computation of air flow patterns, may be of help to develop a better understanding of the water vapour distribution in real situations. In addition, experimental data will be needed to support the simplifying assumptions and to find realistic estimates for boundary conditions.

5.7.6 Model validation.

The word "validation" is often used without a precise definition. In general it is used in the context of testing the correctness of a model. Many different validation techniques have been used in the past:

- analytical validations: checking the model output against known solutions;
- intermodel comparisons: checking the outputs of two or more models;
- empirical validations: checking the model output against experimental results.

Although empirical validation seems to provide the only ultimate truth test for models, it does suffer from many shortcomings. For a complex model a true empirical validation is almost impossible because the output of a model should be tested for all possible combinations of input data. A more severe limitation is that the measured data are often incomplete and many parameters are not precisely known. An empirical validation is even more questionable when a few parameters are fit to measured data. In many cases it is possible to fit any result to measurement results by varying one or two parameters. This is of course no real validation test. The problem of model validation is extensively discussed in a BRE paper [4].

5.8 PARAMETER STUDY

5.8.1 Introduction

The goal of the parameter study is twofold:

1. Investigate the influence of building characteristics and building use on the heat-, air- and moisture-balance of a reference building. This implies the use of a heat-, air- and moisture-model for performing the simulations involved.
2. to develop insight into the practical application and method of use of combined HAM- models

At present heat(energy) flow and air flow are modelled within combined building energy simulation systems. The moisture models in these systems are often very simple and do not take into account hygroscopic behaviour of the building materials. The procedure in this parameter study is to simulate energy flow and air flow with one model and to use a separate moisture model with the output of the first as input. Computing the energy balance in tandem with air flow, implies that time-dependent air flow (predominantly pressure driven) will occur.

Two different procedures are followed:

1. Combining both time-dependent energy and air flow
2. Eliminating the time-dependent air flow by taking a constant value for the infiltration to the building, resulting in an energy flow simulation only.

The second option has the advantage that the parameter study is not disturbed by variations in wind speed and wind direction. It is paramount in this study. Several runs of the first option were made to draw a comparison and to develop insight into the use of combined models, in particular for the interzonal air flow.

The models used and the variants in the study:

- thermal model/air flow model: ESPsim & ESPair (ASL 89, Clarke 85)
- moisture model: Elan_Hum (de Wit 90)

The reference building has a two-zone geometry, consisting of a living room and a kitchen placed behind each other. The separation wall may be removed (open kitchen) resulting in a one-zone geometry.

The occupant behaviour comprises three different items: temperature control, ventilation and moisture production. The temperature set-points are the same for every day and for each room: the first 8 hours of the day 16°C, from 8 to 18 hour 18°C and from 18 to 24 hour 20°C. For the ventilation two different patterns are used: one relatively constant and one with three extra peaks during the day. The day averaged amount of ventilation is the same for each variant, only the pattern differs. The peaks in ventilation and moisture production coincide. The kitchen and the living room have different patterns for the moisture production: the kitchen with a peaked production and a total of about 4 kg/day, the living room with a constant value of 0.1 kg/h from 8 to 24 h. The open kitchen (one zone geometry) has a moisture production which equals the sum of kitchen and living room.

The air tightness of the building envelope is varied by taking a constant value for the infiltration rate of 0.3 h⁻¹ or 0.9 h⁻¹. The used ventilation in the calculation model is the sum of above mentioned ventilation and the infiltration. The different insulation levels stem from the old and new Dutch regulations: the old with R= 1.3 m²K/W and the new one of R = 2 m²K/W. Also the distinction between a heavy or lightweight construction is made. For the calculations with the moisture model, the surface vapour resistance of the walls is a parameter. In one case a 'normal' construction is used, in the second the wall finish has been chosen vapour-tight ($\mu_d = 0.43$ m).

5.8.2. Results

The simulations were performed on an hourly basis over a whole year (8760 hours). The climatic data set used is the reference year developed at the University of Technology in Eindhoven (V.d.Bruggen- 1978). 32 runs were made with the thermal model. The output has been converted to the input format of the moisture model. Then 64 runs were performed with the moisture model, 32 with and 32 without a vapour-tight finish. In this paragraph only a few notable results are given. For a detailed report on this parameter study see: (Pernot- 1990).

For the presentation of the results, a reference situation is chosen and several variants are shown with respect to the reference. The reference is the kitchen (closed kitchen) with the following assumptions:

- heavy construction type;
- isolation;
- airtight building envelope;
- ventilation pattern relatively constant;
- wall finish vapour-tight;

It is likely that in this situation condensation will occur.

The variants that are compared with the reference are:

1. The influence of the geometry, no hygroscopic material; this means that the volume of the kitchen will be increased by removing the separation wall with living room (open kitchen geometry). In fact two effects play a role: the increase of air mass (volume of kitchen + living room) and an increase of the ventilation /infiltration compared with the kitchen only (reference).
2. The influence of the moisture permeability of the wall finish by removing the vapour-tight surface finish.
3. The influence of the infiltration, by switching from 'tight' to 'open' building envelope. This means that the infiltration rate is raised from 0.3 h^{-1} to 0.9 h^{-1}

Presentation of the results

In the top figures the cumulative frequency distribution is shown for the hourly values of the relative humidity over a whole year. The cumulative frequency distribution of the difference between the daily maximum and minimum value of the relative humidity is also indicated. This gives insight into the daily variation of the relative humidity. The bottom figure shows the critical temperature factor for condensation.

This is defined as:

$$\tau_{hi,cr} = \frac{\theta_{dp} - \theta_o}{\theta_i - \theta_o} \quad (5.1)$$

with θ_{dp} : dew-point temperature of the inside air
 θ_o : outside air-temperature
 θ_i : inside air-temperature

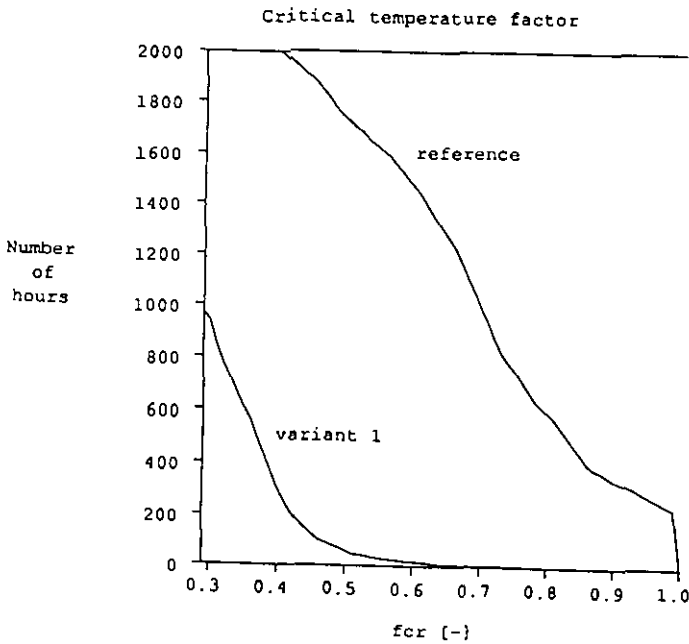
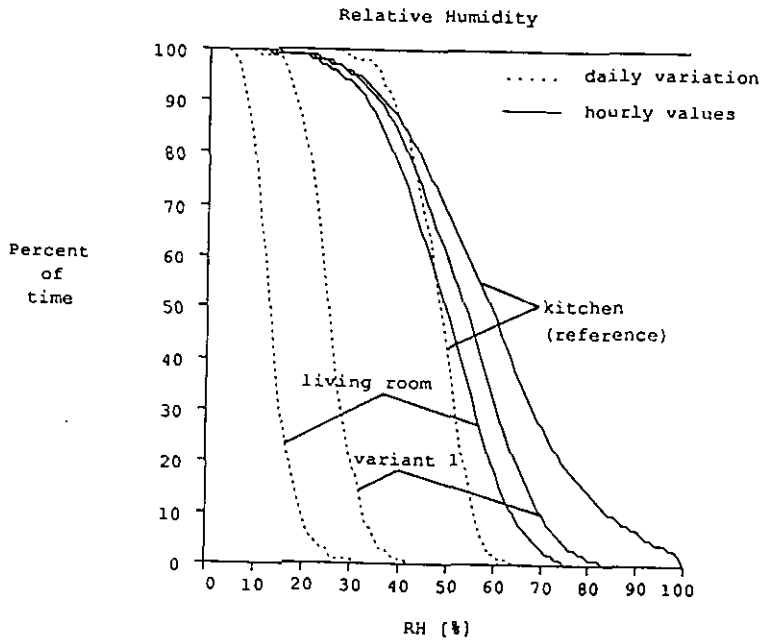


Figure 5.10 Effect of open geometry

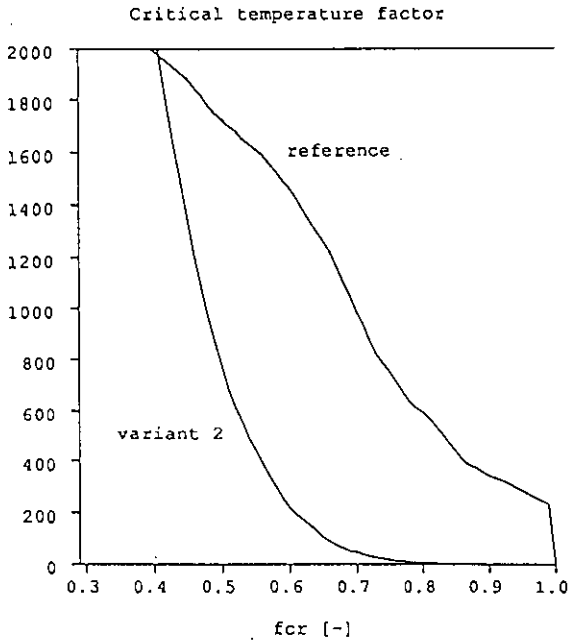
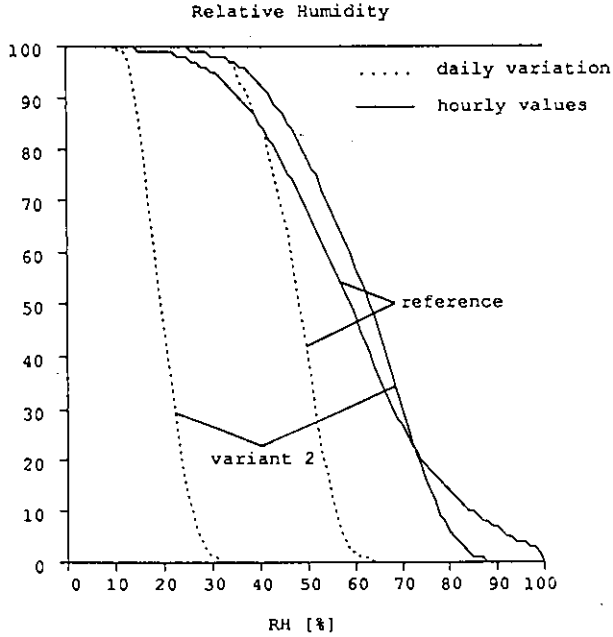


Figure 5.11 Influence of the vapour permeability of the wall finish

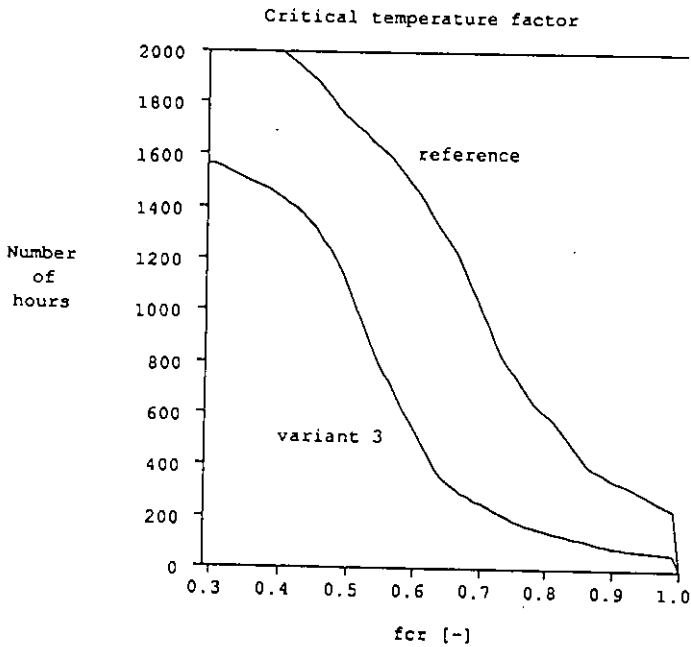
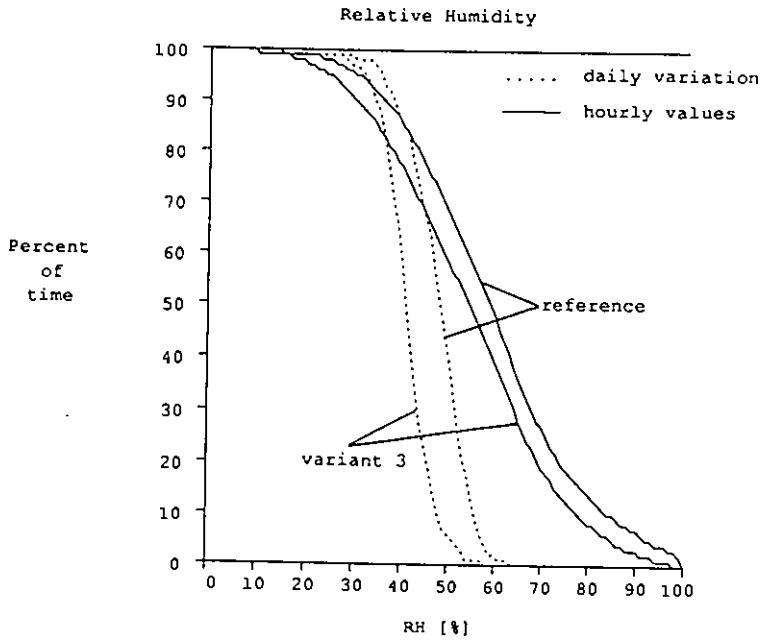


Figure 5.12 Influence of the ventilation

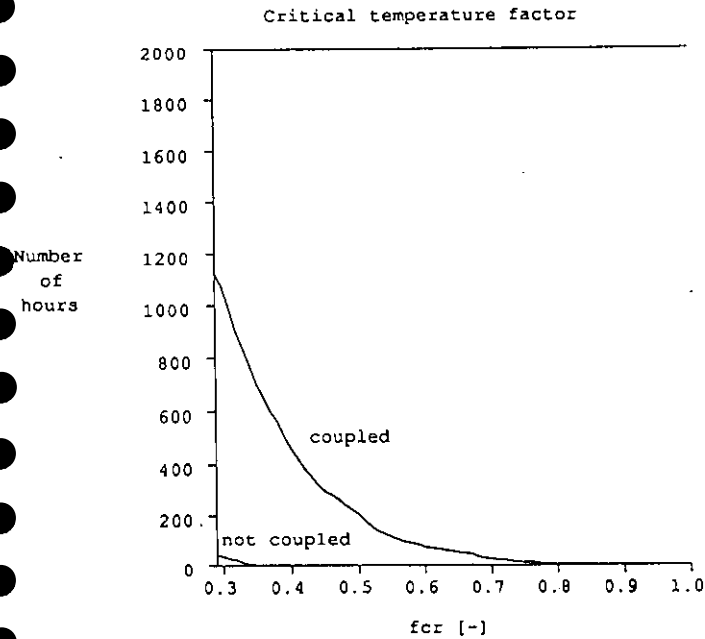
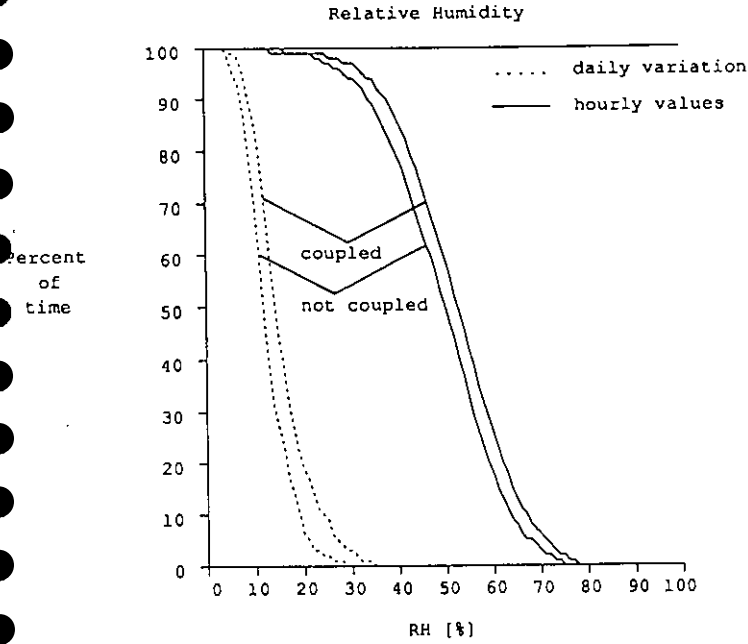


Figure 5.13 Influence of coupled air flow on the living room

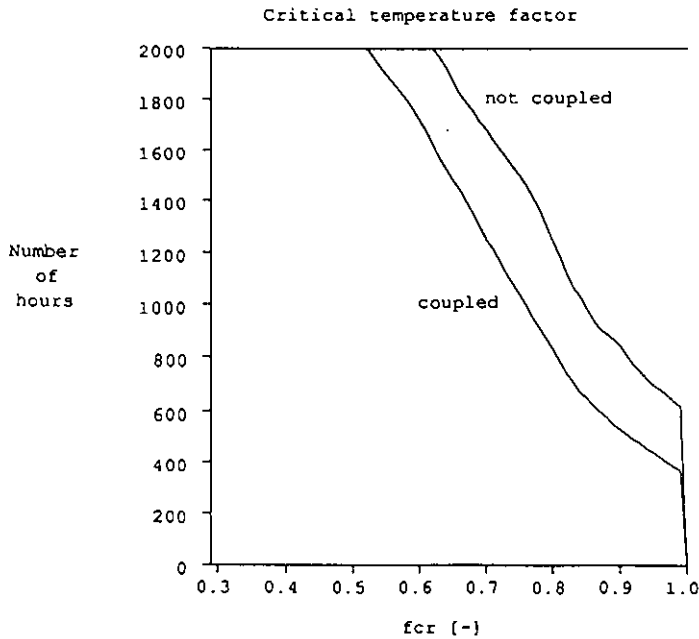
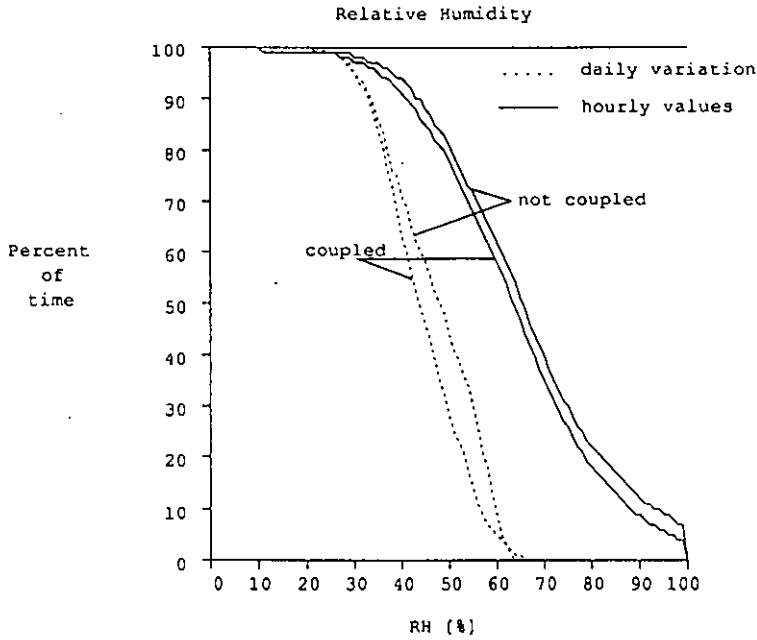


Figure 5.14 Influence of coupled air flow on the kitchen

The temperature factor is defined as:

$$\tau_{hi} = \frac{\theta_{surf} - \theta_e}{\theta_i - \theta_e} \quad (5.2)$$

with θ_{surf} : the surface temperature

If $\tau_{hi,cr} > \tau_{hi}$ condensation will occur. The figures concerning the critical temperature factor indicate if and for how many hours condensation will occur in a comparable situation, once the temperature factor for a typical construction is known.

Comparing the variants

The first variant: influence of the geometry

Figure 5.10 shows the results of the first variant, the reference (the worst case) giving high relative humidities and a high value of the variation of RH over daytime. The influence of the open geometry is very clear: a better situation arises both for the relative humidity and the critical temperature factor. The resulting situation lies between the two distributions for the reference (kitchen) and living room, as indicated in the figure. In the bottom figure there is no contribution for the living room. The model predicts zero hours of a critical temperature factor above 0,7.

The second variant: influence of the finishing layer

Figure 5.11 shows the results of the second variant. The influence of the moisture permeability of the wall finish results in less variation of the relative humidity over daytime. The relative humidity is not higher than 88%. There will be less condensation, as is shown in the diagram for the critical temperature factor.

The third variant: influence of ventilation

Figure 5.12 shows the results of the third variant. The influence of the ventilation results in a better performance of both the relative humidity and the critical temperature factor.

Other variants

Of course it is possible to combine situations to get a configuration with the best performance. Here, only one typical result is given and the possibilities of the models are indicated: Interzonal air flow.

The above simulations have been made without a coupling of the zones in a sense of air transport. One situation has been looked at with the interzonal air flow taken into account. Next results relate to the first option as defined in the introduction. Air flow simulations were made with the model ESPair. Figure 5.13 shows the cumulative frequency distribution of the relative humidity and critical temperature factor for the living room for both the interzonal and non-interzonal air flow case. Figure 5.14 shows the comparable situation for the kitchen. For a clear comparison the infiltration air flow (outside air) is made the same - on average - as in the interzonal air flow case. This yields for the living room an infiltration value of 0.1 and for the kitchen 0.08.

If the interzonal air flow does not exist, than the living room gets only outside air (which will contain less moisture than the living room air) and no extra 'wet' air from the kitchen. This will result in a better performance compared with the interzonal air flow situation. The reverse applies for the kitchen. With no interzonal air flow this zone gets only outside air (containing less moisture than the kitchen air) and no extra 'dry' air from the living room. This will result in a worse performance of the kitchen compared with the interzonal air flow situation.

This expected change in behaviour of the two zones can be seen in the figures. These indicate the difference in predicted behaviour, caused by the difference in approach. The interzonal air flow situation is likely to be the most realistic.

5.8.3 Remarks

This parameter study indicates that the ventilation/infiltration and surface moisture storage are the most important parameters of those covered in this study. In the case of the open kitchen two effects play a role: the increase of air mass (volume of kitchen + living room) but also an increase of the ventilation/infiltration compared with the kitchen only (reference). These two

effects give an important decrease in the number of hours of critical temperature factor as is shown in figure 5.10.

Combining HAM models turned out to provide valuable information on the dynamic behaviour of the room with respect to moisture transport and condensation risk. The work is laborious because of the great amount of information that must be converted to match the input of the following programme. A lot of bookkeeping is required to store all the information properly. To overcome these problems the moisture model should be incorporated in the energy simulation programme. This would also result in a better performance of the combined simulation because thermal effects are involved when condensation occurs.

The validity of the moisture model lies between 20 and 80% relative humidity. This implies that the results give reason for criticism if the relative humidity level exceeds 80%. Also the effect of the hygroscopic material is influenced by the changing physical properties at high relative humidity values (de Wit 90 [34]). The figures indicate that relative humidity is occasionally 100%. At the time that this parameter study was performed, the moisture model did not yet take condensating vapour on constructions into account. In reality these high relative humidities will seldom occur. In this study they are mainly caused by a very pessimistic input e.g. the moisture production is assumed to mix completely with the kitchen air and is not partially extracted by ventilation close to the source.

In real situations, a seasonal effect may play a role. During most simulations, the ventilation rate is the same for every day throughout the year. It is likely that in summer time the ventilation rate is higher than in winter time. It might be interesting to investigate the dependence of the frequency distributions on the season.

It turns out that the distribution of the critical temperature factor is a sensitive indicator for changes in performance. This is clearly illustrated in figure 5.13.

5.10 REFERENCES

- 1 IEA Annex X "System simulations", Synthesis report, University of Liege, 1988
- 2 IEA Annex XVII "Building Energy Management Systems", Annex 17 communications.
- 3 IEA Annex XX "Air flow patterns", Annex XX News Letters
- 4 Bloomfield, An investigation into the analytical and empirical validation techniques for dynamic thermal models of buildings, BRE Executive Summary, december 1988
- 5 Castenmiller, Pijnacker Case Study, Annex XIV report NL-T7-23/1988
- 6 Dalhuijsen, HAM Modelling of swimming halls (in Dutch), TPD-rapport 714.014 (sept. 1988); Novem nr.23.24-006.10.
- 7 Fontaine, Criteria for the evaluation of general ventilation systems: numerical and physical simulations. 2nd International Symposium, London, 20-23, september 1988.
- 8 Hens, Material properties, Annex XIV report B-T2-02/1988
- 9 Kerestecioglu, Theoretical and Computational Investigation of Algorithms for Simultaneous Heat and Moisture Transport in Buildings. Florida Solar research Center, Draft Report FSEC-CR-191-88 (1988)
- 10 Kerestecioglu, Theoretical and Computational Investigation of Simultaneous Heat and Moisture Transfer in Buildings: "Effective Penetration Depth" Theory. To be published in 1990 ASHREA Transactions.
- 11 Kuenzel, Calculation of Moisture Sorption Effects in Buildings. Contributions to Annex XIV meetings
- 12 Liddament, A review and bibliography of Ventilation Effectiveness-Definitions, Measurement, Design and Calculations, Technical Note AIVC 21 (1987)
- 13 Liddament, The validation and comparison of mathematical models of air infiltration, Technical Note AIVC 11 (1983)
- 14 Allen, Air leakage Distribution in buildings. Technical Note AIVC 16 (1985)
- 15 Allen, Wind pressure data requirements, Technical Note AIVC 13.1 (1984)
- 16 Fairy, Dynamic Modelling of Combined Thermal and Moisture Transport in Buildings: Effects on Cooling Loads and Space Conditions. ASHREA Transactions 91 (1985), 461-472
- 17 Cooper, The BERG condensation model. BERG, report June 1987.

- 18 Clarke, A Technical Overview of the ESP System. EC PASSYS-1 report, end 1989
- 19 Cleary, Seasonal Storage of Moisture in Roof Sheathing. Paper 2. AIVG workshop "Airborne Moisture Transfer" (1987)
- 20 Kusuda, Indoor humidity calculations, ASHREA Paper DC-83-12 (1983)
- 21 Oldengarm, Analysis of Moisture Absorption in Dwellings Contribution to IEA Workshop "Condensation and Energy Problems", sept 1985.
- 22 Oldengarm, Crawl Space Ventilation (in Dutch), TPD-TNO report 526.026-3, 1987
- 23 Oldengarm & de Gids, Measurements of airborne moisture transport in a single family in Leidschendam, IEA Annex XIV report, 1990
- 24 Oldengarm, Elkhuisen, Crawl Space Modelling, Paper submitted to CIB Symposium on Moisture, Climate and Energy in Buildings. Rotterdam, september 1990
- 25 Isetti, Predicting Vapour Content of the Indoor Air and Latent Loads for Air-Conditioned Environment: Effect of Moisture Storage Capacity of the Walls. Energy and Buildings, 12 (1988) 141-148
- 26 Becker, The Influence of the Permeability of Materials and Absorption on Condensation in Dwellings, Building and Environment 17,(1982), 125-134.
- 27 Stehno, Praktische berechnung der instationaeren luftzustandsaenderungen in Aufenthaltsraeumen, Bauphysik 4 (1982),128-134
- 28 Riffat, Interzone air movement and its effect on Condensation in houses, Applied Energy 32 (1989) 49-69
- 29 Kohonen, A zone model for room air energy balance, Annex 17 communications between participants, October 1989
- 30 Lemaire, The numerical simulation of air movement and heat transfer in a heated room and a ventilated atrium. TPD-TNO publication 1988
- 31 Plokker, The multi zone computer simulation programme VAl14 for prediction of building thermal performance. XXe International Symposium on Heat and Mass Transfer, September 4-8,1989, Dubrovnik.
- 32 VAl14 Manual Part 1: Instruction Manual (in Dutch), VAl14 Manual Part 2: Model Descriptions (in Dutch)
- 33 Westgeest, Dynamical Crawl Space Model (in Dutch), TPD-TNO report 526.026-4,1987
- 34 Wit, A second order model for the prediction of the indoor humidity, IEA Annex XIV report NL-T4-02/1988

Chapter 6

BOUNDARY CONDITIONS

Authors:

W. Raatschen
DORNIER GmbH, Friedrichshafen (FRG)

H. Erhorn and Z. Herbak
Fraunhofer Institut für Bauphysik, Stuttgart (FRG)

6.0 INTRODUCTION

Mould on building components is, apart from the insulation and building quality factors involved, depending on the boundary conditions: temperature and relative humidity of the outside air and the wind speed, influencing the inside surface temperature, the air change inside the building, and the preloading of the supply air with humidity. Inside, it is the user who affects the indoor air temperature, the amount of moisture emitted and, of course, the air change rate, the last by manipulating the ventilation openings. Room furnishings influence the heat and moisture balance; heating and ventilation systems affect the temperature distribution inside the rooms.

In this last chapter, the boundary conditions will be dealt with in greater detail.

6.1 Moisture Balance of a Room

Humidity conditions inside a room are described by means of the relative humidity or the absolute humidity x [g/kg] or c [g/m³]. In building physics, it is generally the relative humidity that is considered; in investigations of heating or ventilation systems the absolute air humidity is used (see chapter 4, modelling: hygric aspects).

6.2.1 Steady-State Conditions

The relative humidity in steady-state conditions in a room presents an equilibrium determined by the vapour balance. The water vapour produced inside a room (by respiration of occupants, flower plants, cooking, bathing and other water evaporating processes) is added to the moisture, contained in the supply air. As long as there is no surface condensation, the total amount of vapour is discharged back to the outside by the exhaust air (As shown in chapter 4, diffusion doesn't play a big role in this).

6.2.2 Non-Steady-State Effects

In non-steady-state, there are sorption effects caused by moisture fluctuations, which have to be taken into account in addition to the above mentioned moisture balance portions. Depending on the actual sorption behaviour of walls and furnishings, short-term moisture peaks can be buffered. The moisture will be re-released as soon as the indoor air humidity decreases.

6.3 Influence of Inhabitant Behaviour

Occupants have a major impact on the indoor climate. On one hand, humans are a source of pollutants (CO_2 , odours, and moisture), on the other hand they can control the indoor environment when feeling uncomfortable. Humans are not sensitive to all indoor contaminants. For example there is no perception for CO_2 or CO and only a weak sensitivity to very high humidities. The perception of odours is only well functioning for changes of odour intensity (e.g. when entering a room). Occupants respond to room temperature according to their degree of activity and clothing. Therefore occupant behaviour varies very much and is difficult to tackle and to express in mathematical functions.

The interesting questions with regard to mould and surface condensation are:

- how high are room temperatures in practice;
- how high are ventilation rates in practice;
- how high is the humidity production in practice.

In answering these questions, one can differentiate between the kind of rooms (living, functional, and sleeping rooms), between the seasons and climate

variations within a day, between attitudes of occupants towards energy savings, between social status and habits...

In the framework of the IEA-Annex 8, 'Inhabitant Behaviour with Respect to Ventilation', it was tried to answer some of these questions.

6.3.1 Vapour Production Rates in Rooms

Depending on the individual occupants habits, more or less water vapour is emitted in a room, according to the actual degree of physical activity; a man alone releases between 40 g/h and 300 g/h of water vapour every hour. The activities most frequently performed in dwellings will result in a person-related moisture production of about 90 g/h. In bathrooms, the amount of moisture produced is reported in [7] to be about 700 g/h when taking a bath and approximately 2600 g/h when taking a shower. These emission rates correspond well with newer measurements. [30] gives production rates during a shower of 3 resp. 15 minutes duration of 200 resp. 800 g. During cooking processes and other household activities, kitchens experience a moisture load between 600 g/h and 1500 g/h. The daily average amounts to about 100 g/h.

Flower plants and aquaria are also contributing to the indoor moisture load. For instance, plants are evaporating practically all the water supplied; at the most, only 0.2% of this water can be used for growth. Small potted flowers emit between 7 g/h and 15 g/h of vapour; a medium-sized rubber plant yields between 10 g/h and 20 g/h. Although these quantities appear quite insignificantly at first sight, their additive effects must not be underestimated.

Another moisture source are drying processes in dwellings. Even wet laundry that has been spin-dried at full speed still emits between 10 and 50 g/h (per kg dry laundry). Laundry should therefore always be dried in thoroughly ventilated rooms. In Table 6.1 all common moisture emitters present in dwellings have been compiled.

The relevant technical literature (see [3] through [12]) has been screened for moisture loads in dwellings of various sizes. These figures have been collected in Table 6.2-6.5. The average values for moisture loads are presented for a household without children (Table 6.4) and for a household with two children (Table 6.5). During the day, the moisture production is subject to pronounced variations.

Human beings	light activity medium activity hard work	30 - 60 g/h 120 - 200 g/h 200 - 300 g/h
Bathroom	bath shower	about 700 g/h " 2600 g/h
Kitchen	cooking and working daily average	600 - 1500 g/h 100 g/h
Potted flowers e.g. violets (<i>Viola</i>)		5 - 10 g/h
Potted plants e.g. ferns (<i>Comptonia asplenifolia</i>)		7 - 15 g/h
Medium-sized rubber plant (<i>Ficus elastica</i>)		10 - 20 g/h
Aquatic plants e.g. waterlilies (<i>Nymphaea alba</i>)		6 - 8 g/h
Open water surface		about 40 g/m ² h
Young trees (2-3 m) e.g. beech trees (<i>Fagus</i>)		2 - 4 kg/h
Full-grown trees (25 m) e.g. spruce trees (<i>Picea</i>)		2 - 3 m ³ /h
Dry laundry (4.5 kg)	spin-dried dripping wet	50 - 200 g/h 100 - 500 g/h

Table 6.1: Moisture in dwellings emitted by human beings, plants, drying processes, bathroom units, according to [7].

Author	Reference	Households with			
		no child	1 child	2 children	3 children
BH Bau	[3]		10		
BRE	[4]			5 - 10	
BS 5250	[5]				14.4
DQtz/Le Marié	[6]	7	20		
Erhorn/Gertls	[7]			14.6	
Lübke	[8]	13.2	19.9	23.1	
Meyringer	[9]		11.5		
Panzhauser et al.	[10]		5 - 12		
Pfeller	[11]		6 - 10.5		
Stehno	[12]	4.3		13.7	
Average*		8.2	12.1	14.1	14.4

* Average values indicating a range are based on lower limiting values.

Table 6.2: *Compilation of rates of daily moisture loads in dwellings (kg/d) as indicated in the relevant literature.*

Households	Moisture emission rates
no children	8 kg/d = 350 g/h
one child	12 kg/d = 500 g/h
with two children	14 kg/d = 580 g/h
more than two children	15 kg/d = 630 g/h

Table 6.3: *Total quantities of moisture emitted in dwellings of various size.*

Time [h]	Persons present		Total amount of moisture [g/dwelling]			Σm per h [g/dwlg]
	Number	Persons	Cooking	Personal hygiene	Washing	
1	2	120	-	-	-	120
2	2	120	-	-	-	120
3	2	120	-	-	-	120
4	2	120	-	-	-	120
5	2	120	-	-	-	120
6	2	120	240	360	-	720
7	2	120	240	360	-	720
8	-	-	-	-	-	-
9	-	-	-	-	-	-
10	-	-	-	-	-	-
11	-	-	-	-	-	-
12	-	-	-	-	-	-
13	-	-	-	-	-	-
14	-	-	-	-	-	-
15	-	-	-	-	-	-
16	-	-	-	-	-	-
17	-	-	-	-	-	-
18	2	120	-	-	-	120
19	2	120	480	240	-	840
20	2	120	480	240	-	840
21	2	120	-	-	-	120
22	2	120	-	-	-	120
23	2	120	-	-	-	120
0	2	120	-	-	-	120
Σ per day		1680	1440	1200		4320

Table 6.4: Moisture emitted in a family of two, according to [12].

Time [h]	Persons present		Total amount of moisture [g/dwelling]			Σm per h [g/dwlg]
	Number	Persons	Cooking	Personal hygiene	Washing	
1	4	240	-	-	-	240
2	4	240	-	-	-	240
3	4	240	-	-	-	240
4	4	240	-	-	-	240
5	4	240	-	-	-	240
6	4	240	480	720	-	1440
7	4	240	480	720	-	1440
8	2	120	-	-	120	240
9	1	60	-	-	180	240
10	1	60	720	-	180	960
11	2	120	1200	120	-	1440
12	2	120	1200	120	-	1440
13	2	120	480	120	-	720
14	2	120	480	120	-	720
15	2	120	-	-	120	240
16	2	120	-	-	120	240
17	2	120	-	-	120	240
18	4	240	-	-	-	240
19	4	240	480	240	-	960
20	4	240	480	240	-	960
21	4	240	-	-	-	240
22	4	240	-	-	-	240
23	4	240	-	-	-	240
0	4	240	-	-	-	240
Σ per day		4440	6000	2400	840	13680

Table 6.5: Moisture emitted in a family of four, according to [12].

6.3.2 Ventilation Rates

Here we compress the results of IEA-Annex 8 [2].

Window Opening Fabric

windows in apartments are less opened and for shorter periods (except bedrooms) than in houses. If opened at all, than only slightly south-facing rooms with solar gains are more likely to be ventilated than other rooms;

bottom-hung windows and fanlight windows are opened more frequently than other types of windows;

occupants, living in single-glazed window dwellings open windows more, often to remove condensation from the panes, than occupants in double-glazed window dwellings;

windows in centrally heated dwellings were less opened for long periods than those in locally heated dwellings, especially in bedrooms. Dwellings with warm-air central heating are less ventilated than dwellings with radiator systems. There is almost no window opening behaviour difference in dwellings with a natural and dwellings with a mechanical ventilation system as occupants don't understand how to use and operate the system.

Lifestyle

the more occupants in a room, the more the windows are opened. In dwellings, which are left during the day, windows are more likely to be closed during daytime (for security reasons) but more opened during evening and night time; i.e. the duration of window opening over a day is about the same if dwellings are occupied continuously or only at night;

window opening duration in living rooms with smokers is twice that in living rooms with no smokers;

occupants with high thermostat setting open windows less than occupants with low thermostat setting. Most people prefer bedroom temperatures below 17°C and keep bedroom windows open during cold winter days;

there is a correlation between the use of a shower and the opening of the bathroom window.

Socio-economic Variables

elderly people ventilate less than younger people.

Control strategies

- Survey results on why people open their windows also include 'remove stale air or condensation'

Weather Factors

- there is a linear correlation between the percentage of open windows and the outdoor temperature;
- there is an inverse linear correlation between the percentage of open windows and the wind speed
- windows are more often opened when the sun shines
- living and bedroom windows are significantly less opened during rainy days.

Additional Air Change Rates Due to Occupant Behaviour

- Studies from Denmark, Belgium and Switzerland have been evaluated. The results listed in Table 6.6 are remarkably similar. They show an additional ACR due to occupant behaviour between 0.25 and 0.35 h⁻¹.

Source	Country	Description	n _{occ} (ach)
Kvisgard et al	Denmark	Single-family dwellings	0.32
		• naturally ventilated • mechanically ventilated	0.34
Wouters and De Baets	Belgium	Single-family dwellings	0.31
		Apartments	0.21
Faist et al	Switzerland	Apartment	0.25

Table 6.6 Comparison of results for the Danish, Belgian and Swiss projects [2]

6.3.3 Room Temperature

As stated in 6.3.2, most people prefer bedroom temperatures below 17°C. German studies learn, that average living room temperatures are more likely to be higher than 20°C, which is the design value in most building codes. In practice, living room temperatures vary between 20 and 24°C, whereas in Scotland bedroom temperatures were measured as low as down to 0°C.

6.3.4 Air and Humidity Distribution in Buildings

If the interior doors are kept open, rooms with high moisture production will influence the humidity levels in adjacent rooms. A very common behaviour of occupants is to open the doors of a room with high moisture production (especially bathrooms but also laundry rooms and kitchens) to decrease the humidity level in this room. Especially during cold or windy and rainy weather this is done rather than opening windows. This results in an increase of the relative humidity in adjacent rooms (see chapter 5).

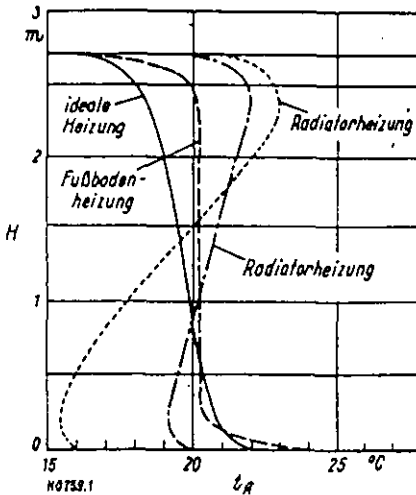


figure 6.1 Room temperature distribution for different heating systems

6.4. Influence of Heating System

6.4.1 Temperature Stratification

The knowledge of the temperature field in a room is important for the investigation of mould problems. Especially the convective surface film coefficient h_{ci} depends on the air temperature close to the surface. How air temperatures are distributed, depends on the heating system.

6.4.1.1 Radiator Heating System

Figure 6.1 shows the temperature distribution as a function of the room height for a radiator heating system, compared to a floor heating system. It can be seen that the temperature gradients are substantially bigger with radiators.

6.4.1.2 Floor and Ceiling Heating System

In rooms with floor heating and a room height of 2,65 m the temperature distribution is pretty uniform [1]. Also under extreme conditions with inside surface temperatures of external walls of 13°C and average room temperatures of 22°C, the temperature difference is max. 2 °C. The difference with respect to the room height increases near the exterior walls. Fig.6.2 shows the temperature distribution with the boundary data and Fig.6.3 gives the velocity distribution for slightly different boundary conditions.

In [34], air temperature and velocity profiles in a room are investigated for 4 different heating systems, 3 infiltration rates and 2 insulation levels. The results are summarized in Table 6.7. Unfortunately, it is not clearly defined in the report whether air, black globe or another temperature was measured.

6.4.2 Operating Modes

The influence of 'night set-back' on mould occurrence has not deeply been examined yet. When heating stops and the room temperature decreases, the relative humidity increases and adsorption starts. When heating starts again the air humidity decreases and moisture is released by the walls. A dutch study [30] reported a rise of 0.4 g/m³ air humidity due to a temperature

Insul. of Facade	Infiltr. h ⁻¹	floor	ceiling	floor* + ceiling	floor + MV**
	0.0	22.0	21.5	21.9	22.0
		+1.0 -1.3	+1.1 -1.0	+1.2 -1.2	+0.8 -0.7
good	0.7	---	---	21.7	---
		+1.4 -1.2	+1.4 -1.7	+1.4 -1.5 +1.5 -1.7	---
	1.2	21.6	21.3	21.5	---
	0.0	22.6	20.9	---	21.8
		+1.4 -1.6	+1.9 -1.8		+1.2 -1.4
poor	0.7	22.0	20.8	21.2	---
		+1.1 -2.0	+2.4 -2.2	+1.9 -2.1	
	1.2	21.4	20.8	21.1	---
		+1.6 -2.4	+2.3 -2.5	+1.6 -2.4	

* Heating power ratio : 1/3 floor, 2/3 ceiling
 ** " " " : 1/2 floor, 1/2 MV (mech. Ventilation)

Table 6.7: Room mean temperatures with maximum and minimum deviation for different heating systems, infiltration rates and insulation quality [34].

increase from 17°C to 21°C; starting at a RH of 35%, the RH after 1 hour was 30%. The total mass of desorbed moisture (living room, 93m³) was 40g. These values are of course dependent on the wall finishes and the furniture in the room.

Some general remarks are given in [25]. During the night the highest moisture production takes place in bedrooms. Most people close bedroom doors at night for privacy and/or keep windows especially during winter times closed. Reducing the room temperature at night lowers the surface temperature of the exterior walls. These conditions increase the probability that the relative humidity against the walls gets too high. So, it is important to give special attention to moisture removal from bedrooms during the night.

Similar effects may take place if the bedrooms are kept cool during the day and warm moist air from the rest of the house comes in.

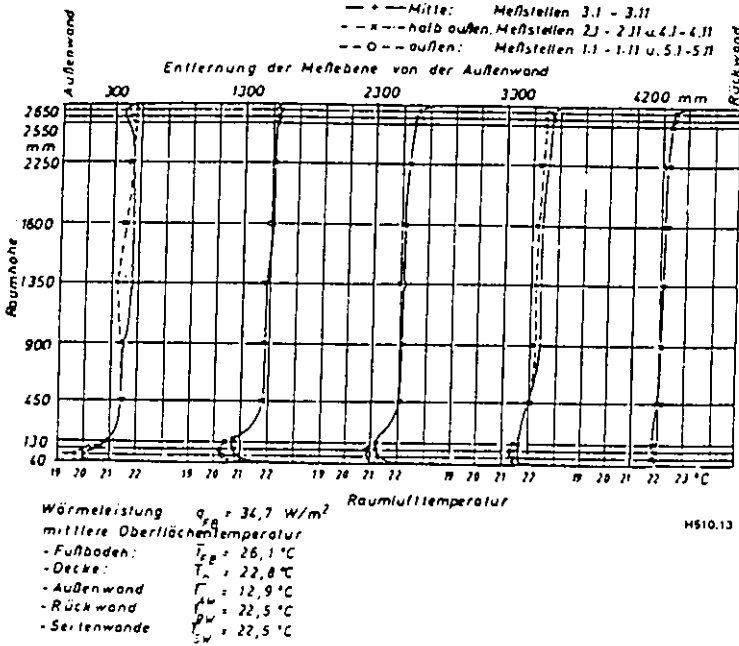


Figure 6.2 Temperature profile in a room with an exterior wall $t_w = 12.9 \text{ }^\circ\text{C}$, $\theta_{\text{air,mean}} = 22.1 \text{ }^\circ\text{C}$, $h/l = 0.54$

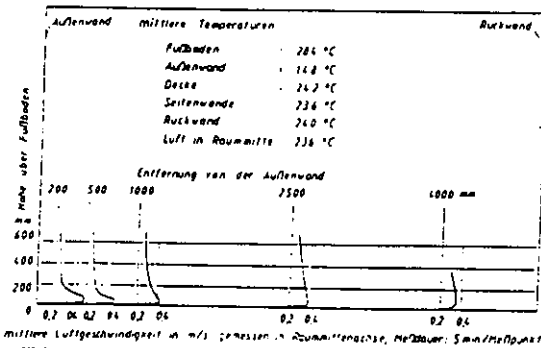


Figure 6.3 Air velocity in a room unit floor heating system and an exterior wall $\theta_{\text{gw}} = 14.8 \text{ }^\circ\text{C}$

6.5 Influence of Ventilation System

One of the causes of mould problems may be poor ventilation. In fact, the poorer the building's insulation, the higher the necessary ventilation. However, also a well insulated building needs an adequate ventilation rate. Most houses are naturally ventilated. Therefore we focus our considerations on this kind of ventilation strategy.

6.5.1 Natural Ventilation

6.5.1.1 Driving Forces

In natural ventilation the driving forces are: wind and stack effect [26].

Wind:

Within the lower regions of the earth's atmosphere the wind is characterized by random fluctuations in velocity which, when averaged over a fixed period of time, give a mean value of speed and direction.

Wind increases the pressure differentials around buildings and increases the air flow through openings. Wind velocity increases with the height above groundlevel. Therefore, the influence of wind on e.g. a high-rise apartment flat is bigger than on low rise buildings.

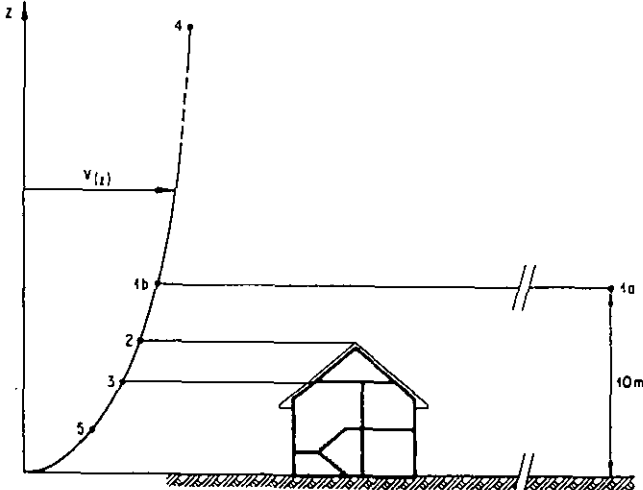


Figure 6.4 Wind velocity profile, which illustrates the effect of wind speed on the ventilation rate [35]

Stack effect:

The stack effect arises as a result of temperature differences and hence air density differences between the inside and the exterior. This creates a vertical pressure difference. When the internal air temperature is higher than the outside temperature, air enters through openings in the lower part and escapes through openings at a higher level of the building. This flow direction is reversed when the internal air temperature is lower than the outside temperature (fig.6.5)

User effect:

Occupants may increase ventilation by opening windows, doors or other purpose provided devices (see paragraph 6.3.2).

6.5.1.2 Component leakage

Timusk et al. [27] investigated moisture problems in timber frame buildings in Canada. It was not possible to explain mould and mildew occurrence solely in terms of thermal bridging, two-dimensional heat flow, hindered air circulation or lack of radiant heat gain.

The authors proved that additional cooling of wall surfaces resulted from defects in the sheathing, which allows the wind to penetrate the wall.

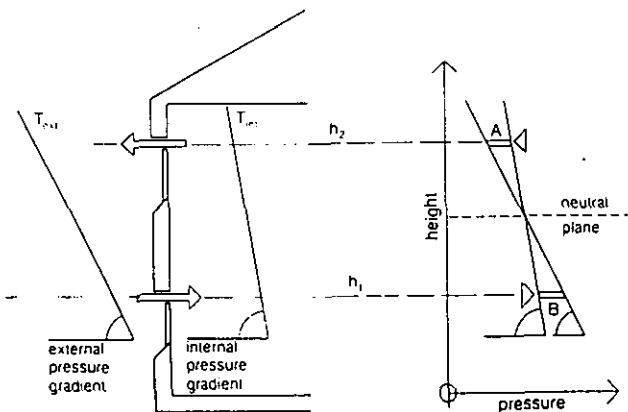


Figure 6.5: Stack induced pressure between two vertically placed openings [26]

construction in corners where a rapid positive- negative change in wind pressure exists. They concluded that defects in the sheathing-siding system permitted wind to blow in and out of the wall cavities without actually entering the building.

For this to occur, there must exist continuous inside - outside air passages into the wall through the siding-sheathing around the corner.. These continuous air passages are due to careless installation of the sheathing, to the air permeability of the glass fibre insulation and to shrinkage cracks between studs and gypsum board. Similarly, air pressure under the wind ward soffit can cause wind to blow through the exposed face of attic insulation. Unfilled corners between the ceiling gypsum board and the attic joints present passages with little resistance to wind. In some instances air velocities into the attic have been sufficiently high to even scour away unprotected cellulose insulation. Wind-driven snow can also blow into the attic through the soffit vents.

Summarised, the above phenomena were believed to be due, to deficiencies in the wind protection of the insulation (allowing forced convection to cool the weather-side of the gypsum wall board to near-outside temperatures).

Powell at al. [28] showed that the influence of air intrusion on the performance of porous insulation can be high and decrease the thermal resistance of a wall substantially. Convective air flows increase the heat transfer in building envelopes which contain air-permeable insulations and therefore decreases indoor surface temperatures. The degradation of the effective thermal resistance of insulation depends on:

- natural or forced convection
- width of the joints between insulation slabs
- air permeability, density and thickness of the insulation
- width of the air spaces on both sides of the insulation layer.

The authors showed that in many cases a correct application of an air barrier reduces significantly the convective air flow, and is effective in preserving the R-value of the insulation.

The hygrothermal consequences of air convection in wall structures was investigated by Ojanen et al. [29] by using a numerical simulation model. The main results are:

- Wind-caused forced convection may increase mean heat losses of the corner area by about 15 %. Here locally heat flux values were even three times higher than without convection.
- Air infiltration causes heat recovery from transmission heat losses. Under uniform infiltration conditions the calculated warming of outdoor air through the porous wall can be 90 %. The total heat recovery effect, related to the total heat balance of the room air, may be 23 %.

We conclude that with respect to 'Energy and Condensation' leakage in wall structures or insulation materials generally increases heat fluxes and, decreases surface temperatures, enhancing the risk of mould and surface condensation.

Exfiltration through gaps, cracks or a porous wall increases significantly the risk of interstitial condensation.

6.5.1.3 Short Intensive Ventilation

Still, it is often proposed to ventilate a room very intensively for a short time (open windows etc.) to re-establish good indoor air quality and low relative humidity with minimal energy losses. To get rid of high moisture concentrations this is not a good advice. Many tests show that just after intensive ventilation (windows closed) vapour is released again from room and furniture surfaces with the result that the relative humidity in the room air is about the same value as before (see Figure 6.6).

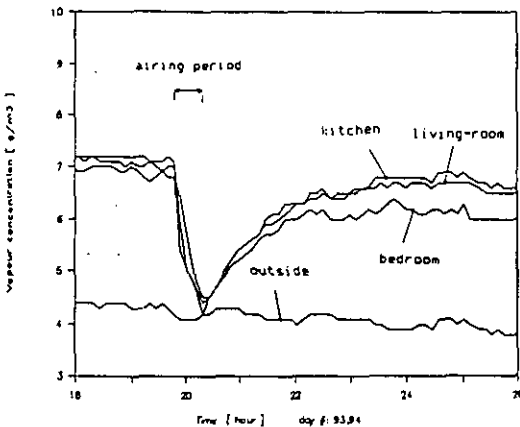


Figure 6.6 Moisture behaviour due to airing [30]

6.5.1.4 Ventilation strategy

A possible ventilation strategy to cope with moisture problems and to minimize energy consumption is adjusting the air flow rates, according to the variation in relative humidity in the building zone.

From the point of view of energy conservation (and not yet from an economic point of view) an air tight building with a humidity controlled ventilating system, could be a good choice, which should be looked at closer.

6.5.2 Climatic Influences

The impact of the local climate on ventilation is twofold:

- due to outdoor humidity and temperature changes the leakage characteristics of the building component openings may vary. Especially affected are timber components which shrink during dry and cold winters and swell during wet summers;
- as discussed in paragraph 6.5.1 the driving forces of natural ventilation - wind pressure and stack effect - are largely dependent of the meteorological conditions.

Fig. 6.7 qualitatively shows the infiltration characteristics of a building. Such a curve is constructed using a numerical model to calculate the infiltration rate for fixed increments in wind speed and temperature, covering the climatic range of the locality (graphs and text partly taken from the Air Infiltration Calculation Techniques Guide [26]).

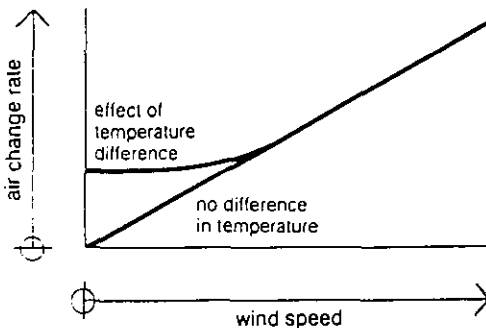


Figure 6.7 Infiltration characteristic [26]

This approach provides an invaluable aid to the visualization of air infiltration performance for specific design conditions. By constructing such curves for different topographic conditions, it is also possible to analyse the influence of shielding. In addition this approach enables an approximate indication of air change rates for a wide range of wind and temperature conditions.

In practice it is inevitable that certain combinations of wind and temperature result in too much or too little infiltration. Therefore it may be necessary to calculate the air infiltration rates in a further stage of design process by determining the frequency of time intervals for which unsuitable conditions prevail. This is possible using statistical climatic data of hourly mean wind speed and air temperature to produce hour-by-hour frequency distributions of air infiltration. Typical results are illustrated in figure 6.8 in the form of a histogram and an accumulative frequency plot. This figure also illustrates how climatic severity influences the distribution.

These results may be used to analyse the extra energy losses associated with natural ventilation or to investigate the need for controlled ventilation. According to the maximum allowable relative humidity in a room one can estimate, how often supply air is insufficient to remove moisture and how often excessive (unnecessary) air with regard to moisture production is supplied throughout a year. To do such calculations, the meteorological data base is given in Appendix A.

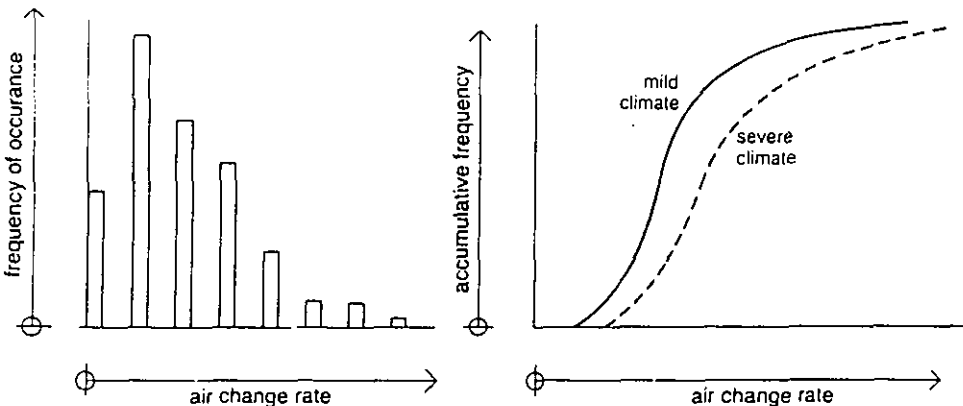


Figure 6.8: Distribution of infiltration rates throughout a heating season [26]

6.5.3 Moisture distribution within a zone (intrazonal moisture distribution)

The characteristics of the moisture sources are different: intermittent release through cooking and showering or other special activities, more uniform release through flower plants, aquaria and sometimes cloth drying. Adsorption and desorption are also generation sources, where adsorption (negative generation) can happen quite fast, especially when condensation occurs, while desorption of a previously adsorbed amount of water can take 10 - 15 times longer [30]. It is proven that the characteristic of the source, the ventilation system and the heating system influence the intra-zonal moisture distribution.

In naturally ventilated rooms vapour production by sources with low and uniform release is usually homogeneously mixed throughout the room. Door usage and the often applied radiator heating promote good mixing of room air. If temperature stratification occurs, relative humidities may vary but the absolute water content will be about the same, as experiments show [36].

A different behaviour is observed with intermittent moisture sources. Experiments in a dutch living room [30] with open kitchen indicate the following:

- vapour concentration (in mg/m^3) decreases with the distance from the source due to mixing (dilution) and fast adsorption;
- vapour concentrations beneath the ceiling are higher, sometimes by a factor of 2, compared to locations above the floor (measured at the same x-y coordinates with different height). This is, because water vapour at the boiling point is much lighter than air and accumulates beneath the ceiling;
- depending on the operation mode of the ventilation system and the use of air supply devices it takes between 2 to 4 hours, before vapour concentrations in the room have equalized
- if no mechanical ventilation system is in operation, doors and vents are closed, and an infiltration rate of 0.6 h^{-1} is assumed, than the adsorption process lasts for about 2 hours after moisture generation. Then a desorption period follows with a duration of 6 hours

- with the support of an extract fan, the adsorption and the desorption process is accelerated.

Similar experiments were undertaken in Germany [31]. In a living room moisture was generated using an air humidifier. Contrarily to the dutch experiment, the moisture was mixed with the air and the temperature of the emitted vapour air mixture was only slightly above room temperature. Relative humidity was measured at 5 locations in the room. In that case, at all locations almost the same values were measured, no gradients being found from the floor to the ceiling or away from the source.

6.5.4 Interzonal Moisture Transfer

Studying the transport of moisture, one has to realize that the airflow through an open door, due to turbulence and even small temperature differences, is relatively high in relation to the flow rates with the door closed [30]. For instance 1K temperature difference easily causes a flow rate of approximately 100 dm³/s. With the door closed, in the same situation, the flow is about 0.5 dm³/s. The flow rate over a closed door due to wind or mechanical extraction normally is, for instance with 2 Pa pressure difference across it, approximately 10 dm³/s. This is of course depending on the air permeance of the door perimeter joint.

Experiments in [30] reveal that after a 30 min cooking process and opened door between living room and landing only a slight relative humidity increase was observed in the landing. The results of a 15 minutes showering experiment (810 g evaporated in a 9.3 m³ bathroom) reveals that the vapour concentration in adjacent rooms goes up to 85 % of the peak level of the bathroom, when the fan is off and the door in between open. The drying of both rooms took 4 hours. With the fan off and the door closed there was almost no increase of humidity in the adjacent room. The drying of the bathroom was determined by natural ventilation and took about 28 hours.

Using an extract fan, which provides an ACR of 6.6 h⁻¹, and keeping the bathroom door open the peak level in the adjacent room could be reduced to about 40 % of the peak in the bathroom.

6.6 Meteorological Conditions

The outdoor climate has a major impact on the inside vapour concentration. Humid air enters a building by infiltration, natural ventilation or by a mechanical ventilation system. Infiltration and natural ventilation are strongly influenced by wind speed and direction and by the temperature difference between inside and outside.

The knowledge of outdoor temperature, outdoor relative humidity, wind speed, and wind direction is important. For case studies and research projects these parameters have to be recorded. For more global considerations e.g. comparison of different locations or calculations, monthly averages are of interest. Appendix A contains the monthly averaged outdoor temperature, absolute humidity, and wind speed for the 5 countries, involved in Annex XIV.

6.6.1 Influence of the Local Climate on the Indoor Air Humidity

By ventilation or infiltration, outdoor air is brought into a building. How much air enters, depends on the ventilation strategy (natural ventilation, balanced ventilation, etc.). How humid this entering air is, depends on the local climate. There are locations which are fairly dry but others which are humid. Also the season plays a role.

Independent of the building quality, the ventilation strategy and occupant behaviour, we tried to compare for different locations the impact of the local climate on the indoor air humidity level. The reason for these calculations is not to report theoretical ventilation rates and energy saving factors, but to visualize trends and to qualitatively emphasize the impact of different parameters on ventilation and energy consumption in relation to the moisture balance of a building.

For the calculations, a meteorological data base, the Test Reference Year (TRY), which gives hourly mean values of the local climates of Germany, was used.

In many locations of Europe the most critical time of the year is early fall. It can be seen in Figure 6.9 and 6.10 that e.g. in Bremerhaven in the north-west part of Germany and in Friedrichshafen at Lake Constance in the very south of the country during some days in October the calculated differences

are close to zero, sometimes even negative. This means that the amount of supply air for a given vapour emission rate has to be substantially higher than during the cold months, were the outdoor air is drier and therefore the difference $(x_i)_m - x_e$ bigger. These facts may not be severe with regard to mould growth, as these conditions do not last very long. Using monthly mean values, one would obtain in most cases uncritical conditions.

The considered cases are idealized, but they show that sometimes only small rates of moisture production in a building can make the difference $(x_i)_m - x_e$ negative and, if this situation stays for a considerable time, it increases the risk on mould growth. These small difference $(x_i)_m - x_e$ ask high ventilation rates.

Example:

We consider as reference house, a one zone building with a mean "inside surface - outside" heat permeance $P' = 1.15 \text{ W/m}^2\text{K}$. The inside surface film coefficient is $h_i = 4.0 \text{ W/m}^2\text{K}$. Calculations are performed with a room air temperature of 20°C and 16°C . The outdoor air passes through the zone where it is heated from outdoor to room temperature. If mould problems should be avoided, the monthly mean humidity against the surface should not exceed the empirically derived ' a_w '-value, see chapter 2 of [32].

Out of the steady-state moisture balance (see chapter 4), we calculated the mean inside vapour concentration, $(x_i)_m$ of the zone.

A plot of $(x_i)_m - x_e$ vs. time shows:

- for positive $(x_i)_m - x_e$, how much vapour can be produced for a given ventilation rate or how much outside air has to be supplied for a given vapour production to avoid mould risks;
 - if $(x_i)_m - x_e$ is zero, that no moisture should be released into the room;
 - if $(x_i)_m - x_e$ is negative, that without dehumidification of the supply air the maximum ' a_w '-value at the surface considered will be exceeded.
-

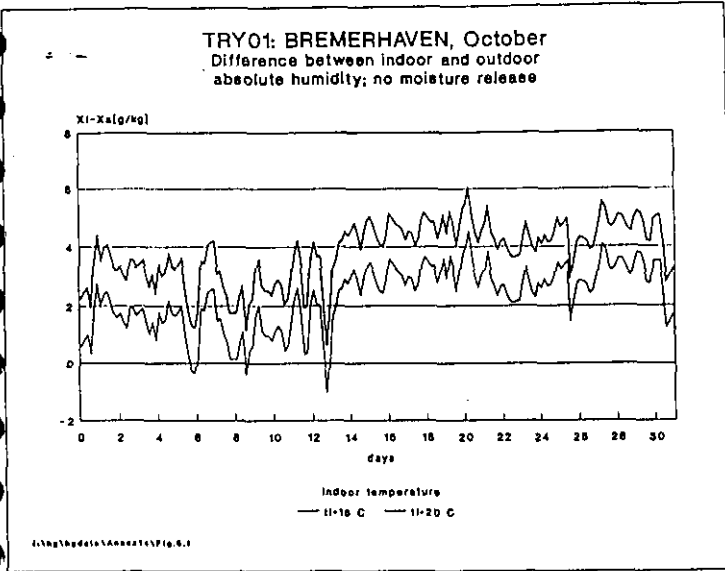


Figure 6.9

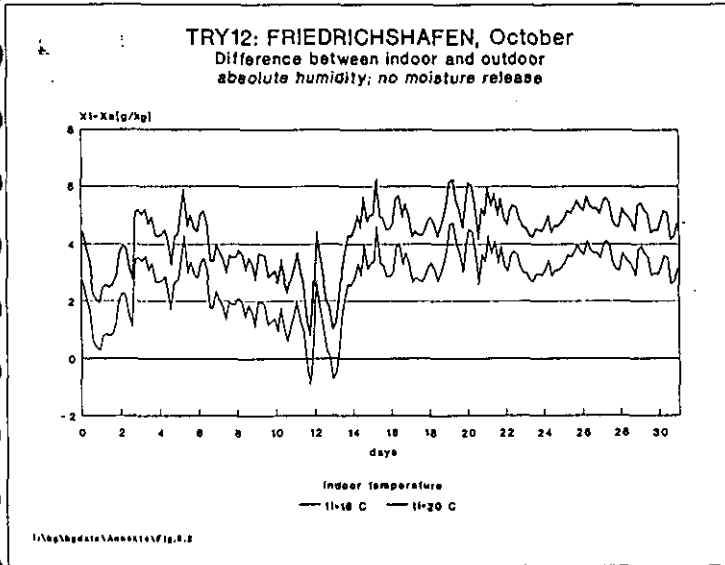


Figure 6.10

6.6.2 The Influence of the Local Climate on the Ventilating Rates

We consider the same reference house as in 6.6.1 and calculate the accumulated supply air flow, necessary to fulfil the condition not to exceed the maximum 'a_w'- RH-value against the wall surface. Furtheron we assume, that the moisture release is uniform throughout the day: 8 kg/day. There is no heating from June to August and also during days outside this period, when the mean daily outdoor temperature is above 15°C. The energy consumption calculated, refers only to the ventilation losses without taking into account the energy consumption by fans or the savings through heat recovery (See appendix B) Figures 6.11 and 6.12 shows monthly accumulated ventilation flows and energy consumption for Essen, in the west of Germany, necessary to keep the indoor relative humidity low enough to have no exceeding of the mould condition against indoor surfaces.

Remark:

It should be kept in mind, that the purpose of ventilation is not only to evacuate moisture, but also to remove odours, stale air, tobacco smoke etc. Especially during winter times, when removing moisture only demands small ventilation rates, it may be possible that other factors dominate and govern the necessary ventilation rate. Here we only try to evaluate the influence of the moisture load (local climate, indoor generation processes), coupled to the mould condition, on ventilation rate and energy consumption, with exclusion of all other factors.

Figure 6.11 shows, that, depending on the indoor temperature, the necessary ventilation rates are highest during summer and lowest during wintertime. This is obvious, because - assuming a uniform generation rate throughout a year - the warm humid air in summer can not take up so much moisture as the dry cold air in winter, after being heated. This increases the ventilation rate in summertime.

Figure 6.12 shows the energy demand for two different indoor temperatures. As it can be seen, it is not always possible to save on ventilation energy demand with a lower room temperature, if the adequate amount of air should be supplied to avoid mould problems.

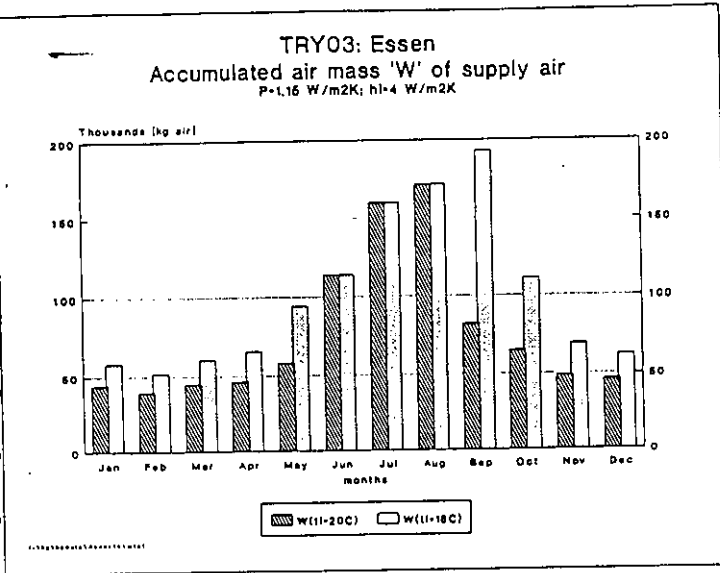


Figure 6.11

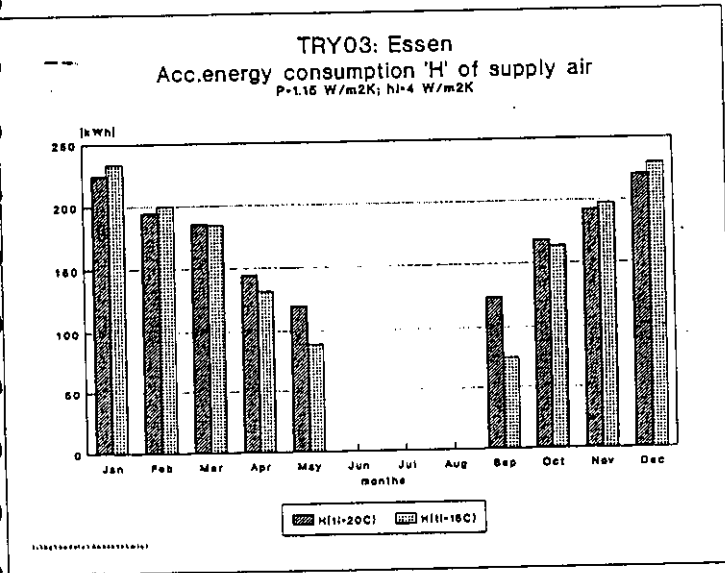


Figure 6.12

If the monthly average values over a year of the ventilation flows 'W' and the energy consumption 'H' are added, we see, according to Table 6.8, that the total air flow all over the year has to be increased by 32%, if the air temperature is reduced to 16°C. This increased air flow reduces the energy savings by a lower inside temperature to only 4%. Calculations for other locations had been made with the result, that a decrease of room temperature can led to an even higher energy consumption for air heating.

Usually one would assume to save energy with a reduced room temperature. This would be true if the ventilation rate is constant. But as be seen in Figure 6.11 and 6.12, to avoid mould, an increased ventilation rate is needed with decreasing room temperature. This overcompensates the effect of the outdoor air, to be heated to a lower room temperature.

All calculations performed base on the assumption, that the ventilation system installed is able to exactly adjust the air change rate to the need, i.e. not to exceed the ' a_w '-RH-value against indoor surfaces. Such a system doesn't exist yet. One step towards this goal could be relative humidity controlled ventilating systems.

If different ventilation strategies are compared with regard to energy consumption, such a comparison only makes sense when all strategies make sure, that on a monthly base the relative humidity against indoor surfaces will not exceed the ' a_w '-value.

Room- temperature	accumulated air flow [kg] during a year	energy consumption [kWh] during a year
$\theta_i = 20^\circ\text{C}$	920360 (100%)	1578 (100%)
$\theta_i = 16^\circ\text{C}$	1212330 (132%)	1507 (96%)

Table 6.8: Accumulated air mass and energy consumption during a year at different room temperatures based on values from Figure 6.11

Air flow rates 'W' and energy consumption 'H' for supplied air for international locations

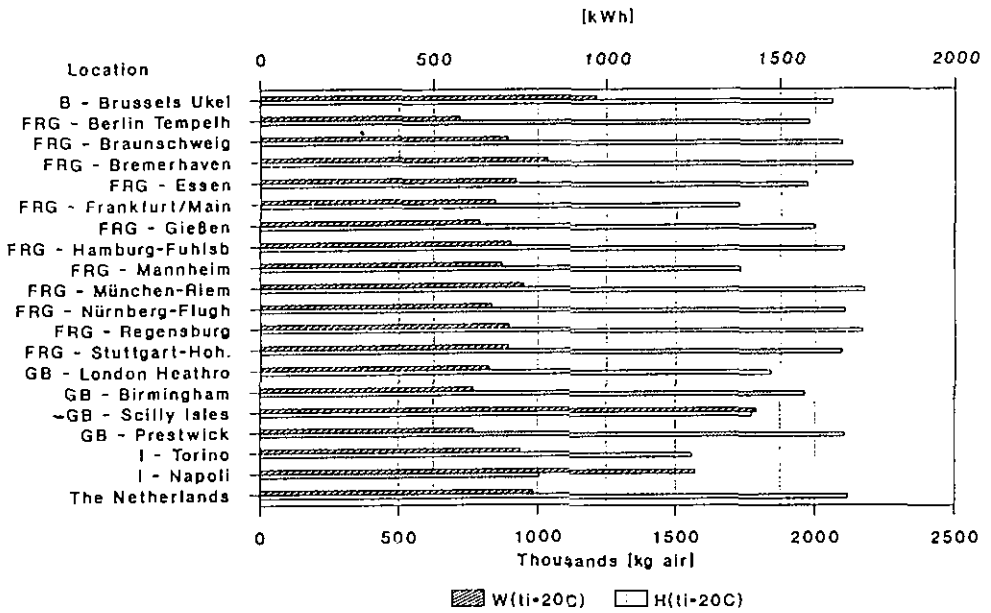


Figure 6.13

Based on the previous calculations, we tried to compare the air flow rates needed, and the energy demand for locations in the countries participating in this Annex, to see how the different climates effect the necessary ventilation. Used are the monthly mean outdoor temperature and relative humidity values of Appendix A.

The results are shown in Figure 6.13. If the reference house with a vapour generation rate of 8 kg/day is placed on the Scilly Isles (CB), the accumulated air mass flow on yearly basis reaches $1.8 \cdot 10^6$ kg air; Napoli (I) holds the second place with $1.6 \cdot 10^6$ kg air and Brussels (B) ranges on the third place with approx. $0.95 \cdot 10^6$ kg air. All other areas don't differ that much. Energy demand is due to the warmer climate lowest in Napoli (I): 750 kWh, and Torino (I): 1200 kWh. The third lowest energy consumption can be found on the Scilly Isles: 1400 kWh, where ventilation rates are highest. Energy demand of the other locations vary between 1300 and 1700 kWh.

6.6.3 Summary of Findings - Comparison to common Ventilation Strategies

Assuming that it is possible to control the indoor air humidity in a way that the ' a_w '-value, is not exceeded, the results can be summarized as follows:

1. At a constant room temperature the necessary supply air with respect to the relative humidity control can be substantially higher (factor 3 in Figure 6.11) in summer than in winter. The energy consumption during the cold months (Dec./Jan) can be twice that of the warmer months May and Sept.
2. A decrease of the room temperature increases the necessary supply air and can even lead to more energy consumption.

As previously said, it only makes sense to compare those ventilation strategies, which make sure that the ' a_w '-value is not exceeded.

Coming back to the energy consumption of Figure 6.12, these values are really the minimum amounts needed, if indoor humidity is the dominant control parameter and when the system always operates, coupled to the ' a_w '-value needed. Therefore, such a system would from a relative humidity -control point of view be the optimum one.

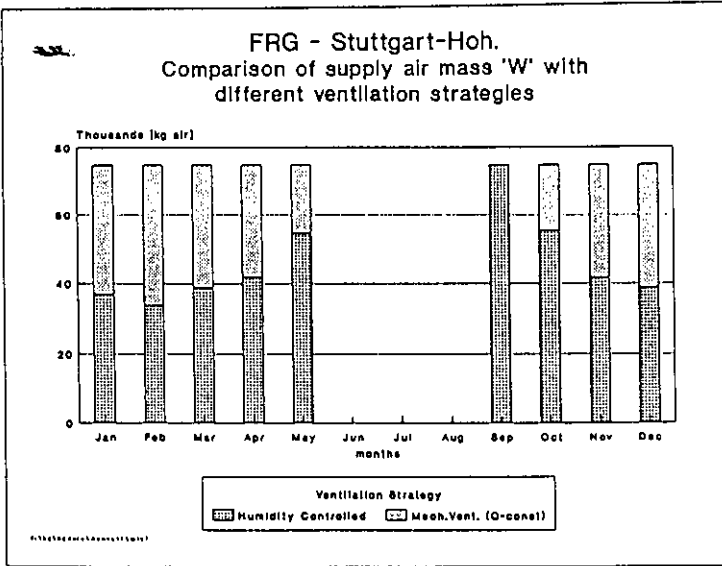


Figure 6.14

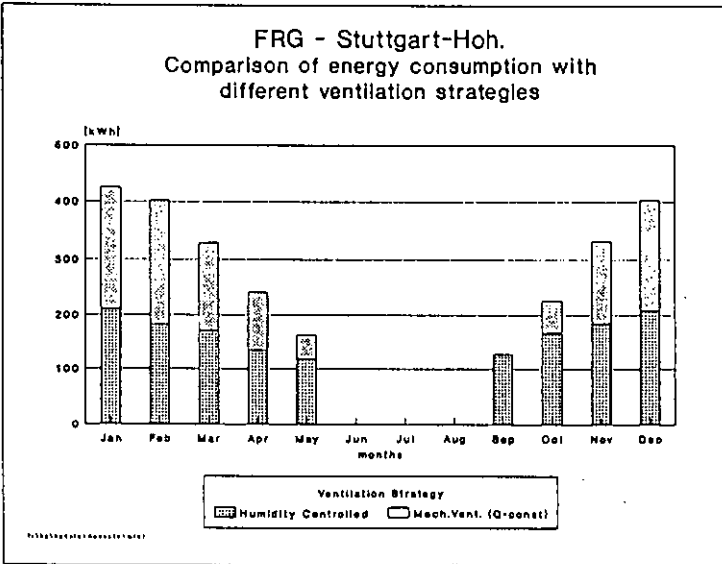


Figure 6.15

In the following we discuss the potential energy savings with more advanced ventilation strategies, compared to the traditional ones.

Natural ventilation

Due to the driving forces, which are higher in winter than in summer, the demand with a natural ventilation system is adverse to the potential. However, the occupant is able to react on too high relative humidities by using the devices. Practice shows that this is not always done.

To calculate energy savings, comparing natural ventilation systems with humidity controlled ones in a global way is not possible because the physics of natural ventilation are too complex to generalise specific results. Comparisons can only be made case per case. Nevertheless, it can qualitatively be summarized, that a natural ventilation system, which works on the 'a_w'-value during the warm months, must supply without users interference too much during cold months. This results in a waste of energy.

Mechanical Ventilation

Most systems operate with a constant volume flow rate. Sometimes there is a time control which allows a higher ventilation in the bedrooms during night times. A mechanical ventilation system, which operates on a constant flow rate throughout the heating season at such a high rate to meet the requirements during the critical month of September, will supply too much air during all other months. Figure 6.14 shows the excess air mass (light dotted area) in a specific case. The excess energy, to heat this extra air mass is shown in Figure 6.15 (light dotted area). On yearly basis, humidity controlled system needs 1500 kWh, the constant flow ventilation system 2650 kWh, 76% more.

Also other ventilation strategies are possible. E.g. the flow rate is manually adjusted 2 or 3 times a year depending on the season. This will increase the cost efficiency. However, all calculations assume that the indoor relative humidity is the dominant control parameter throughout the year for the whole building. In reality, the influence and the dominance of other parameters (odours, CO₂ etc.) may in well insulated buildings supersede, especially during the winter. Unfortunately the impact of such parameters as a function of season and room-use are not really known yet.

6.7. Measurement Techniques

To cure moisture problems, the cause has to be detected. This being not always clear on a first glance, a thoroughly study and measurements may be necessary. In the following, various methods and instrumentation to measure temperatures, humidities and air change rates are explained. They vary in expenditure and preciseness. There are scientific techniques and those suited for in-situ measurements. One has to choose which method is adequate for a given case. The different techniques are not explained in detail: they are sketched briefly and their applicability in mould and moisture damage evaluation outlined.

6.7.1 Temperature

6.7.1.1 Basics

Important temperatures are: the room temperatures, (the outdoor temperature) and the inside surface temperatures. We deal with mean conditions. Fast changes in temperature are not of major interest.

Important are temperature plots over a day, a week or longer. However, before temperature measurements are performed, one should define which temperature one is interested in:

- air, or more generally, medium temperature;
- black globe temperature;
- dry resulting temperature;
- ping-pong ball temperature.

Chapter 3 'Thermal Modelling', explains that the precise definition of the reference temperature is essential for surface heat transfer calculations.

Medium temperature:

The medium temperature is defined by the location (x,y,z-coordinates in the medium) and the medium itself (air, solid material, surface). E.g. measuring the air temperature means, protecting the measuring device with a radiation shield.

Black globe temperature (BGT):

The black globe temperature is defined by the location (room coordinates) in the medium and the medium itself. To measure BGTs e.g. in air, the resultant temperature depends on the local air temperature and on the temperature of the surrounding surfaces. In practice, the BGT can be measured, when the measuring device is placed in the centre of a black sphere of 8 cm diameter. The black sphere is in radiative heat exchange with the surrounding walls and the measuring device. The globe should not be mounted close to a window to avoid direct solar radiation on it.

Dry resulting temperature (DRS):

The dry resulting temperature can not be measured. It is a defined temperature, with as weighting factors for the air and radiation temperature (index r) 0.5:

$$\theta_{rs} = 0,5. \theta_a + 0,5. \theta_R$$

Ping-pong ball temperature (PPBT):

The PPBT is measured by putting the measuring device into a white ping-pong ball. PPBT combines the air temperature with the radiation temperature of the surrounding surfaces. The PPBT and the BGT differ due to the different absorption and emission coefficients. PPBT is less sensitive to direct solar radiation. The device is also less expensive than a black globe.

Black globe and ping-pong ball, including the measuring device have some inertia. A rhythm in data acquisition of 1 log per 3 to 5 minutes is acceptable.

6.7.1.2 Measurement Techniques.

Commonly used for temperature measurements are mechanical contact thermometers:

- Liquid Filled Thermometers (LFT);
- Metal Expansion Thermometers (MET);
- Thermocouples;
- Resistance Thermometers (RT).

Liquid Filled Thermometers (LFT)

Most often used are mercury thermometers. If not calibrated, the uncertainty range can be considerable. LFTs only give instantaneous information (with a few exceptions they generally do not allow to record temperatures). Therefore they are not well suited for moisture damage research.

Metal Expansion Thermometers (MET)

The working principle of these thermometers is measuring the change of length due to a change in temperature: the length change or the angle change of a spirale than is a measure for the temperature. The most used and preferred group of METs are bimetal spirals.

For recording outdoor and indoor air temperatures, they are very well suited. Thermographs often use this principle. They are available for time intervals of 1,7, or 30 days. Measuring tolerances are 1,5 %.

Thermocouples

Working principle is the thermoelectric effect: if two wires of different metals are connected at both ends, a current flows, when the two ends are on a different temperature. From this, only temperature differences can be measured with thermocouples. To get an absolute temperature signal in °C, one has to keep one end at a fixed temperature, normally 0°C. This can be done using a DEWAR-bottle filled with melting ice or a PELTIER-thermostat. As temperatures are usually recorded during several days, the ice in the DEWAR-bottle has to be checked and stirred every hour whereas a Peltier-thermostat is easier to handle and works automatically. Very useful are electronic monitors or recorders, with the reference temperature device incorporated. Permissible tolerances for NiCr-Ni, Fe-Konst, Cu-Konst, Pt 30 Rh-Pt 6, Rh Pt 10 Rh-Pt, Pt 13 Rh-Pt thermocouples are ± 3 K according to DIN 43710. To have more confidence in the measured data, it is recommended to calibrate the thermocouples. This achieves tolerances of ± 0.5 K. The output voltage is a non-linear function of the temperature. So, the temperature must be calculated using a mathematical calibration curve, or can be taken from a graph.

Thermocouples exist in very small dimensions, i.e. that room air temperatures as well as surface temperatures can be measured. There are covered thermocouple types, which only should be used for air temperatures. They are not suited for surface temperatures because the contact to the surface is too

bad. This often results in substantial errors. Better for surface measurements are folio-thermocouples. The folio is 0.05 - 1 mm thick. One side is coated with adhesives, so it is easy to attach the folio also to rough surfaces. To measure the surface temperature without radiation influence the folio should be attached to the surface and then covered with a larger folio with the same absorption as the surface.

Thermocouples are suited for datalogging or for recording the signal on a plotter over the measuring period. Thermocouples are very robust, reliable and not expensive.

Resistance Thermometers (RT)

Here, the principle of the electrical resistance of a material, changing with temperature, is used. In contrast to thermocouples, an auxiliary power supply is needed. But whereas only temperature differences can be measured with thermoelements, resistance thermometers give absolute temperatures.

RT work very precisely in the temperature range important in buildings.

Most common are Platin RT. They are usually specified by the resistance at 0°C. For example Pt 100 is a RT out of Platin (Pt) with a resistance of 100 Ω at 0°C.

There are also semi-conductor resistance elements available. The advantage to Platin RT is that the resistance change due to a temperature variation is higher. Therefore, the influence of connecting wires can usually be neglected. They are cheap and have an accuracy of 0.1 - 1 % of the measuring interval. RT exist in very small design so that they are suited for both air and surface temperature measurements. The length of the connecting wires can have a substantial influence on the accuracy of Platin RT, due to their own resistance. To avoid these problems, a four wire technic has been introduced.

An expensive accurate device is needed to measure the change in resistance of Platin RT. The electric resistance is a non-linear function of temperature to be described with a quadratic or cubic power series. The permissible tolerances are much smaller compared to thermocouples and are in the considered temperature range here max. 0,5 K according to DIN 43760.

Concerning radiation protection for air temperature measurements the same rules apply to RT as to thermocouples.

6.7.2 Humidity

6.7.2.1 Basics

Humidity measurements are essential in moisture research. Procedures exist for point and continuous measurements. Continuous measurements are much more interesting. In spite of this also the point measurement procedures are briefly outlined, as they are often used to calibrate the continuously operating devices.

Together with the relative humidity, it is essential to measure the air temperature at the same time and location. Further information on atmospheric relative humidity measurement methods is given in ref. [17].

6.7.2.2 Measurement Techniques

Dew Point Indicator

A copperplate, covered with a gold layer, is cooled through a Peltier element. The room air passes over this plate. When the plate temperature is below the dew point, water vapour condenses at the surface and a concentrated light beam scatters on the gold mirror it is directed to. The change from a specular to a diffuse reflection is detected with a photoresistant. This controls the Peltier cooler in such a way that the golden surface is kept on the dewpoint temperature. This temperature is precisely recorded with a Pt 100. With the air temperature known, the relative humidity can be calculated. The accuracy of the Pt 100 is $0,1^{\circ}\text{C}$.

The dewpoint indicator is a precise but also expensive way to measure relative humidities. This accuracy is not necessarily needed for the purpose here. Dewpoint Indicators are usually point-wise operated but also continuously logging devices are available. They are suited for calibration purposes.

Psychrometer

Psychrometers consist of a dry and a wad wetted thermometer. Over both the air is sucked by a small fan. The difference between both temperatures - the so-called 'psychrometric difference' - determines the relative humidity.

Most common is the ASSMANN-Psychrometer. Psychrometers can be continuously operated but one has always to make sure that the wad is wet. This makes the psychrometer not so suited for measuring periods longer than $\frac{1}{2}$ day.

Hair and polyethylen-stripe hygrometers

These hygrometers contain a hair with a changing length for about 2 % for a humidity change from 0 to 100 % RH. Also other hygroscopic materials like silk, cotton and synthetic materials are in use. A disadvantage of the device is the necessity of regular recalibration. The hysteresis is between 2-5 %.

The length change of the sensor stripe often works on a potentiometer to give the required analogous electric output signal. Low cost hair hygrometers often have unaccuracies of more than 10% RH. Therefore, it is recommended never to use this hygrometer type without former calibration. Hygrographs very often use the hair or polyethylen-stripe technique. The use of hair hygrographs is one of the simplest ways for in-situ measurements. The response time is fast enough to detect also short humidity peaks in bathrooms. Coupled with a thermograph, they represent a valuable and compact tool.

Capacitive Hygrometers

These use a humidity sensitive folio which is placed between 2 electrodes. A change in relative humidity causes a capacity change. Additional electronics (beside the sensor) is needed to get an analogous output signal in Ohm, Ampere or Volt. Linearization and temperature compensation is often necessary. Capacitive humidity sensors are, depending on accuracy and response time, fairly cheap. Unfortunately they are sensitive to contaminated air (dust, organics).

Conductance-film Hygrometer

An electrode is placed on a plastic ground plate and covered with a hygroscopic layer, where the conductivity changes with humidity. The result is a change of the electric current. This sensor type should have high accuracy and short response times, no recalibration or maintenance.

Lithiumchloride Sensors

Uses the thermodynamic equilibrium between humid air and a salt solution. The lithium chloride solution absorbs water vapour from the air till the total pressure of the solution is the same as the partial pressure of water vapour in the air. Accuracy is between 1-3%. The measuring element consists of a thermocouple enclosed in a glass-fibre sleeve soaked in LiCl solution. The sleeve contains a bifilar thread connected to a power source. Assuming that the LiCl solution is unsaturated, the electrical current gradually heats it so that the equilibrium vapour pressure rises. If it rises above that of the predominant vapour pressure in the air, water will evaporate from the solution, so that it first becomes saturated and then crystallizes, reducing the amount of liquid solution. This leads to a rise in resistance and a fall in current, bringing the rise in temperature to a halt. When equilibrium is reached the temperature of the solution and therefore of the sensor provides a direct measurement of the predominant vapour pressure.

6.7.2.3 Constructive hints

It is essential to measure the air temperature and RH, as the relative humidity alone gives not a complete information. Before a measurement is started, one should check the sensor's performance, when the humidity is 100 %. There are sensors which need days to recover after condensation has occurred on their surface. It's advisable to check and/or calibrate humidity sensors during a measuring campaign at least weekly.

6.7.3 Air Change Rates

6.7.3.1 Basics

The knowledge of the Air Change Rate (ACR) or hourly air change rate (HACR) is very valuable in moisture research. But one has to be very careful in using the concept of air change rates and be aware of the 'assumptions'. The ACR n is defined as:

$$n = G_a / V$$

with G_a : the volume flow rate
 V : room volume

In this definition the volume flow rate can be defined as the sum of air entering the considered zone or the sum of air leaving the room. They don't have to be the same. Depending on the temperature difference between indoors and outdoors the differences go up to 10 %. If a mechanical ventilation system is considered, the supply can differ from the exhaust due to infiltration.

The question how to determine the room volume V is not that trivial. Is it really 'length x width x height' or is it only a part of this. When measuring ACRs one has to define carefully the effective volume, this is the volume, where the air really passes through. Techniques to determine the effective volume are discussed elsewhere [18].

The volume flow rates are used to establish moisture balances for a zone under the assumption that there is no moisture gradient in the zone, i.e. complete mixing of air and moisture. This assumption is often true, especially in dwellings with natural ventilation, where purpose provided devices and cracks are equally distributed around the zone and radiators, warmer and colder surfaces support intensive convection. But in mechanically ventilated spaces one has to check the assumption of complete mixing. Therefore the expression 'air change rate' is meaningless and in newer literature substituted by the expression 'nominal air change rate'.

In most moisture problem cases, we have rooms with natural ventilation. Infiltration is caused by temperature differences between inside and outside (stack effect) and by wind pressure. In a naturally ventilated zone the HACR can vary daily with a factor of up to three [13]. If occupants open windows, the HACR can increase considerably according to [14]. In this paper some values of the thumb are published; with an opened hopper window HACR are 0.8 to 4.0 h^{-1} , with half-opened vertically-pivoted windows HACR increase to 5 to 10 h^{-1} and with a complete opened window HACRs are 9 to 15 h^{-1} . If there is additionally cross ventilation HACRs can be up to 40 h^{-1} .

From this, one can conclude that punctual HACRs values are of minor value. As mould growth is a very slow process, a time plot of the ACR is needed to derive an average ACR and the standard deviation.

6.7.3.2 Measurement Techniques

Decay Method

To measure the ACR in most cases a tracer gas is used. This is a special but non-toxic gas (common are SF_6 , N_2O or CO_2) which is released into the zone. The tracer gas is homogeneously distributed by mechanical fans till a state of complete mixing is achieved, i.e. the concentration gradients should be less than 5 %.. Then the fans are turned off, the time set to zero and the decay of concentration, which occurs due to infiltration and air entering from other zones, recorded. To have reliable results one has to watch that also during the decay period, the assumption of complete mixing is fulfilled.

For example, a house with a central heating system can be treated as one completely mixed zone [13]. For rooms with natural ventilation and heights not higher than 2,5 m complete mixing is a good assumption. Bigger heights can result in temperature stratification and a stratification of the tracer gas [15]. If between the rooms on one floor the doors are open, they can be treated as well mixed [19]. If they are closed, each room has to be treated as a single zone [20].

Under the assumption of a permanent and complete mixing, the HACR can simply be derived by a mass balance of the tracer gas in the zone. In a plot, it is given by the slope of the logarithm of tracer-gas concentration versus time (linear).

If one measures the ACR in that way, the result is only of limited value. One can not say where the air which diluted the tracer gas in the zone came from : from outdoors or from one or even more adjacent rooms. The uncertainty can be substantial if a decay experiment is used to establish a vapour balance of a zone.

Constant Emission Technique

The technique that is probably most suitable for moisture damage investigations is the constant emission technique. It was developed in Brookhaven National Laboratory [21,22]. A small capsule (32 mm length and 7 mm diameter), called a passive constant injection source constantly emits a very small amount of a perfluorocarbon tracer (PFT) into the zone. Concentrations in the zone are of the order of 10^{-9} ppm. At a distance of 2-3 m of the PFT

another capsule called the passive diffusion tube sampler is placed which adsorbs the emitted gasses. After a period of some days, a week, one or 3 months the sampler is taken away and analyzed in the laboratory. There the sampler is heated which causes a release of the PFT. The amount adsorbed is measured with a gas chromatograph. This technique allows the measurement of an average ventilation rate over more or less long periods with an accuracy of $\pm 0.2 \text{ h}^{-1}$. Uncertainties occur, when the air change rates are very high (open windows).

The assumption behind this technique is complete mixing in the zone. To fulfil this requirement in larger zones, 2 emitters are used. The result with PFT-techniques is about the same as with the decay method, the only difference being that the decay method gives an average ACR over the measuring period (1-2 h), whereas PFTs give an average value over weeks or months. It can not be said from where (outside or other adjacent rooms) the air came to dilute the tracer. To get into more complex measurements with more detailed results one can use 3 to 4 different PFTs in different zones. There is only one passive sampler placed in each zone which now adsorbs the different tracers. After sampler analysis one knows the interzonal volume flow rates. The 4 available PFTs have different source strengths, which should be considered for the placement of the PFTs.

The disadvantage of this technique at this time is the long time it takes to get the samplers analyzed in the lab (1-2 months).

Two Zone Technique with One Tracer

This technique has been intensively applied to measure the transport of Radon from the soil into the crawl space or into the living area of houses [13,23]. The tracer gas is released in zone 1 and completely mixed by fans. Then concentrations in zone 1 and zone 2 are measured and plotted versus time. One gets a usual decay for zone 1; for zone 2 the concentration will increase and then decay. From these plots one can calculate the volume flow rates from zone 1 to zone 2 and reverse as well as infiltration rates for both zones. This technique is straightforward and could be used to measure for example the volume flow rate from a warm humid bathroom into a cooler room.

Constant Concentration Method

The simple decay method and the constant injection technique suffered from the fact that there is no information about from where the air entered the zone. Especially for air quality considerations a technique was developed to test, if all zones in a building are adequately ventilated, i.e. to measure the infiltration rate in every zone. The tracer-gas technique is called the constant concentration method [13]. There is one gas analyzer and a multiplexer, from which a tube for sampling and a tube for emitting tracer goes into every zone. In defined time intervals the multiplexer takes a sample from each zone, analyzes it and calculates the amount of tracer to supply into the zone in that way, that the tracer-gas concentration remains constant and equal in all zones at all times. As all zones have the same concentration, interzonal airflows will not change the concentration. Only air flows which enter the room from outside may cause changes. The measurement is sophisticated, taking a lot of time to set up and demands experienced assistance. The constant concentration method can be applied continuously, i.e. so that infiltration histories can be obtained. Therefore, it is very suited to study the variation of infiltration rates due to changing outside climate conditions and occupant behaviour.

6.8. References

1. Schlapmann, D.: Konvektiver Wärmeübergang an beheizten Fußböden, HLH 34, 1983, Nr. 3 März (in german)
2. Dubrul, D.: Inhabitant Behaviour with Respect to Ventilation - a Summary Report of IEA Annex VIII, TN AIVC 23, March 88
3. Bundesministerium für Raumordnung, Bauwesen und Städtebau (Eds.): Merkblatt "Richtig Heizen und Lüften - Schutz vor Gesundheits- und Bauschäden". Sanitär- und Heizungstechnik 22 (1983), v. 1, p. 18
4. Building Research Establishment (Eds.): Surface condensation and mould growth in traditionally-built dwellings. Building Research Establishment Digest 297, Garston, Watford (Max 1985) England
5. BS 5250: Code of basic data for the design of buildings: The control of condensation in dwellings. Edition 1975 (British standard)
6. Dütz, A.; Le Marié, A.: Energieeinsparung und Bauschäden. DBZ 119 (1985), nr. 10, p. 1317-1323
7. Erhorn, H.; Gertis, K.: Mindestwärmeschutz oder/und Mindestluftwechsel? GI 107 (1986)
8. Lübke, P.: Mindestluft gegen Feuchte - Beitrag zur praktischen Bestimmung des bauphysikalischen Mindestluftstromes zur Vermeidung von Tauwasserbildung in Außenecken. HLH 36 (1985), nr. 6, p. 292-296
9. Meyringer, V.: Lüftungserfordernisse zur Vermeidung von Feuchteschäden in Wohnungen: unpublished manuscript
10. Panzhauser, E. et al: Die Luftwechselzahlen in österreichischen Wohnungen. Research report F 287 of the Austrian Federal Ministry for Building and Technology, Vienna (1984)
11. Pfeiler, W.: Die Beseitigung von Kondenswasser und Schimmelpilzbildung in Wohnungen. Research report of the Austrian Federation of Public Building Associations
12. Stehno, V.: Einfluß von Wärmeschutz, Wärmespeicherung und Wohnungslüftung auf die Feuchtigkeitsbeanspruchung von Wänden und Decken. Der Ausbau 9 (1981) nr. 9, p. 3509-361
13. Harrje, D.T.; Dutt, G.S.; Bohac, D.L.; Gadsby, K.L.: Documenting Air Movements and Infiltration in Multicell Buildings Using Various Tracer-Gas Techniques. Preprint, ASHRAE Transaction 1985, Vol. 91, Pt 2, HI-85-40 No. 3
14. Gertis, K.; Hauser, G.: Energieeinsparung durch Stoßlüftung, HLH 30, 1979 Nr. 3

15. Maldonado, E.A.B.; Woods, J.E.: Ventilation Efficiency as a Means of Characterizing Air Distribution in a Building for Indoor Air Quality Evaluation, ASHRAE Transactions, 1983, Vol. 89 pt. 2 A + B
16. Standaert, P.: Surface Heat Transfer in Rooms, 5. May 1989, IEA-Annex 14 report
17. Dulk den, F.W.: Study of Methods for Measuring Atmospheric Humidity, NOVEM Nederlandse Maatschappij Voor Energie en Milieu b.v., Utrecht (NL), Report No.: M.87.235.1, Oct. 1988
18. O'Neill, P.J.; Crawford, R.R.: Multizone Flow Analysis and Zone Selection Using a New Pulsed Tracer Gas Technique, 10th AIVC Conference, Dipoli, Finland, Sept. 1989
19. Hitchin, E.R.; Wilson, C.B.: A Review of Experimental Techniques for the Investigation of Natural Ventilation in Buildings, Building Science 1967, Vol. 2., p. 59-82
20. Laschober, R.R.; Healy, J.H.: Air leakage in split-level residences ASHRAE trans, vol. 70, p. 364 - 374
21. Dietz, R.N.; Cote, E.A.: Air Infiltration Measurements in a Home Using a Convenient Perfluorocarbon Tracer Technique, Environment International Vol. 8, p. 419 - 433
22. Dietz, R.N.; Goodrich, R.W. et al: Detailed Description and Performance of a Passive Perfluorocarbon Tracer System for Building Ventilation and Air-Exchange Measurements, ASTM-Symposium on Measured Air Leakage Performance of Buildings, Philadelphia, PA, 2. - 3. April 1984
23. Hernandez, Tel.; Ring, J.W.: Indoor Radon Source Fluxes, Experimental Test of a Two-Chamber Model, Environment International, Special Issue on Indoor Air Pollution, 1982, Vol. 2, pp 45 - 57
24. N.N.: DIN 4710, Meteorologische Daten, Bent Verlag GmbH, Berlin, Nov. 1982
25. Achenbach, P.R.: Moisture management in buildings, Symposium on air infiltration, ventilation and moisture transfer Fort Worth, Texas, USA; Building Thermal Envelope Coordinating Council, 1988, p 73-81 AIVC # 2003]
26. Liddament, M.W.: Air Infiltration Calculation Techniques, Air Infiltration and Ventilation Centre, Bracknell GB, June '86
27. Timusk, J.; Seskus, A.L.; Ary, N.: The Control of Wind Cooling of Wood Frame Building Enclosures, 6th Annual International Energy Efficient Building Conference Portland, Maine, USA, April 27-29, 1988
28. Powell, F.; Krarti, M; Tuluca, A.: Air Movement Influence on the Effective Thermal Resistance of Porous Insulations. A Literature Survey, Journal of Thermal Insulation, V12, Jan 1989, p 239-251

29. Ojanen, T.; Kohonen, R.: Hygrothermal Influence of Air Convection in Wall Structures, Conf. on 'Thermal Performance of the Exterior Envelopes of Buildings IV, Orlando, Florida, Dec. 4-7, 1989
30. Elkhuizen, P.A.; Oldengarm, J.; de Gids, W.F.; van Schijndel, L.L.M.: Measurement of airborne moisture transport in a single family dwelling at Leischendam the Netherlands, Novem P.O. Box 8242, NL-3502 RE Utrecht
31. Werner, A. et al: Fortschrittliche Systeme für Wohnungslüftung, Fraunhofer Institut für Bauphysik, Holzkirchen, Germany, IBP-report EB-21/1989, part B (in german)
32. Hens, H.: Practice report, IEA-Annex 14, draft of Oct.'89
33. Lillich, K.-H.: Auslegung der elektrischen Fußboden-Speicherheizung, HLH 22. Okt. 1971, Nr.10 (in german)
34. IC-IB, Recherches sur les performances dans le batiment, Confort Thermique, Recherche subventionnée par l'IRSIA, convention 2377, rapport final, juin 1977, 185pp (in french)
35. Moor, H.: Physikalische Grundlagen der Gebäudedynamik im Hinblick auf die Berechnung des Luftaustausches, Eidg. Materialprüfungs- und Versuchsanstalt (EMPA), Abtl. Bauphysik, Jan. 1987, Dübendorf, Switzerland (in german)
36. Weersink, A.: Results of investigations on the distribution of moisture in a climate room, Techn. Uni. of Eindhoven, 1988

APPENDIX A: METEOROLOGICAL DATA BASE

Data of Belgium 1/1

BRUSSELS (Ukkel)

Month	θ [°C]	x [g/kg]	v [m/s]	ϕ [%]	P [Pa]
January	2.6	4.0	4.3	86	633
February	3.5	4.1	4.1	84	659
March	5.5	4.5	4.0	79	713
April	9.0	5.5	3.8	77	884
May	12.7	7.0	3.6	76	1116
June	15.5	8.5	3.4	77	1356
July	17.1	9.7	3.4	79	1540
August	16.8	9.5	3.4	79	1511
September	14.6	8.6	3.4	82	1362
October	10.5	6.9	3.6	86	1091
November	6.1	5.1	3.9	87	819
December	3.3	4.2	4.2	86	665
Year	9.8	6.5	3.8	82	1029

Data of Germany 1/2

Month	Berlin Tempelhof			Braunschweig			Bremenhasen			Zweuen			Frankfurt/Main			Gießen		
	$\bar{\rho}_a$ [°C]	\bar{x}_a [g/kg]	\bar{v}_w [m/s]	$\bar{\rho}_a$ [°C]	\bar{x}_a [g/kg]	\bar{v}_w [m/s]	$\bar{\rho}_a$ [°C]	\bar{x}_a [g/kg]	\bar{v}_w [m/s]	$\bar{\rho}_a$ [°C]	\bar{x}_a [g/kg]	\bar{v}_w [m/s]	$\bar{\rho}_a$ [°C]	\bar{x}_a [g/kg]	\bar{v}_w [m/s]	$\bar{\rho}_a$ [°C]	\bar{x}_a [g/kg]	\bar{v}_w [m/s]
Jan.	-0.7	3.2	3.8	-0.2	3.3	3.4	0.9	3.6	4.6	1.6	3.7	4.6	1.1	3.4	2.6	0.2	3.3	2.1
Febr.	-0.3	3.2	4.1	0.0	3.4	3.9	0.9	3.8	6.2	2.2	3.7	4.4	2.0	3.6	3.2	1.0	3.4	2.7
March	3.3	3.6	4.4	3.3	3.8	4.2	3.4	4.0	5.2	6.1	4.2	4.0	5.7	4.1	3.2	4.4	3.9	2.8
April	8.6	4.6	4.0	6.0	4.9	4.0	7.4	5.0	5.8	8.8	5.0	4.2	10.1	5.1	3.9	8.8	4.8	3.0
May	13.3	6.0	3.9	12.2	6.3	3.6	11.7	6.4	4.9	12.6	6.4	3.5	14.1	6.5	3.3	12.7	6.2	2.4
June	17.5	7.7	3.8	15.9	8.0	3.2	15.3	8.1	4.8	16.7	8.0	3.4	17.5	8.3	3.0	16.3	7.8	2.3
July	18.5	8.6	3.6	17.0	9.0	3.4	16.5	9.2	5.3	17.0	9.0	3.4	18.9	9.1	3.2	17.6	8.7	2.3
August	17.9	8.5	3.4	16.7	8.9	3.0	16.5	9.2	4.4	16.7	9.0	3.3	18.1	9.0	2.9	16.9	8.6	2.1
Sept.	14.7	7.5	3.0	14.0	7.8	3.2	14.3	8.1	4.6	14.6	8.0	3.5	15.1	8.0	3.0	14.0	7.6	2.0
Oct.	10.1	6.1	3.4	9.8	6.3	3.4	10.2	6.7	4.7	10.7	6.6	3.7	10.3	6.3	3.6	9.4	6.1	2.2
Nov.	4.6	4.5	5.0	4.6	4.6	4.7	5.4	4.9	6.7	5.8	4.9	6.0	5.4	4.0	3.6	4.5	4.5	3.1
Dec.	0.9	3.6	4.0	1.3	3.7	4.3	2.2	4.0	5.9	2.8	4.1	4.7	2.2	3.8	4.0	1.4	3.6	2.6
Year	9.1	5.6	3.9	8.6	5.9	3.7	8.8	6.1	5.2	9.5	6.1	4.0	10.1	6.0	3.2	9.0	5.7	2.5

: Monthly mean values of outdoor temperature, absolute humidity and wind velocity for different locations in West Germany

Data of Germany 2/2

Month	Hamburg-Fahh.			Mannheim			München-Riem			Nürnberg-Flugh.			Regensburg			Stuttgart-Rob.		
	$\bar{\vartheta}_a$ [°C]	\bar{x}_a [g/kg]	\bar{v}_w [m/s]															
Jan.	0.5	3.4	4.4	1.2	3.5	1.8	-1.8	3.0	2.0	-1.0	3.1	2.3	-2.1	2.9	1.7	-0.3	3.2	1.8
Febr.	0.4	3.3	4.7	2.1	3.0	2.5	-0.4	3.2	3.0	0.2	3.3	2.8	-0.8	3.1	2.4	0.8	3.4	2.8
March	3.2	3.7	4.9	5.8	4.1	2.4	3.4	3.0	3.3	3.0	3.8	2.8	3.2	3.8	2.3	4.3	3.9	2.6
April	7.3	4.7	4.5	10.2	5.1	2.8	6.1	5.0	3.7	8.4	5.0	3.2	8.4	5.0	2.6	8.5	4.9	3.2
May	11.6	6.1	4.2	14.3	6.6	2.4	11.9	6.6	3.1	12.6	6.4	2.7	12.4	6.5	1.9	12.2	6.4	2.5
June	16.3	7.8	3.8	17.6	8.4	2.4	16.6	8.5	3.0	16.4	8.1	2.6	16.2	8.4	1.7	15.6	8.3	2.4
July	16.4	8.8	4.0	19.2	9.2	2.3	17.5	9.2	2.8	17.8	8.8	2.4	17.7	9.1	1.6	17.3	8.9	2.2
August	16.1	8.8	3.4	18.3	9.2	2.1	16.7	9.0	2.6	16.7	8.8	2.3	16.8	9.0	1.5	16.6	8.8	2.1
SepL	13.8	7.8	3.7	16.3	8.2	2.3	13.9	7.9	2.4	13.8	7.7	2.0	13.7	7.7	1.4	13.9	7.9	1.8
Oct.	9.6	6.3	3.8	10.3	6.4	2.2	8.8	6.0	3.2	9.1	6.1	2.4	8.4	5.9	1.5	9.2	6.2	2.3
Nov.	4.9	4.7	5.6	5.4	4.7	2.9	3.6	4.3	3.8	4.1	4.5	3.1	3.3	4.3	2.3	4.1	4.5	2.8
Dec.	1.8	3.8	5.0	2.2	3.8	2.4	-0.2	3.4	3.3	0.0	3.4	2.8	-0.5	3.3	2.1	0.7	3.6	2.4
Year	8.4	5.8	4.3	10.2	6.1	2.4	6.1	5.8	3.1	8.5	5.8	2.6	8.1	5.8	1.9	8.6	5.8	2.4

· Monthly mean values of outdoor temperature, absolute humidity and wind velocity for different locations in West Germany

Data of Italy 1/3



Data of Italy 2/3

Mean value of:

T = air temperature [°C]
 x = absolute humidity [g/kg]
 v = wind speed [m/s]

Torino Caselle 45°11' N 7°39' E 282 m Genova 44°25' N 8°51' E 3 m Milano Linate 45°26' N 9°46' E 103 m

Torino Caselle			Genova			Milano Linate					
T	x	v	T	x	v	T	x	v			
[°C]	[g/kg]	[m/s]	[°C]	[g/kg]	[m/s]	[°C]	[g/kg]	[m/s]			
JAN	0.1	3.2	0.5	JAN	7.6	6.3	5.5	JAN	-0.8	3.5	1.0
FEB	1.6	3.5	0.8	FEB	9.2	5.4	4.8	FEB	2.8	3.9	1.3
MAR	7.2	3.4	1.1	MAR	11.6	5.4	3.7	MAR	8.8	5.7	1.5
APR	11.0	4.6	1.3	APR	14.0	6.3	3.4	APR	12.8	7.1	1.6
MAY	15.5	7.2	1.1	MAY	17.6	8.9	2.9	MAY	16.8	8.2	1.5
JUN	19.2	10.1	1.0	JUN	20.8	10.0	2.5	JUN	20.0	11.3	1.5
JUL	22.0	11.3	1.4	JUL	23.6	13.2	2.6	JUL	22.8	10.7	1.3
AUG	20.4	11.9	0.8	AUG	23.5	12.6	2.7	AUG	22.0	12.5	1.0
SEP	17.2	8.8	0.6	SEP	21.6	12.5	3.3	SEP	18.8	11.9	0.8
OCT	11.6	6.9	0.5	OCT	17.2	8.4	4.3	OCT	12.8	8.6	0.7
NOV	5.6	5.0	0.5	NOV	11.6	5.5	4.8	NOV	7.2	5.8	0.9
DEC	1.6	3.6	0.5	DEC	7.6	5.1	5.4	DEC	2.0	4.0	0.8

Bolzano 46°28' N 11°19' E 241 m Verona Villafranca 45°24' N 10°53' E 68 m Trieste 45°39' N 13°45' E 20 m

Bolzano			Verona Villafranca			Trieste					
T	x	v	T	x	v	T	x	v			
[°C]	[g/kg]	[m/s]	[°C]	[g/kg]	[m/s]	[°C]	[g/kg]	[m/s]			
JAN	-0.8	2.1	0.4	JAN	1.2	3.5	0.7	JAN	4.4	3.5	3.1
FEB	2.0	2.7	0.7	FEB	2.8	3.2	1.1	FEB	5.2	4.1	2.8
MAR	7.6	3.9	1.3	MAR	7.2	4.9	1.4	MAR	9.2	5.1	2.9
APR	12.0	5.2	1.5	APR	12.0	5.7	1.5	APR	14.0	5.8	2.5
MAY	16.0	7.4	1.4	MAY	16.8	8.1	1.1	MAY	18.8	8.1	2.2
JUN	19.2	9.8	1.2	JUN	20.4	10.8	1.1	JUN	21.6	10.8	1.9
JUL	20.8	10.3	1.2	JUL	23.2	12.6	0.9	JUL	24.0	10.9	2.2
AUG	19.6	10.4	0.9	AUG	22.0	11.6	0.8	AUG	23.2	10.4	2.2
SEP	17.2	8.3	0.7	SEP	18.4	9.8	0.7	SEP	20.4	11.0	2.3
OCT	10.0	6.1	0.4	OCT	13.2	7.0	0.7	OCT	15.2	8.7	2.9
NOV	4.4	4.2	0.3	NOV	8.4	5.8	0.8	NOV	11.6	7.0	2.9
DEC	0.0	2.4	0.3	DEC	2.4	4.1	0.7	DEC	6.4	4.1	2.9

Udine Campoformido 46°02' N 13°11' E 92 m Bologna Borgo Panigale 44°31' N 11°18' E 49 m Pisa San Giusto 43°41' N 10°24' E 11 m

Udine Campoformido			Bologna Borgo Panigale			Pisa San Giusto					
T	x	v	T	x	v	T	x	v			
[°C]	[g/kg]	[m/s]	[°C]	[g/kg]	[m/s]	[°C]	[g/kg]	[m/s]			
JAN	2.8	3.6	2.0	JAN	1.2	3.8	1.3	JAN	6.4	4.7	2.8
FEB	4.0	3.9	1.9	FEB	2.5	4.4	1.5	FEB	7.2	5.4	3.0
MAR	8.0	4.5	2.1	MAR	8.0	5.1	1.8	MAR	9.2	5.6	2.1
APR	11.5	4.9	1.9	APR	12.8	6.6	2.0	APR	12.8	6.6	2.5
MAY	16.8	8.4	1.7	MAY	17.6	8.6	2.1	MAY	16.0	9.7	2.1
JUN	19.6	10.5	1.4	JUN	21.6	11.3	2.0	JUN	19.6	10.0	2.1
JUL	22.0	11.6	1.4	JUL	24.0	11.8	2.0	JUL	23.2	12.4	2.0
AUG	21.9	12.6	1.5	AUG	23.6	11.9	1.8	AUG	22.4	12.7	2.1
SEP	19.2	10.2	1.5	SEP	19.6	9.6	1.5	SEP	19.2	10.4	2.1
OCT	14.8	7.0	1.6	OCT	13.6	7.5	1.3	OCT	15.2	9.5	2.3
NOV	9.2	5.6	1.8	NOV	7.2	5.7	1.3	NOV	11.6	7.1	2.7
DEC	3.2	3.3	1.8	DEC	2.4	4.2	1.2	DEC	3.6	5.5	2.7

Data of Italy 3/3

Ancona 43°47' N 13°31' E 105 m				Roma Ciampino 41°48' N 12°36' E 137 m				Napoli Capodichino 40°53' N 14°18' E 72 m			
	T [°C]	x [g/kg]	v [m/s]		T [°C]	x [g/kg]	v [m/s]		T [°C]	x [g/kg]	v [m/s]
JAN	5.6	5.0	4.0	JAN	7.6	5.1	3.0	JAN	8.4	5.1	2.6
FEB	7.0	5.1	3.7	FEB	8.0	4.9	3.1	FEB	9.2	5.2	3.1
MAR	8.8	6.0	3.4	MAR	10.0	5.2	3.1	MAR	10.8	5.5	2.9
APR	12.4	7.6	3.1	APR	13.2	6.6	2.9	APR	13.6	6.9	2.5
MAY	16.8	8.1	2.8	MAY	17.2	8.7	2.5	MAY	17.2	8.4	2.1
JUN	20.4	11.5	2.7	JUN	21.2	11.0	2.4	JUN	21.2	11.3	2.0
JUL	23.6	12.3	2.8	JUL	24.4	11.4	2.4	JUL	23.6	11.2	1.9
AUG	23.6	13.3	2.8	AUG	24.0	12.4	2.3	AUG	23.6	12.4	1.7
SEP	20.8	12.8	2.9	SEP	20.8	10.9	2.3	SEP	20.8	11.0	1.7
OCT	16.0	9.6	3.0	OCT	16.0	8.4	2.4	OCT	16.0	8.9	2.0
NOV	8.4	7.1	3.5	NOV	12.4	7.1	3.2	NOV	13.2	7.0	2.3
DEC	7.6	5.2	3.8	DEC	8.4	5.6	3.1	DEC	10.0	5.7	2.6

Brindisi 40°40' N 17°57' E 10 m				Catania Fontanarossa 37°28' N 15°04' E 16 m				Cagliari Elmas 39°15' N 9°03' E 18 m			
	T [°C]	x [g/kg]	v [m/s]		T [°C]	x [g/kg]	v [m/s]		T [°C]	x [g/kg]	v [m/s]
JAN	9.2	6.1	5.8	JAN	10.0	5.2	3.4	JAN	9.2	5.9	3.6
FEB	10.0	5.0	5.9	FEB	10.4	5.8	3.8	FEB	9.2	5.4	4.2
MAR	11.6	6.0	5.5	MAR	12.0	6.1	3.5	MAR	12.0	5.8	4.2
APR	14.0	7.0	5.0	APR	14.0	7.0	3.5	APR	13.6	7.0	4.4
MAY	18.0	9.2	4.8	MAY	18.0	9.1	3.0	MAY	17.6	8.4	4.1
JUN	22.0	9.8	4.5	JUN	22.0	11.3	2.9	JUN	21.2	10.3	4.3
JUL	24.8	14.7	5.2	JUL	25.2	12.0	2.8	JUL	23.6	12.2	4.3
AUG	24.8	13.7	4.7	AUG	25.6	13.6	2.6	AUG	24.0	12.5	4.9
SEP	22.0	13.5	4.4	SEP	23.2	12.0	2.6	SEP	22.0	11.4	4.1
OCT	18.0	9.1	4.8	OCT	18.4	9.1	2.9	OCT	18.0	8.9	3.3
NOV	14.4	7.8	5.1	NOV	15.2	7.4	3.1	NOV	14.4	7.6	3.1
DEC	11.2	6.7	5.5	DEC	11.6	5.7	3.2	DEC	11.6	7.0	3.8

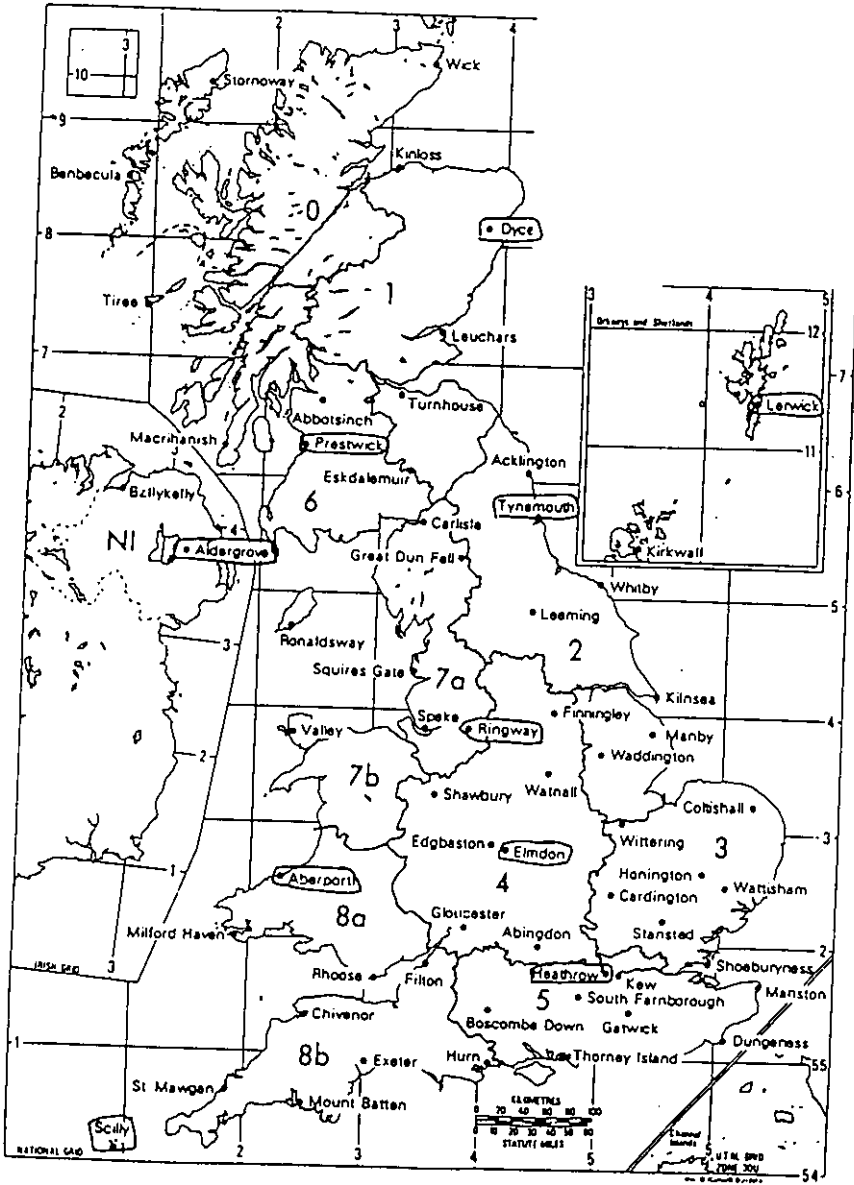
Data of The Netherlands 1/1

KLIMAATJAREN 1961-1970

	Temp max (C.)	Temp min (C.)	Temp gem (C.)	KV max (g/kg)	KV Emin (g/kg)	KV max (g/kg)	KV min (g/kg)	KV gem (g/kg)
JAAR: 1	11.9	-17.8	1.3	6.9	0.7	7.6	0.7	3.8
JAAR: 2	16.2	-16.2	2.4	5.5	0.9	8.0	0.9	3.9
JAAR: 3	23.8	-10.0	4.3	6.5	1.6	7.9	1.2	4.1
JAAR: 4	27.0	-4.8	8.1	6.8	2.4	10.3	1.4	5.2
JAAR: 5	28.5	-2.5	12.1	12.4	3.1	13.1	2.9	6.5
JAAR: 6	31.2	1.5	15.3	12.3	4.0	14.9	3.4	7.9
JAAR: 7	31.7	3.6	16.1	10.6	4.6	16.0	4.4	8.8
JAAR: 8	31.1	4.6	16.1	11.2	4.8	15.6	4.5	9.0
JAAR: 9	28.0	1.8	14.2	12.8	4.3	17.1	3.9	8.2
JAAR: 10	23.3	-1.1	10.7	10.2	3.3	12.4	0.3	6.9
JAAR: 11	19.9	-7.9	5.5	9.0	2.0	9.9	0.5	5.0
JAAR: 12	13.8	-12.6	1.2	8.9	-	9.0	0.8	3.8

Indien aandgegevens ontbreken van een klimaatjaar
zijn de hierboven weergegeven waarden bepaald over
de resterende jaren.

Data of the United Kingdom 1/4



Data of the United Kingdom 2/4

LONDON HEATHROW
51:28N 0:19W 5m

MONTH	TEMP :C	X :g/kg	V :m/s
JAN	4.2	4.4	4.8
FEB	4.5	4.2	5.2
MAR	6.6	4.4	5.2
APR	9.5	5.3	5.0
MAY	12.6	6.3	4.8
JUN	15.9	7.6	4.5
JUL	17.5	8.5	4.4
AUG	17.1	8.6	4.4
SEP	14.9	8.2	4.2
OCT	11.6	7.1	4.2
NOV	7.5	5.3	4.8
DEC	5.3	4.4	4.7
YEAR	10.6	6.2	4.7

BIRMINGHAM
52:29N 1:56W 163m

MONTH	TEMP :C	X :g/kg	V :m/s
JAN	3.4	4.3	4.8
FEB	3.8	4.1	5.1
MAR	5.9	4.3	5.3
APR	8.5	5.1	5.0
MAY	11.5	6.1	4.7
JUN	14.7	7.4	4.4
JUL	16.3	8.0	4.4
AUG	16.1	8.1	4.6
SEP	13.7	7.7	4.3
OCT	10.1	6.7	4.4
NOV	6.7	5.1	4.9
DEC	4.7	4.3	4.8
YEAR	9.6	5.9	4.7

SCILLY ISLES
49:56N 6:18W 48m

MONTH	TEMP :C	X :g/kg	V :m/s
JAN	7.7	5.6	7.9
FEB	7.3	5.3	7.6
MAR	8.5	5.6	6.8
APR	9.9	6.4	6.7
MAY	11.9	7.3	6.0
JUN	14.4	8.6	4.8
JUL	16.0	9.5	4.6
AUG	16.3	9.8	4.9
SEP	15.1	9.2	5.5
OCT	12.9	8.1	6.4
NOV	10.2	6.4	7.7
DEC	8.7	5.9	8.4
YEAR	11.6	7.3	6.4

Data of the United Kingdom

3/4

ABERPORTH
52:08N 4:34W 133m

MONTH	TEMP :C	X :g/kg	V :m/s
JAN	5.4	4.7	7.6
FEB	4.8	4.4	7.4
MAR	6.8	4.7	7.1
APR	8.5	5.5	6.2
MAY	10.8	6.4	5.8
JUN	13.4	7.8	5.0
JUL	14.9	8.6	4.8
AUG	15.3	8.6	5.7
SEP	14.0	8.1	6.0
OCT	11.2	7.1	6.6
NOV	8.2	5.4	7.3
DEC	6.4	4.8	8.1
YEAR	10.0	6.3	6.5

MANCHESTER RINGWAY
53:21N 2:16W 75M

MONTH	TEMP :C	X :g/kg	V :m/s
JAN	3.3	4.3	4.8
FEB	3.7	4.0	5.2
MAR	5.7	4.2	5.4
APR	8.3	5.0	4.9
MAY	11.3	5.9	4.7
JUN	14.3	7.3	4.2
JUL	15.7	7.9	4.0
AUG	15.5	8.1	4.2
SEP	13.7	7.6	4.2
OCT	10.5	6.7	4.3
NOV	6.5	4.9	4.7
DEC	4.3	4.3	4.6
YEAR	9.4	5.8	4.6

BELFAST ALDERGROVE
54:39N 6:13W 68m

MONTH	TEMP :C	X :g/kg	V :m/s
JAN	3.5	4.5	5.6
FEB	3.8	4.3	5.7
MAR	5.7	4.6	5.8
APR	7.9	5.2	5.4
MAY	10.4	6.2	5.2
JUN	13.3	7.6	4.9
JUL	14.4	8.0	4.8
AUG	14.3	8.4	4.7
SEP	12.7	7.8	5.0
OCT	10.1	6.3	5.4
NOV	6.4	5.1	5.1
DEC	4.6	4.6	5.1
YEAR	8.9	6.1	5.2

Data of the United Kingdom 4/4

TYNEMOUTH
55:01N 1:25W 33m

MONTH	TEMP :C	X :g/kg	V :m/s
JAN	3.9	4.3	5.0
FEB	4.1	4.1	5.6
MAR	5.5	4.3	5.4
APR	7.7	5.0	4.9
MAY	9.7	6.0	4.4
JUN	12.9	7.3	3.8
JUL	14.7	7.9	3.8
AUG	14.6	8.3	3.8
SEP	13.3	7.8	3.8
OCT	10.7	6.7	3.9
NOV	6.9	5.2	5.1
DEC	4.9	4.3	5.0
YEAR	9.1	5.9	4.5

PRESTWICK
55:29N 4:34W 10m

MONTH	TEMP :C	X :g/kg	V :m/s
JAN	3.1	4.4	5.2
FEB	3.9	4.1	5.2
MAR	5.6	4.5	5.7
APR	7.8	5.1	5.1
MAY	10.8	6.1	4.8
JUN	13.5	7.6	4.6
JUL	15.6	7.9	4.6
AUG	14.8	8.2	4.4
SEP	12.6	7.7	4.4
OCT	9.5	6.7	4.9
NOV	6.1	5.0	5.0
DEC	4.4	4.5	4.8
YEAR	8.9	6.1	4.9

ABERDEEN DYCE
57:08N 2:08W 52m

MONTH	TEMP :C	X :g/kg	V :m/s
JAN	2.5	3.9	4.9
FEB	2.7	3.9	5.2
MAR	4.5	4.1	5.6
APR	6.8	4.6	4.7
MAY	9.0	5.5	4.6
JUN	12.1	7.0	4.2
JUL	13.7	7.3	4.3
AUG	13.3	7.6	4.2
SEP	11.9	7.1	4.4
OCT	9.3	6.1	4.7
NOV	5.3	4.5	4.8
DEC	3.7	4.0	5.0
YEAR	7.9	5.4	4.7

APPENDIX 6.B:

Calculation Procedure to Determine the accumulated Supply Air

Mass 'W' and the Energy Consumption 'H'

Hourly mean values of p_o , θ_o and ϕ_o are taken from weather data files. The absolute outdoor humidity x_o [g/kg] is calculated:

$$x_o = \frac{p_s(\theta_o)}{\frac{100 \cdot p_o}{\phi_o} - p_s(\theta_o)} \cdot 622 \quad (6B-1)$$

With p_o barometric pressure (Pa)
 θ_o outdoor temperature (°C)
 ϕ_o outdoor relative humidity (%)

The initial inside temperature θ_i^* is an input value. The following is assumed: the space heating system of the house is not in operation during days, where the daily mean outdoor temperature $\theta_{o,m}$ is above 15°C, and from June 1st to August 31st. In this case the room temperature is independent of the initial room temperature θ_i and set to $\theta_i = (\theta_{o,m} + 20)/2$, during all other times $\theta_i = \theta_i^*$.

The surface temperature θ_{si} at the coldest location of the building, where we have a normalised heat transmission coefficient k_N and a surface heat transfer coefficient h_i , is calculated with:

$$\theta_{si} = \theta_i - \frac{k_N \cdot (\theta_i - \theta_{o,m})}{h_i - k_N \cdot (h_i/h_{iN} - 1)}$$

with h_{iN} : the normalised surface film coefficient

As 'a_w'-value, the threshold relative humidity against the wall surface is taken:

$$a_w = 5.3 \cdot 10^{-4} \theta_{si}^2 - 2.7 \cdot 10^{-2} \theta_{si} + 1.13$$

This assumption differs from $a_w = 0.8$, accepted as threshold relative humidity by the Annex. It takes into account the dependance of a_w on the temperature.

With a_w and θ_{si} , the maximum allowable indoor humidity ϕ_i in the room at room temperature θ_i is calculated, using the relationship:

$$x_i(\theta_i) = x_s(\theta_s)$$

If $x_i(\theta_i)$ and $x_s(\theta_s)$ are expressed as in equation (6B-1), ϕ_i can be determined as:

$$\frac{\phi_i}{100} = \frac{P_n}{\frac{P_i(\theta_i)}{P_s(\theta_s)} \cdot \left[\frac{P_a}{a_w} - P_s(\theta_i) \right] + P_s(\theta_i)}$$

which leads to a maximum absolute indoor humidity of

$$x_i = \frac{\phi_i \cdot P_s(\theta_i)}{P_i - \phi_i \cdot P_s(\theta_i)} \cdot 622 \quad (\text{g/kg})$$

Figure 6.9 and 6.10 show now the difference $x_i - x_e$.

For a constant vapour emission G_p in the building the necessary accumulated supply mass of outside air W_t is calculated in such a way, that the value x_i in the room is not exceeded.

$$W_t = \frac{G_m}{x_i - x_e} \cdot \Delta t \quad (\text{kg})$$

For those short periods, where $x_i - x_e < 0$, i.e. the absolute outdoor absolute humidity is higher than the allowed maximum indoor value and more humidity is supplied to the building by ventilation than exhausted, we set $W_t = 0$.

$$W = \sum_{\text{month}} (W_t)$$

The energy H to heat the outside air to room temperature is:

$$Q_t = W_t \cdot c_p \cdot (\theta_i - \theta_e)$$

We set $Q_t = 0$ from June 1st to Aug. 31st and for days with $\theta_{e,m} > 15^\circ\text{C}$.

